A regulatory network of Mdm2 and members of the Polycomb Group (PcG) family

---

Dissertation

for the award of the degree

“Doctor rerum naturalium”

of the Georg-August-Universität Göttingen,

within the doctoral program

“Molecular Biology of Cells”

of the Georg-August University School of Science (GAUSS)

submitted by

Maria Magdalena Wienken

from Quakenbrück, Germany

Göttingen 2015

Thesis Committee

Prof. Dr. Matthias Dobbelstein, Institute of Molecular Oncology, University Medical Center Göttingen (UMG)

PD Dr. Halyna Shcherbata, Research Group Gene Expression and Signaling, Max Plack Institute for Biophysical Chemistry (MPI-bpc)

Prof. Dr. Michael Zeisberg, Department of Nephrology and Rheumatology, University Medical Center Göttingen (UMG)

Members of the Examination Board

Referee: Prof. Dr. Matthias Dobbelstein, Institute of Molecular Oncology, University Medical Center Göttingen (UMG)

2nd Referee: PD Dr. Halyna Shcherbata, Research Group Gene Expression and Signaling, Max Plack Institute for Biophysical Chemistry (MPI-bpc)

Further members of the Examination Board

Prof. Dr. Michael Zeisberg, Department of Nephrology and Rheumatology, University Medical Center Göttingen (UMG)

Prof. Dr. Steven Johnsen, Clinic for General, Visceral and Pediatric Surgery, University Medical Center Göttingen (UMG)

Prof. Dr. Heidi Hahn, Department of Human Genetics, University Medical Center Göttingen (UMG)

Dr. Roland Dosch, Department of Developmental Biochemistry, University Medical Center Göttingen (UMG)

Date of oral examination: 11.01.2015

AFFIDAVIT

Herewith I declare that I prepared the PhD Thesis: “A regulatory network of Mdm2 and members of the Polycomb Group (PcG) family” on my own and with no other sources and aids than quoted.

Göttingen, 20.11.2015 _____

(Maria Magdalena Wienken)

ACKNOWLEDGEMENTS

I would like to use the opportunity to thank several people for their support, enthusiasm and scientific input:

Prof. Matthias Dobbelstein, for the possibility to work on this fascinating project and for all the fruitful scientific discussions that we had during the last couple of years.

PD Dr. Halyna Shcherbata and Prof. Dr. Michael Zeisberg, for the constructive discussions during the annual thesis committee meetings; Prof. Dr. Steven Johnsen, Prof. Dr. Heidi Hahn, and Dr. Roland Dosch, for serving as my extended thesis committee.

The “Studienstiftung des deutschen Volkes”, for their financial and ideational support.

The Göttingen Graduate School for Neurosciences, Biophysics, and Molecular Biosciences (GGNB), for accepting and guiding me as a student of their program.

My project partners Antje Dickmanns and Xin Zhang, for all their work before I joined this project and for everything we worked on together. It has not always been easy but I’m very proud of what we achieved together.

My collaboration partners of the Moll and Johnsen group. Special thanks here go to Prof. Dr. Ute Moll and Prof. Dr. Steven Johnsen, for the constructive discussions; to Alice Nemajerova, for performing the iPSC experiments; to Zeynab Najafova and Wanhua Xie, for their incredible patience when helping me with the RNA- and ChIP-Seq analysis.

My office partners Antje, Cathrin, Veena, Kamila, Merit, Franzi, and Christin, for all the emotional and chocolatey support during my time in your office and for all the laughter that made my stay so enjoyable even in times of scientific crisis.

The whole Molecular Oncology Department, for lots of science, cake and fun.

Frank, Daniela, Lydia, Veena, Katharina and Shelley, for proofreading this manuscript.

My family and friends, for your unrestricted love and support. Without you I would not be where I am right now and the next 150 pages would still be in scientific nirvana – Thank you!

Table of Contents

List of Tables

List of Figures

Abbreviations

A/BA	Acrylamide/Bisacrylamide
°C	Degree Celcius
ΔN	Delta N
µg	Microgram
µL	Microliter
µM	Micromolar
Aa	aminoacid
Ac	Acetylation
APS	Ammonium persulfate
Bp	Base pair
BSA	Bovine serum albumine
CA/CA	C462A/C462A
cDNA	Complementary DNA
ChIP	Chromatin immunoprecipitation
ChIP-Seq	Chromatin immunoprecipitation coupled with deep sequenzing
CMV	Cytomegalievirus
Co-IP	Complex immunoprecipitation
CpG	Cytosine-phosphatidyl-Guanine
Ct	Cycle threshold
C-terminus	Carboxy terminus of a protein
Ctrl	control
DBD	DNA-binding domain
DiffBind	Differential binding analysis of ChIP-Seq peak data
DMEM	Dulbecco`s modified Eagle medium
DMSO	Dimethylsulfoxide
DNA	Deoxyribonucleic acid
dNTP	Deoxynucleotide triphosphate
DTT	Dithiotreitol
E.coli	Escheria coli
EDTA	Ethylene diamine tetraacetic acid
EGTA	Ethylene glycol tetraacetic acid
EPZ6438	Tazemetostat
Et al	Et alii, and others
EtOH	Ethanol
EZH2	Enhancer of zeste homolog 2
FCS	Fetal calf serum
GFP	Green fluorescent protein
H	Hour
HAT	Histone acetyl transferase

Hepes	4-(2-Hydroxyethyl)piperazine-1-ethanesulfonic acid
H3K27	Histone H3 lysine 27
H2AK119	Histone H2A lysine 119
hMSC	Human mesenchymal stem cell
HMT	Histone methyl transferase
HRP	Horseradish peroxidase
IP	immunoprecipitation
iPSC	induced pluripotent stem cell
K	Lysine
Kd	Knock down
Ki	Knock In
Ko	Knock out
kDa	Kilodalton
LiCl	Lithium chloride
lncRNA	Long non-coding RNA
M	Molar
MACS	Model-based Analysis of ChIP-Seq
Max.	Maximal
Mdm2	Murine double minute 2
MEF	Murine embryonic fibroblast
Mg	Milligram
MG132	N-(benzyloxycarbonyl)leucinylleucinylleucinal Z-Leu-Leu-Leu-al, proteasome inhibitor
Min	Minute
mL	Milliliter
mM	Millimolar
MMulv	Moloney murine leukemia virus
mRNA	Messenger RNA
n	Sample size
n.s.	Not significant
NaDoc	Sodium deoxycholate
$NaHCO_3$	Sodiumhydrogencarbonate
ng	Nanogram
nM	Nanomolar
No.	Number
NP-40	Nonidet P-40 substitute
N-terminus	Amino-terminus of a protein
P	Phosphorylation
PBS	Phosphate buffered saline
PCA	Principal Component Analysis
PcG	Polycomb group family
PCR	Polymerase chain reaction
PIC	Protease inhibitor cocktail
pmol	Pico-mol

PRC	Polycomb repressive complex
PRE	Polycomb response element
PTM	Posttranslational modification
qPCR	Quantitative real-time PCR
R	Arginine
RING1B	RING finger protein 1B
RNA	Ribonucleic acid
Rpm	Rounds per minute
RT	Room temperature; Reverse transcriptase
S2	Safety level 2
SDS	Sodium dodecyl sulfate
SDS-PAGE	Sodium dodecyl sulfate polyacrylamide gel electrophoresis
SEM	Standard error of the mean
Ser	Serine
shRNA	Small hairpin RNA
siRNA	Small interfering ribonucleic acid
SUZ12	Suppressor of zeste 12 protein homolog
TBST	Tris buffered saline + Tween 20
TEMED	Tetramethylethylenediamine
Tris	Trisamine
UCSC	University of California Santa Cruz
UTR	Untranslated region
UV	Ultraviolet
VSV-G	Vesicular stomatitis virus glycoprotein
WB	Western Blot, Immunoblot
WT	Wild type

1 Abstract

The E3 ubiquitin ligase MDM2 is the most well-known physiological antagonist of the tumor suppressor P53. P53 induces cell cycle arrest or apoptosis in the case of DNA damage, whereas MDM2 targets it for proteasomal degradation during unstressed conditions. Loss of MDM2 in the murine organism is embryonically lethal but can be rescued by a concomitant loss of P53, which led to the assumption that MDM2's only function is based on P53 regulation. Still, several tumor species have been identified which are supported by high levels of MDM2 even in the absence of P53.

In this project, we have analyzed a P53-independent and stemness maintaining function of MDM2 which supported the de-differentiation process of induced pluripotent stem (iPS) cells. It furthermore inhibited differentiation of mesenchymal stem cells (MSCs) into osteoblasts and accelerated clonogenic cancer cell survival in the absence of P53. In each system, loss of MDM2 resulted in the deregulation of Polycomb group (PcG) family target genes. The PcG consists of the two protein complexes, PRC1 and PRC2, and silences gene expression through methylation of histone H3K27 (PRC2) and ubiquitination of H2AK119 (PRC1), which is often essential for stemness maintenance and cancer cell survival. MDM2 directly interacted with the PRC2 proteins EZH2 and SUZ12 and was recruited to PcG target gene promoters through EZH2. On the chromatin, MDM2 enhanced H3K27me3 and H2AK119ub1 which correlated to its gene regulatory function. H2AK119 is mainly ubiquitinated by the PRC1 protein RING1B. Loss of both E3 ligases, MDM2 and RING1B, decreased H2AK119ub1 levels and induced target gene expression further than the loss of each factor alone. Moreover, loss of RING1B and MDM2 was synthetically lethal in primary mouse- and cancer cells.

A close homolog of the MDM2 protein is MDM4. MDM2 and MDM4 support each other in the regulation of P53 but they cannot compensate each other according to *in vivo* loss of function studies. Preliminary data in our setting indicated a similar gene regulatory and H3K27me3 stabilizing function of MDM4 as detected for MDM2.

Taken together, MDM proteins enhanced the repression of lineage specific genes in cooperation with the PcG family, in the absence of P53. Thus, the oncogenic function of MDMs is not limited to controlling P53, but extended to chromatin modification and a stem-like cell phenotype.

2 Introduction

2.1 The MDM family – evolution, structure and functions

Murine double minute 2 or MDM2 is one of the most frequently studied oncoproteins worldwide. In the following paragraphs MDM2 evolution and structure will be discussed and it will be explained how MDM2 got one of the most important targets of the pharmaceutical industry to fight cancer.

2.1.1 MDM family structure and evolution

As its full name already suggests, MDM2 was originally identified on double minute chromosomes from transformed mouse 3T3DM cells roughly 30 years ago (Cahilly-Snyder et al, 1987). Double minutes are extrachromosomal DNA fragments that result from DNA amplification processes. MDM2 is not the only MDM protein; MDM4 (also known as MDMX) is a paralog of MDM2 that emerged from a gene duplication event around 440 M years ago (Momand et al, 2011; Shvarts et al, 1996). Both proteins are expressed in most vertebrate organisms whereas *Drosophila* and *Caenorhabditis* genomes do not encode any *MDM* sequences. This absence was long taken as reverse evidence that MDM proteins just classify to the vertebrates. However, recent studies identified coding sequences in several invertebrate organisms that resemble up to 27% of the human MDM2 (Momand et al, 2011). This makes it possible to trace back the MDM family for 1.5 billion years (Lane & Verma, 2012; Momand et al, 2011). 440 M years of evolution caused some independent development, but overall, the structures of MDM2 and MDM4 are quite similar. Since my project mainly focused on MDM2, the upcoming chapters will address mostly MDM2 but some specific features of MDM4 will be highlighted as well.

In jawed vertebrates the domain structure of MDM2 is highly conserved. In general, an acidic and a zinc finger domain are flanked by the aminoterminal P53-binding domain (Chen et al, 1993; Kussie et al, 1996) and a carboxyterminal RING (really interesting gene) domain (cf. Figure 2-1) (Fang et al, 2000; Honda et al, 1997) Among these domains, the RING domain is the most conserved (Momand et al, 2011). In MDM2, the RING domain encodes the E3 ubiquitin ligase function which is responsible for the mono- or polyubiquitination of several target proteins (cf. paragraphs 2.1.2.2 and 2.1.5.1) as well as MDM2 itself (Fang et al, 2000; Honda et al, 1997). Nuclear export and localization signal (NES/NLS) domains located between the P53-binding- and acidic domain ensure proper nuclear-cytoplasmic shuttling. The acidic and the zinc

finger domain are necessary for the interaction of MDM2 with multiple partners, influencing MDM2 posttranslational modifications, activity and function (cf. paragraph 2.1.3.2).

The MDM proteins differ by length in only one amino acid (aa) (Figure 2-1) and share 31 % amino acid identity. Highest conservation between the two proteins was detected in the P53-binding domain and the RING domain. MDM4 does not have intrinsic ubiquitin ligase activity. Instead, the RING domain promotes dimerization with MDM2 and was found to influence MDM2 RING domain function (Shvarts et al, 1997; Shvarts et al, 1996; Tanimura et al, 1999).

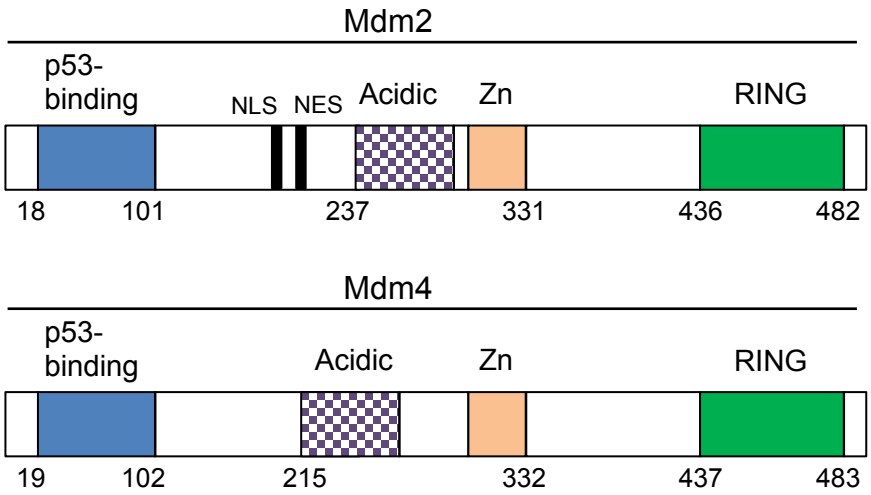

Figure 2-1 Domain structure of MDM2 and MDM4.

The different domains of MDM2 and MDM4 are shown together with the respective flanking amino acids (Wienken et al, under review).

2.1.2 P53 regulation by the MDM proteins

MDM2 and MDM4 are the main physiological antagonists of the tumor suppressor P53. The following paragraphs will introduce the MDM-P53 network and explain its importance.

2.1.2.1 *The tumor suppressor P53*

The P53 tumor suppressor, encoded by the *TP53* gene on chromosome 17p13.1, is one of the most studied proteins worldwide because of its significant role during tumor development and progression. Originally described in 1979 by Levine et al and Lane and colleagues as a 54 kDa protein which interacts with the SV40 large T antigens (Lane & Crawford, 1979; Linzer & Levine, 1979), P53 reactivation in a tumor is now the common goal of most future cancer therapies

(Wade et al, 2013). Together with its family member p73 and p63, P53 is the main mediator of cell cycle arrest and apoptosis in any case of cellular stress. It ensures proper heritage of the genomic information onto arising daughter cells and protection against accumulation of oncogenic mutations (Levrero et al, 2000).

In unstressed cells, P53 levels and activity are tightly controlled via numerous mechanisms, including the regulation by the MDM protein family as outlined in 2.1.2.2 (Gu & Zhu, 2012). Upon genotoxic stress e.g. via UV radiation, P53 is posttranslationally modified especially via phosphorylation and acetylation, leading to its stabilization, accumulation and activation (for illustration see also Gu et al, 2012). When activated, P53 can assemble as a homo-tetramer and bind to specific DNA binding sites, leading to the transactivation of genes involved in cell cycle arrest-, DNA repair, senescence and apoptosis (cf. Figure 2-2). The classic and probably most well-known target of P53 is the *CDKN1A* gene encoding the cyclin dependent kinase 1A (also known as p21), which mediates induction of G1 cell cycle arrest (El-Deiry et al, 1993). Several outstanding reviews have tried to gather published data (22,000 publications on PubMed only in the last 5 years) on the functions of P53 (Oren, 2003; Vogelstein et al, 2000; Vousden, 2000).

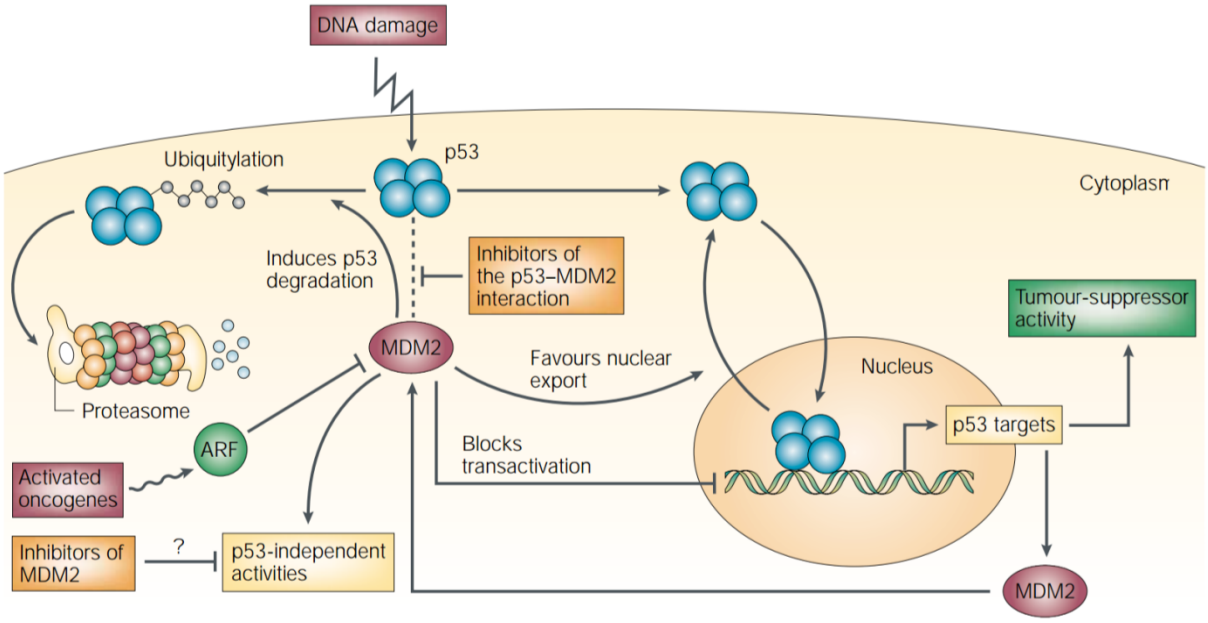

Figure 2-2 The regulation of P53 by MDM2 and its potential for cancer drug development.

MDM2 targets P53 for proteasomal degradation in an unstressed cell. Upon cell stress, P53 gets activated leading to the induction of target genes. Reactivation of wt p53 functions in malignant cells through inhibitor treatments is intensively studied to improve cancer therapy (Chene, 2003).

2.1.2.2 *P53 regulation by MDM2 and MDM4*

5 years after the first description of MDM2, a paper published by Arnold Levine and colleagues described the first interaction of MDM2 with the tumor suppressor P53. To that point, P53 had gained a lot of scientific interest but a major associated regulatory pathway was still lacking. Levine targeted this question by analyzing interaction partners of P53 and came across the p90 protein. Purification processes revealed that p90 was already described as the MDM2 protein important in murine fibroblast transformation and further analyzes identified its ability to abrogate P53 mediated cell cycle regulation functions (Momand et al, 1992). It took yet another 5 years to understand the main function of this interaction and new aspects of the P53 regulation by the MDM family are still getting published.

Haupt and Oren published in 1997 that MDM2 directly mono- and polyubiquitinates P53 and therefore targets it for proteasomal degradation (cf. Figure 2-2) (Haupt et al, 1997). As most embryonic and adult cells do not produce high wt P53 protein levels, proteasomal degradation explained the considerably high levels of P53 mRNA (Marine et al, 2006). Less well defined in the scientific community is the extent of MDM2 specific ubiquitination of P53. Degradation by the proteasome is dependent on Lysine 48-linked polyubiquitination of multiple lysines in the P53 C-terminus (amongst them are e.g. K370, K372, K373, K381, K382, and K386) (Michael & Oren, 2003). Depending on its expression levels, MDM2 is able to both, mono- and polyubiquitinate P53. P53 is monoubiquitinated when MDM2 is present in a low concentration and this modification rather seems to mediate nuclear export than decay (Li et al, 2003). On the other hand, high abundance of MDM2 leads to P53 polyubiquitination (Li et al, 2003). Due to this discrimination in MDM2 levels, it was discussed whether MDM2 might also need additional help in the elongation of ubiquitin chains on P53. p300 was speculated to be a possible candidate for this function although this is still under investigation (Grossman et al, 2003).

Next to its ubiquitination function, MDM2 can directly bind an α-helix in the P53 transactivation domain through its P53-binding domain and thereby inhibit the interaction of P53 with the basal transcription machinery (Momand et al, 1992; Oliner et al, 1993). This hypothesis was supported *in vitro* by the inability of an MDM2 mutant, lacking parts of the P53 binding domain, to efficiently inhibit P53 transactivation function (Haines et al, 1994). Although the data looked promising, recent *in vivo* studies in genetically engineered mouse models so far failed to directly support the theory that MDM2 masks P53 transactivation (Francoz et al, 2006; Toledo et al, 2006). Most interestingly, Toledo and colleagues developed a p53 mutant lacking the proline

rich domain which had decreased transactivation activity. When introduced into the $Mdm2^{-/-}$ mouse the $p53^{\Delta P}$ was not able to rescue embryonic lethality (see also paragraph 2.1.4).

In contrast to MDM2, the regulatory pattern of P53 by MDM4 is less well defined. So far, it is known that MDM4 does not ubiquitinate P53 because it does not contain any intrinsic E3 ligase function. MDM4 rather builds up heterodimers with MDM2 via their RING domains and enhances MDM2 ubiquitination of P53 (Linares et al, 2003). Quite recent data also indicates that heterodimerization of MDM2 with MDM4 changes MDM2 function from mono-ubiquitination to poly-ubiquitination (Wang & Jiang, 2012). Like MDM2, MDM4 is also able to mask the P53 transactivation domain and ablate the assembly of a functioning transcription machinery. In contrast to MDM2, this hypothesis also was supported by *in vivo* data, since overexpression of $p53^{\Delta P}$ (see paragraph before) rescued the $Mdm4^{-/-}$ phenotype (Francoz et al, 2006; Toledo et al, 2006).

2.1.3 Pre- and posttranslational regulation of MDM2

According to the human protein atlas (http://www.proteinatlas.org/) and the Universal Protein Resource database (www.uniprot.org/) the MDM2 protein is detected especially in the nuclear compartment of a cell. It is highly expressed in embryonic stem cells and only to low extent in developed tissues (data generated by Northern Blot; tissue array data on MDM2 protein expression controversial, due to the presence of many unspecific antibodies used) (Montes de Oca Luna et al, 1995). By regulating the tumor suppressor P53, a tight regulation of *MDM2* expression and activity is needed to ensure cell proliferation under normal conditions and p53 release during cell stress situations.

2.1.3.1 *Transcriptional regulation of MDM2*

MDM2 expression is regulated through the two distinct promoters, P1 and P2. P1 mediates constant basal expression whereas P2 is highly regulated and responsible for dynamic expression changes (Barak et al, 1994). In fact, one main transcription factor activating MDM2 expression through the P2 promoter is P53 itself (cf. Figure 2-2) (Wu et al, 1993). It is thereby ensured that P53 induced cell cycle arrest and apoptosis induction is reversed after P53 activation. This so called autoregulatory feedback loop is a crucial tool to mediate cellular survival as soon as the damage that initially activated P53 is repaired.

Furthermore, the P2 promoter is bound by several other transcription factors e.g. activated members of the ETS (E26 transformation-specific) family and SP1 (specificity protein 1) (Bond et al, 2004; Truong et al, 2005) which can rapidly induce MDM2 expression (Figure 2-3) (Wade et al, 2013).

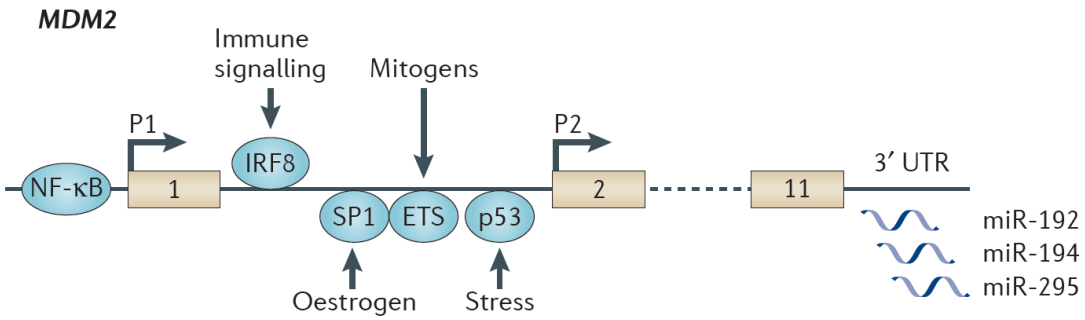

Figure 2-3 Transcriptional regulation of MDM2.

Expression of the *MDM2* gene is induced by multiple transcription factors through the two distinct promoters P1 and P2. Resulting transcripts are further controlled via miRNA mediated mRNA destabilization processes (Wade et al, 2013).

2.1.3.2 *Posttranscriptional and –translational regulation of MDM2*

Both *MDM2* promoters give rise to the same transcripts which differ in their 5' untranslated region (UTR). However, the P2 transcript is translated much more efficiently due to interaction of the 5'UTR with La antigen (Trotta et al, 2003). The P1 transcript does not only lack La binding properties but also contains two open reading frames slowing down the translational process (Zhao et al, 2014). In addition, many micro RNAs (miRNA) as well as other RNA binding proteins like RNPC1 can bind to the 3' UTR of MDM2 (and to some extent also MDM4) transcripts and target it for destabilization and degradation (cf. Figure 2-3) (Xu et al, 2013). These miRNAs provide further regulation (e.g. also by P53) and their MDM2 regulation is quite frequently lost during tumor formation (Zhao et al, 2014).

Upon translation, the MDM2 protein is characterized by a high turnover rate and many posttranslational modifications (cf. Figure 2-4) and protein interactions (cf. Figure 2-5). MDM2 is e.g. stabilized through phosphorylation of Ser166 and Ser186 by the kinase AKT for a more effective inhibition of P53 (highlighted in Figure 2-4). On the other hand, DNA-dependent protein kinase (DNA-PK) dissociates MDM2 from P53 through Ser17 phosphorylation in the case of genotoxic stress (Mayo et al, 1997). Activation of the DNA damage cascade also induces the kinase ATM, which phosphorylates MDM2 at the RING domain associated Ser-395. This

impairs the MDM2 mediated export of P53 from the nucleoplasm as well as diminishes E3 ligase function (Maya et al, 2001). Dephosphorylation of Ser-395 by the protein phosphatase 1D (Wip1) stabilizes MDM2 and in return leads to P53 inhibition (Lu et al, 2007).

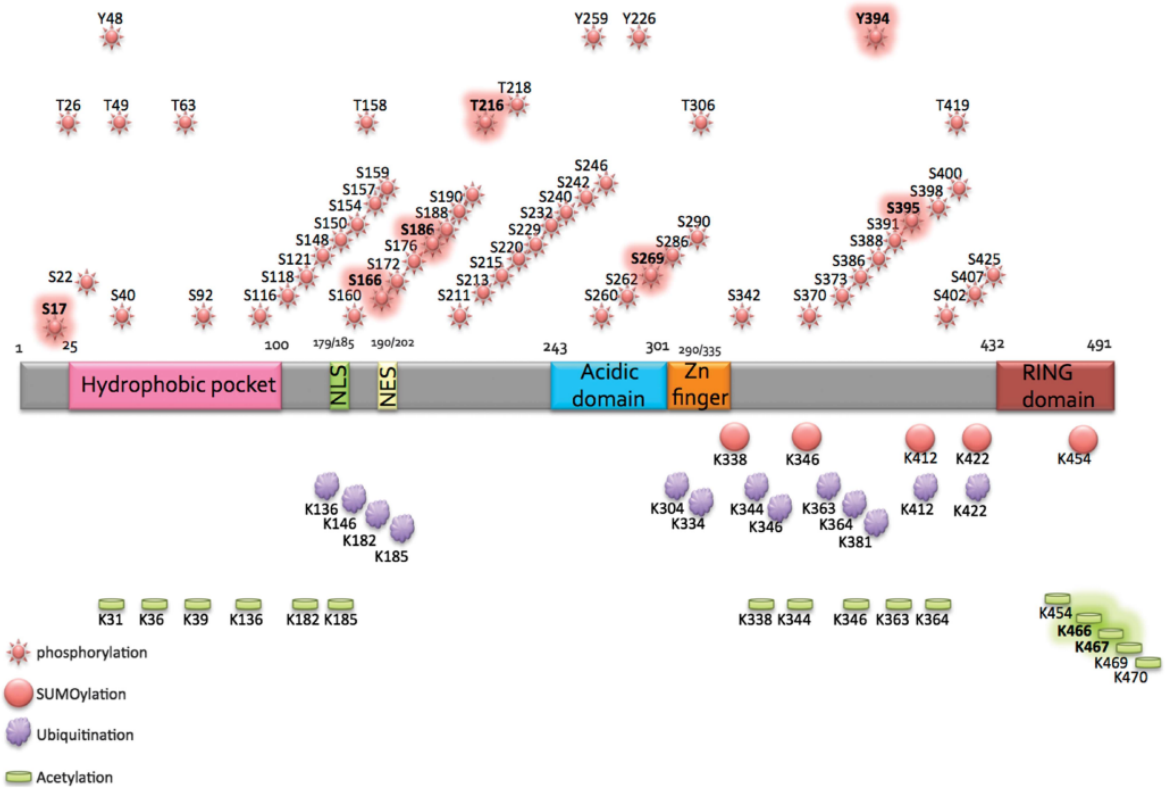

Figure 2-4 Posttranslational modifications of MDM2.

After translation, the MDM2 protein is modified by a variety of posttranslational modifications including phosphorylation, sumoylation, ubiquitination and acetylation. These modifications determine MDM2 protein activity, protein-protein interactions and stability (Fåhraeus & Olivares-Illana, 2013; Wade et al, 2013)

As already indicated in paragraph 2.1.1, the MDM2 protein is interacting with a large group of proteins and also RNA. The acidic domain is the major platform for protein interactions whereas the RING domain interacts both with proteins as well as RNA. Figure 2-5 shows a fraction of the so far identified interaction partners of MDM2. One important protein is the main physiological antagonist of MDM2 – $p14/p19^{ARF}$. ARF sequesters MDM2 and localizes it to the nucleolus during the activation of oncogenes like c-Myc (Zindy et al, 1998). Furthermore, MDM2 also interacts with proteins under p53 independent conditions. Nbs1 and E2F1 are interesting candidates here and are introduced further in paragraph 2.1.5.1.

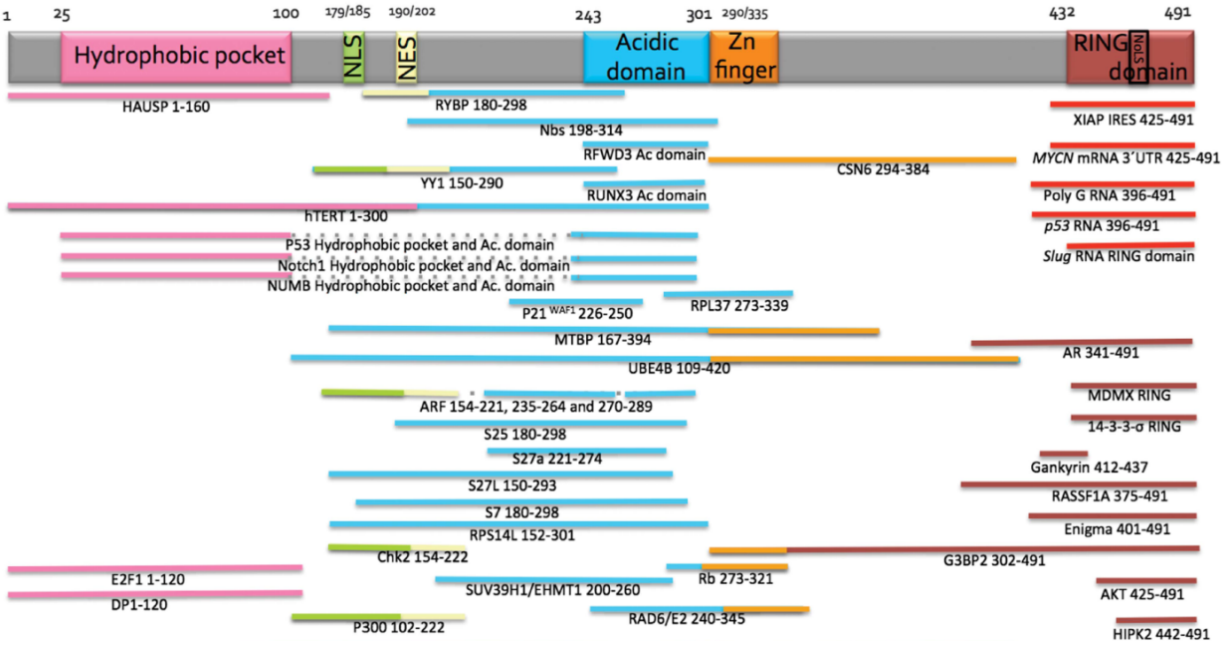

Figure 2-5 The many interaction partners of MDM2.

Apart from the well-studied interaction with P53, MDM2 interacts with a variety of proteins, mainly through its acidic domain (Fåhraeus & Olivares-Illana, 2013)

2.1.4 Knock out studies of MDM genes and P53 – jumping to conclusions too soon?

Due to their significance in cellular survival and oncogenesis, P53 and MDM2 were amongst the first genes to be analyzed in genetically engineered mouse models.

Remarkably, homozygous P53 deletion did not affect embryonic development. $P53^{-/-}$ mice develop normally but generate a variety of neoplasms at a later developmental stage (Donehower et al, 1992). Analysis of the P53 family members p63 and p73, indicated though that the main developmental functions might be carried out by p63 and – to some extent – also p73 (Levrero et al, 2000).

The absence of MDM2 as well as MDM4 is embryonically lethal due to a massive upregulation and activation of P53 (Jones et al, 1995; Montes de Oca Luna et al, 1995; Parant et al, 2001). These studies further led to two important notions:

1) Although MDM2 and MDM4 share P53 regulatory functions, they control P53 in a non-redundant manner. However, Steinmann and colleagues published that overexpression of MDM2 was able to overcome MDM4 knock out (ko) lethality (Steinman et al, 2005).

2) Whereas MDM2 ko is lethal due to apoptosis in the pre-implantation phase, MDM4 ko lethality only occurs later during mid-gestation and is characterized by cell cycle arrest. This time dependency is hinting at possible independent roles of each factor as well as a temporal spatial distribution of their activity (Finch et al, 2002; Jones et al, 1995; Migliorini et al, 2002; Montes de Oca Luna et al, 1995; Parant et al, 2001). This was further supported by conditional MDM2/MDM4 ko studies in the heart; whereas loss of MDM2 was lethal due to embryonic heart failure, loss of MDM4 did not affect heart development at all (Grier et al, 2006).

Most interestingly Montes de Oca Luna et al., as well as Jones and colleagues showed in their studies that the MDM ko phenotype was reversed with a concomitant p53 deletion. $P53^{-/-}$ $Mdm2^{/-}$ as well a $p53^{-/-}$ $Mdm4^{-/-}$ mice developed normally. In respect to late stage cancer generation these mice behaved comparably to the single P53 ko mouse. Oca Luna mentioned though subtle abnormalities in the reproduction of the double ko mice, since the mice had only few litters and also only few pubs within a litter (Montes de Oca Luna et al, 1995).

The same phenotype was found for mice carrying a mutation in the RING domain (C462A) of MDM2 and MDM4. The C462A mutation in MDM2 abrogated E3 ligase function and interfered with MDM2/MDM4 heterodimer formation but not with the binding to P53. Along the same line, C462A mutation in MDM4 disintegrated MDM2 binding, but P53 interaction stayed intact. $MDM2/MDM4^{C462A/C462A}$ mice were embryonically lethal due to P53 upregulation and lethality was reversed by additional loss of P53. These findings revealed the following: 1) Insufficient E3 ubiquitin ligase function of MDM2 is enough to drive embryonic lethality. The lethal activation of P53 cannot be rescued by the binding of the MDM proteins to P53. 2) The MDM2-MDM4 heterodimerization through their RING domains is necessary for efficient MDM2 ubiquitination function which explains why neither homolog can compensate the other (Huang et al, 2011; Itahana et al, 2007; Pant et al, 2011).

The P53/MDM2 ko studies provided a distinct insight into the relevance of the system in development and embryogenesis. However, the simple conclusions that were drawn – no developmental regulation by P53 and only P53 dependent functions for MDM2/4 in development – are facing now strong counter-arguments. It is still a fact that a murine organism can develop without P53 but already in 1995, two independent groups related an increase in embryonic lethality to the loss of P53. According to their data, this was caused by developmental defects especially during neural tube closure (Armstrong et al, 1995; Sah et al, 1995). Until now, these findings were supported by many different publications. P53 represses the reprogramming of

differentiated cells into iPS cells (Hong et al, 2009; Kawamura et al, 2009) and is involved in stem cell differentiation, self-renewal and plasticity (Aloni-Grinstein et al, 2014). It e.g. controls the differentiation of mesenchymal stem cells and cells of the B-cell lineage and regulates transcription of the stem cell factors Oct4 and Nanog as well as different factors of the homeodomain containing transcription factor family (Aloni-Grinstein et al, 1993; Molchadsky et al, 2008; Villasante et al, 2011). The insights into P53/MDM2 activity in stemness and differentiation are quite controversial and will need further elucidation during the upcoming years.

2.1.5 MDM proteins in cancer

As MDM2 mediates the regulation of P53 levels and activity, amplification of its corresponding genes as well as inhibition of any negative MDM2 regulation pattern was assumed to drive tumorigenesis. Indeed, roughly 10 % of all human cancers are characterized by an overexpression of *MDM2*, being most abundant in soft tissue tumors and osteosarcomas, but also in hematologic malignancies, gliomas, colorectal-, bladder- and breast cancer (Momand et al, 1998; Onel & Cordon-Cardo, 2004).
Deregulation was identified to be mediated through gene amplification processes, release of p14/p19ARF regulation and induction of gene expression (cf. paragraph 2.1.3.1) (Li & Lozano, 2013).

Defining the carcinogenic role of MDM2 in *in vitro* cell-based studies revealed that MDM2 alone was not always sufficient to drive proper cell transformation; stable overexpression of MDM2 was even correlated with cellular toxicity making it hard to draw any conclusions from these studies. Only in the presence of pre-existing genetic changes (e.g. in immortalized NIH3T3 cells) supra-physiological expression manifested MDM2 oncogenic functions (Fakharzadeh et al, 1991). In *in vivo* studies in mice though, overexpression of a MDM2 transgene was responsible for increased polyploidy and genomic instability independent of the P53 status (Lundgren et al, 1997). These genomic aberrations were correlated to the appearance of induced sarcomas, lymphomas and carcinoma.

The role of MDM4 in tumorigenesis is less well defined. MDM4 protein levels are elevated in several cancers, most prominently retinoblastoma and overexpression is mainly caused by gene amplification. In addition, Gilkes and colleagues postulated the upregulation of MDM4 through the ERK induced transcription factors c-Ets-1 and Elk-1 in colon cancer (Gilkes et al, 2008).

All of these findings support the relevance of the MDM proteins in tumorigenesis, but mainly in the context of repressing wt P53. However, there are several hints to P53 independent functions of MDM2. Jones and colleagues described already in 1998 the predisposition of a P53 ko mice with a transgenic MDM2 towards increased occurrence of sarcomas and spontaneous tumor formation (Jones et al, 1998). Heterozygous loss of MDM2 in $P53^{-/-}$ mice changes the tumor spectrum towards sarcomas (McDonnell et al, 1999) and similarly, close observations revealed a faster tumor onset in mice lacking MDM4 and P53 in comparison to P53 alone (Matijasevic et al, 2008).

2.1.5.1 *P53-independent functions of the MDM proteins in cancer and beyond*

As Jones and colleagues already suggested, MDM2 influences oncogenesis and tumor cell survival not only through P53 but also via independent functions. This hypothesis was supported by the identification of human sarcomas and bladder cancers which overexpressed MDM2 even in the absence of wt P53 (Cordon-Cardo et al, 1994; Lu et al, 2002). Moreover, Eμ-*myc* driven lymphomas overexpress MDM2 when generated in a P53 null or mutated background (Eischen et al, 1999) and tumors were identified that overexpressed MDM2 splice variants that are unable to bind P53 (Sigalas et al, 1996).

One of the earliest explanations was brought up by two different groups who described the destabilization of the retinoblastoma (Rb) protein and subsequent activation of the cell cycle regulator E2F1 through MDM2. Rb negatively regulates E2F1, a transcription factor driving cell cycle and survival. Through Rb decay, E2F1 is released of its negative regulation and can itself be activated by MDM2, which increases proliferation and genomic instability (Martin et al, 1995; Uchida et al, 2005; Xiao et al, 1995; Zhang et al, 2005). Most interestingly, in a context-specific situation in which E2F1 induces apoptosis, MDM2 has been detected to rather mediate E2F1 degradation than activation (Loughran & La Thangue, 2000).

As outlined in Figure 2-6, MDM2 is also responsible for the degradation of the negative cell cycle regulators p21 and hnRNP (Jin et al, 2003; Moumen et al, 2005) as well as the antiapoptotic protein FOXO3a (Yang et al, 2008). Furthermore, MDM2 does not only control cellular self-renewal but also plasticity. The epithelial marker protein E-cadherin, which is important during normal and malignant epithelial to mesenchymal transition processes (EMT) can be directly targeted for degradation by MDM2 which facilitates cell migration and metastasis (Yang et al, 2006). Quite recently Mulay and colleagues also reported a role of MDM2 in

inflammation and wound healing through interaction with NFκB and co-localization on its NFκB - target gene promoters (Mulay et al, 2012).

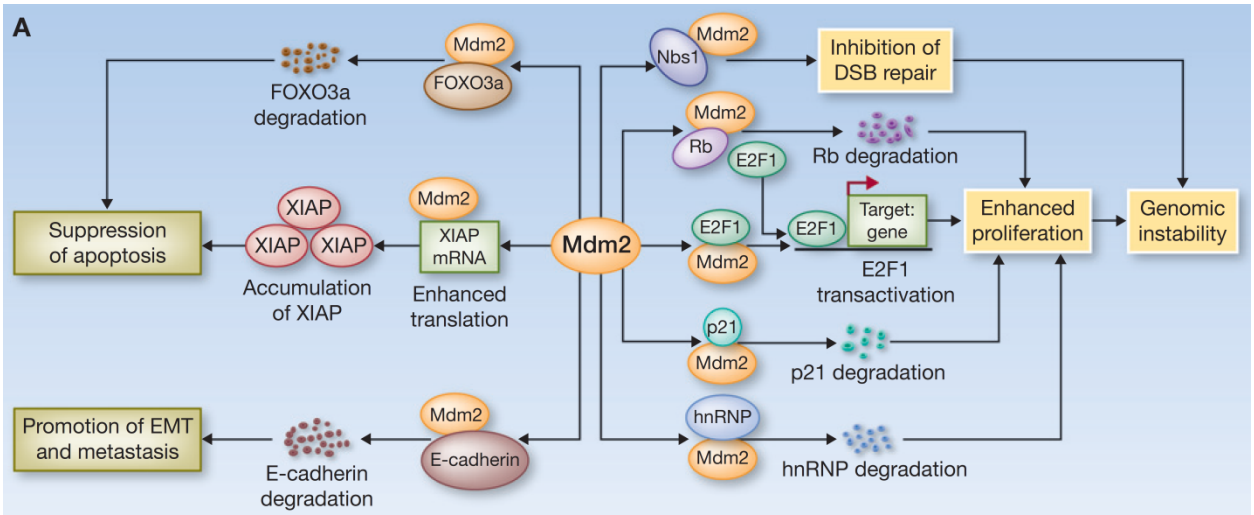

Figure 2-6 P53-independent functions of the MDM2 protein.

MDM2 is mainly known for its regulation of the tumor suppressor P53. Since its' first description in 1998 P53 –independent functions of the MDM protein have been intensively studied and are summarized in the context of cancer relevance (Li & Lozano, 2013)

2.1.6 The role of MDM2 in gene expression, epigenetics and development

2.1.6.1 *MDM2 in gene expression regulation and epigenetic control*

P53 is the major scientific focus of gene expression regulation by MDM2/4. As a matter of fact, there is a distinct regulation of P53 inducible genes by MDM2 and MDM4. Whereas the effects of MDM2 ko can be delayed by the additional loss of the pro-apoptotic gene *Bax*, MDM4 ko was partially rescued through loss of p21 (Chavez-Reyes et al, 2003). Indeed, further *in vitro* studies in MEF cells confirmed that MDM2 and MDM4 affect P53 activation through defined target gene selection (Barboza et al, 2008). MDM2 does not only influence gene expression through P53 but also via independent mechanisms. Apart from the P53 independent regulation of E2F1 (cf. paragraph 2.1.5.1) other transcription pathways have been identified to depend on MDM2 signaling, among them the NFκB and TGFβ pathways (Biderman et al, 2012). Of note, most of the data concerning MDM2 as a regulator of transcription was generated in malignant cells and normal physiological relevance needs to be determined.

Concerning epigenetic relevance, it was published that MDM2 associates to chromatin in several different settings. MDM2 was immunoprecipitated from P53 target gene chromatin in the presence of P53. According to the authors, MDM2 bound P53 directly on the chromatin of the *CDKN1a* promoter and inhibited transcription through the abrogation of transcription machinery binding, as outlined in 2.1.2.2 (Arva et al, 2005). In addition, MDM2 can recruit the histone methylases SUV39H1 and EHMT1 to P53 target gene promoters and thereby convert them to repressive chromatin (Chen et al, 2010). Most interestingly, Minsky and colleagues developed a P53 deficient *in vitro* system, in which MDM2 was still able to repress gene expression from a luciferase reporter plasmid. This repressive function was dependent on the MDM2 RING finger domain and was mediated through ubiquitination of histone H2A and H2B (Minsky & Oren, 2004).
So far, a chromatin associated function of MDM4 has not been published.

2.1.6.2 *P53-independent functions of MDM2 in development*

For most scientists, the results obtained in the genetically modified mouse models outlined in 2.1.4 were reason enough to doubt any possible p53-independent roles of the MDM proteins during stemness and differentiation. Several follow-up publications which used conditional MDM ko models in specific organs supported this assumption. Hence, a role in organ development and stem cell differentiation has been so far only been analyzed in a P53 proficient context, describing MDM2 and MDM4 as important factors for stem cell survival due to P53 shut-down (Abbas et al, 2010; Hilliard et al, 2014; Lengner et al, 2006).
However, the same studies also implicated, that there is no major function of P53 during development which was proven wrong at least *in vitro* when several groups in parallel indentified a stem cell barrier function of P53 in the generation of induced pluripotent stem cells (iPSCs) (Hong et al, 2009; Kawamura et al, 2009). If the developmental role for p53 is more complex than a ko mouse model can explain, it will most probably also not be the final answer for the MDM protein family.

During my master thesis project I observed a stemness maintenance function of MDM2 which works through the interaction with the well-known stemness- and epigenetic related Polycomb group family (PcG).

2.2 Chromatin modifications regulate gene expression

2.2.1 DNA compaction – not just a matter of storage

In a multicellular organism, each cell contains the same genetic information. To produce diverse cell differentiation, a highly complex system must regulate which genes are switched on and off, resulting in a specific gene expression code that determines cell fate. One mechanism, which was already introduced via p53, is the usage of distinct transcription factors that can either transactivate or repress gene expression. Another mechanism which can act more broadly covers the modification of the chromatin as such (Yan et al, 2010).

In general, DNA is not just loosely contained within the cell nucleus but is highly compacted together with histone and non-histone proteins into a dynamic polymer called chromatin as highlighted in Figure 2-7 (GM., 2000; Yan et al, 2010). The DNA double helix is wrapped around an octamer of four core histones (H2A, H2B, H3 and H4) building up a nucleosome, which is secured by the addition of the linker histone H1 (Rothbart & Strahl, 2014). This nucleosome structure is further coiled and condensed, ensuring proper chromosome structure during mitosis.

The chromatin structure is the basis of several regulation patterns as indicated in Figure 2-7. The DNA itself can be methylated at DNA stretches rich in CpG dinucleotides – so called CpG islands. This methylation is associated with repressed gene expression and is one of the major epigenetic changes during stem cell differentiation and malignant transformation (Reik et al, 2001).

Furthermore, non-coding RNAs regulate gene expression through various and not yet completely understood ways. e.g. inhibition of gene expression through direct binding but also through the recruitment of histone modifying enzymes (Bernstein & Allis, 2005).

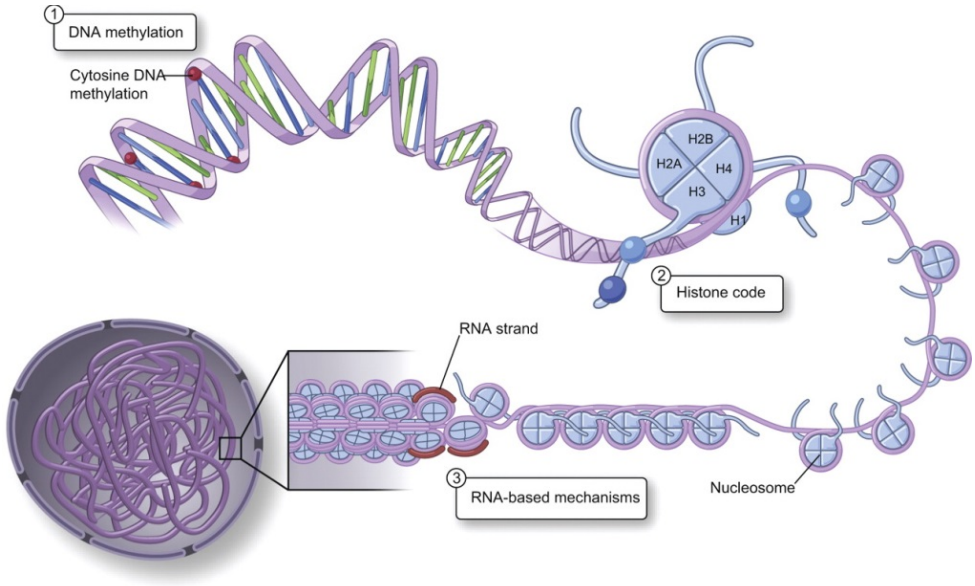

Figure 2-7 The three fundamental mechanisms of epigenetic regulation.

Epigenetic regulation of gene expression consists of three defined processes. (1) DNA is methylated at CpG rich regions, so called CpG islands, which represses gene expression (Reik et al, 2001). (2) Histone proteins are post-translationally modified at amino acid residues on their N- and C-terminal tails. These modifications alter DNA or effector protein binding and therefore modulate gene expression (Rothbart & Strahl, 2014). (3) Non-coding RNA structures can modify chromatin dynamics through direct binding or recruitment of other epigenetic effector proteins (Bernstein & Allis, 2005). Each of these mechanisms can act on its own but can also influence the others (Yan et al, 2010).

2.2.2 The histone code

Apart from regulation through DNA methylation and RNA-based mechanisms, histones are covalently modified, especially on their N- and C-terminal domains. This leads to alterations in the nucleosome compaction and/or the binding of specific DNA binding proteins. Since the first description in 2000, the histone code has been slowly revealed and was found to be defined by writers (proteins that modify histones), erasers (proteins that remove the modifications) and readers (proteins that bind to the modifications) (Strahl & Allis, 2000; Turner, 2000). Histones can be acetylated, methylated, phosphorylated, ubiquitinated, sumoylated, citrullinated and ADP ribosylated which is partly summarized in Figure 2-8. Many other modifications have been described but most lack any regulatory explanation yet. Apart from amino acid modifications, histone variants can be incorporated by protein replacement (Talbert & Henikoff, 2010).

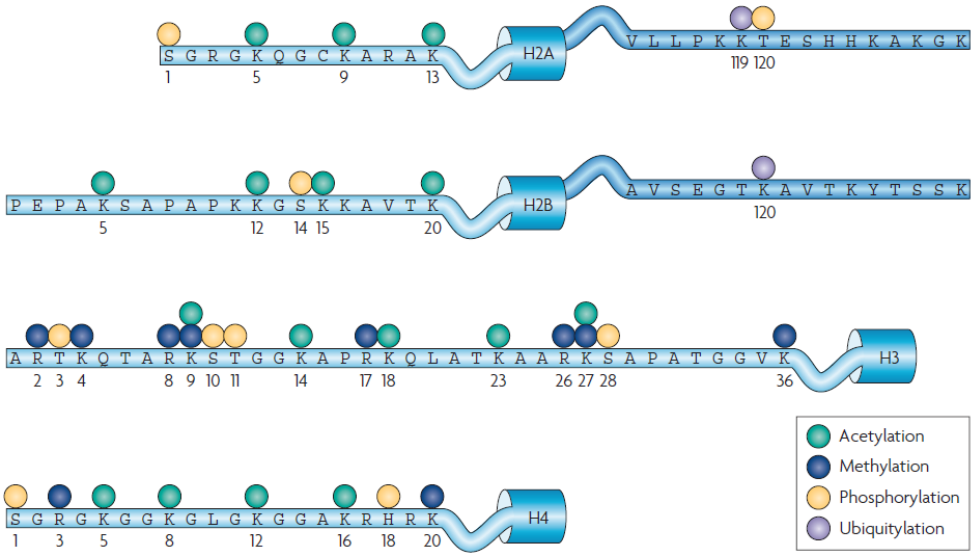

Figure 2-8 The histone code hypothesis - simplified.

Amino acid residues of histone proteins are post-translationally acetylated, methylated, phosphorylated and ubiquitinated, which influences their interaction with the DNA and other DNA binding proteins. Histone-DNA interaction is a major source of gene expression regulation (Spivakov & Fisher, 2007).

Histone acetylation and methylation are among the most widely studied modifications and were already described in 1964 by Allfrey and colleagues (Allfrey et al, 1964). Histones are acetylated by histone acetyl transferases (HATs) which will reduce the positive charge of the nucleosome and thus weaken the DNA histone interaction (Shogren-Knaak et al, 2006). The lack of compaction will facilitate transcription machinery binding and gene expression is favored. Furthermore, effector proteins containing a bromo-domain are able to bind to acetylated histones and further facilitate transcription (Dhalluin et al, 1999).

The contributions of histone methylation are less well defined. Methylation can either repress or activate gene expression, depending on the residue which is methylated and also on the number of methyl groups added (Spivakov & Fisher, 2007). For example, histone 3 lysine 27 trimethylation (H3K27me3) generally represses gene expression whereas H3K4me3 is associated with active expression (Santos-Rosa et al, 2002; Schwartz & Pirrotta, 2007). Monomethylated H3K4 was identified in gene enhancer regions whereas trimethylated H3K4 was linked to promoter regions (Greer & Shi, 2012).

This project mainly focused on the histone methyl transferase (HMT) Enhancer of Zeste Homolog 2 (EZH2) which methylates lysine 27 and 9 on histone 3. EZH2 is acting in a defined

epigenetic complex which is responsible for gene expression control in a variety of different physiological contexts.

2.3 The Polycomb Group family proteins (PcG)

The Polycomb group family is a sophisticated protein machinery which establishes histone modifications important in gene repression. This repression is important in cellular self-renewal and - plasticity, X-chromosome inactivation and malignant transformation (Breiling, 2015; Richly et al, 2011; Simon & Kingston, 2013). The group of PcG proteins was clustered together in 1985 by Jürgens and colleagues since mutants of all of their genes lead to a similar fly phenotype - additional sex comb structures on male legs. This was roughly 40 years after the first description of the so called Polycomb mutant (Jürgens, 1985; Slifer, 1942).
The similar phenotypes were caused by the ectopic upregulation of homeotic transcription factor expression in each PcG mutant. These transcription factors typically ensure specific cell identity along the embryonic axis and distortion of their expression transforms embryo segments and body structures (Lewis, 1978). It is now believed that the PcG and their highly conserved vertebrate homologs not only repress homeotic transcription factors (also known as Hox genes) but also many other genes, which maintain cell cycle and embryonic development (Boyer et al, 2006; Lee et al, 2006; Schwartz et al, 2006)

2.3.1 Polycomb repressive complex 2 (PRC2)

The Polycomb Repressive Complex 2 (PRC2) is one of the two well-known repression machineries of the PcG family and consists of four different complex proteins. The PRC2 methylates H3 on lysine 27 and 9 (mono-, di- and trimethylation) and histone 1 on lysine 26, however, its main catalytic target is H3K27 (Kuzmichev et al, 2004; Margueron et al, 2008). PRC2 catalytic activity is provided by EZH2, the *Drosophila* homolog of the *Enhancer of Zeste E(z)* gene (Czermin et al, 2002). EZH2 is a SET domain containing histone methyl transferase, which is only catalytically active when assembled with SUZ12 (Suppressor of Zeste 12) and EED (ESC in flies) (Cao & Zhang, 2004; Ketel et al, 2005; Pasini et al, 2004). This interaction was highly conserved from fly to human and homologs can be found even in plants but not in yeast (Ito & Sun, 2009; Whitcomb et al, 2007).

Apart from the intrinsic factors, PRC2 can build complex specifying interactions with accessory proteins like PCL1-3 (homologs of the fly protein PCL) and JARID2 (Kaneko et al, 2014;

Landeira et al, 2010; Nekrasov et al, 2007; Walker et al, 2010). Both, PCL proteins and JARID2, have been described to be involved in the recruitment of the PRC2 to specific and also broader target sites. As an example, PCL2 recruits the PRC2 especially to the X-chromosome whereas PCL3 stabilizes overall PRC2 mediated H3K27me3 (Hunkapiller et al, 2012; Walker et al, 2010). PCL proteins can also boost the enzymatic activity of EZH2, facilitating the conversion of H3K27me2 into H3K27me3 (Nekrasov et al, 2007). Chromatin occupancy of PRC2 proteins largely overlap with the second multiprotein complex of the PcG family – the PRC1 (Schuettengruber & Cavalli, 2009) and both complexes are tightly linked according to numerous studies (Comet & Helin, 2014)

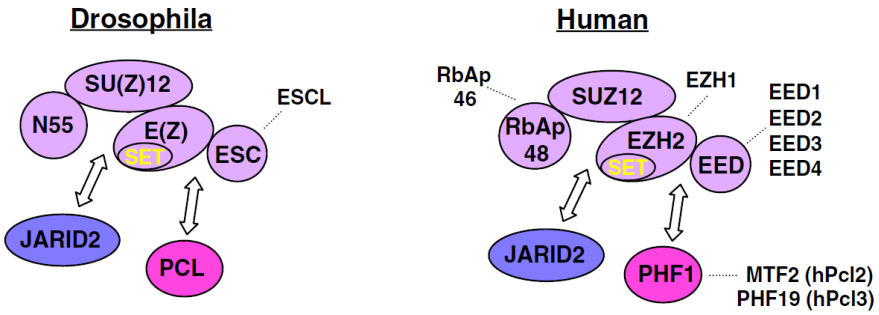

Figure 2-9 Composition of the Polycomb Repressive Complex 2 (PRC2) in fly and human.

The canonical subunits building up the fly and human PRC2 are shown. Lavender colored proteins are essential core subunits of the fly proteins and their respective homologs in human. Arrows indicate the conserved interaction of the PRC2 with JARID2 and PCL proteins (Simon & Kingston, 2013)

2.3.2 Polycomb repressive complex 1 (PRC1)

Three years before detection of the PRC2, the Polycomb repressive complex 1 (PRC1) was introduced (Shao et al, 1999). The original core components isolated from *Drosophila* were Polycomb (PC), Polyhomeotic (PH), Posterior sex combs (PSC), and Sex combs extra (SCE/dRING) (Shao et al, 1999). A few years later homologs of each gene were isolated from mammalian species, each had faced duplication events and evolutionary development (Levine et al, 2002). The PC protein evolved into five different CBX proteins which contain a chromo-domain and can bind to H3K27me3 (Fischle et al, 2003). PH and PSC became three (PHC1-3) and six different homologs (PSC: Polycomb group RING fingers, PCGF1–6), respectively. Two different dRING proteins (RING1A and RING1B) make up the catalytic part of the complex and ubiquitinate histone H2A at lysine K119 (H2AK119ub1) (Wang et al, 2004). In addition, many

other proteins were described to interact with the PRC1 (cf. Figure 2-10). Only from the number of homologs present of all PRC1 complex members can one estimate how many different composition forms can be built up. According to Gao and colleagues, six biochemically distinct PRC1 complexes can be defined which do not only differ in their composition but also harbor complex specific functions (Gao et al, 2012).

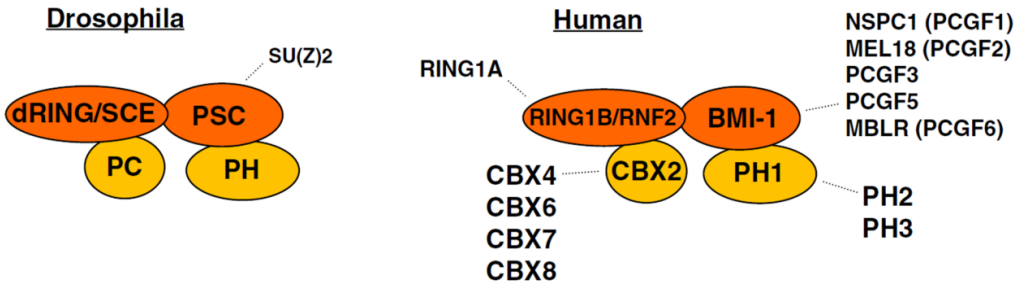

Figure 2-10 Composition of the Polycomb Repressive Complex 1 (PRC1) in fly and human.

The canonical core subunits of the fly and human PRC1 are shown. PRC1 is built up of the 4 proteins PC, PH, PSC and dRING in fly and diverse set of its homologs in human (Simon & Kingston, 2013).

The PRC1 was long thought to be a downstream effector of the PRC2 mediating its function especially through ubiquitination of H2AK119. Thereby, a CBX (= chromo-domain) containing PRC1 complex can recognize amino acids methylated by the PRC2 leading to its chromatin recruitment. Subsequent ubiquitination of H2AK119ub1 blocks chromatin remodeling and halts RNA polymerase II mRNA elongation (Cao et al, 2005). Spreading of PRC1 protein complexes along the downstream regions further compacts the chromatin structure for repression maintenance (Francis et al, 2004). The idea behind the repressive functions of PRC1 ubiquitination is generally accepted but the whole molecular mechanism of PRC1 functioning as well as its recruitment is not completely solved yet. In fact, Eskeland and colleagues demonstrated that chromatin compaction by PRC1 is independent of its ubiquitination function (Eskeland et al, 2010). This correlated nicely with a publication by Francis and colleagues who defined the compaction ability as histone tail independent (Francis et al, 2004). In addition, although all PRC1 complexes contain RING1A/B, only specific PRC1 setups seem to be important for the placement of H2AK119ub1 (Blackledge et al, 2014).

2.3.3 Recruitment of the PcG proteins to their target gene chromatin

Although sequencing analysis and motif predictions of chromatin immunoprecipitation approaches are increasing in computational strength, it is not defined clearly yet, how the PRC2 is localized to its target sites in mammalian cells. In *Drosophila* this question was answered more straightforward. In 1993 and 1994 two distinct groups published the existence of cis-regulatory Polycomb response elements (PREs) which are bound by specific DNA-binding proteins that can recruit PcG complexes (Chan et al, 1994; Simon et al, 1993). Being located upstream of the gene promoters the PREs are thought to interact through protein interactions with the promoter via loop formation (Kahn et al, 2006). The only known homologue of these DNA binding proteins in mammalian cells is PHO/YY1 and so far only two mammalian PRE-like elements were identified. This makes it hard to believe that the PRE mechanism is the main driver of PcG recruitment here (Sing et al, 2009; Woo et al, 2010).

In mammalian cells the PRC2 is thought to be recruited through interactions with specific DNA binding proteins (cf. paragraph 2.3.1), CpG dinucleotides (CpG islands) (Ku et al, 2008) and non-coding RNA (Plath et al, 2003). According to Tanay and colleagues, the presence of CpG islands correlates with PcG binding in the absence of methylated CpGs and transcriptional activators. The PRC2 interaction partner PCL3 is able to direct the PRC2 towards unmethylated CpG islands and facilitate interaction with Tet1, an important factor in DNA demethylation (see also Figure 2-11 a) (Hunkapiller et al, 2012; Wu et al, 2011).
Apart from the recruitment to CpG sites, non-coding RNAs were found to direct the PRC2 to its target sites. Two prominent examples are the long non-coding RNAs (lncRNAs) X-inactive specific transcript (XIST) (Plath et al, 2003) and HOTAIR (Gupta et al, 2010).
Chromatin dynamics can further modify PcG recruitment. Activating histone marks, such as trimethylated H3K4 and H3K36 have been reported to prevent PRC2 binding and subsequent methylation of H3K27 (Schmitges et al, 2011; Voigt et al, 2012), whereas H3K27me3 and H2AK119ub1 stimulate PRC2 enzymatic activity (Hansen et al, 2008; Kalb et al, 2014). In addition, recognition of nucleosome density (Yuan et al, 2012) as well as specific PRC2 cofactor engagements (cf. paragraph 2.3.1) modify PRC2/chromatin interaction and gene repression.

The general opinion about PRC1 recruitment is still mainly based on the recognition of methylated H3K27 via the PRC1 chromo-domain containing CBX proteins. This idea was analyzed through CBX chromatin immunoprecipitation experiments in PRC2 wt and mutant cells and proven true for many PcG target sites (Boyer et al, 2006; Cao et al, 2002; Fischle et al,

2003) (see also Figure 2-11 a). However, two publications in 2007 and 2010 demonstrated retention of PRC1 on the chromatin even in the absence of PRC2 in pluripotent as well as differentiated cells (Leeb et al, 2010; Pasini et al, 2007; Tavares et al, 2012) and they postulated other recruitment strategies.

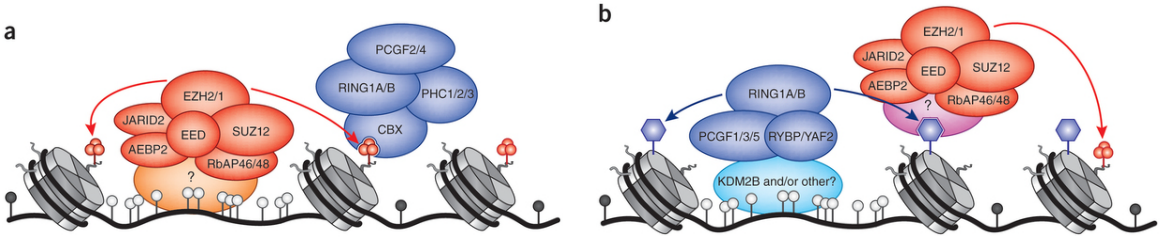

Figure 2-11 Recruitment of PcG proteins by unmethylated CpG islands.

PRC2 and PRC1 can be recruited through accessory binding partners to unmethylated CpG islands. This recruitment is speculated to facilitate their interaction with each other in a non-hierarchical fashion (Comet & Helin, 2014).

One striking and recent finding in this context was that only CBX protein containing PRC1 complexes are dependent on methylated histone 3 for recruitment whereas RYBP containing PRC1 can mediate H2AK119ub1 independent of H3K27me3 (Tavares et al, 2012). RYBP and CBX presence exclude each other due to a mutually exclusive binding site on RING1A/B (Wang et al, 2010), giving rise to two distinct PRC1 targeting strategies and the termination of canonical (CBX-containing) and variant (RYBP-containing) PRC1.

In 2014, Blackledge and colleagues further extended this finding and postulated PRC2 recruitment and H3K27me3 placement through variant PRC1 occupancy at specific target sites (see also Figure 2-11 b). This recruitment was H2AK119ub1 dependent and loss of catalytic activity dramatically reduced H3K27me3 and PRC2 levels at these target sites in murine ESCs (Blackledge et al, 2014). Kalb and colleagues confirmed this dependency of the PRC2 on PRC1 and postulated that JARID2–Aebp2–containing PRC2 complexes can bind H2AK119ub1 and methylate H3K27 on monoubiquitinated nucleosomes (Kalb et al, 2014).

As already mentioned for the PRC2, CpG islands can also recruit the PRC1 when it is assembled to the protein KDM2B/FBXL10 (cf. Figure 2-11 b). The PRC1-KDM2B interaction not only directs the complex to CpG island but also facilitates H2AK119ub1 at these sites (Wu et al, 2013). In accordance with the PRC2 binding pattern, the PRC1 is only recruited to non-methylated CpG islands, since methylation inhibits KDM2B binding. In the context of variant PRC1, Blackledge and colleagues identified CpG recruitment of a PCGF1 containing PRC1

variant as a requirement for PRC2 levels at specific CpG islands, which was necessary for embryonic development (Blackledge et al, 2014).

2.3.4 PcG gene regulation in stem cells and cancer

2.3.4.1 *Stem cell plasticity regulated by the PcG*

Stem cells are characterized by continuous self-renewal and the ability to differentiate into specialized cell types (Morrison et al, 1997). Stem cell self-renewal and specification is a major target of epigenetic regulation and especially regulation via the PcG family (Spivakov & Fisher, 2007).

Before anything was known about the PcG regulatory mechanism, their corresponding fly mutants had revealed their importance in embryonic development and especially body segmentation (cf. paragraph 2.3). In mice, loss of the main three PRC2 proteins (EZH2, SUZ12 and EED) as well as RING1B, the main catalytic subunit of the PRC1, leads to early embryonic lethality (Faust et al, 1995; O'Carroll et al, 2001; Pasini et al, 2004; Voncken et al, 2003). Mice deficient of the PRC1 members BMI1 and PHC1 are suffering from malformation in the anterior-posterior patterning and severe anemia due to reduced self-renewal of hematopoietic stem cells (Lessard & Sauvageau, 2003; Ohta et al, 2002).

The striking influence of PcG proteins on organism development was supported by genome wide analysis, mapping their gene regulatory function to key stem cell factors, cell cycle regulators, X-chromosome inactivation as well as stem cell plasticity and also tumor progression (Breiling, 2015; Simon & Kingston, 2013). Upon differentiation of pluripotent embryonic stem cells (ESCs) PcG proteins delocalize from specific lineage associated transcription factors and subsequently silence stem cell associated genes. In concordance total PcG protein levels decrease during the onset of differentiation (Lee et al, 2006; Simon & Kingston, 2013) and loss of the epigenetic regulation by the PcG accelerates differentiation capacity in many different directions (Chou et al, 2011).

In 2012 Onder and colleagues verified the importance of PRC2 regulation also in the reprogramming of differentiated fibroblasts into iPS cells. According to their study, loss of EZH2 weakens reprogramming efficiency (Onder et al, 2012). This finding correlated to the finding of Boyer et al., who proposed the regulation of Yamanaka factor target genes by PcG mediated epigenetic regulation (Boyer et al, 2006). Yamanaka and colleagues published in 2006 that the

generation of pluripotent stem cells is highly dependent on the 3 (4) different transcription factors – Oct3/4, Klf4 and Sox2 (sometimes also c-myc) (Takahashi & Yamanaka, 2006).

2.3.4.2 *PcG deregulation in cancer*

Already in 1983, it was published that cancer cells are characterized by an altered DNA methylation landscape (Feinberg & Vogelstein, 1983). Although no one really understood what these findings meant at that point it was clear that transformation had changed the epigenetic landscape (or vice versa) and that this must be correlated by the intensive shut down of specific gene clusters (Baylin et al, 1991). Next to the deregulation of DNA methylation processes histone modifications go awry during tumorigenesis (Fraga et al, 2005; Seligson et al, 2005). In parallel, many tumor types were identified that dependent on flawed PcG signaling, among them hormone-refractory metastatic prostate cancer, breast- and bladder cancer as well as melanoma (Hochedlinger et al, 2005; Lee et al, 2006). It is believed that the PcG proteins are able to repress gene loci important in cell arrest and apoptosis to support malignancy. One quite early identified and important locus for this is the *CDKN2a* locus which encodes the *INK4A* and *ARF* genes (Jacobs et al, 1999) INK4A is a regulator of the Rb pathway and ARF regulates the activity of MDM2 (cf. Figure 2-2) and both genes encode crucial tumor suppressive functions (Sherr, 2001).

The underlying mechanisms how PcG signaling is malignantly changed are versatile and not yet completely understood. BMI1, SUZ12 and EZH2 have all been found to be aberrantly upregulated in different tumor cells, which did not only alter the epigenetic landscape of these tumors but was also highly correlated with their aggressiveness and resistance towards chemotherapy. (Iliopoulos et al, 2010; Malekzadeh Shafaroudi et al, 2008; Weikert et al, 2005). Upregulation of PcG proteins can be caused by e.g. gene amplification and translocation processes. Moreover, loss of miRNA-mediated PcG regulation pathways is a key mechanism for cellular transformation (Beà et al, 2001; Godlewski et al, 2008; Smith et al, 2003; Varambally et al, 2008). In addition, the upregulation of associated factors and deregulation of interacting lncRNAs like HOTAIR that are involved in PcG recruitment have been described to mediate PcG hypersilencing (Gupta et al, 2010; Tange et al, 2014).

2.3.4.3 *PcG proteins and their connection to cancer stem cells*

The interconnection of the PcG proteins in both, stem cell maintenance and malignant transformation has raised an interesting discussion about its contribution to the hypothesis of

cancer stem cells (CSC) (Richly et al, 2011; Sparmann & van Lohuizen, 2006). According to the hypothesis of CSCs, the majority of tumors are characterized by very heterogeneous cell populations which can be separated into a small number of proliferating “stem cells” (CSCs) and a larger amount of more differentiated daughter cells (cf. Figure 2-12) (Kreso & Dick, 2014; Pardal et al, 2003). CSCs and normal stem cells share the capacity of continuous self-renewal and dedifferentiation and recent studies have shown that CSCs have a similar gene expression and epigenetic profile when compared to normal stem cells, even in the absence of the same driver mutation that initiated malignancy (Bartholdy et al, 2014; Eppert et al, 2011). In fact, several independent groups were able to isolate CSCs and proved that only the cancer stem cells proliferated extensively, were able to form new tumors in nude mice and mainly conferred towards chemoresistance (Al-Hajj et al, 2003; Bonnet & Dick, 1997; Singh et al, 2003). However, the whole concept is under intensive debate since there are tumors which are not built up by a clear CSC vs. non-CSC structure.

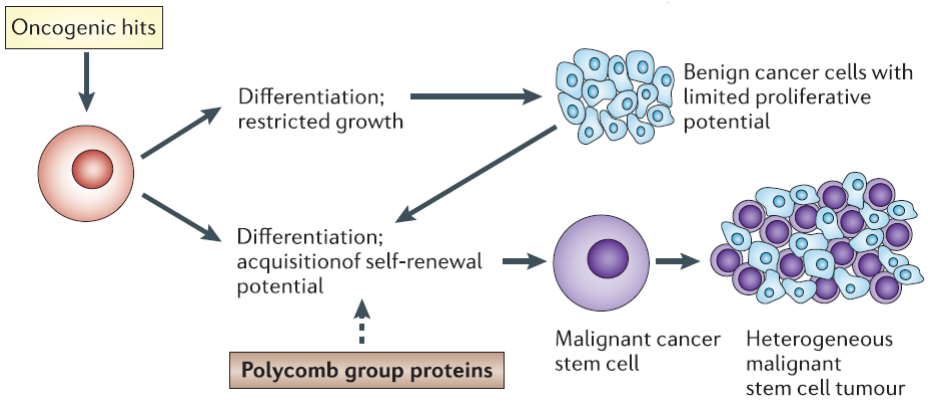

Figure 2-12 Cancer stem cells and their possible dependence on PcG signaling

According to the concept of CSCs, the majority of tumors are characterized by heterogeneous cell populations which can be separated into a small number of proliferating “stem cells” (CSCs) and a larger amount of more differentiated daughter cells. Gene expression regulation mediated by PcG proteins is speculated to be responsible for the generation and maintenance of the CSC population (Sparmann & van Lohuizen, 2006)

The PcG proteins EZH2 and Bmi1 have been extensively discussed in the field of CSC research. As an example, elevated EZH2 and H3K27me3 levels were detected in breast and prostate cancer CSCs. Inhibitor or shRNA mediated decrease in EZH2 protein significantly reduced prostate CSC spheroid formation and frequency, and intracranial tumor formation from glioblastoma CSCs, respectively (Crea et al, 2011; Suvà et al, 2009; van Vlerken et al, 2013).

2.4 Previous work

This PhD thesis deals with a functional network of the oncoprotein MDM2 and the PcG family. The project design was based on experimental data that I had obtained during my 6 months master thesis project. Before I started my thesis, initial work had indicated a functional interaction of MDM2 and members of the PRC2 via exogenous protein interaction and co-localization assays. The major question to answer in my master thesis was whether we can identify any functional relevance of this interaction. Therefore, I depleted multiple cancer cell lines of MDM2 and EZH2 and analyzed the expression of single PRC2 target genes. Surprisingly, several PRC2 target genes were upregulated not only in the absence of EZH2 but also MDM2, even in the absence of p53.

Since PcG proteins silence genes important for stem cell differentiation and cellular survival (cf. paragraphs 2.3.4.1 and 2.3.4.2) we further tested whether the regulation of PRC2 target genes via MDM2 was also connected to this function. Indeed, loss of MDM2 accelerated the differentiation of human mesenchymal stem cells (hMSCs) and impeded cancer cell survival, both in the absence of p53.

2.5 Project Aim

This project was conducted to further define the cellular consequences and molecular mechanism behind the gene regulatory function of MDM2 on PRC2 target genes.

Since differentiation experiments of hMSCs had already pointed out a stem cell maintenance function of MDM2 we wanted to investigate its relevance also in pluripotent reprogramming.

The generation of iPSCs had already highlighted an unexpected stemness barrier function for P53 (cf. paragraph 2.1.4). Based on the data we received from our MSC system we expected less efficient reprogramming of differentiated cells into iPS cells in the absence of MDM2.

Since we already knew about a possible gene regulatory function of MDM2 on single PRC2 target genes we wanted to approach the gene expression modulation in a global way. Via whole transcriptome sequencing or hybridization approaches we wanted to identify possible MDM2 target genes in different cell types including primary murine embryonic fibroblasts (MEFs), cancer- and stem cells and analyze these for PcG correlated enrichment. We were thinking to identify specific pathways that are enriched by the MDM2 gene regulatory function and which could also serve as a link that connects MDM2s' influence on stemness and malignancy. Because malignant transformation processes are supported by stem cell pathways the question arose whether the MDM2-PC2 interconnection could serve these processes.

PcG gene silencing is mediated by or at least correlated to changes in the epigenetic organization of their target genes (cf. paragraph 2.3). In the case of a joint gene regulatory function for MDM2 and PcG proteins we wanted to address several questions:
1) Does MDM2 itself bind to the target gene promoters and could it also be recruited there through interactions with proteins of the PRC2? MDM2 has indeed been found to bind chromatin in a p53 dependent- and independent manner (cf. 2.1.6) and localization experiments had already indicated a relocalization of MDM2 with EZH2 in specific nuclear compartments. This encouraged us to determine the MDM2 occupancy on the identified target genes via chromatin immunoprecipitation (ChIP).
2) Are the gene expression changes accompanied by changes in the respective H3K27me3 or H2AK119ub1 levels on the target gene promoters? In the case of repression release we were expecting a change of the epigenetic landscape associated with the gene promoter so that the transcription machinery can access the transcriptional start site and gene body. Interestingly, MDM2 had already been reported once to ubiquitinate H2A at lysine 119 (Minsky & Oren, 2004) leading to gene repression. Genome wide profiles of H3K27me3 and H2AK119ub1 would serve us for a more global analysis if we found a connection between MDM2 and histone modification changes.
3) Is MDM2 somehow involved in the recruitment of the PcG proteins to their target gene promoters or does it influence its activity? As it was already introduced in paragraph 2.3.3 there are versatile mechanisms by that PcG proteins get recruited to their target genes. Interaction with accessory proteins that can direct target gene binding has been detected and MDM2 could be involved by binding to the PRC2 proteins. Furthermore, a possible influence on activity could be rendered by ubiquitination processes directed either at decay or at changes of enzymatic activity and complex formation.

On the long run, analyzing the mechanisms of a p53-independent gene regulatory function of MDM2 which is not only mediating stemness maintenance but also cancer cell survival will be of utmost interest in the development of therapeutic cancer drugs. So far, many different compounds which are already tested in clinical trials are all aiming at the reactivation of P53 mostly through inhibiting the interaction of MDM2 with P53 (Li & Lozano, 2013). In case of PRC2 target gene regulation by MDM2 (and also other p53-independent functions cf. paragraph 2.1.6.2), this therapeutic approach might not be enough and it will be necessary to expand the drug design to interfere with the chromatin modifier function of MDM2 as well.

3 Material and Methods

3.1 Material

3.1.1 Technical devices

Table 3-1 Technical devices

Device	Company
Autoclave DX-200	Systec GmbH
Blotting chamber	Biozym, Hessisch Oldendorf, Germany
Cell counting chamber Neubauer improved	Brand, Wertheim, Germany
Centrifuge 5415R	Eppendorf, Hamburg, Germany
Centrifuge 5810R	Eppendorf, Hamburg, Germany
Centrifuge Megafuge 1.0R	Heraeus, Thermo Scientific, Waltham, MA, United States
Chemiluminescence imager Chemocam HR 16 3200	Intas Science Imaging Instruments, Göttingen, Germany
DNA gel chamber	Biotch Service Blu
DynaMag™-2	Life Technologies, Thermo Scientific, MA, United States
Electrophoresis system for SDS-PAGE	Amersham Biosciences, GE Healthcare
Freezer -20°C	Liebherr, Bulle, Switzerland
Freezer -80°C	Heraeus, Thermo Scientific, Waltham, MA, United States
Heating Block	Grant Instruments
Ice machine B100	Ziegra
Incubator for bacteria	Memmert, Schwabach, Germany
Incubator for cell culture Hera Cell 150	Heraeus, Thermo Scientific, Waltham, MA, United States
Laminar flow cabinet Hera Safe	Heraeus, Thermo Scientific, Waltham, MA, United States
Liquid nitrogen tank LS 4800	Taylor-Wharton, Theodore, AL, United States
betic stirrer MR Hei-Standard	Heidolph, Schwabach, Germany
Microscope Axiovert 40C	Zeiss, Oberkochen, Germany
Microwave	Cinex, Lippstadt, Germany
Mini Centrifuge MCF-2360	LMS, Tokyo, Japan
PCR machine for qPCR CFX96, C1000	Bio-Rad Laboratories
PCR machine Thermocycler T personal	Biometra, Göttingen, Germany
pH-meter WTW-720	WTW, Weilheim, Germany
Pipets Multipipet	Eppendorf, Hamburg, Germany
Pipets Eppendorf Research Series 2100 (0.1-2.5µL; 0.5-10µl; 2-20µL; 20-200µL; 100-	Eppendorf, Hamburg, Germany

1000µL)	
Power supply unit Powerpack P25T	Biometra
Qubit 2.0 Fluorometer	Invitrogen
Refrigerator 4°C	Liebherr
Roller RM5 V-30	CAT, Staufen, Germany
Rotator PTR 300	Grant Instruments
Scales Acculab ALC-6100.1	Sartorius, Göttingen, Germany
Scales LE623S	Sartorius, Göttingen, Germany
Scanner CanoScan 8600F	Canon
Shaker PROMAX 2020	Heidolph
Sonication device Bioruptor®	Diagenode, Liège, Belgium
Sonication device Bioruptor® Pico	Diagenode, Liège, Belgium
Spectrophotometer NanoDrop ND-1000	PeqLab, Erlangen, Germany
Thermomixer comfort	Eppendorf, Hamburg, Germany
UV-transilluminator Intas UV system Gel Jet Imager	Intas Science Imaging Instruments
Vacuum pump	IBS Integra Biosciences, Fernwald, Germany
Vortex Genie 2	Scientific Industries, Bohemia, NY, United States
Water bath TW 20	Julabo Labortechnik, Seelbach, Germany

3.1.2 Consumables

Table 3-2 Consumables

Product	**Company**
96-well plates for qPCR	4titude, Wotton, United Kingdom
Bacteria culture dishes	Sarstedt, Nümbrecht, Germany
Bacteria culture vials (14 cm)	Becton Dickinson
Bioruptor® Pico Microtubes with Caps (1.5 ml)	Diagenode
Cell culture dishes (10 cm, 15 cm)	Greiner, Frickenhausen, Germany
Cell culture plates (6-well, 12-well)	Greiner, Frickenhausen, Germany
Cell scraper (16 cm, 25 cm)	Sarstedt, Nümbrecht, Germany
Cryo tubes Cryoline	Nunc, Thermo Scientific
DNA LoBind tubes (1.5 mL)	Eppendorf
Filter tips (10 µL)	Starlab, Hamburg, Germany
Filter tips (20 µL, 200 µL, 1,000 µL)	Sarstedt, Nümbrecht, Germany
Parafilm	Brand
Pipet tips (10 µL, 20-200 µL, 1,000 µL)	Greiner, Frickenhausen, Germany
Protran nitrocellulose transfer membrane, 0.2 µM	Whatman, Dassel, Germany
Reaction tube (0.2 mL)	Sarstedt, Nümbrecht, Germany
Reaction tube (0.5 mL, 1.5 mL, 2.0 mL)	Eppendorf, Hamburg, Germany

Falcon reaction tube (15 mL, 50 mL)	Greiner, Frickenhausen, Germany
Safe-lock reaction tube (1.5 mL)	Eppendorf, Hamburg, Germany
Sterile filter (0.2µM and 0.45µM)	Millipore, Merck
Syringe, 1mL, 5mL, 10mL, 50mL	Henke-Sass, Wolf, Tuttlingen, Germany
Syringe canules (different sizes)	B.Braun, Melsungen, Germany
Transparent sealing foil for 96-well plate	4titude, Wotton, United Kingdom
Whatman paper	Whatman, Dassel, Germany

3.1.3 Chemicals and reagents

Table 3-3 Chemicals and reagents

Substance	**Company**
Acetic Acid	Roth
Acrylamide/bisacrylamide (A/BA)	Roth
Agar	Sigma-Aldrich
Agarose	Roth
Agencourt AMPure XP	Beckman Coulter
Albumin Fraction V (Bovine Serum Albumine, BSA) for molecular biology	Roth
Ammonium persulfate (APS) p.a.	Roth
Ammonium sulphate ((NH4)2SO4) >99.5%, p.a.	Roth
Ampicillin	Roth
Bromophenol blue	Sigma-Aldrich
Calcium chloride dihydrate (CaCl2 x 2H2O) >99%, p.a., ACS	Roth
Chloroform, Rotipuran	Roth
Complete Mini Protease Inhibitor EDTA free	Roche, Basel, Schweiz
Deoxynucleotide triphosphates (dNTPs)	Primetech
Deoxyribonucleotide triphosphates (dNTPs) in single tubes	Primetech
Dimethyl sulfoxide (DMSO)	AppliChem
Dithiotreitol (DTT)	Roth
DNA ladder GeneRuler	Fermentas, Thermo Scientific
DNA stain clear G (39804)	Serva
Ethanol 99.8%	Roth
Ethylene glycol tetraacetic acid (EGTA)	Roth
Formaldehyde, 37% solution	Roth
Glucose	Roth
Glycerol, >99%, p.a.	Roth
Glycerophosphate (ß-) dissodium salt hydrate	Sigma-Aldrich
Glycine, >99%, p.a.	Roth
Glycogen, molecular biology grade	Roth
HEPES Pufferan >99%, p.a.	Roth

Hexadimethrine bromide (Polybrene)	Sigma
Hydrogen chloride (HCl)	Roth
Igepal (NP-40), Ca-630	Sigma-Aldrich
Isopropanol	Roth
Lipofectamine RNAiMAX	Invitrogen, Life Technologies
Lipofectamine 2000	Invitrogen, Life Technologies
Lithium chloride	Roth
Magnesium chloride hexahydrate (MgCl2 x 6H2O)	Roth
Magnesium sulfate (MgSO4)	AppliChem
Methanol >99% (MetOH)	Roth
Nonidet P-40 substitute (NP-40)	Fluka
Nuclease free water	Ambion, Life Technologies
Page Ruler™ Prestained Protein Ladder	Fermentas, Thermo Scientific
Pefabloc SC protease inhibitor	Roth
Pepstatin A	AppliChem
Phenol solution (pH 8,0) for ChIP	Sigma-Aldrich
Ponceau S	Roth
Potassium chloride (KCl)	Applichem
Potassium hydrogenphosphate (KH2PO4)	Roth
Powdered milk	Roth
Protein A/G Agarose	Santa Cruz
Puromycin	Sigma-Aldrich
Random Hexamer Primer (0.2µg/µL)	Thermo Scientific fisher
RNase inhibitor	Fermentas, Thermo Scientific
Rotiphorese Gel 30	Roth
Sodium (di-) hydrogenphosphate dihydrate (Na2HPO4 x 2H2O) >99%, p.a.	Roth
Sodium acetate (NaAc)	Roth
Sodium chloride (NaCl)	Roth
Sodium deoxycholate	Applichem
Sodium dodecyl sulphate (SDS)	Biorad
Sodium Ethylene diamine tetraacetatic acid (Na-EDTA)	Roth
Sodium hydrogen carbonate (NaHCO3), >99,5%, p.a., ACS, ISO	Roth
Sodium hydrogenphosphate monohydrate (NaHPO4 x H2O), p.a.	Roth
Sodium hydroxide (NaOH), pellets	Sigma-Aldrich
SYBR green	Invitrogen, Life Technologies
Tetramethylethylenediamine (TEMED)	Merck
Trehalose dehydrate	Usb corporation, Cleveland
Trisamine (Tris) Pufferan, >99% p.a.	Roth
Triton X-100, molecular biology grade	Applichem

Trizol	Invitrogen, Life Technologies
Tryptone	Roth
Tween 20	Applichem

3.1.4 Buffers and solutions

6x Laemmli buffer

Tris pH 6.8	0.35 M
Glycerin	30.00%
SDS	10.00%
Dithiotreitol	9.30%
Bromophenol blue	0.02%
dissolved in H2O	

Tris buffered saline + Tween 20 (TBST), pH 7.6

Tris	50 mM
NaCl	150 mM
Tween 20	0.10%
dissolved in H2O	

10x qPCR reaction buffer (RB)

Tris (pH 8.8)	750 mM
(NH4)2SO4	200 mM
Tween 20	0.10%
dissolved in H2O	

10x Western Salt buffer, pH 8.3

Tris	250 mM
Glycin	1,92 M
SDS	0.02%
dissolved in H2O	

WB transfer buffer, pH 8.3

10x Western Salt buffer	10%
MetOH	20%
dissolved in H2O	

Phosphate buffered saline (PBS), pH 7.4

NaCl	24.00 mM
KCl	0.27 mM
Na2HPO4 x 7H2O	0.81 mM
KH2PO4	0.15 mM
dissolved in H2O	

WB blocking solution

milk powder	5%
dissolved in TBST	

RIPA lysis buffer, pH 7.5

Triton X-100	1.00%
Sodium deoxycholate	1.00%
SDS	0.10%
NaCl	150 mM
EDTA	10 mM
Tris-HCl, pH 7.5	20 mM
dissolved in H2O	

Cell lysis buffer

Urea	2 M
RIPA lysis buffer	100%
protease inhibitors:	
Pefabloc	10 µM
Pepstatin A	1 µg/ml
Leupeptin/Aprotinin	1 µg/ml

SDS running buffer

Tris	25.0 mM
Glycin	86.1 mM
SDS	3.5 mM
dissolved in H2O	

qPCR reaction mix, 25x	
10x qPCR RB	1x
SybrGreen	0,001620
MgCl2	3.0 mM
Trehalose in 10 mM Tris (pH 8.5)	300.0 mM
dNTPs	0.2 mM
Triton X-100	0.25%
Taq polymerase	20 U/mL
dissolved in H2O	

Buffer B for chromatin harvest (for ChIP)	
Triton X-100	0.25%
EDTA, pH 8.0	10 mM
EGTA, pH 8.0	0.5 mM
HEPES pH 7.6	20 mM
dissolved in H2O	

Buffer C for chromatin harvest (for ChIP)	
NaCl	0.15 M
EDTA, pH 8.0	1 mM
EGTA, pH 8.0	0.5 mM
HEPES pH 7.6	50 mM
dissolved in H2O	

Washbuffer 3 for ChIP	
LiCl	0.25 M
NaDOC	0.50%
NP-40	0.50%
EDTA, pH 8.0	1 mM
EGTA, pH 8.0	0.5 mM
HEPES pH 7.6	20 mM
dissolved in H2O	

Washbuffer 4 for ChIP	
EDTA, pH 8.0	10 mM
EGTA, pH 8.0	5 mM
HEPES pH 7.6	200 mM
dissolved in H2O	

Ponceau S Solution	
Ponceau S	0.50%
Acetic acid	1.00%
dissolved in H2O	

Buffer A for chromatin harvest (for ChIP)	
NaCl	0.1 M
EDTA, pH 8.0	1 mM
EGTA, pH 8.0	0.5 mM
HEPES pH 7.6	50 mM
dissolved in H2O	

Crosslinking buffer for chromatin harvest	
PFA	1.1 %
Buffer A	7 %
dissolve in PBS	

Washbuffer 1 for ChIP	
SDS	0.10%
NaDOC	0.10%
Triton-X-100	1%
NaCl	0.15 M
EDTA, pH 8.0	1 mM
EGTA, pH 8.0	0.5 mM
HEPES pH 7.6	20 mM
dissolved in H2O	

Washbuffer 2 for ChIP	
SDS	0.10%
NaDOC	0.10%
Triton-X-100	1%
NaCl	0.5 M
EDTA, pH 8.0	1 mM
EGTA, pH 8.0	0.5 mM
HEPES pH 7.6	20 mM
dissolved in H2O	

Elutionbuffer for ChIP	
SDS	1%
NaHCO3	0.1 M
dissolved in H2O	

CoIP buffer	
Tris-HCl, pH 7.5	50 mM
Sodium chloride	300 mM
NP-40	0.5 %
Sodium deoxycholate	0.1 %
Complete Mini, Protease Inhibitor Mix	1 x
dissolved in H2O	

HBS Buffer	
NaCl	68 mM
KCl	2,5 mM
Dextrose/Glucose	0,2 %
Hepes	10,5 mM
Na2HPO4x7H2O	0,37 mM
dissolved in H2O	
pH between 6.8 and 7.0 with 1M NaOH	
Re-pH a day or two later again	

Incubationbuffer stock for ChIP, 5x	
SDS	0.75%
Triton-X-100	5%
NaCl	0.75 M
EDTA, pH 8.0	5 mM
dissolved in H2O	

TAE buffer	
Tris	40 mM
Acetic acid	20 mM
EDTA	2 mM
dissolved in H2O	

DNA gel loading buffer, 6x	
Sucrose	40%
Glycerin	10%
Bromophenol blue	0.25%
dissolved in H2O	

3.1.5 Enzymes and buffers

Table 3-4 Enzymes and buffers

Reagent	Company
Buffer for M-MuLV RT, 10x	New England Biolabs (NEB)
Buffer for Taq (KCl+, -MgCl2), 10x	Fermentas, Thermo Scientific
M-MuLV Reverse transcriptase (RT)	New England Biolabs (NEB)
Maxima SYBR Green qPCR Master Mix	Thermo Scientific
Taq DNA polymerase (Taq)	Fermentas, Thermo Scientific
Taq DNA polymerase (Taq) for qPCR	Primetech

3.1.6 Kits

Table 3-5 Kits

Name	Company
Immobilon Western HRP Substrate Peroxide Solution	Millipore, Merck
Leukocyte Alkaline Phosphatase Kit (86R-1KT)	Sigma

NEBNext® Ultra™ DNA Library Prep Kit for Illumina®	New England Biolabs
NEBNext® Multiplex Oligos for Illumina® (Index Primers Set 1 and 2)	New England Biolabs
MinElute PCR Purification Kit	Qiagen
Pierce BCA Protein assay kit	Thermo Scientific fisher
PureYield Plasmid Midiprep System	Promega
Qubit dsDNA HS Assay Kit	Invitrogen
SuperSignal West Femto Maximum Sensitivity Substrate	Thermo Scientific fisher
TruSeq RNA Sample Preparation Kit	Illumina

3.1.7 Plasmids

Table 3-6 Plasmids

Plasmid	Origin
pcDNA3	Invitrogen
pcDNA3 Mdm2 301-491	cloned from pcDNA3 Mdm2 wt by site directed mutagenesis (QuikChange, Stratagene)
pcDNA3 Mdm2 wt	Addgene (#16233)
pcDNA3 SUZ12 Flag	S. Wu (Cao & Zhang, 2004)
pCMV-dR.8.91	Plasmidfactory Bielefeld
pCMV EZH2 HA	K. Helin (Bracken et al, 2003)
pCMV Mdm2	B. Vogelstein (Oliner et al, 1992)
pCMV-myc3-HDM2	Addgene (#20935)
pCMV β-gal	M. Dobbelstein (Dobbelstein et al, 1999)
pMD2.G (VSV-G)	Addgene (#12259)
pTY-Control	Y. Zhang (He et al, 2008)
pTY-shRing1b	Y. Zhang (He et al, 2008)
M420 GFP	from AG Dietrich, GSH Frankfurt

3.1.8 Antibodies

Table 3-7 Primary antibodies used for immunoblot, ChIP and Co-IP

Antibody	species	Amount used	Catalog #	Source
Anti-Flag Affinity Gel	mouse	10 µl for 300 µl cell lysate	A2220	Sigma
EZH2	rabbit	ChIP 2 µg	C15410039	Diagenode
EZH2 (AC22)	mouse	WB 1:1000; Co-IP 3 µg	3147	Cell Signaling
GAL4(DBD) (RK5C1)	mouse	ChIP 2 µg	sc-510	Santa Cruz
H2AK119ub	rabbit	ChIP 2 µg	C15410002	Diagenode

H3	rabbit	ChIP 2 µg; WB 1:5000	ab1791	abcam
H3K27me3	rabbit	ChIP 2 µg; WB 1:5000	pAb-069-050	Diagenode
IgG	rabbit	ChIP 2 µg; Co-IP 3 µg	ab46540	Abcam
Mdm2	mouse	WB 1:500; ChIP 2 µg; Co-IP 3 µg	IF2, OP46	Millipore
RING1B (D22F2)	rabbit	WB 1:500; ChIP 2 µg	5694	Cell Signaling
SUZ12 (D39F6)	rabbit	WB 1:500; Co-IP 3 µg	3737	Cell Signaling
β-actin	rabbit	WB 1:10000	ab8227-50	Abcam
β-actin (AC15)	mouse	WB 1:10000	ab6276-100	Abcam
β-galactosidase	mouse	Co-IP 3 µg, WB 1:5000	Z378B	Promega

Table 3-8 Secondary antibodies used for immunoblot

Antibody	Company	Cat. No.	Dilution
HRP-coupled AffiniPure F(ab')2 fragment, anti mouse IgG (H+L)	Jackson Immunoresearch	711-036-152	1:10,000
HRP-coupled AffiniPure F(ab')2 fragment, anti rabbit IgG (H+L)	Jackson, Immunoresearch	715-036-150	1:10,000

3.1.9 Inhibitors

Table 3-9 Inhibitors

Name	Target/Function	Company
EPZ 6438	EZH2 inhibitor	Epizyme
MG132	Proteasome inhibitor	Calbiochem

3.1.10 Bacteria

Table 3-10 Bacteria strains used for plasmid amplification

Strain	Description	Source
DH10B™	chemically competent *E.coli*	self-made, originally from Thermo Scientific

Table 3-11 Bacteria growth medium

2YT medium	
Tryptone	1.60%
Yeast extract	1.00%
NaCl	0.50%

2YT agar	
YT agar	15%
2YT medium	100%

3.1.11 Cell culture

Table 3-12 Human and mouse cell lines

Name	Source
HCT116 $p53^{-/-}$	p53-deficient human colon carcinoma cell line (Bunz et al, 1998)
HEK 293T	human embryonic kidney cells, harbouring SV40 antigen
H1299	human non-small cell lung carcinoma cell line, homozygous partial deletion of P53 gene
$p53^{-/-}$ MEF $p53^{-/-}$ $Mdm2^{-/-}$ MEF	p53- and p53 Mdm2 deficient mouse embryonic fibroblasts; generated by Lozano lab, MD Anderson Cancer Center, Texas USA (Montes de Oca Luna et al, 1995)
$p53^{-/-}$ MEF $p53^{-/-}$ $Mdm2^{-/-}$ MEF $p53^{-/-}$ $Mdm2^{C462A/C462A}$ MEF	p53-deficient mouse embryonic fibroblasts with additional Mdm2 knock out or RING finger mutation knock in; generated by Zhang lab, UNC Medial School, North Carolina, USA (Clegg et al, 2012)
SJSA	human osteosarcoma cell line, overexpression of Mdm2 due to gene amplification

Table 3-13 Cell culture media

Reagent	Company
Antibiotic-Antimycotic (100X)	Gibco, Life Technologies
Dulbecco's Modified Eagle Medium (DMEM), powder	Gibco, Life Technologies
Fetal Calf Serum (FCS)	Gibco, Life Technologies
L-Glutamine	Gibco, Life Technologies
Minimal essential medium (MEM)	Gibco, Life Technologies
Opti-MEM® I Reduced Serum Media	Gibco, Life Technologies
PBS (tablets)	Gibco, Life Technologies
Penicillin/Streptomycin	Gibco, Life Technologies
Trypsin/EDTA	Gibco, Life Technologies
McCoy's medium	Gibco, Life Technologies
DMEM (dissolved in H_2O)	
DMEM, powder	10.0 g/L
$NaHCO_3$	3.7 g/L

HEPES	5.96 g/L
dissolved in H_2O	
DMEM with supplements	
DMEM	
FCS	10%
L-Glutamine	200 µM
Penicillin/Streptomycin	100 U/ml
McCoy's medium with supplements	
McCoy's medium	
FCS	10%
L-Glutamine	200 µM
Penicillin/Streptomycin	100 U/ml
MEM with supplements	
MEM	
FCS	10%
L-Glutamine	200 µM
Antibiotic-Antimycotic (100x)	1x

3.1.12 Oligonucleotides

Table 3-14 Human siRNAs from Ambion/Life Technologies

Target	Catalogue No./ID	Sequence
EZH2 (a)	4390828 (customer select)	sense: 5'-GACUCUGAAUGCAGAAGCUtt-3' antisense: 5'-AGCAACUGCAUUCAGAGUCtt-3'
EZH2 (b)	4390828 (customer select)	sense: 5'-CGGUGGGACUCAGAAGGCAtt-3' sense: 5'-UGCCUUCUGAGUCCCACCGtt-3'
MDM2 (a)	4390829 (customer select)	sense: 5‘-GCCAUUGCUUUUGAAGUUAtt-3’ antisense: 5’-UAACUUCAAAAGCAAUGGCtt-3'
MDM2 (b)	4390824, s8630 (silencer select)	sense: 5‘-AGUCUGUUGGUGCACAAAAtt-3’ antisense: 5‘-UUUUGUGCACCAACAGACUtt-3’
P53	4390824, s605 (silencer select)	sense: 5‘-GUAAUCUACAGGGACGGAAtt-3’ antisense: 5‘-UUCCGUCCCAGUAGAUUACca-3’
RING1B (a)	4392420, s12068 (silencer select)	sense: 5‘-CAAACGGACCAAAACAUCUtt-3’ antisense: 5‘-AGAUGUUUUGGUCCGUUUGtt-3’
RING1B (b)	4392420, s12069 (silencer select)	sense: 5‘-GGAGUGUUUACAUCGUUUUtt-3’ antisense: 5‘-AAAACGAUGUAAACACUCCtt-3’
siRNA negative control 1	4390843	Undisclosed

Table 3-15 Primer sequences for gene expression studies in human cells

hn36B4 forward	5'-GATTGGCTACCCAACTGTTG-3'
hn36B4 reverse	5'-CAGGGGCAGCAGCCACAAA-3'
hnALPL forward	5'-TGGGCCAAGGACGCTGGGAA-3'
hnALPL reverse	5'-AAGGCCTCAGGGGGCATCTCG-3'
hnBGLAP forward	5'-GCCCTCACACTCCTCGCCCT-3'
hnBGLAP reverse	5'-CGGGTAGGGGACTGGGGCTC-3'
hnBMP4 forward	5'-GAGTATCTAGCTTGTCTCCCCG-3'
hnBMP4 reverse	5'-ACAAACTTGCTGGAAAGGCTC-3'
hnCXCR4 forward	5'-CGCCTGTTGGCTGCCTTACT-3'
hnCXCR4 reverse	5'-ACAGAGGTGAGTGCGTGCTG-3'
hnDUSP4 forward	5'-ATGCTGGACGCCCTGGGCAT-3'
hnDUSP4 reverse	5'-CCCACGGCAGTCCTTCACGG-3'
hnEZH2 forward	5'-5'-AGCCGCCCACCTCGGAAATTT-3'
hnEZH2 reverse	5'-AGGAAGTGCGCCTGGGAGCT-3'
hnGDF6 forward	5'-ACTCCATCGCTGAGAAGCTG-3'
hnGDF6r reverse	5'-AGGAGTGTGCGAGAGATCG-3'
hnIGF2 forward	5'-CTCCTGGAGACGTACTGTGC-3'
hnIGF2 reverse	5'-ACGTTTGGCCTCCCTGAAC-3'
hnKLF2 forward	5'-TGCGGCAAGACCTACACCAAGAGT-3'
hnKLF2 reverse	5'-AGCCGCAGCCGTCCCAGTT-3'
hnMDM2 forward	5'-TCAGGATTCAGTTTCAGATCAG-3'
hnMDM2 reverse	5'-CATTTCCAATAGTCAGCTAAGG-3'
hnRNPK forward	5'-GACCGTTACGACGGCATGGTTGG-3'
hnRNPK reverse	5'-ATCCGGAGCCACCCTGTGGTT-3'
hnSNX31 forward	5'-ACAGTGAGGATAGTTGCTGGC-3'
hnSNX31 reverse	5'-AGTCTTTCTGCTGGCTTTGTTG-3'
hnTEX261 forward	5'-TGGACTCTATTACCTGGCAGAAC-3'
hnTEX261 reverse	5'-GCGCTCAAAGACGTAGAGG-3'
hnTIMP3 forward	5'-CTGTGCAACTTCGTGGAGAG-3'
hnTIMP3 reverse	5'-TCACAAAGCAAGGCAGGTAG-3'
hnWNT6 forward	5'-CAACTGCACAACAACGAGGC-3'
hnWNT6 reverse	5'-GCGAAATGGAGGCAGCTTCTG-3'

Table 3-16 Primer sequences for gene expression studies in murine cells

mmHhip forward	5'-GCCTCACGACCACATTCTTC-3'
mmHhip reverse	5'-CAGAAACACCCTGGCTGTTC-3'
mmHoxb13 forward	5'-ATTCTCTGCTTCCCGTGGAC-3'
mmHoxb13 reverse	5'-CATACTCCCGCTCCAACTCC-3'
mmHoxc10 forward	5'-TCGGATAACGAAGCTAAAGAGGA-3'
mmHoxc10 reverse	5'-TCCAATTCCAGCGTCTGGTG-3'
mmHoxc13 forward	5'-AGTCTCCCTTCCCAGACGTG-3'
mmHoxc13 reverse	5'-GATGAATTTGCTGGCTGCGT-3'
mmHprt forward	5'-CGTCGTGATTAGCGATGATGAAC-3'
mmHprt forward	5'-CATCTCGAGCAAGTCTTTCAGTC-3'
mmNotch1 forward	5'- GTCAATGCCTCGCTTCTGTG-3'
mm Notch1 reverse	5'- ACAGAAGGTTACACAGGGACC-3'
mmJag1 forward	5'- CCTGTCATCGGGGGTAACAC-3'
mm Jag1 reverse	5'- CGAAGTGGGCAATCCCTGTG-3'
mmTxnip forward	5'- GAGTTCCAGTTCATGCCCCC-3'
mmTxnip reverse	5'- TTGCCACCCATCTTGAGGAG-3'

Table 3-17 Primer sequences for targeted ChIP qRT-PCR in human cells

CXCR4 for	5'-CAAATAAGCCCGGAGAGATG-3'
CXCR4 rev	5'-TTCTGATTCGTGCCAAAGC-3'
DUSP4 for	5'- GAGCCTCTTCTTCCCTGTCC-3'
DUSP4 rev	5'- GCGGTCCTCTCTCGTAAACAC-3'
FGF1 for	5'-TTCTTTCCTAGTGCCCATCG-3'
FGF1 rev	5'-TGTGTCAGCTCAGGGTTTTG-3'
GAPDH for	5'-TACTAG CGGTTTTACGGGCG-3'
GAPDH rev	5'-TCGAACAGGAGGAGCAGAGAGCGA-3'
KLF2 for	5'-TCAGGAGAGGAGGATGCGG-3'
KLF2 rev	5'-CTGCTTGCCTTTTACCACCC-3'
MYO for	5'- CTCATGATGCCCCTTCTTCT-3'
MYO rev	5'- GAAGGCGTCTGAGGACTTAAA -3'
TEX261 for	5'-AAAGGAAGTTGCCCTGGGTC-3'
TEX261 rev	5'-GGGAATTAGGCCGGAGGATG-3'
TGFBI for	5'-GCTCTCTGGGTACAGCAAGG-3'
TGFBI rev	5'-CCCCATTTGAACAGTGTGTG-3'
TLR3 for	5'-CGAGAGTGCCGTCTATTTGC-3'
TLR3 rev	5'-GAGAGACCCTGCCCAGTAAG-3'
UAS_for	5'-ACGCCAAAAACATAAAGAAAGGC-3'
UAS_rev	5'-CCAGCGGTTCCATCCTCTAGAG-3'

Table 3-18 Primer sequences for targeted ChIP qRT-PCR in murine cells

Eomes forward	5`-AAATTCCACCGGCACCAAAC-3`
Eomes reverse	5`-TAAACACCCTAAGCAGAGCCC-3`
Evx1 forward	5`-TGGCAGCAGC CTTAAACCTT-3`
Evx1 reverse	5`-AGCTGCAGTA GACCGTTGAC-3`
Gapdh forward	5`-TCCTGGCTTCTGTCTTTGGC-3`
Gapdh reverse	5`-GCATCCTGACCTATGGCGTA-3`
Hhip forward	5`-TAATCCGGGAAGGCTTATGGG-3`
Hhip reverse	5`-TCAAGGCAGAGATTGGGTACAG-3`
Hoxb13 forward	5`-GGGTCGGAATCTAGTCTCCC-3`
Hoxb13 reverse	5`-CACTGCTTTGGTGGCTCTG-3`
Hoxc10 forward	5`-TTCAACTGCGGGGTGATGAG-3`
Hoxc10 reverse	5`-AGAGGTAGGACGGGTAGGTG-3`
Hoxc11 forward	5`-GTGCTCGGGGAGAGAGACTA-3`
Hoxc11 reverse	5`-CGTTCTCTTCTCCTGCCTCC-3`
Hoxc13 forward	5`-CGAGCTATGCTGAGGAATGC-3`
Hoxc13 reverse	5`-GATTGCTTCACTCTGGACCC-3`
Tuba1a forward	5`-AGGTAATCTCTCCCCCACCC-3`
Tuba1a reverse	5`-CTTTCCACCCCTCCCCAAC-3`

3.1.13 Software and databases

Table 3-19 Software

Name	Company
AxioVision 3.0	Zeiss
CFX Manager Software for qPCR cycler	Bio-Rad
Excel	Microsoft, Redmond, WA, United States
Graph Pad Prism	GraphPad Software, Inc., CA, USA
INTAS lab ID	Intas Science Imaging Instruments
NanoDrop Software	Peqlab
R studio	R studio, Boston, USA
UV imager software	Intas Science Imaging Instruments
IGV 2.3	Broad Institute of MIT and Harvard, Boston, USA (Robinson et al, 2011; Thorvaldsdottir et al, 2013)
Galaxy Galaxy/Cistrome Galaxy/deepTools	www.usegalaxy.org; www.cistrome.org/ap/root; open source, web-based platform for data intensive biomedical research; used for ChIP-Seq analysis (Blankenberg et al, 2010; Giardine et al, 2005; Goecks et al, 2010; Liu et al, 2011; Ramírez et al, 2014)

Table 3-20 Databases

Name	Details
Ensembl Genome Browser	www.ensembl.org software system for automatic annotation on selected eukaryotic genomes; used for gene expression primer design
UCSC genome browser	www.genome.ucsc.edu information on ENCODE analysis, finding functional elements on the human and mouse genome; used for ChIP-Seq track analysis and ChIP targeted PCR primer design
NCBI Pubmed	www.ncbi.nlm.nih.gov/pubmed; literature search
NIH Roadmap Epigenomics	www.ncbi.nlm.nih.gov/epigenomics; genome viewer for genome-wide maps of DNA and histone modifications from diverse epigenomic data sets; used for protein-chromatin binding prediction and targeted ChIP PCR primer design
Primer3web	www.primer3.ut.ee; used for primer design

3.2 Methods

3.2.1 Cell Biology

3.2.1.1 *Transformation of chemically competent* E.coli

For heat shock transformation of chemically competent *E.coli*, 1 µl of DNA was incubated with 50 µl of competent cells for 30 min on ice, 10 min at 37 °C and another 10 min on ice. Afterwards, 200 µl of LB was added and cells were mildly shaken at 37 °C for 30-60 min. The cells were then plated onto an 2YT Agarplate with the appropriate antibiotic (Ampicillin 100 µg/mL, Kanamycin 50 µg/ml) and incubated overnight at 37 °C. After overnight incubation a single colony was picked using an autoclaved 10 µl pipet tip which was then given into 5 ml of 2YT medium containing antibiotic. The 5 ml culture was kept at 37 °C shaking for 8-12h and was then transferred into 45 ml of 2YT medium overnight (37°C, shaking).

3.2.1.2 *Culture of adherent cells*

Cell culture work was conducted under sterile conditions and human as well as mouse cells were grown in cell culture dishes in a humidified atmosphere at 37 °C and 5 % CO_2. The different cell lines used were cultured in specific media (Table 3-13 and Table 3-21) and were sub-cultured 2-3 times a week dependent on confluence. For this purpose, growth medium was removed the cells were washed with pre-warmed PBS and detached using a 3-5 min incubation with 0.1 % trypsin/EDTA. An appropriate portion of the detached cells were transferred to a new culture plate and taken up in new growth medium to stop the trypsinization process and for continuous culture.

Table 3-21 Specific culture medium for cell culture

Cell line	Growth medium
HCT116 $p53^{-/-}$	McCoy's with supplement
hMSCs	MEM with supplements
H1299	DMEM with supplements
MEF	DMEM with supplements
SJSA	DMEM with supplements
PANC1	DMEM with supplements

For experimental purposes the cells were seeded in appropriate amounts into specific culture dishes. For counting, the cells were taken up into fresh medium after trypsinization and were counted using a Neubauer counting chamber.

3.2.1.3 *Freezing and thawing of cells*

For long term storage, cells were expanded in 15cm culture dishes and harvested using trypsin/EDTA as described above. After detaching, the cells were transferred into a falcon tube of appropriate size and counted. After determination of the cell number the cell suspension was centrifuged at RT and 1000 g for 5 min and settled cells were taken up in pre-cooled FCS supplemented with 10 % DMSO to a final concentration of $1x10^6$ cells/ml. Cryo vials were filled with 1 ml of the cell suspension and frozen for 24 h at -80 °C before moving them into -196 °C liquid nitrogen.

For thawing, the cryo vials were taken out of the liquid nitrogen and the cells were transferred as quickly as possible into pre-warmed growth medium into 15cm dishes and grown as described. As soon as the cells had settled, the medium was exchanged in order to get rid of residual DMSO.

3.2.1.4 *Transient siRNA knock down in human cells*

Transient knock down of gene expression was done with a reverse siRNA transfection procedure using final concentrations of 10 or 15 nM siRNA (Table 3-14). Therefore, the transfection reagents were prepared according to the following scheme:

Table 3-22 siRNA transfection set up

Cell line	Culture plate	Cell number	Solution A	Solution B	final volume
HCT116 p53$^{-/-}$	6 well	400,000	250 µl DMEM(-), 100 nM siRNA	250 µl DMEM(-), 5 µl Lipofectamine 2000	2.5 mL
hMSCs	12 well	100,000	250 µl Opti_MEM(-), 2.5 µl Lipofectamine RNAiMax, 60 nM siRNA		1 mL
MCF7	6 well	400,000	250 µl DMEM(-), 100 nM siRNA	250 µl DMEM(-), 5 µl Lipofectamine 2000	2.5 mL
PANC1	6 well	180,000	250 µl DMEM(-), 100 nM siRNA	250 µl DMEM(-), 5 µl Lipofectamine 2000	2.5 mL
SJSA	6 well	125,000	250 µl DMEM(-), 100 nM siRNA	250 µl DMEM(-), 5 µl Lipofectamine 2000	2.5 mL

Solution A and B were vortexed and incubated for 5 min at RT before they were mixed and incubated at RT for another 20 min. For hMSC transfection only one solution was made

containing all transfection reagents at once. In the 20 min incubation time, target cells were detached from their culture plate via trypsinization and counted as described before (cf. paragraph 3.2.1.2). The transfection mixture was transferred into the culture plate and cells were added in the appropriate volume in growth medium without antibiotics. For proper distribution the culture plate was shaken gently. 24 h after transfection the transfection medium was removed and cells were grown further in normal growth medium with supplements.

For better knock down efficiency, the cells were treated with a double transfection protocol. 48 h after the first transfection, cancer cells were reverse transfected again following the protocol as before. hMS cells were treated with a forward transfection 72 h after the first knock down (kd), giving the transfection reagent directly onto the attached cells.
After 96h of knock down in total the cancer cells were harvested for RNA and protein isolation.

3.2.1.5 *Transient vector transfection of human cells*

For expression vector transfection a forward transfection procedure of the plasmid DNA (cf. Table 3-6) in H1299 cells was followed. 280,000 cells were seeded 24 h before transfection into the wells of a 6-well plate. The transfection solutions A and B (specific volumes described in Table 3-23) were handled as described in 3.2.1.4. 6 h after transfection the transfection medium was removed and the cells were grown in normal growth medium with supplements. 24 h after transfection the cells were harvested.

Table 3-23 Plasmid transfection set up

Cell line	culture dish	cell number	solution A	solution B	final volume
H1299	6 well plate		200 µl DMEM(-), 2.4 µg DNA	200 µl DMEM(-), 8 µl Lipofectamine	2.4 mL

3.2.1.6 *Differentiation of human mesenchymal stem cells into osteoblasts*

To analyze the effect of gene expression kd on stem cell differentiation, human mesenchymal stem cells (hMSCs) were transfected with siRNA as described in 3.2.1.4. Differentiation of MSCs was started 24 h after the first transfection via culturing the cells in osteoblast differentiation medium (cf. Table 3-24), which was described by Karpiuk and colleagues (Karpiuk et al, 2012). Differentiation media was exchanged every 24 h for 5-7 days and cells were then harvested for RNA and protein isolation as well as alkaline phosphatase staining.

Alkaline phosphatase staining was done using the Leukocyte Alkaline Phosphatase Kit by Sigma (cf. Table 3-5).

Table 3-24 Osteoblast differentiation medium by Karpiuk and colleagues

Osteoblast Differentiation Media	
MEM with supplements (Table 3-13)	
β-Glycerophosphate disodium salt hydrate	10 mM
Ascorbate	0.2 mM
Vitamin D	10 nM

3.2.1.7 *Induction of pluripotent stem cells from murine embryonic fibroblasts*

This procedure was carried out by Alice Nemajerova from the Department of Pathology of the Stony Brook School of Medicine according to a method described previously (Nemajerova et al, 2012). Briefly, human Klf4, Oct4 and Sox2 in the retroviral vector Rebna were transfected into packaging Phoenix E cells using Lipofectamine. 24 hours later, transfected Phoenix E cells were selected with 2 ug/ml puromycin for 2-3 days. Viral supernatants were collected and filtered through a 0.45-μm cellulose acetate filter. MEFs were plated at a density of 2×10^5 cells per 6-cm plate and incubated with the viral supernatant overnight. After four successive infections, cells were switched to knockout serum replacement (KSR) medium consisting of DMEM/F12 containing 10% KSR (Invitrogen), 1 × nonessential amino acids, 1 × Glutamine, 1 × Pen/Strep, 0.1 μM β-mercaptoethanol and 1000 U/ml leukemia inhibitory factor (Millipore). The transduction efficiency of MEFs was determined by extrapolation from parallel infections with GFP-expressing control viruses. Efficiency of iPSC production was determined based on their undifferentiated morphology. Also, all hand-picked iPSC colonies (11-21 dpi) were transferable and could be further propagated on feeder cells (irradiated mouse embryo fibroblasts, GlobalStem).

3.2.1.8 *Clonogenic assay of MCF7 cells*

MCF7 cells were transfected with siRNAs as described above (3.2.1.4). 48 hrs post-transfection, cells were trypsinized, counted and seeded in 6-well plates (40,000 cells/well). After 7 days of growth, cells were washed with PBS and fixed with methanol at 4°C for 30 min. Cells were then stained with crystal violet solution (10% formaldehyde, 1 mg/ml crystal violet) overnight.

3.2.1.9 *Generation of stable Ring1b kd MEFs using shRNA*

To generate stable knock down cells, lentiviral constructs expressing pTY-Puro-shRing1b were generated in HEK293T cells (pTY constructs were kindly provided by Prof. Yi Zhang (He et al, 2008)). Briefly, HEK cells were seeded in 10 cm cell culture dishes and transfected with 2.5 µg shRNA construct, 1.6 µg pCMV-dR.8.91 and 1 µg pMD2.G (VSV-G) packaging plasmid (Naldini et al, 1996; Stewart et al, 2003) using calcium phosphate transfection (Graham & Van der Eb, 1973). For control purposes lentiviruses expressing GFP were generated in addition. Plasmids and buffers were set up in the following ratios per 10 cm dish:

2x HBS buffer (see also 3.1.4)	500 µl
Sterile H_2O	440 µl – plasmid volume
2 M $CaCl_2$	60 µl (added last, followed by vigorous shaking)

24 h after transfection the medium was changed. MEF cells were seeded accordingly (one well of a 6-well plate was transduced with virus produced from a 10 cm dish Plat-E cells) and transduced twice with generated virus (48 and 72h after transfection). For transduction, virus supernatant was filtered through a 0.45 µm sterile filter and supplemented with final concentrations of 8 µg/ml polybrene.

72h after the first transduction, MEF cells were splitted as appropriate and stable kd cells were selected using final concentrations of 1.5 µg/ml puromycin in growth medium. After selection, puromycin was removed and cells were used for qRT-PCR and cell growth analysis.

3.2.1.10 *Proliferation assay (Celigo)*

Cells were transfected with siRNA as described above (3.2.1.4), and cell proliferation was measured using automated light microscopy with quantitative image analysis (Celigo, Nexcelom, software version 2.0). 24 h after the second transfection, cells were harvested via trypsinization and counted. From each transfection sample, three replicates of 20.000 cells (HCT116 cells; 10,000 cells taken for experiments with SJSA and PANC1 cells) were seeded into 12-well plates, and cell confluence was measured every 24 h for 4-6 days.

3.2.1.11 *Protein harvest of cultured human and mouse cells*

For protein isolation, cells were handled on ice to avoid proteolytic degradation. For all cancer cells as well as the hMSCs one well of a 6-well plate was sufficient for the protein amounts desired. MEF cells were harvested from one 10cm dish.

6-well plates were kept on ice and the cells were scraped from the plate directly in the growth medium using a cell scraper. Cell containing medium was then transferred into a 2 mL Eppendorf tube which was centrifuged at 3000 g and 4 °C for 5 min. The supernatant was removed without disturbing the cell pellet and cells were washed with ice-cold PBS. After removal of PBS, the cells were taken up in Cell Lysis Buffer (cf. paragraph 3.1.4) and boiled at 95 °C for 5min before sonication for 10 min at high power using 30 s on/off cycles. 150-200 µl of cell lysis buffer was used depending on cell confluence.

MEF cell proteins were harvested directly in the 10 cm culture dish. For this the growth medium was removed and cells were washed in the dish with ice-cool PBS. After removal of PBS the cells were scraped from the plate directly in cell lysis buffer. The lysate was transferred into an Eppendorf tube and treated by sonication as described before. 250 µl of cell lysis buffer was used per dish.

In order to determine the protein concentration, a Bicinchoninic Acid (BCA) test was performed (cf. Table 3-5) as indicated by the manufacturer's instructions. Protein samples with adjusted concentration were then incubated with 6x Laemmli buffer (cf. paragraph 3.1.4) for 5 min at 95 °C in the ratio 2:3.

3.2.2 Molecular Biology

3.2.2.1 *Isolation of plasmid DNA*

Plasmid DNA was isolated from a 50 ml culture of transformed E.coli using the PureYield Plasmid Midiprep System according to the manufacturer's instructions (Table 3-5). Elution was done using 500 µl of nuclease free H_2O and plasmid concentration was determined using the NanoDrop ND-1000.

3.2.2.2 *Gene Expression Analysis*

To evaluate mRNA expression in target cells, RNA was isolated from cells, reverse transcribed into cDNA and analyzed via quantitative real-time PCR (qRT-PCR) or whole transcript

hybridisation or -sequencing. For all cells that were handled, one well of a 6-well plate was enough to harvest sufficient amounts of RNA.

3.2.2.2.1 RNA isolation

Cells were washed with PBS directly in the plate and lysed for 5 min in 1 mL TRIzol® RNA Isolation Reagent and isolation procedure was continued according to the manufacturer's instructions. The lysate was transferred into an Eppendorf tube and mixed 1:5 with chloroform via shaking for 15 s and incubation at RT for 3 min. Afterwards the mixture was centrifuged at 12.000 g for 20 min at 4 °C and the colorless upper phase was mixed in a new tube with 500 µl isopropanol and incubated for 10 min at RT. The tube was centrifuged at 12.000 g and 4 °C for at least 30 min, the supernatant was discarded and the resulting RNA pellet was washed twice with 500 µl of 75 % EtOH. The supernatant was discarded and the pellet was dried at 37°C for 15 min and resuspended in 10-30 µl (depending on pellet size) RNase-free water via incubation at 55 °C for 3 min.

For purification purposes, isolated RNA was mixed via vortexing with 1-2 µl GlycoBlue, 1:10 v/v 3 M NaAc (pH 5.2) and 2.5 time volume µl of EtOH abs. and centrifuged for another 15 min at 12.000g. The resulting (blue) pellet was washed with 70 % EtOH, dried and resuspended in 10-30 µl RNase-free water. RNA concentration and purity was measured with the spectrophotometer NanoDrop ND-1000, using absorbance values at 230, 260 and 280 nm. Absorbance at 260 nm was used for concentration analysis whereas contamination with protein and/or aromatic solvents was determined with the 230 and 280 nm absorbance ratios. The following ratios were used as purity standards:

A260/A280 > 1.8

A260/A230 > 2.0

3.2.2.2.2 cDNA synthesis

Reverse transcription of the harvested RNA into a complementary DNA (cDNA) library was done using a reverse transcriptase (RT) derived from moloney murine leukemia virus (M-MuLV, see also Table 3-4) (Spiegelman et al, 1971). After determination of RNA concentration, 1 µg of total RNA was mixed with 2 µl of combined primers (50 µM Oligo $dT_{23}VN$ Primer and 15 µM random nonamer primer), 4 µl of 2.5 mM dNTP mixture and RNase-free water to a final volume of 16 µl and was incubated at 70 °C for 5 min. After this, the reagents were spun down and put on ice. To each reaction 4 µl of the following master mix was given for a final volume of 20 µl. For control purposes all samples were prepare with and without the addition of reverse

transcriptase (-RT control) to avoid signal contamination with DNA that could have been co-purified together with the isolated RNA.

Table 3-25 cDNA synthesis master mix

Component (for 1 reaction)	Volume [µl]
10x Reaction Buffer for M-MuLV Reverse Transcriptase	2
RNase Inhibitor (10 U)	0.25
M-MuLV Reverse Transcriptase (25 U)	0.125
H2O	1.625

The reverse transcription reaction was carried out for 1 h at 42 °C with subsequent enzyme inactivation at 95 °C for 5 min and storage at 4 °C. Before usage, the resulting cDNA was diluted 1:50 and 5 µl of cDNA was used for qRT-PCR analysis

3.2.2.2.3 Quantitative real time polymerase chain reaction (qRT-PCR)

qRT-PCR was conducted via real time analysis of PCR amplification with SYBR green fluorescent dye incorporation for quantitative analysis (PCR originally described by Mullis and colleagues (Saiki et al, 1985) and further developed for quantification by Higuchi et al. (Higuchi et al, 1993). The reaction set up was pipetted as follows for a total reaction volume of 25 µl. For enzyme and buffer information see also Table 3-4 and 3.1.4. Each PCR reaction was conducted in triplets via the following program shown in Table 3-27.

Table 3-26 qRT-PCR reaction set up

Component	Stock	[µl] for 1 reaction
qPCR reaction mix		14
forward primer	100 pmol/µl	0.1
reverse primer	100 pmol/µl	0.1
H_2O		5.8
cDNA		5

Table 3-27 qRT-PCR protocol for gene expression studies

Step	Temperature	Time
1	95	2 min
2	95	15 s
3	60	30 s
4	fluorescence read	
back to step 2, 39 times more		
5	melting curve, 55-95 °C	

Analysis was done using the ΔΔCt method according to Livak and colleagues (Livak & Schmittgen, 2001). Gene expression was normalized to the housekeeping gene 36B4, an acidic ribosomal phosphoprotein P0 (RPLP0) for all cancer cell lines and HPRT1 for all MEF cells. MSC gene expression was normalized to the heterogeneous nuclear ribonucleoprotein K (hnRNPK). Primer sequences that were used for qRT-PCR analysis are listed in Table 3-15 and Table 3-16.

3.2.2.2.4 Global gene expression analysis using microarray

Microarray analysis was performed to generate global expression data from HCT116 and hMS cells that had undergone Mdm2 knock down. For each approach, RNA of a minimum of two replicates per sample was isolated (3.2.2.2.1) and given to the transcriptome analysis laboratory (TAL) Göttingen. Via Bioanalyzer measurements RNA quality and concentration was determined and 200 ng of total RNA were reverse transcribed into cDNA. Cy3-CTP labelled antisense RNA was subsequently generated from the cDNA using dNTPs (including Cy3-CTP) and T7 RNA polymerase and was hybridized to a microarray slide in the presence of complementary oligonucleotides. For the visualization of complementary bound probes the microarray slides were excited with a laser beam of defined wavelength and fluorescent emission of the Cy3 signal intensity was measured. In the case of intensive gene transcription strong fluorescence emission was expected, and vice versa. According to this principle control- and target kd samples were compared and analyzed which was done by Claudia Pommerenke (former bioinformatician at TAL). Biological replicates were combined and the threshold of differentially regulated mRNA expression was set to 1 given as log2 induction values.

3.2.2.2.5 Global gene expression analysis using RNA-Sequencing

For RNA-sequencing the quality of total RNA was determined with the Bioanalyzer 2100 from Agilent. All samples analyzed exhibited a RIN>8. Library preparation was conducted by using the TruSeq RNA LT SamplePrep Kit (Illumina) starting from 1000 ng of total RNA. Barcodes for sample preparation were used according to the indications given by the protocol. Accurate library quantitation of cDNA libraries was performed with the QuantiFluor™dsDNA System (Promega). The size range of final cDNA libraries was determined applying the DNA 1000 chip on the Bioanalyzer 2100 from Agilent (290-310 bp). cDNA libraries were amplified and sequenced via cBot and HiSeq 2000 from Illumina (SR, 1×50 bp, 6 Gb/sample ca. 30 million reads per sample). Sequence images were transformed with Illumina software BaseCaller to bcl

files, which were demultiplexed to fastq files with CASAVA (version 1.8.2). Quality check was done via FastQC (version 0.10.1, Babraham Bioinformatics). Fastq files were mapped to the mm9 reference transcriptome (UCSC) using Bowtie 2 (version 2.1.0) (Langmead & Salzberg, 2012). Read counts for each sample and each gene were aggregated using a custom Ruby script. DESeq (version 1.14.0) was used for measuring differential expression (Anders & Huber, 2010) and heatmaps were calculated via the heatmap.2 function of the R package gplots. RNA library preparation and sequencing was done by the Transcriptome and Genome Analysis Laboratory (TAL, University Medical Centre, Göttingen) as also published before (Pirouz et al. 2015).

3.2.2.3 *Preparation of a ChIP-sequencing (ChIP-Seq) library*

ChIP-Seq libraries were prepared according to the instructions given in *NEBNext Ultra™ DNA Library Prep Kit for Illumina*. Before preparation, the concentration of precipitated DNA was measured using the Qubit Fluorometer and the Qubit dsDNA HS Assay Kit. 10 ng of input DNA and 2.5 ng of histone ChIP DNA were taken up in a total volume of 55.5 µl in nuclease free water, using DNA LoBind tubes, and were sonicated in the Biorupter Pico (20 cycles, 30 s on, 30 s off). This additional sonication step ensured fragment DNA fragment size around 300 bp. Fragment end preparation and adapter ligation was done as described in the manual. For adaptor ligation the adaptors were diluted 1:15 for input ChIP DNA and 1:20 for histone ChIP DNA. Afterwards a cleanup of adaptor-ligated DNA without size selection was performed using 77.85 µl (0.9x) Agencourt AMPure XP magnetic beads per sample and the DynaMag™-2 magnetic rack for magnetic separation. PCR amplification and subsequent cleanup of PCR amplification was done according to the manufacturer's advice. Different index primers were taken for each sample and the PCR cycling protocol was conducted using 13 cycles for 10 ng and 17 cycles for 2.5 ng of starting ChIP DNA material. The concentration of the prepared library samples were measured using the Qubit Flourometer and were analyzed for size distribution on an Agilent high sensitivity chip (done by TAL, University Medical Center, Göttingen). Library preparations were expected to have an average fragment size of 280-320 bp and no contamination with adaptor dimers as shown in Figure 3-1. In the case of adaptor dimer presence the last AMPure XP bead cleanup was repeated and the samples were analyzed again. Library sequencing was done as described in 3.2.2.4.

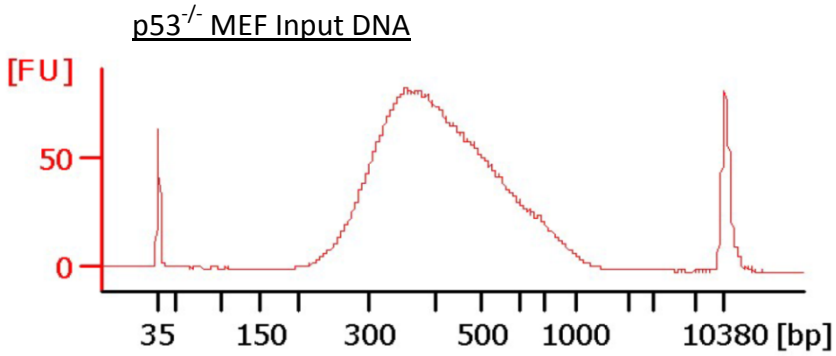

Figure 3-1 ChIP-Seq library size distribution analysis on an Agilent high sensitivity chip

A ChIP-Seq library was prepared from $p53^{-/-}$ MEFs input ChIP DNA and was analyzed for size distribution and adaptor dimer contamination on an Agilent high sensitivity chip.

3.2.2.4 *Sequencing of ChIP-Seq libraries and subsequent analysis*

Sequencing of prepared ChIP DNA libraries was performed by the TAL using the Illumina HiSeq 2500. Libraries were amplified and sequenced by using cBot and HiSeq 2000 from Illumina (SR, 1×50 bp, ca. 25 million reads per sample). Sequence images were transformed with Illumina software BaseCaller to bcl files, which were demultiplexed to fastq files with CASAVA (version 1.8.2). Quality check was done via FastQC (version 0.10.1, Babraham Bioinformatics). Resulting reads were mapped to the mouse genome (UCSC mm9) using Bowtie 2 (Galaxy Tool Version 0.4) (Langmead et al, 2009) and peak calling was performed using MACS (Galaxy Tool Version 1.0.1) (Zhang et al, 2008). Coverage was determined by normalizing the total number of mapped reads per hundred million and the data was visualized using the Integrative Genome Viewer (Thorvaldsdottir et al, 2013). Differential methylation and ubiquitination patterns were determined using DiffBind analysis in R (Stark & Brown, 2011). Gene body coordinates and TSSs were obtained from UCSC Table Browser (Karolchik et al, 2004). Aggregation plots around defined regions were calculated using the “computeMatrix” and “heatmapper” function in Galaxy/deeptools (Ramírez et al, 2014). Galaxy/deeptools functions were also used for the generation of fused RNA-Seq and ChIP-Seq data.

3.2.3 Protein biochemistry

3.2.3.1 *SDS-PAGE*

In 1967, Shapiro and colleagues developed a method called SDS-PAGE (Sodium dodecyl sulfate polyacrylamide gel electrophoresis) which they used for protein separation depending on electrophoretic mobility and molecular weight (Shapiro et al, 1967). Therefore, they denatured

their protein samples in a buffer devised by Laemmli and colleagues (Laemmli, 1970), which was characterized by the anionic detergent sodium dodecyl sulfate (SDS). Thereby they ensured a constant negative charge of the protein and a tendency to move to the anode in an electric field. The proteins are run in a two-phase gel which consists of an upper stacking gel and a lower separation gel and are separated according to the principle that lower weight proteins migrate faster through the gel than those with larger weight.

Within the stacking gel, which is characterized by an acrylamide/bisacrylamide (A/BA) concentration of 5 %, a pH of 6.8 and relatively large gel pores, the denatured proteins are stacked between the leading chloride ions and the trailing Glycine ions. Protein separation is then conducted in the lower gel part with A/BA concentration of 12 % and a pH of 8.8. Depending on the separation grade higher or lower percentage separation gels can be used.

Gels for protein separation were casted as described in Table 3-28 between two glass plates. First the stacking gel was applied and overlaid with 2-Propanol to avoid air bubble formation at the top. After polymerization, 2-Propanol was removed and stacking gel was applied. For protein application into the gel, 10- or 15-slot combs were inserted into the not yet polymerized stacking gel.

Table 3-28 Stacking and separating gel composition for SDS-PAGE

Compound	Stacking gel	Running gel
Acrylamide-bisacrylamide	5%	12%
Tris-HCl, pH 6.8 (0.5 M)	125 mM	-
Tris-HCl, pH 8.8 (1.5 M)	-	380 mM
SDS (10%)	0.1%	0.1%
APS (10%)	0.1%	0.06%
TEMED	0.2%	0.06%

Cell lysates were prepared as described in 3.2.1.7. Before gel application the proteins were boiled for another 5 min at 95 °C. Gel combs were removed and the gels were placed into the electrophoresis system containing 1 x SDS running buffer. 20-45 µl of protein samples were applied into each slot together with at least one lane containing 5 µl of protein marker and gels were run at constant current of 20 mA per gel.

3.2.3.2 *Immunoblotting*

Proteins that are separated by SDS-PAGE can be specifically analyzed using immunoblotting (also known as Western Blotting, WB), which enables visualization of protein levels as well as

post-translational modification and interaction. The blotting procedure hereby follows the original protocol developed by Renart et al. as well as Towbin and colleagues (Renart et al, 1979; Towbin et al, 1979). The separated proteins were transferred onto a 0.2 µm pore size nitrocellulose membrane via the wet-blot application (Bittner et al, 1980) using WB transfer buffer for 1.5 h at 100 V. To estimate transfer efficiency, the membrane was stained with Ponceau S and then washed with TBST. For blocking purposes, the membrane was subsequently incubated for at least 45 min in WB blocking solution and was then labelled with the appropriate primary antibody (see also Table 3-7) diluted in blocking solution at 4 °C overnight. After primary antibody binding the nitrocellulose was washed 3x 10 min in blocking solution before incubation with donkey anti-mouse or anti-rabbit secondary antibody (see Table 3-8). Used secondary antibodies were coupled to horseradish peroxidase (HRP) and applied 1:10000 diluted in blocking solution for 1 h at RT. Before antibody binding detection, the membrane was washed again three times for 10 min in blocking solution.

Antibody binding was detected using either Super Signal West Femto Maximum Sensitivity Substrate for expected weak signals, or Immobilon Western Chemiluminescent HRP Substrate for expected strong signals. HRP coupled to the secondary antibody oxidizes the luminol contained in the substrate solution, emitting light that can be detected on a light sensitive film or by a chemiluminescent sensitive camera.

3.2.3.3 *Complex Immunoprecipitation (Co-IP)*

Co-IP was performed to detect interaction between Mdm2 and PRC2 complex members. In this project Co-IP was done either with endogenous protein levels or after exogenous overexpression. For exogenous Co-IP, cells were transfected and harvested from a 6-well plate (cf. paragraph 3.2.1.5). Endogenous Co-IP was performed in SJSA cells and cells from one 15 cm dish were harvested for one antibody precipitation. Before harvesting, cells were treated with the protease inhibitor MG-132 for 6-8 h (20 µM final concentration, only for endogenous Co-IP). Reagents volumes used in the protocol are depicted in Table 3-29. Co-IP samples were always handled on ice or at 4 °C.

Table 3-29 Co-IP set up

Cells	Protein	Format	Co-IP Buffer	Lysate per antibody	Beads per precipitation
SJSA	Endogenous	15 cm dish	1 mL	1 mL	50 µl + 50 µl
H1299	Exogenous	6-well plate	0.5 mL	0.5 mL	50 µl + 50 µl

Before cells were harvested for Co-IP, protein G sepharose (PGS) was equilibrated. Therefore, the 50/50 slurry beads per sample were washed 3 times with Co-IP buffer (cf. paragraph 3.1.4) with intermediate centrifugation at 3000 rpm for 2 min. Afterwards the beads were taken up in equal volumes of fresh Co-IP buffer.

Growth medium was removed from the cells and the cells were washed with pre-cooled PBS. Co-IP buffer was added to the washed cells and cells were scraped from the plate and transferred into a tube. The cell lysate was homogenized via pushing it through a 26G syringe (5x) and sonicated using a Bioruptor® at medium power for 10min (30 s on, 30 s off) for DNA disruption. For the removal of cellular debris the lysate was then centrifuged at maximum speed for 10 min and the supernatant was transferred into a new tube. For control purposes a supernatant sample and the cell pellet were taken up in 6x Laemmli to test protein solubility.

In order to get rid of unspecific bead reactions, the protein lysates were pre-cleared with 50 µl of prepared PGS beads via incubation for one hour on a rotator. The beads were centrifuged down and pre-cleared cell lysates were transferred into a new tube. 20-50 µl of each lysate were boiled with equal amounts of 6 x Laemmli buffer and taken as input control.

For immune-reaction, each cell lysate was now substituted with 2 µg of antibody binding the protein of interest on a rotating device overnight. For background control, one sample of each lysate was also incubated with a non-specific IgG antibody. For immunoprecipitation, PGS beads were prepared as described before and 50 µl were added to each sample tube and incubated further on a rotating device for 2 h.

After antibody-PGS coupling, all samples were washed 5 times with 800 µ of Co-IP buffer via inverting the tubes 5-10 times and subsequent centrifugation at 3000 rpm for 2 min. The last spin-down was performed at 6000 rpm and all supernatant was carefully discarded before taking up the beads in 50 µl of 6x Laemmli buffer with subsequent incubation at 95 °C for 5 min. The samples were stored at -20 °C or directly used for SDS-PAGE and immunoblot analysis.

3.2.3.4 *Chromatin harvest for chromatin immunoprecipitation (ChIP)*

Chromatin immunoprecipitation was used as a method to detect protein-DNA interaction in the cell and was done according to Denissov and colleagues (Denissov et al, 2007). For chromatin harvest, two 15 cm cell culture dishes with 80-90 % confluent MEF or SJSA cells were taken to get roughly 800 µl of chromatin (depending on confluence). The cells were washed with room

temperature PBS and protein and DNA were crosslinked directly in the dish with crosslinking buffer for 20 min at RT. The crosslinking procedure was quenched for 5 min using final concentration of 125 mM glycine. Afterwards the cells were washed twice with ice cold PBS and lysed in the plate with 2 mL of pre-cooled Buffer B for 10 min at 4 °C. After incubation, the cells were scraped from the plate into a 2 mL Eppendorf tube on ice and centrifuged at 4 °C for 5 min at 1600 rpm. After centrifugation the cells were washed in 2 mL ice-cold Buffer C, centrifuged at the same speed for 10 min and the nucleus was lysed in 800 µl of 1x Incubation buffer supplemented with 0.375 % SDS and 1 x protease inhibitors (Roche). The DNA was fragmented using the Bioruptor sonicator (Diagenode) for 25 cycles of 30 seconds on and 30 seconds off at highest power with intermediate ice-water changes. Afterwards remaining cellular debris were centrifuged down at maximum speed and the chromatin was either directly used for immunoprecipitation or was frozen at -80 °C.

For MDM2 ChIP, the cells were fixed in 1.1 % PFA for 30 min. Fixation was stopped as before and the cells were lysed in a lysis buffer containing 0.1 % SDS. Sonication was done using the Pico sonicator (Diagenode) in Biorupter microtubes for 10 cycles.

3.2.3.5 *Chromatin Immunoprecipitation*

For the immunoprecipitation procedure, the chromatin was incubated together with protein A/G coupled beads as well as the antibody targeting the protein of interest (cf. Table 3-7); samples were always kept at 4°C or on ice. 50 µl of the 1:5 bead solution were taken per precipitation, centrifuged at 4 °C and 4000 rpm for 2 min and washed twice with 100 µl per reaction of wash buffer (1x Incubation buffer supplemented with 0.2 % BSA). Afterwards the beads were taken up in wash buffer in half of the initial volume. 30 µl of the washed beads were pipetted into a 1.5 ml Eppendorf tube with 1x incubation buffer substituted with 0.1 % BSA and 1 x protease inhibitors (Roche) to a final volume of 178 µl. To this, 120 µl of chromatin and 2 µg of antibody (see Table 3-7) were added and precipitation was conducted over night on a rotator in the cold room. 12 µl of chromatin input was kept also at 4 °C.

After incubation, the beads were washed two times with 400 µl washbuffer 1, once with washbuffer 2 and 3 and twice with wash buffer 4 using intermediate centrifugation at 4 °C and 4000 rpm for 2 min. Afterwards the input samples were included and antibody-bead interaction was reversed by a 20 min RT incubation with 200 µl of incubation buffer on a rotating device. The beads were centrifuged down for 1 min at maximum speed and the supernatant was

transferred to a new Eppendorf tube. DNA and protein were de-crosslinked via incubation with final concentrations of 200 mM NaCl for 4-5 h at 65 °C shaking.

The DNA was then isolated following the instructions of the MinElute PCR Purification Kit (Qiagen). After purification the input DNA was diluted 1:10 and PCR was conducted with 5 µl of ChIP product. For this Maxima SYBR Green qPCR Master Mix (2X) and primers given in

Table 3-18 were taken. The PCR protocol was programmed as described in the master mix manual.

3.2.4 Statistical evaluation of scientific data

If not stated otherwise, statistical testing was performed using Graph Pad Prism 6. An unpaired t test was calculated and multiple comparisons were corrected using the Sidak Bonferroni method with an assumed significance for p-values ≤ 5%. Asterisks represent significance in the following way:

*** = $p \leq 0.001$

** = $p \leq 0.01$

* = $p \leq 0.05$

The term “n.s.” indicates results that are not significant.

4 Results

In order to avoid confusion there has not been any notation separation between mouse and human annotation before. However, in the following paragraphs it will be discriminated between cell systems derived from mouse (Mdm2, p53, Ezh2 etc.) and human (MDM2, P53, EZH2 etc.).

4.1 Accession Numbers

The NCBI Gene Expression Omnibus accession number for RNA-Seq-, microarray- and ChIP-Seq data reported in this thesis is GSE73602.

4.2 Mdm2 enables stemness and cell proliferation through PRC2 target gene regulation

4.2.1 Mdm2 attenuates iPS cell generation from MEFs

In corroboration of the results obtained previously we wanted to identify whether a possible stem cell maintenance function of Mdm2 can be further validated in the system of induced pluripotent stem cells (iPSCs). MEFs from $p53^{-/-}$ and $p53^{-/-}$ $Mdm2^{-/-}$ mice were obtained from Guillermina (Gigi) Lozano at the MD Anderson cancer center and reprogrammed into iPSCs following the widely accepted protocol of Yamanaka and colleagues (Takahashi & Yamanaka, 2006) (cf. 3.2.1.7). Reprogramming protocols included transduction of OSK (Oct3/4, Sox2 and Klf4), OS (Oct3/4 and Sox2) and OK (Oct3/4 and Klf4). All three reprogramming protocols led to the successful generation of iPS cell colonies from $p53^{-/-}$ cells, with the 2-factor protocols resulting in a 10-fold decrease of colony numbers compared to the 3-factor protocol (cf. Figure 4-1 A-C). Loss of Mdm2 significantly decreased the generation of iPSC colonies up to 80 % compared to $p53^{-/-}$ cells (Figure 4-1 A-C). This reduction was continuously observed regardless of the reprogramming protocol. For comparison, we also investigated the potential difference of iPSC generation from wt MEFs. As published before, wt MEFs were reprogrammed less efficiently than $p53^{-/-}$ MEFs (Hong et al, 2009), but the efficiency was still higher than the one observed in $p53^{-/-}$ $Mdm2^{-/-}$ cells (Figure 4-1 D).

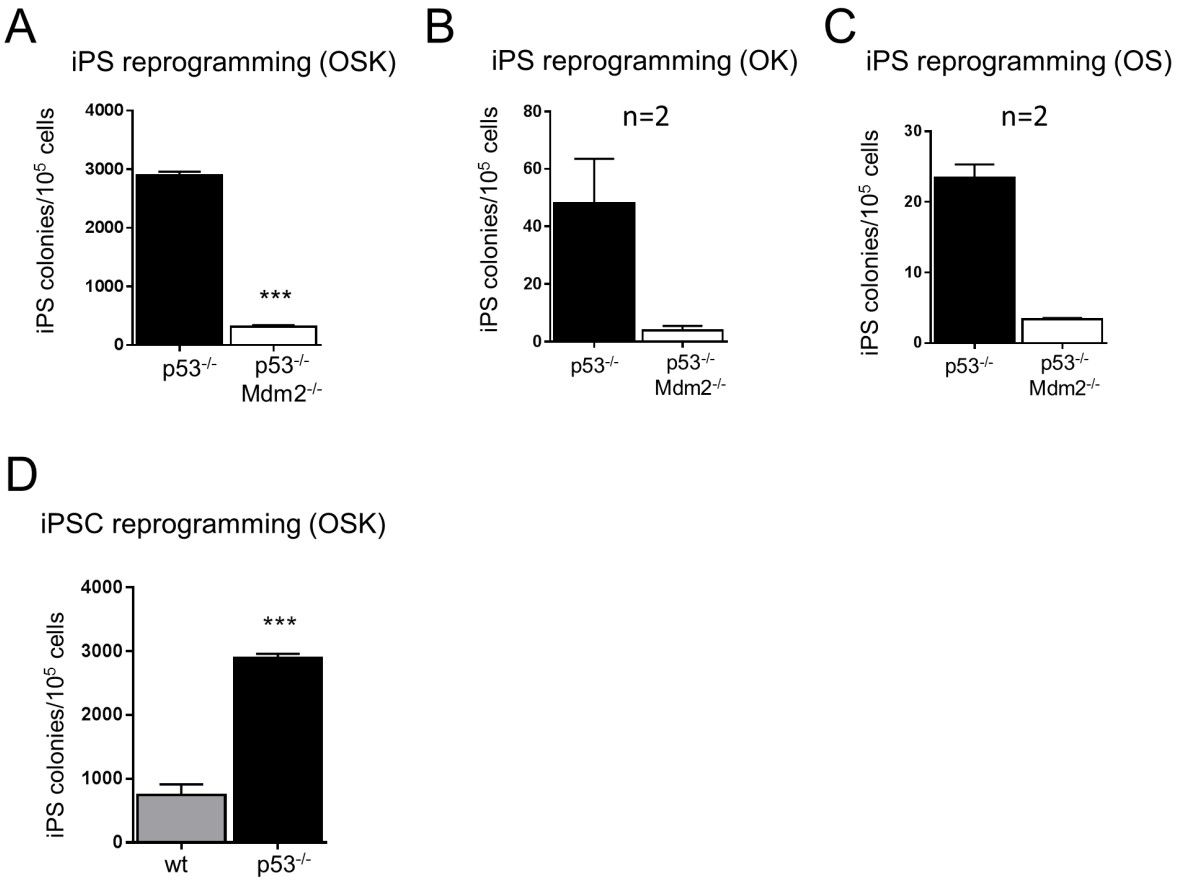

Figure 4-1 Mdm2 is required for iPS cell generation from murine embryonic fibroblasts (MEFs).

(A) $p53^{-/-}$ and $p53^{-/-}$ $Mdm2^{-/-}$ MEFs were reprogrammed into induced pluripotent stem (iPS) cells using the 3-factor protocol described in paragraph 3.2.1.7 (Oct4, Sox2, and Klf4; OSK). The number of obtained iPS colonies per MEFs was determined (mean ± SEM, n=3). (B, C) Same MEF cell preparations were reprogrammed into iPS cells using a 2-factor protocol (OS: Oct4, Sox2; OK: Oct4, Klf4) and obtained iPS colonies per MEFs were counted (mean ± SEM, n=2). (D) For comparison, wt MEFs were reprogrammed as described.
All reprogramming experiments were conducted by Alice Nemajerova, Department of Pathology, School of Medicine, Stony Brook University, USA. Figure data and legend also published in Wienken et al, *under review*.

4.2.1.1 *Mdm2 regulates gene expression in MEF cells*

Reprogramming of differentiated cells into iPSCs is associated with a major change of the expression profile (Tanaka et al, 2015). Hence we hypothesized that the differences in iPSC reprogramming in Figure 4-1 were caused by a differential gene expression pattern of $p53^{-/-}$ and $p53^{-/-}$ $Mdm2^{-/-}$ MEFs. RNA was isolated from MEFs that had undergone different time

points of reprogramming and global gene expression was analyzed via microarray hybridization. Essentially, unsupervised clustering separated the gene expression profile from $p53^{-/-}$ and $p53^{-/-}$ $Mdm2^{-/-}$ MEFs regardless of reprogramming. Several genes were identified that were continuously differentially regulated between the two cell types (Figure 4-2 A-B). Interestingly, we found factors important in stemness, development and differentiation (e.g. *Hoxc11*, *Hoxc13*, *Hoxb13* and *Notch1*) (Artavanis-Tsakonas et al, 1999; Shah & Sukumar, 2010).

4.2.1.2 *The RING domain in Mdm2 is important for gene regulation*

A gene regulatory function of Mdm2 in MEFs is displayed in Figure 4-2. Global gene expression was further validated in the $p53^{-/-}$ $Mdm2^{-/-}$ MEFs by sequencing RNA from MEFs generated in the laboratory of Yanping Zhang, University of North Carolina. Zhang also provided us with $p53^{-/-}$ $Mdm2^{C462A/C462A}$ knock in (KI) MEFs (further always referred to as $p53^{-/-}$ $Mdm2^{CA/CA}$) (Itahana et al, 2007). These MEFs expressed a RING finger mutant of Mdm2 which is unable to elicit E3 ligase function but still binds to p53. We used these cells to determine possible dependency of the gene regulatory function of Mdm2 on ubiquitin ligase function.

RNA-Seq analysis revealed that many genes were deregulated after total loss of Mdm2 as well as after loss of ubiquitin ligase function when compared to $p53^{-/-}$ MEFs (Figure 4-3 A). RNA-Seq data were validated via qRT-PCR analysis which corroborated the upregulation of several Hox genes (*Hoxb13*, *Hoxc10* and *Hoxc13*) as well as *Hhip* (Figure 4-3 B) and downregulation of the genes *Notch1*, *Tgfb2* and *Txnip* (Figure 4-3 C). These genes were of particular interest for us, as they had been associated before with stemness and development before. Hox genes encode a family of homeotic transcription factors that are conserved from fly to human. They ensure specific cell identity along the embryonic axis (cf. paragraph 2.3) (Dolle et al, 1993; Lewis, 1978; Zacchetti et al, 2007) and are thus major drivers of embryonic development (Shah & Sukumar, 2010). On the other hand, *Notch1* and *Tgfb2* are usually supporting the self-renewal of pluripotent cells and have been identified to support stem cell maintenance (Duncan et al, 2005; Stier et al, 2002). Repression and activation of differentiation factors and stem cell factors, respectively, explained why $p53^{-/-}$ $Mdm2^{-/-}$ MEFs were not reprogrammed efficiently into iPSCs (cf. Figure 4-1).

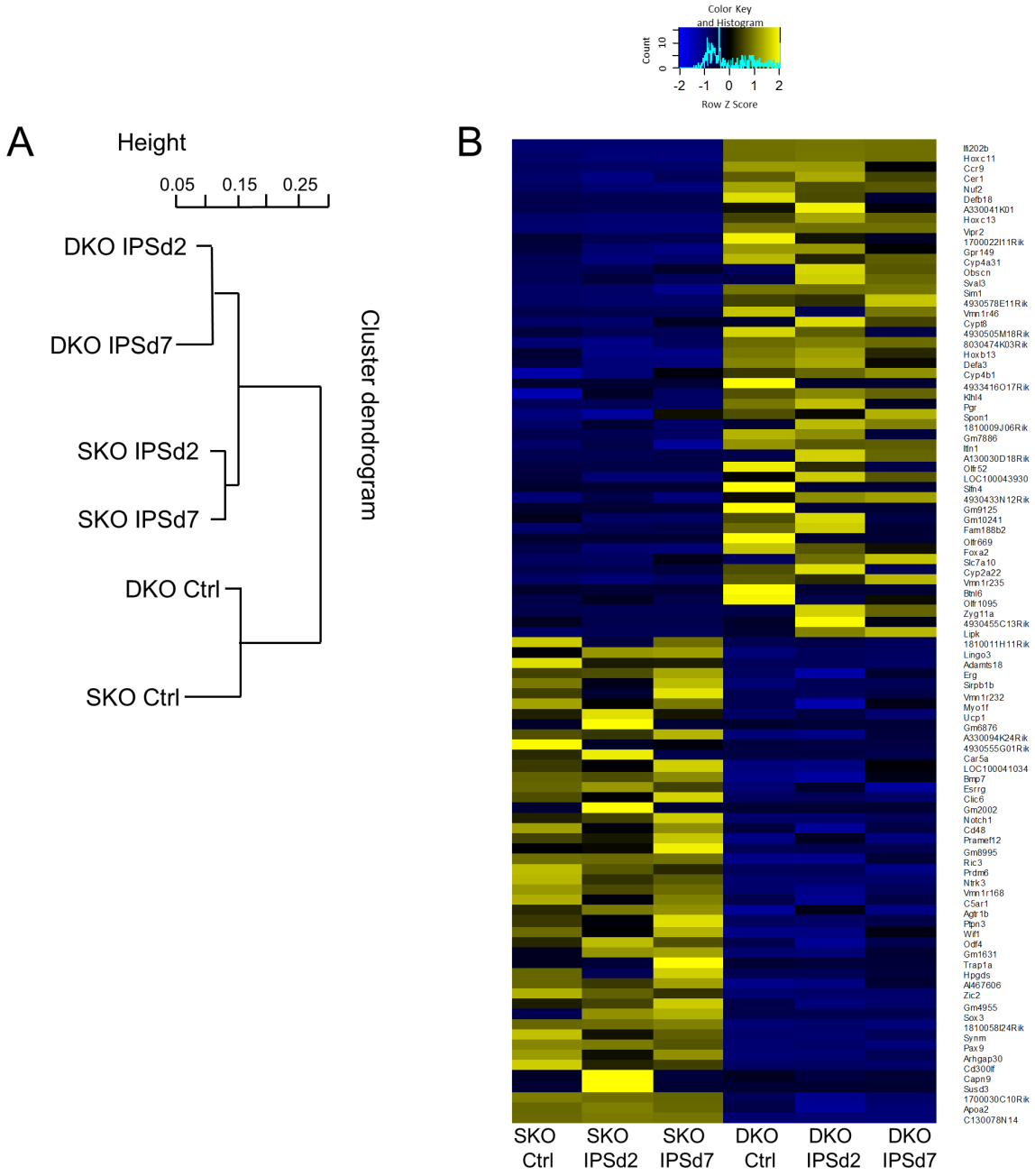

Figure 4-2 p53$^{-/-}$ and p53$^{-/-}$ Mdm2$^{-/-}$ MEFs are characterized by a differential gene expression pattern which is not influenced by cellular reprogramming.

p53$^{-/-}$ and p53$^{-/-}$ Mdm2$^{-/-}$ MEFs were reprogrammed into iPSCs using the 3-factor protocol for two and seven days (cf. Figure 4-1; Oct4, Sox2, and Klf4). mRNA expression was quantified using microarray analysis and cell clustering according to gene expression was determined. **(A)** Cluster dendrogram was generated using a hierarchical approach with the average linkage-method. Distances were measured as 1 - Pearson's Correlation Coefficient. **(B)** From the normalized gene expression data, continuously differentially regulated genes were identified and are displayed in a heatmap (SKO = p53$^{-/-}$, DKO = p53$^{-/-}$ Mdm2$^{-/-}$ MEFs). Figure data and legend also published in Wienken et al, *under review*.

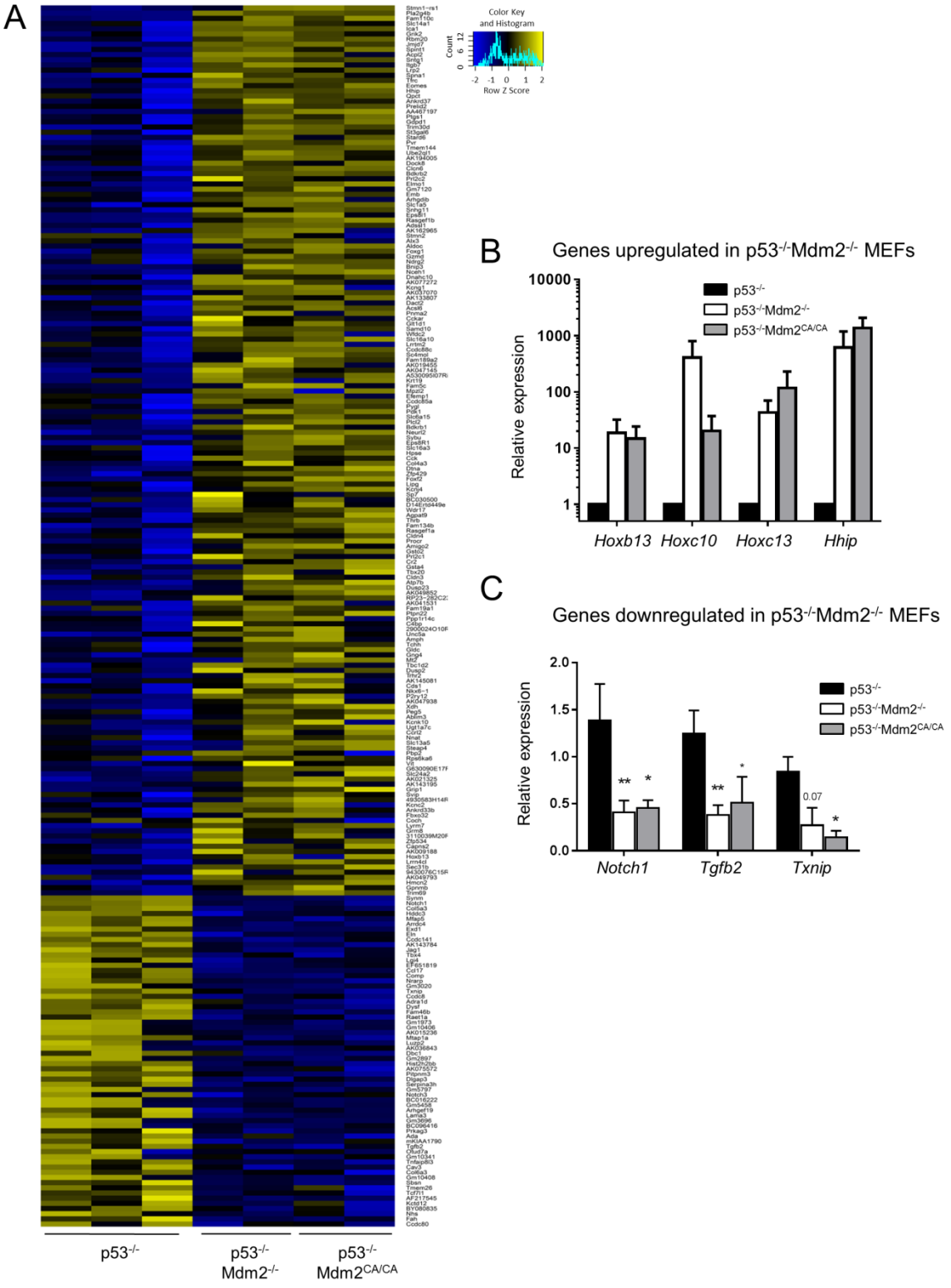
A
Color Key and Histogram
Count
Row Z Score
p53-/-
p53-/- Mdm2-/-
p53-/- Mdm2CA/CA
B
Genes upregulated in p53-/-Mdm2-/- MEFs
Relative expression
p53-/-
p53-/-Mdm2-/-
p53-/-Mdm2CA/CA
Hoxb13
Hoxc10
Hoxc13
Hhip
C
Genes downregulated in p53-/-Mdm2-/- MEFs
Relative expression
Notch1
Tgfb2
Txnip
0.07

Figure 4-3 Mdm2 regulates gene expression in MEFs through its RING domain.

(A) Gene expression of $p53^{-/-}$, $p53^{-/-}$ $Mdm2^{-/-}$ and $p53^{-/-}$ $Mdm2^{CA/CA}$ ($Mdm2^{CA/CA}$ = $Mdm2^{C462A/C462A}$) MEFs was analyzed via next generation RNA-sequencing. Differentially expressed genes were identified using the DESeq analysis in R (cf. paragraph 3.2.2.2.5) and are shown as a heat map. **(B-C)** Differentially upregulated **(B)** and downregulated **(C)** genes were re-evaluated by qRT-PCR (mean ± SEM, n=4 for upregulated-, n=3 for downregulated genes). For RNA-Seq data see also Table S2 in Wienken et al, *under review*. Figure data and legend also published in Wienken et al, *under review*.

4.2.1.3 *Stem cell and development associated genes in MEFs are regulated by Mdm2*

Mdm2 repressed a group of genes in MEFs and we investigated their functional annotation via GO term analysis. According to C5 GSEA and DAVID Mdm2 repressed genes involved in development and differentiation (Figure 4-4 A, C). Genes belonging to this annotation were, among others, the Hox genes (cf. Figure 4-3). This enrichment correlated with the decreased ability of $p53^{-/-}$ $Mdm2^{-/-}$ MEFs to de-differentiate into iPSCs (cf. Figure 4-1). According to C5 GSEA, genes activated by Mdm2 were also partially involved in development, but this finding was not supported by corresponding data from DAVID (Figure 4-4 B,D).

In order to identify a common regulatory pathway of the deregulated genes, C2 GSEA was performed (Figure 4-5). Several upregulated gene sets in $p53^{-/-}$ $Mdm2^{-/-}$ MEFs were characterized by PRC2- and H3K27me3 epigenetic regulation (Figure 4-5 A). Downregulated genes on the contrary were enriched for the H3K27me3 opposite mark – H3K4me3 (Figure 4-5 B, cf. 2.2.2) (Santos-Rosa et al, 2002) and also to some extent PRC2 regulation. H3K27me3 is the hallmark of PRC2 gene repression which is highly important during early differentiation processes of stem cells as well as reprogramming into iPSCs (cf. paragraph 2.3.4). One well known gene family that is regulated by PRC2 is the *Hox* gene family (cf. paragraph 2.3), from which *Hoxb13, Hoxc10 and Hoxc13* had already been confirmed to be Mdm2 target genes (cf. Figure 4-3). In line with our iPSC reprogramming data, gene sets were upregulated in $p53^{-/-}$ $Mdm2^{-/-}$ MEFs that are normally downregulated in stem cells (e.g. BOQUEST_STEM_CELL_DN or LIM_MAMMARY_STEM _CELL_DN) (Figure 4-5 A). Vice versa, stem cell specific gene sets were identified to be downregulated in $p53^{-/-}$ $Mdm2^{-/-}$ MEFs (e.g. WONG_EMBRYONIC_STEM_ CELL_CORE or BOQUEST_STEM_CELL_ UP (Figure 4-5 B). Among those sets *Notch1* and *Tgfb2* were found.

A C5 GSEA of genes upregulated in p53$^{-/-}$Mdm2$^{-/-}$ MEFs

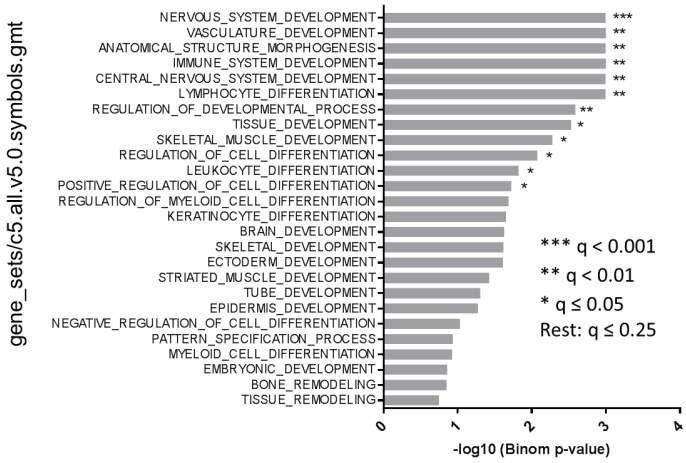

B C5 GSEA of genes downregulated in p53$^{-/-}$Mdm2$^{-/-}$ MEFs

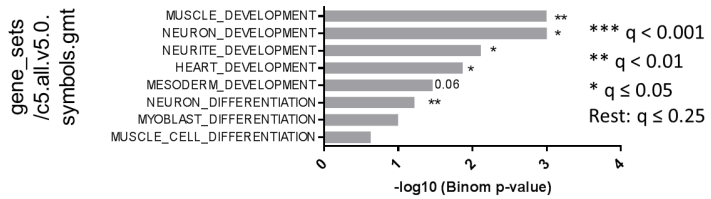

C DAVID GO analysis of genes upregulated in p53$^{-/-}$Mdm2$^{-/-}$ MEFs

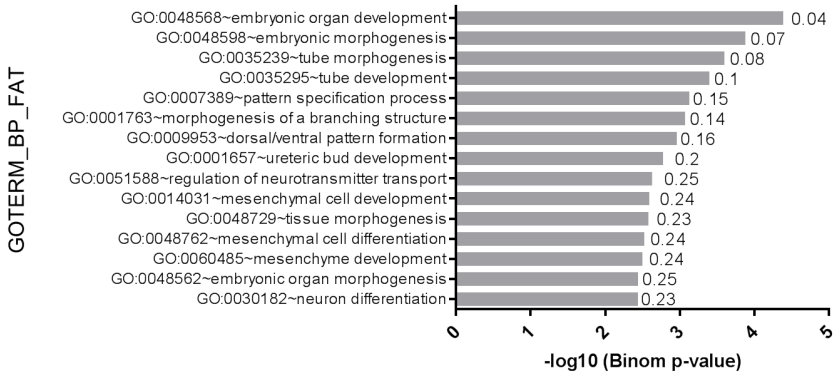

D DAVID GO analysis of genes downregulated in p53$^{-/-}$Mdm2$^{-/-}$ MEFs

Functional annotation with DAVID was performed but no significant classification with q value < 0.25 could be detected .

Figure 4-4 Mdm2 regulated genes are involved in stemness and differentiation.

(A-B) Gene set enrichment analysis (GSEA) from C5 GO gene sets (provided by the Molecular Signatures Database (MSigDB) v5.0) was performed using normalized RNA-Seq

reads from Figure 4-3 (Mootha et al, 2003; Subramanian et al, 2005). Enriched gene sets were filtered for the cues “development”, “differentiation”, “stem_cell” and “remodeling” and are displayed for genes upregulated in $p53^{-/-}$ $Mdm2^{-/-}$ MEFs **(A)** and genes downregulated in $p53^{-/-}$ $Mdm2^{-/-}$ MEFs **(B)**. q-values indicate false discovery rate (FDR); the threshold of significant enrichment ($q \leq 0.25$) was implied according to the GSEA standards (http://www.broadinstitute.org/gsea/doc/ GSEAUserGuideFrame .html) for this and all following GSEA and DAVID analyses (for the total analysis see Table S3 in Wienken et al, *under review*). **(C-D)** For comparison, differentially expressed genes that had already been identified by DESeq were also subjected to GO term analysis by DAVID (https://david.ncifcrf.gov/) and are shown according to their significance by p-value and FDR according to Benjamini Hochberg (Huang et al, 2008) (for the total analysis see Table S3 in Wienken et al, *under review*). Figure data and legend also published in Wienken et al, *under review*.

A

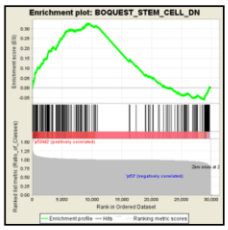

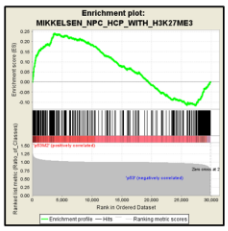

C2 GSEA of genes upregulated in $p53^{-/-}Mdm2^{-/-}$ MEFs

NAME	NOM p-val	FDR q-val
BOQUEST_STEM_CELL_DN	< 0.001	< 4.90E-06
MIKKELSEN_NPC_HCP_WITH_H3K27ME3	< 0.001	< 4.90E-06
MIKKELSEN_MCV6_HCP_WITH_H3K27ME3	< 0.001	< 4.90E-06
MEISSNER_BRAIN_HCP_WITH_H3K27ME3	< 0.001	< 4.90E-06
MEISSNER_NPC_HCP_WITH_H3K4ME2_AND_H3K27ME3	< 0.001	< 4.90E-06
LIM_MAMMARY_STEM_CELL_DN	< 0.001	< 4.90E-06
MEISSNER_NPC_HCP_WITH_H3K4ME3_AND_H3K27ME3	< 0.001	< 4.90E-06
BOQUEST_STEM_CELL_CULTURED_VS_FRESH_UP	< 0.001	< 4.90E-06
MIKKELSEN_NPC_HCP_WITH_H3K4ME3_AND_H3K27ME3	< 0.001	< 4.90E-06
LEE_NEURAL_CREST_STEM_CELL_DN	< 0.001	< 4.90E-06
PASINI_SUZ12_TARGETS_DN	< 0.001	< 4.90E-06
ACEVEDO_LIVER_CANCER_WITH_H3K27ME3_UP	< 0.001	4.90E-06
JAATINEN_HEMATOPOIETIC_STEM_CELL_UP	< 0.001	2.85E-05
MIKKELSEN_MEF_ICP_WITH_H3K27ME3	< 0.001	2.90E-05
MEISSNER_NPC_HCP_WITH_H3K4ME2	< 0.001	3.14E-05
MIKKELSEN_NPC_ICP_WITH_H3K4ME3	< 0.001	3.50E-05
JAATINEN_HEMATOPOIETIC_STEM_CELL_DN	< 0.001	6.20E-05
IZADPANAH_STEM_CELL_ADIPOSE_VS_BONE_UP	< 0.001	6.26E-05
MATSUDA_NATURAL_KILLER_DIFFERENTIATION	< 0.001	6.53E-05

B

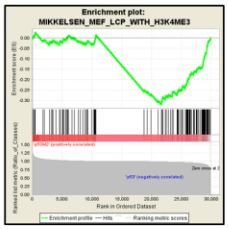

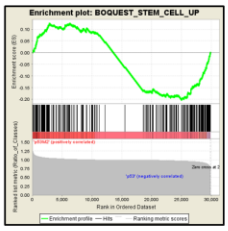

C2 GSEA of genes downregulated in $p53^{-/-}Mdm2^{-/-}$ MEFs

NAME	NOM p-val	FDR q-val
MIKKELSEN_MEF_LCP_WITH_H3K4ME3	< 0.001	< 2.15E-05
WONG_EMBRYONIC_STEM_CELL_CORE	< 0.001	< 2.15E-05
RIZ_ERYTHROID_DIFFERENTIATION	< 0.001	< 2.15E-05
BOQUEST_STEM_CELL_UP	< 0.001	< 2.15E-05
LIM_MAMMARY_STEM_CELL_UP	< 0.001	< 2.15E-05
GAL_LEUKEMIC_STEM_CELL_DN	< 0.001	< 2.15E-05
SCHAEFFER_PROSTATE_DEVELOPMENT_6HR_DN	< 0.001	< 2.15E-05
REACTOME_DEVELOPMENTAL_BIOLOGY	< 0.001	< 2.15E-05
FOURNIER_ACINAR_DEVELOPMENT_LATE_2	< 0.001	< 2.15E-05
LU_EZH2_TARGETS_UP	< 0.001	< 2.15E-05
KAMMINGA_EZH2_TARGETS	< 0.001	< 2.15E-05
MIKKELSEN_NPC_LCP_WITH_H3K4ME3	< 0.001	4.78E-05
URS_ADIPOCYTE_DIFFERENTIATION_DN	< 0.001	1.04E-04
REACTOME_TRANSCRIPTIONAL_REGULATION_OF_WHITE_ADIPOCYTE_DIFFERENTIATION	< 0.001	1.30E-04
LE_NEURONAL_DIFFERENTIATION_DN	< 0.001	1.66E-04
IVANOVA_HEMATOPOIESIS_STEM_CELL	< 0.001	1.69E-04
ST_DIFFERENTIATION_PATHWAY_IN_PC12_CELLS	< 0.001	2.02E-04
YAMASHITA_LIVER_CANCER_STEM_CELL_UP	< 0.001	2.37E-04
MIKKELSEN_MCV6_LCP_WITH_H3K4ME3	< 0.001	2.50E-04
RIZ_ERYTHROID_DIFFERENTIATION_CCNE1	< 0.001	2.94E-04

Figure 4-5 Mdm2 preferentially regulates stemness related genes controlled by the Polycomb Repressive Complex.

(A-B) Gene set enrichment analysis (GSEA) from C2 curated gene sets (provided by the Molecular Signatures Database (MSigDB) v5.0) was run from normalized RNA-Seq reads (cf. Figure 4-3). Enriched gene sets were filtered for the cues “H3K27me3”, “H3K4me3”, “Ezh2”, “Suz12”, “development”, “differentiation” and “stem_cell” and are displayed for genes upregulated in $p53^{-/-}$ $Mdm2^{-/-}$ MEFs **(A)** and genes downregulated in $p53^{-/-}$ $Mdm2^{-/-}$ MEFs **(B)**. Selected enrichment plots are provided as examples. (for the total analysis see Table S4 in Wienken et al, *under review*). Figure data and legend also published in Wienken et al, *under review*.

4.2.1.4 *Genes regulated by Mdm2 are direct targets of PRC2 regulation*

In order to proof whether Mdm2 regulated genes were direct targets of PcG regulation, $p53^{-/-}$ and $p53^{-/-}$ $Mdm2^{-/-}$ MEFs were treated with the selective Ezh2 inhibitor EPZ6438 (Knutson et al, 2013). EZH2 is the catalytic subunit of the PRC2 which drives H3K27me3 (O'Carroll et al, 2001). According to our data, Mdm2 especially regulated genes which were characterized by regulation through H3K27me3 (Figure 4-5). If the putative Mdm2 target genes from Figure 4-3 B are directly repressed by the PRC2, treatment with EPZ 6438 will activate gene expression through loss of H3K27me3. If the gene repression is furthermore dependent on Mdm2, a higher gene induction upon inhibitor treatment will be expected in the $p53^{-/-}$ MEFs in comparison to the $p53^{-/-}$ $Mdm2^{-/-}$ cells.

EPZ6438 treatment lowered overall H3K27me3 levels in both cell lines without affecting Ezh2 levels (Figure 4-6 A). Additionally, it released the gene repression of the target genes *Hoxc10, -c13, -b13* and *Hhip* in the $p53^{-/-}$ and in the $p53^{-/-}$ $Mdm2^{-/-}$ MEFs. Remarkably, this induction was much higher in the $p53^{-/-}$ MEFs than in the $p53^{-/-}$ $Mdm2^{-/-}$ MEFs, which emphasized that Mdm2 regulates PRC2 target genes epistatically (Figure 4-6 B). For further analysis, H3K27me3 levels at the gene promoters were evaluated via ChIP (cf. 3.2.3.4 and 3.2.3.5). Upon EPZ6438 treatment, H3K27me3 promoter levels were reduced to 40 % in the $p53^{-/-}$ cells. This reduction was less pronounced in $p53^{-/-}$ $Mdm2^{-/-}$ MEFs; overall the difference was not significant (Figure 4-6 C).

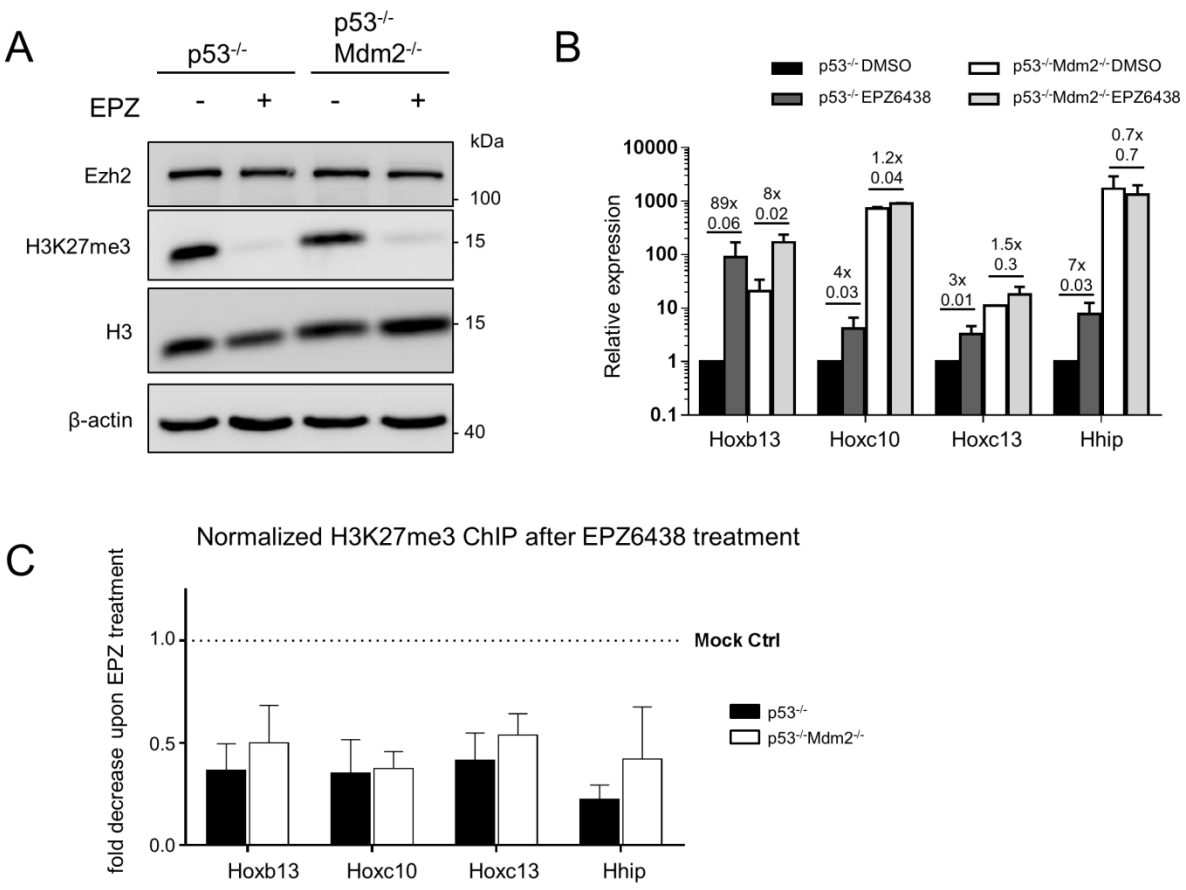

Figure 4-6 Ezh2 inhibitor treatment reveals epistatic regulation of Mdm2/PRC2 target genes by Mdm2.

(A) Ezh2 was inhibited via 48 h incubation with 5 µM EPZ6438 in $p53^{-/-}$ and $p53^{-/-}$ $Mdm2^{-/-}$ MEFs. Downregulation of H3K27me3 after Ezh2 inhibition was visualized via immunoblot analysis. **(B)** Gene expression was quantified using qRT-PCR analysis and (**C-D**) H3K27me3 promoter levels were analyzed via targeted ChIP. ChIP results are shown as fold decrease upon EPZ6438 treatment normalized to corresponding mock control **(C)**. Figure data and legend also partly published in Wienken et al, *under review*.

4.2.2 Osteoblast differentiation is repressed by Mdm2

Mdm2-mediated gene regulation executed stem cell maintenance function since its depletion abolished de-differentiation of fibroblasts into iPSCs (Figure 4-1 and Figure 4-3). Consequently, we asked the question whether loss of Mdm2 could vice versa drive stem cells into accelerated differentiation. As a suitable model, human mesenchymal stem cells (hMSCs) were differentiated into osteoblasts as described before (cf. 3.2.1.6 and Karpiuk et al, 2012). Since hMSCs were P53 wt cells, they were depleted of MDM2 and P53 and both in combination to focus on P53-independent functions of MDM2. Furthermore, *EZH2* gene expression was repressed.

According to our data in Figure 4-5 and Figure 4-6, Mdm2 regulated PRC2 target genes. Moreover, loss of PRC2 members had already been published to accelerate stem cell differentiation including the differentiation into osteoblasts (Dudakovic et al, 2014; Ezhkova et al, 2009; Pasini et al, 2007). EZH2 kd was included to compare the effects of both EZH2 and MDM2 kd in parallel and to overlap their gene regulatory profiles. If MDM2 executes PRC2 target gene regulation also in hMSC cells, we will expect a de-repression of specific target genes and most probably also an alteration of differentiation.

Knock down was done via double siRNA transfection and monitored via immunoblot after 96h of kd and after 7 days of differentiation using RNA expression data (differentiation started 48h after the first kd). According to Figure 4-7, protein expression was successfully abolished after 96 h of kd (Figure 4-7 A). As expected, kd of MDM2 alone induced P53 regarding protein levels and activity since its depletion elevated protein levels of the P53 target p21. Gene expression of *MDM2* and *TP53* was at low levels after the additional differentiation time of 7 days according to Figure 4-7 B. *EZH2* gene expression had already recovered from kd but was still diminished by 20 %.

MDM2 indeed repressed the differentiation of hMSC-Tert cells into osteoblasts. Its depletion increased alkaline phosphatase activity and expression (*ALPL*) as well as *BGLAP* (osteocalcin) expression, both established markers of osteoblast differentiation (Weinreb et al, 1990). This differentiation barrier function of MDM2 was independent of P53 but comparable to that of EZH2. (Figure 4-8 A-C).

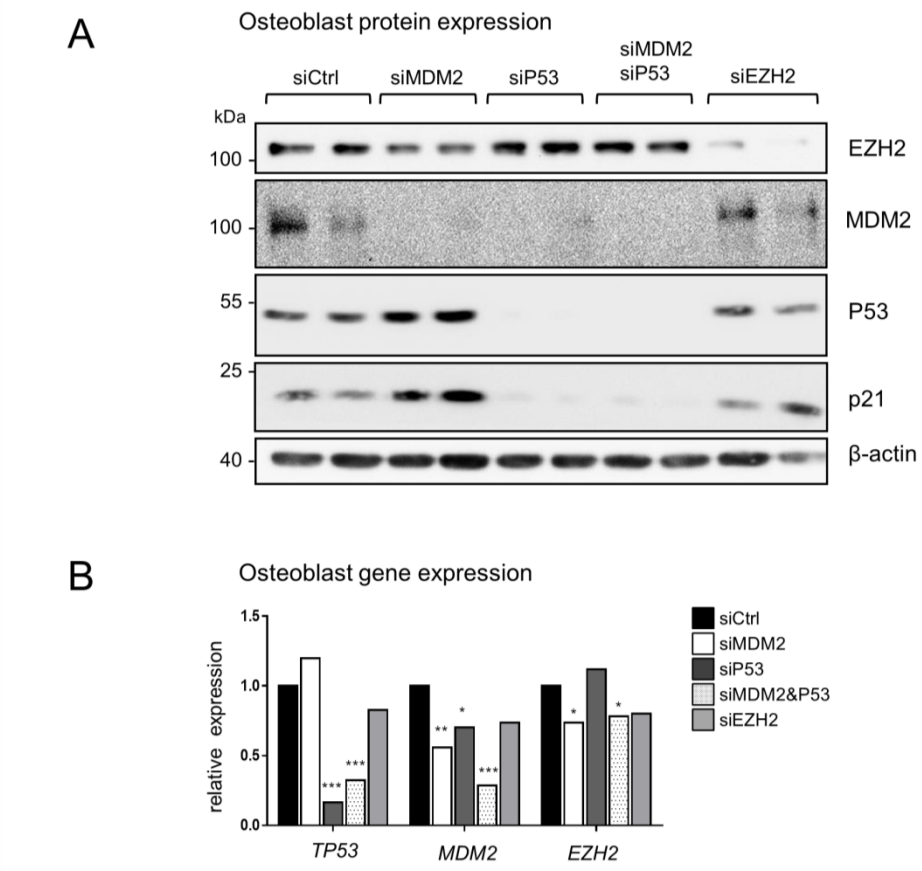

Figure 4-7 MDM2, P53 and EZH2 kd in hMSCs monitored by immunoblotting and gene expression analysis.

(A-B) MDM2, P53 and EZH2 were knocked down in hMSCs using siRNA transfection for 96 h (cf. paragraph 3.2.1.4 and 3.2.1.6). Knock down efficiency was verified 96 h after transfection via immunoblotting (**A**, n=2, already published in my master thesis) and after additional 7 days of differentiation using microarray data (**B**, n=2, microarray data shown in Figure 4-8). Figure data and legend also published in Wienken et al, *under review*.

As already indicated in Figure 4-8 C, loss of MDM2 altered the gene expression of two differentiation marker genes in differentiating osteoblast which is why global gene expression was monitored via microarray analysis from these samples. EZH2 kd samples were also included to compare gene regulatory profiles from both, MDM2 and EZH2 kd samples.

Loss of MDM2 (single kd and co-kd with P53) and loss of EZH2 cooperatively deregulated a vast number of genes. Figure 4-8 D shows a heatmap of the 50 most significantly up- and downregulated genes in the EZH2-, MDM2- and MDM2 & P53 kd samples in comparison to control- and single P53 kd. In total, loss of MDM2 together with P53 led to the deregulation of 747 genes and around 50 % of these were coregulated by EZH2 (Figure 4-8 E). Interestingly, around 90 % of the coregulated genes were regulated in the same direction, either up (yellow) or down (blue) in comparison to control. For microarray validation, qRT-PCR analysis was performed from the known PRC2 target genes *TIMP3* and *GDF6* (Sher et al, 2012; Shin & Kim, 2012) and from the additional osteoblast differentiation marker genes *BMP4* and *IGF2* (Twine et al, 2014) (Figure 4-8 F).

4.2.2.1 *The differentiation barrier function of MDM2 is P53 independent*

Due to the fact that P53 kd significantly decreased osteoblast differentiation (cf. Figure 4-8 A-C) microarray data were used to confirm that the differentiation barrier function of MDM2 was indeed p53 independent. First evidence was given by the unsupervised clustering of the expression data from MDM2 kd and MDM2&P53 kd samples together with EZH2 kd samples and apart from siCtrl and siP53 in Figure 4-8 D. Principal component analysis (PCA) from the whole array data mirrored this finding (Figure 4-9 A). Furthermore, differential gene expression from P53 kd samples did only overlap to some extent with MDM2-, MDM2 & P53- and EZH2 kd samples (Figure 4-9 B).

In addition, P53 responsive genes were identified via comparison of MDM2 kd samples (assuming P53 induction; cf. Figure 4-7 A, p21 induction) and MDM2&P53 kd samples (assuming P53 repression, cf. Figure 4-7 A). These genes included the known P53 target genes *INPP5D* and *CLCA2* (Figure 4-9 C) (Lion et al, 2013; Tanikawa et al, 2012) and only overlapped to a minor extent with previously identified MDM2/PRC2 target genes (Figure 4-9 D; MDM2/PRC2 target genes from Figure 4-8 E).

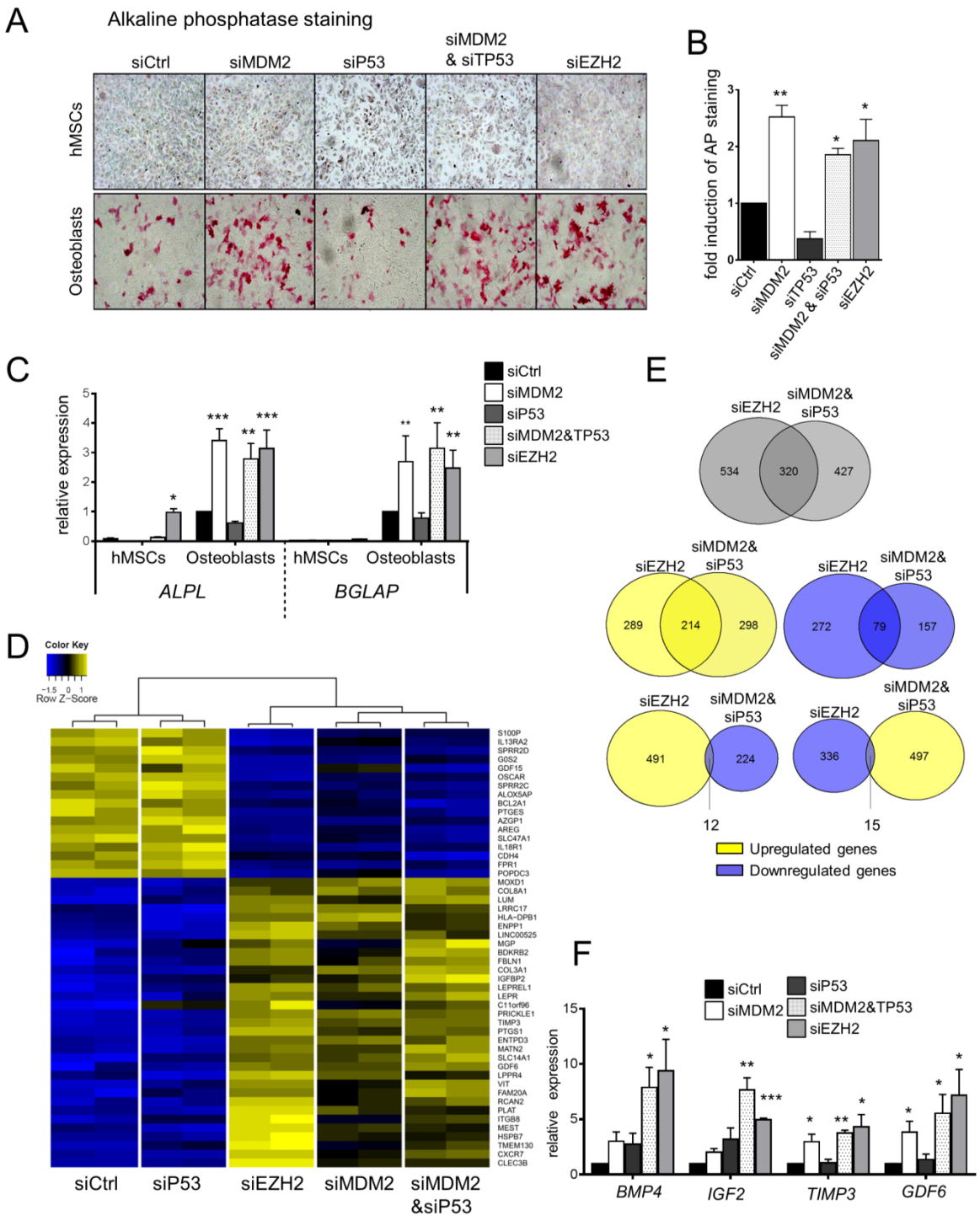

Figure 4-8 MDM2 hinders the differentiation of human mesenchymal stem cells (hMSCs) into osteoblasts and contributes to the regulation of PRC2 target genes.

(A) MDM2, P53 and EZH2 depleted hMSCs were differentiated into osteoblasts (cf. Figure 4-7). At day 7, alkaline phosphatase (AP) activity was detected via AP staining (cf. 3.2.1.6). **(B)** Quantification of AP activity from A was done using automated light microscopy with

quantitative image analysis (Celigo cytometer, mean ± SEM, n=3). **(C-D)** RNA from the differentiated osteoblasts was quantified by qRT-PCR of the differentiation genes *ALPL* and *BGLAP* (**C**, n=3; A-C already published in master thesis) and array hybridization (**D**, n=2; the 50 most significantly deregulated genes are shown). **(E)** Venn diagrams present overlapping gene sets that respond to EZH2 and MDM2 & P53 depletion. Grey color indicates overall deregulated genes whereas blue and yellow coloring corresponds to downregulated- and upregulated genes, respectively, in comparison to control. **(F)** Differentially expressed osteoblast differentiation marker genes (*BMP4* and *IGF2*) as well as known PRC2 target genes (*TIMP3* and *GDF6*) identified in (C) were validated via qRT-PCR analysis (mean ± SEM, n=3). For microarray data see also Table S5 in Wienken et al, *under review*. Figure data and legend also published in Wienken et al, *under review*.

4.2.2.2 *MDM2 target genes in hMSCs are characterized by stemness functions and PRC2 regulation*

According to C5 GSEA, genes upregulated upon loss of MDM2 (& P53) in osteoblasts were enriched for development-, differentiation- and bone morphogenesis annotations whereas no significant annotation was withdrawn from identified downregulated genes (Figure 4-10 A-B). DAVID analysis was conducted for the genes co-regulated by MDM2 and EZH2 (cf. Figure 4-8 E). Cooperatively upregulated genes were comparably annotated as seen before in A (Figure 4-10 C). DAVID also identified annotations for some significantly downregulated gene sets which were involved in the immune response (Figure 4-10 D). Overall, the functional annotation of MDM2 repressed genes in MEFs and hMSCs overlapped (cf. Figure 4-4).

C2 GSEA analysis of the Mdm2 target genes in MEFs had revealed a connection to PRC2 gene regulation (cf. Figure 4-5) and EPZ6438 treatment had confirmed direct regulation of these target genes by Ezh2 (cf. Figure 4-6). Thus we tested a possible enrichment of H3K27me3 and PRC2 gene sets in the MDM2&P53 kd samples of differentiated osteoblasts. Indeed, similar epigenetic gene sets were enriched in the osteoblast samples after loss of MDM2 together with P53 (Table 4-1 A and B). Furthermore, this enrichment was much more pronounced in genes upregulated after loss of MDM2 than compared to downregulated ones. This overlap in gene set regulation supported our theory that MDM2 is a potential PRC2 gene repression partner not only in primary MEF cells but also in human mesenchymal stem cells. MDM2 hereby maintained stemness not only through favoring iPSC generation but also through inhibition of MSC differentiation into osteoblasts.

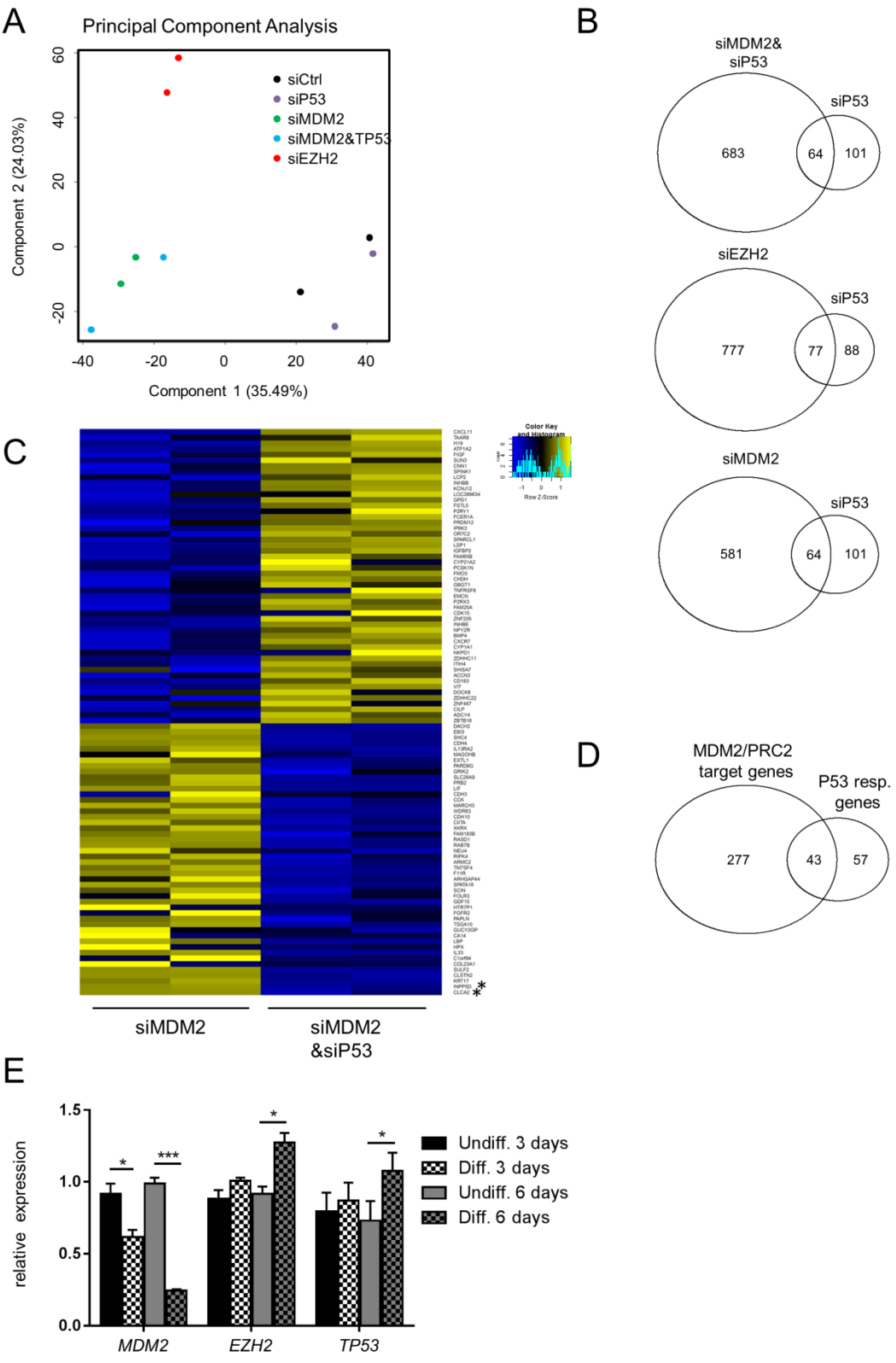

Figure 4-9 Differentiation barrier function of MDM2 is P53 independent.

(A) Principal component analysis (PCA) of microarray data (cf. Figure 4-8 D). PCA was performed using the princomp-function in the R software. To estimate the average group values for each gene and assess differential gene expression, a simple linear model was fitted to the data, and group-value averages and standard deviations for each gene were obtained. **(B)** Venn diagrams present overlapping gene sets that respond to P53 depletion and also to the depletion of MDM2&P53, EZH2 or MDM2 alone. Note that this overlap does not discriminate between positive or negative regulation of genes. **(C)** P53-responsive genes were identified comparing microarray data from MDM2 and MDM2&P53 depleted samples. Well-known P53 target genes like *INPP5D* and *CLCA2* are marked with an asterisk (Lion et al, 2013; Tanikawa et al, 2012). **(D)** Overlap of P53 responsive genes identified in C with PRC2/MDM2 target genes is shown in a Venn diagram. **(E)** Expression of *TP53*, *MDM2* and *EZH2* during osteoblastic differentiation of mesenchymal stem cells was analyzed via qRT-PCR at different time points post differentiation induction. cDNA from hMSCs was kindly provided by Simon Baumgart, University Medical Center Göttingen. Figure data and legend also published in Wienken et al, *under review*.

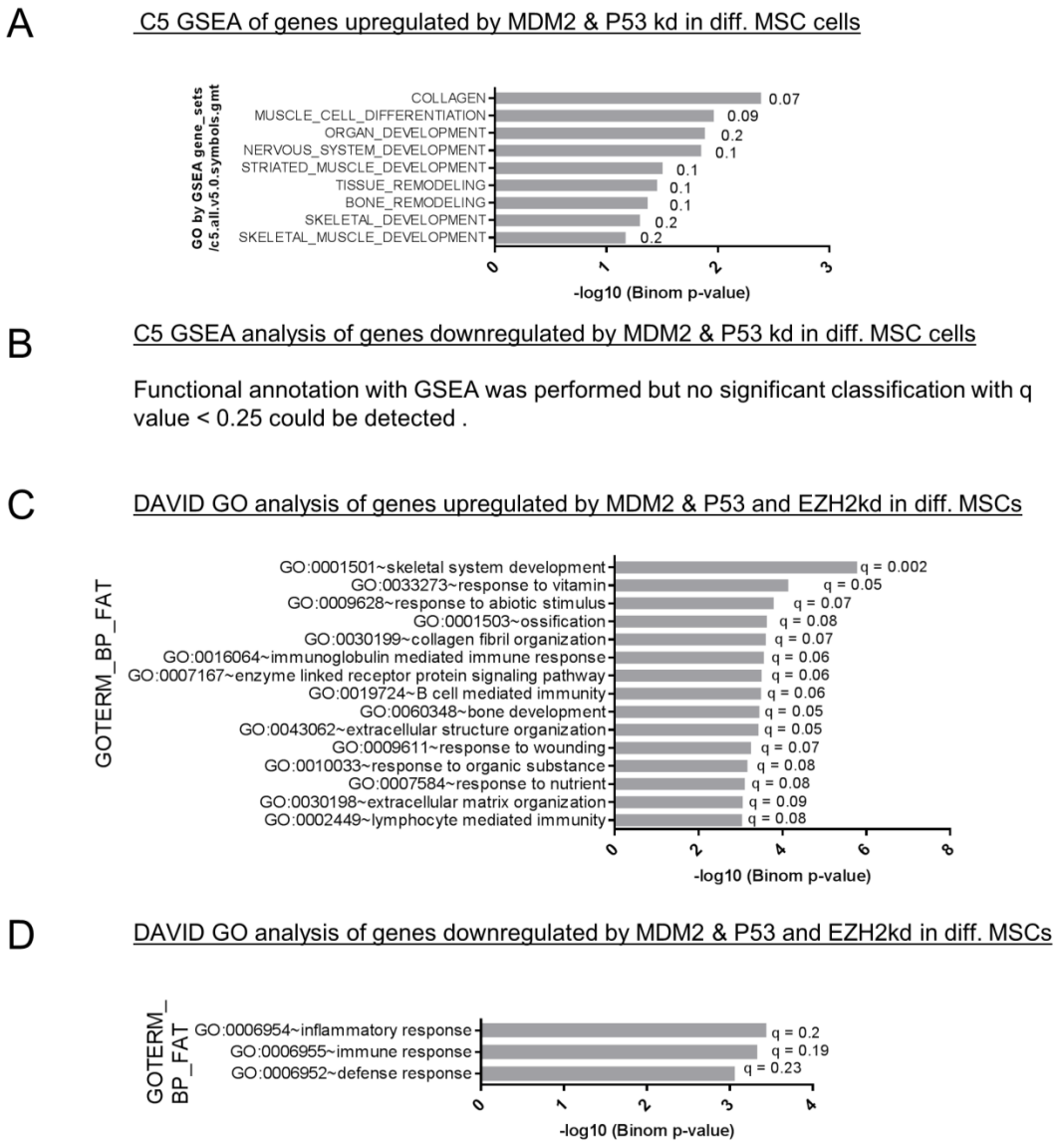

Figure 4-10 Functional annotation of genes regulated by MDM2 and coregulated by MDM2 and EZH2.

(A-B) C5 GSEA was performed based on normalized microarray data comparing siCtrl to MDM2&P53 knock down (kd) samples (cf. Figure 4-8). Enriched gene sets were filtered as described before (cf. Figure 4-4 A-B) for genes upregulated **(A)** and downregulated in P53&MDM2 kd samples **(B)**. **(C-D)** For comparison, DAVID annotation analysis was conducted from genes that were coregulated by MDM2 as well as EZH2 (comparing siMDM2&P53 and siEZH2, each vs siCtrl) (cf. Figure 4-8 E). For the whole data set please refer to Table S4 in Wienken et al, *under review*. Figure data and legend also published in Wienken et al, *under review*.

Table 4-1 MDM2 regulated genes in hMSCs are characterized by PRC2 and H3K27me3.

(A-B) C2 GSEA was performed on normalized microarray data comparing siCtrl to MDM2&P53kd samples (cf. Figure 4-8). Enriched gene sets were filtered as described before (cf. Figure 4-5) and are displayed for genes upregulated in P53&MDM2 kd samples **(A)** and genes downregulated in P53&MDM2 kd samples **(B).** For the whole data set please refer to Table S4 in Wienken et al, *under review*. Figure data and legend also published in Wienken et al, *under review*.

A C2 GSEA of genes upregulated by MDM2 & P53 kd in diff. MSC cells

NAME	NOM p-val	FDR q-val
BOQUEST_STEM_CELL_UP	< 0.01	1.03E-05
MIKKELSEN_ES_ICP_WITH_H3K4ME3_AND_H3K27ME3	< 0.01	2.73E-04
MIKKELSEN_MEF_ICP_WITH_H3K27ME3	< 0.01	2.83E-04
BOQUEST_STEM_CELL_CULTURED_VS_FRESH_DN	< 0.01	3.09E-04
BOQUEST_STEM_CELL_DN	< 0.01	3.95E-04
IZADPANAH_STEM_CELL_ADIPOSE_VS_BONE_DN	< 0.01	5.83E-04
GENTLES_LEUKEMIC_STEM_CELL_DN	< 0.01	7.12E-04
KAMMINGA_EZH2_TARGETS	< 0.01	8.03E-04
WONG_EMBRYONIC_STEM_CELL_CORE	< 0.01	0.001347
KONDO_PROSTATE_CANCER_WITH_H3K27ME3	< 0.01	0.001528
MIKKELSEN_NPC_HCP_WITH_H3K27ME3	< 0.01	0.001763
LIM_MAMMARY_STEM_CELL_UP	< 0.01	0.001892
JAATINEN_HEMATOPOIETIC_STEM_CELL_UP	< 0.01	0.002365
GAL_LEUKEMIC_STEM_CELL_DN	< 0.01	0.00363
MEISSNER_NPC_HCP_WITH_H3K4ME2_AND_H3K27ME3	< 0.01	0.004236
JAATINEN_HEMATOPOIETIC_STEM_CELL_DN	< 0.01	0.004249
CAIRO_LIVER_DEVELOPMENT_UP	< 0.01	0.004886
LEE_NEURAL_CREST_STEM_CELL_DN	< 0.01	0.005722
FOURNIER_ACINAR_DEVELOPMENT_LATE_2	< 0.01	0.00871
MEISSNER_BRAIN_HCP_WITH_H3K27ME3	< 0.01	0.010253
ACEVEDO_LIVER_CANCER_WITH_H3K27ME3_UP	< 0.01	0.01218

B C2 GSEA of genes downregulated by MDM2 & P53 kd in diff. MSC cells

NAME	NOM p-val	FDR q-val
MIKKELSEN_MEF_HCP_WITH_H3K27ME3	< 0.01	< 7.20E-04
MIKKELSEN_MCV6_HCP_WITH_H3K27ME3	< 0.01	< 7.20E-04
MIKKELSEN_MEF_LCP_WITH_H3K27ME3	< 0.01	7.20E-04
SCHLESINGER_H3K27ME3_IN_NORMAL_AND_METHYLATED_IN_CANCER	< 0.01	0.008082
MIKKELSEN_MCV6_LCP_WITH_H3K27ME3	< 0.01	0.030868

4.2.3 MDM2 ensures cancer cell proliferation independent of P53

So far, murine primary cells as well as human adult stem cells were identified as systems in which MDM2 represses PRC2 target genes and enables stemness. Differentiated cells gather stem cell like features as they de-differentiate and self-renew in an unlimited manner to transform into a tumor cell (Reya et al, 2001). This requires a radical shift in the epigenetic- and gene expression profile of the cell (cf. paragraph 2.3.4).

As MDM2 had already been identified as an important oncogene and we now defined an important role for MDM2 in stemness maintenance, different cancer cell lines were screened for related P53-independent gene regulatory functions. In the previous systems, MDM2 cooperatively regulated gene expression with the PRC2. Loss of PRC2 proteins is fatal to cancer cell survival in several systems as outlined in 2.3.4.2. If MDM2 was indeed able to regulate PRC2 target genes also in cancer cells, we will expect P53-independent diminished cell survival after MDM2 depletion.

In a panel analysis of different cancer cell lines (cf. Table 4-2) MDM2 gene expression was knocked down via siRNA (Figure 4-11 A, C, E and G) and cell survival was evaluated via automated microscopy (Figure 4-11 B, F, H) and colony formation assays (Figure 4-11 D). Cells bearing wt P53 were additionally depleted from P53 to focus on the P53-independent functions of MDM2. As outlined in paragraph 2.3.4.2, cancer cells depend on the presence of PRC2 and specifically EZH2. EZH2 was therefore depleted as a control for our study. Cell survival of all different cancer cell lines was diminished upon loss of MDM2 – even in the absence of P53 – as it was for EZH2 (Figure 4-11 B,D,F,H). This phenotype supported our idea that MDM2 might have gene regulatory functions on PRC2 target genes also in cancer cells. It was tested via global expression analysis of MDM2 and EZH2 kd samples from the HCT116 $p53^{-/-}$ cell system.

Table 4-2 Cancer cell lines used for panel analysis shown in Figure 4-11

Cell line	Origin	P53 status
HCT116 $p53^{-/-}$	Colon cancer	-
MCF7	Breast cancer	wt
SJSA	Osteosarcoma	wt
PANC1	Pancreatic cancer	mt

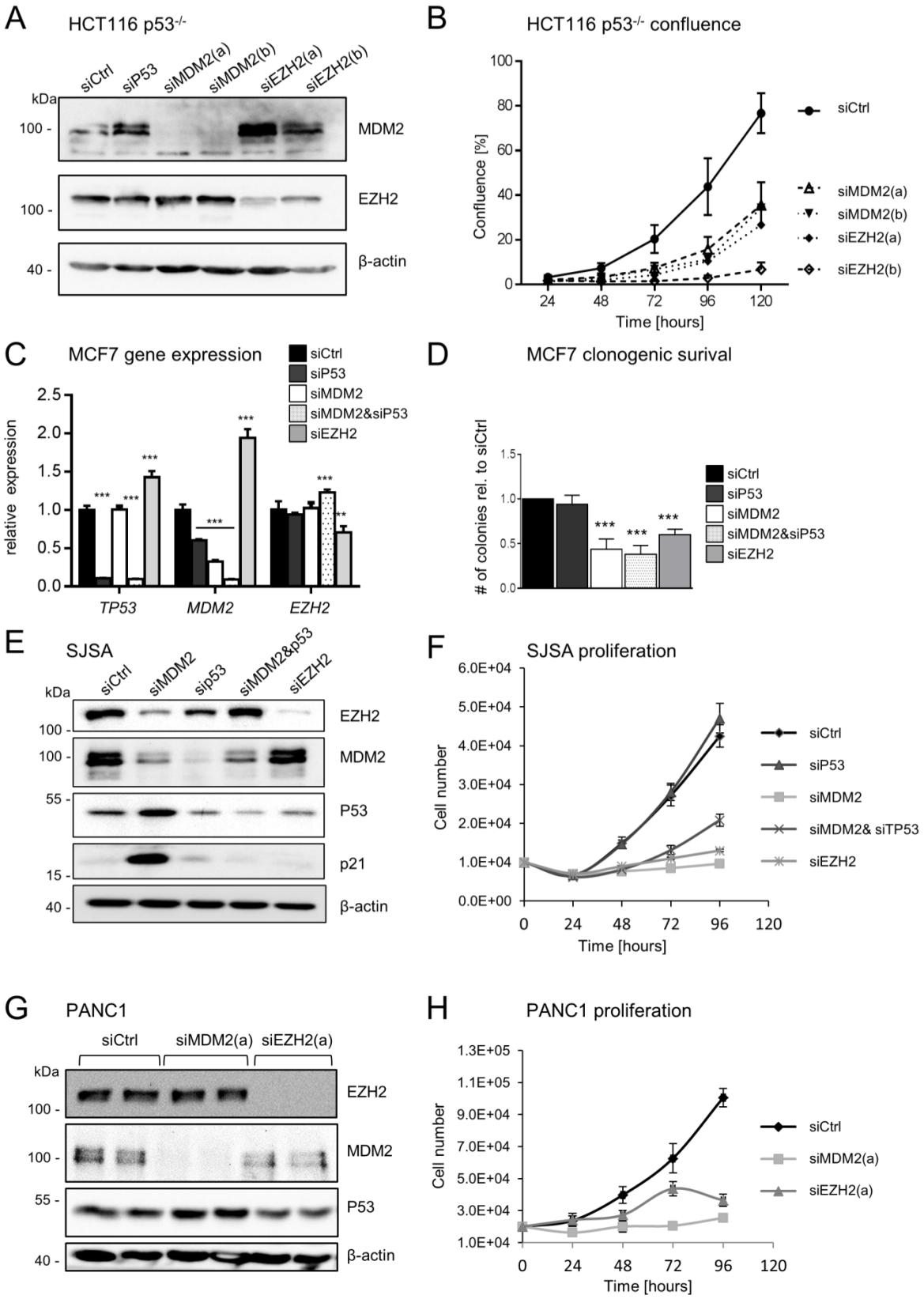
A
HCT116 p53-/-
siCtrl
siP53
siMDM2(a)
siMDM2(b)
siEZH2(a)
siEZH2(b)
kDa
100 -
MDM2
100 -
EZH2
40 -
β-actin
B
HCT116 p53-/- confluence
Confluence [%]
Time [hours]
siCtrl
siMDM2(a)
siMDM2(b)
siEZH2(a)
siEZH2(b)
C
MCF7 gene expression
relative expression
siCtrl
siP53
siMDM2
siMDM2&siP53
siEZH2
TP53
MDM2
EZH2
D
MCF7 clonogenic surival
# of colonies rel. to siCtrl
E
SJSA
siCtrl
siMDM2
sip53
siMDM2&p53
siEZH2
EZH2
MDM2
P53
p21
β-actin
F
SJSA proliferation
Cell number
Time [hours]
siCtrl
siP53
siMDM2
siMDM2& siTP53
siEZH2
G
PANC1
siCtrl
siMDM2(a)
siEZH2(a)
EZH2
MDM2
P53
β-actin
H
PANC1 proliferation
Cell number
Time [hours]
siCtrl
siMDM2(a)
siEZH2(a)

Figure 4-11 MDM2 mediates cell survival in several different cancer cell lines independent of P53.

(A, C, E, G) The cancer cell lines HCT116 $p53^{-/-}$(A), MCF7 (C), SJSA (E) and PANC1 (G) were depleted of MDM2 and EZH2 using double siRNA transfection for 96 h. Knock down efficiency was verified by immunoblotting or qRT-PCR (TP53 co-knockdown was done in cells bearing wt TP53). **(B, F, H)** Cell proliferation of HCT116 $p53^{-/-}$, SJSA and PANC1 cells was determined using automated light microscopy with quantitative image analysis (Celigo cytometer), mean ± SEM, n=3), and **(D)** the amount of MCF7 cells displaying clonogenic survival, regardless of TP53 co-kd(mean ± SEM, n=3). Note, that the results for HCT116 $p53^{-/-}$ cells were already partly published in my master thesis; MCF7 data were kindly provided by Dr. Xin Zhang. Figure data and legend also published in Wienken et al, *under review*.

MDM2 represses PRC2 target genes in different cancer cells

HCT116 $p53^{-/-}$ cells were chosen for microarray analysis, because they provided us with a clean P53 ko system (Bunz et al, 1998). MDM2 and EZH2 were depleted, each using two different siRNAs, and gene expression was compared to control kd (siCtrl) and P53 kd (cf. Figure 4-11 A; since the cells were $P53^{-/-}$, siP53 was used as a control siRNA). As it was already observed before, loss of MDM2 deregulated a group of genes which was also regulated by EZH2 (Figure 4-12 A). In total, 150 genes were differentially up- or downregulated upon MDM2 kd whereas EZH2 depletion deregulated nearly 1500 target genes. Most interestingly, 70 % of the MDM2 target genes were coregulated by EZH2 and none of these were regulated by EZH2 and MDM2 in a differential pattern (they were either downregulated (blue) or upregulated (yellow), Figure 4-12 B). qRT-PCR analysis of the PRC2 target genes *CXCR4*, *DUSP4*, *KLF2 and TEX261* was used for array validation (Figure 4-12 C-D; *TEX261* was selected as target due to H3K27me3 and EZH2 ChIP-Seq tracks on the UCSC genome browser; other genes were selected from literature (Lin et al, 2011; Nie et al, 2015; Vanharanta et al, 2013)). In parallel to HCT116 cells (Figure 4-12 C), MDM2 repression of these PRC2 target genes was also observed in MCF7 cells (Figure 4-12 D).

C2 GSEA which had previously indicated the relation of MDM2 and PRC2 target gene regulation (cf. Figure 4-5 and Table 4-1) revealed a similar gene regulation annotation. Genes upregulated by the loss of MDM2 were often associated with H3K27me3 (Figure 4-13 A) whereas downregulated genes are stem cell associated (Figure 4-13 B). Functional annotation via C5 GSEA on MDM2 regulated genes did not give us any significant enrichment of gene sets (Figure 4-13 C-D). According to DAVID analysis MDM2/EZH2 target genes were involved in transcription (Figure 4-13 E-F).

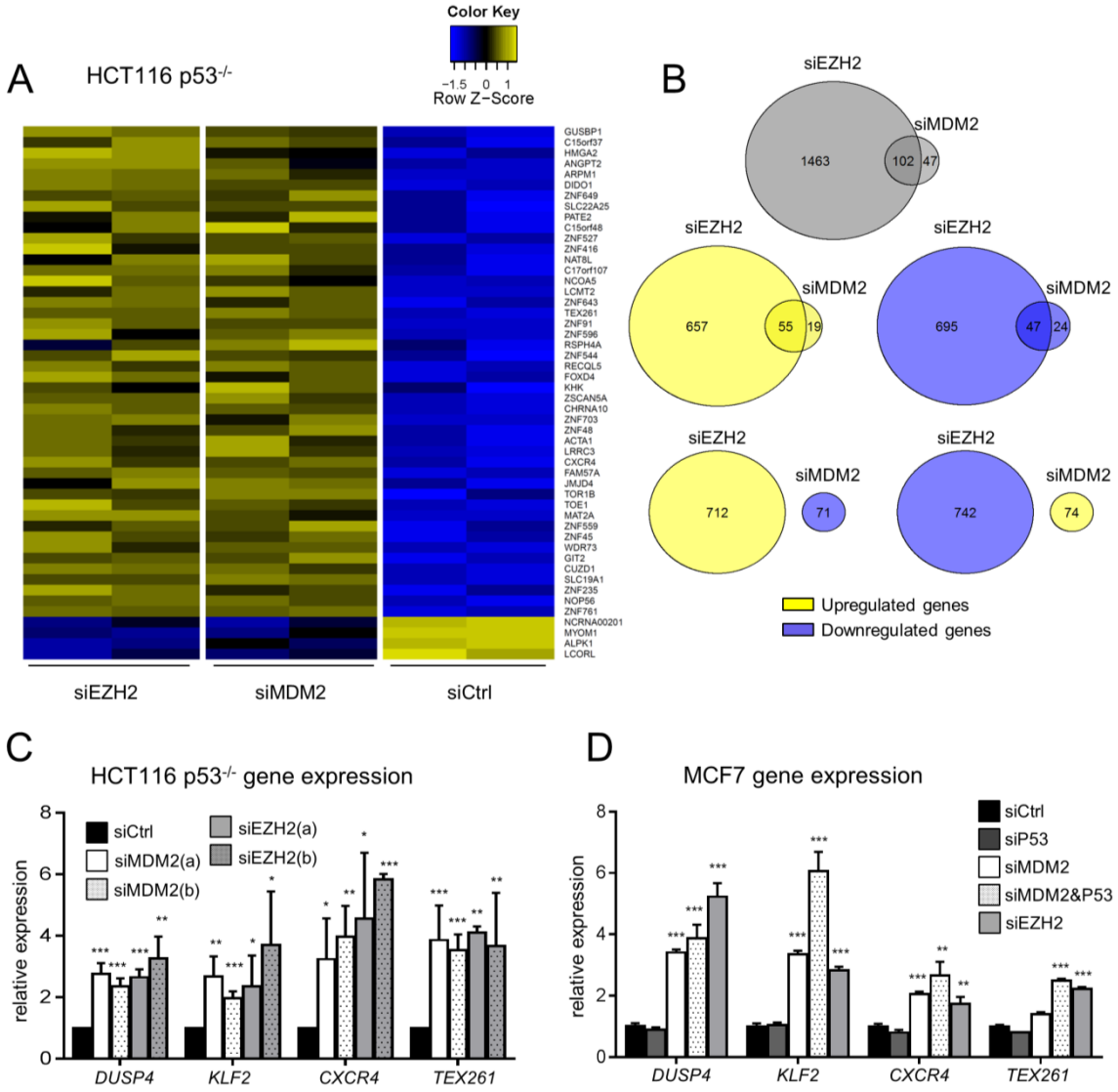

Figure 4-12 MDM2 represses PRC2 target genes in HCT116 p53$^{-/-}$ and MCF7 cells.

(A) Differential gene expression was determined via microarray analysis of HCT116 p53$^{-/-}$ cells which were depleted of MDM2 and EZH2 (cf. Figure 4-11). The 50 most significantly deregulated genes are depicted in a heatmap **(B)** Overlap of gene sets regulated by both MDM2 and EZH2 are shown as Venn diagrams; note the absence of genes with opposite regulation. Grey color indicates overall deregulated genes whereas blue and yellow coloring corresponds to downregulated- and upregulated genes, respectively, in comparison to control. **(C, D)** Verification of identified target genes was conducted via qRT-PCR analysis in HCT116 p53$^{-/-}$ **(C)** and MCF7 **(D)** cells (mean ± SEM, n=3). MCF7 data was kindly provided by Dr. Xin Zhang. For microarray data see also Table S6 in Wienken et al, *under review*. Figure data and legend also published in Wienken et al, *under review*.

A C2 GSEA of genes upregulated by MDM2 kd in HCT116 p53$^{-/-}$ cells

NAME	NOM p-val	FDR q-val
KONDO_PROSTATE_CANCER_WITH_H3K27ME3	< 0.001	0.010268
BOSCO_EPITHELIAL_DIFFERENTIATION_MODULE	0.001093	0.030315
MIKKELSEN_MCV6_LCP_WITH_H3K27ME3	0.006313	0.130856
JAATINEN_HEMATOPOIETIC_STEM_CELL_DN	0.00504	0.176841
PECE_MAMMARY_STEM_CELL_UP	0.003086	0.177931
MIKKELSEN_MCV6_HCP_WITH_H3K27ME3	< 0.001	0.190977
MIKKELSEN_IPS_WITH_HCP_H3K27ME3	0.010593	0.211196
FOURNIER_ACINAR_DEVELOPMENT_LATE_2	0.004008	0.214383
MEISSNER_NPC_HCP_WITH_H3K4ME2_AND_H3K27ME3	0.002	0.245104

B C2 GSEA of genes downregulated by MDM2 kd in HCT116 p53$^{-/-}$ cells

NAME	NOM p-val	FDR q-val
WONG_EMBRYONIC_STEM_CELL_CORE	< 0.001	< 0.004
BHATTACHARYA_EMBRYONIC_STEM_CELL	< 0.001	0.004433
ADDYA_ERYTHROID_DIFFERENTIATION_BY_HEMIN	0.011111	0.070773
MA_MYELOID_DIFFERENTIATION_UP	0.013245	0.074581
ZHAN_VARIABLE_EARLY_DIFFERENTIATION_GENES_DN	0.025316	0.07791
LE_NEURONAL_DIFFERENTIATION_DN	0.100358	0.215054
FOURNIER_ACINAR_DEVELOPMENT_EARLY_UP	0.055794	0.152536

C C5 GSEA analysis of genes upregulated by MDM2 kd in HCT116 p53$^{-/-}$ cells

Functional annotation with GSEA was performed but no significant classification with q value < 0.25 could be detected .

D C5 GSEA analysis of genes downregulated by MDM2 kd in HCT116 p53$^{-/-}$ cells

Functional annotation with GSEA was performed but no significant classification with q value < 0.25 could be detected .

E DAVID GO analysis of genes upregulated by MDM2 and EZH2 in HCT116 p53$^{-/-}$ cells

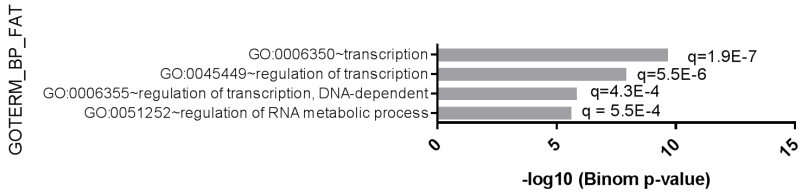

F DAVID GO analysis of genes downregulated by MDM2 and EZH2 in HCT116 p53$^{-/-}$ cells

Functional annotation with DAVID was performed but no significant classification with q value < 0.25 could be detected .

Figure 4-13 C2 GSEA and GO term analysis of MDM2 and MDM2/EZH2 regulated genes.

(A-B) C2 GSEA on normalized microarray data, comparing siCtrl to siMDM2 samples. Enriched gene sets were filtered as described before (Figure 4-5) and are displayed for genes upregulated in MDM2 kd samples **(A)** and genes downregulated in MDM2 kd samples **(B,** for the total analysis see Table S3 in Wienken et al, *under review*) **(C-D)** C5 GSEA comparing siCtrl to siMDM2 kd samples. Enriched gene sets were filtered as described

before (cf. Figure 4-4) and are displayed for genes upregulated in MDM2 kd samples **(C)** and genes downregulated in &MDM2 kd samples **(D)**. No significant classification was detected in these cases. **(E-F)** For comparison, annotation was analyzed via DAVID from genes that were coregulated by MDM2 and EZH2 (in comparison to siCtrl) (cf. Figure 4-12 B). For the total analysis see Table S3 in Wienken et al, *under review*. Figure data and legend also published in Wienken et al, *under review*.

4.3 MDM2 is recruited to target gene promoters by the PRC2

4.3.1 MDM2 directly interacts with the PRC2 members EZH2 and SUZ12

We detected a gene repressive function of MDM2 on PRC2 target genes in three distinct cell systems – mouse embryonic fibroblasts, human mesenchymal stem cells and at least two different human cancer cell lines. Due to this regulatory relationship we wanted to know whether MDM2 directly interacted with members of the PRC2. Therefore, endogenous MDM2 protein levels were boosted using the proteasome inhibitor MG132 over 6 hours in SJSA cells and MDM2 and the PRC2 members EZH2 and SUZ12 were immunoprecipitated. Endogenous levels of MDM2 were detected by immunoblotting in the precipitates of EZH2 and SUZ12 indicating an interaction of the two proteins. Vice versa, the precipitation of MDM2 pulled down EZH2 and SUZ12 (Figure 4-14 A). The interaction of EZH2 with its protein partner SUZ12 was also detected as a positive control.

When being transiently overexpressed in the cell line U2OS, MDM2 again bound to both, EZH2 and SUZ12, which indicated a direct interaction pattern (Figure 4-14 B and C). It was furthermore also possible to perform these interaction studies in MEF cells. For MEFs we immunoprecipitated endogenous Ezh2 from transiently overexpressed murine Mdm2 in $p53^{-/-}$ $Mdm2^{-/-,}$ MEFs indicating a conversation of the MDM2-PRC2 interaction from mouse to human (please refer to Wienken et al, *under review*)

Further exogenous Co-IP experiments with deletion mutants of MDM2 identified a 300 amino acid (aa) stretch in the N-terminal domain as critical for EZH2 and SUZ12 binding (Figure 4-14 D). The first 300 aa of MDM2 comprise the P53-binding- as well as the acidic domain. At least for EZH2 the P53 binding domain did not play any role in this interaction since P53-binding domain deletion mutants still interacted with EZH2. Deletion mutants covering the acidic domain also persisted EZH2 and SUZ12 binding, which leaves a 130 aa stretch between the two domains as most possible interaction platform.

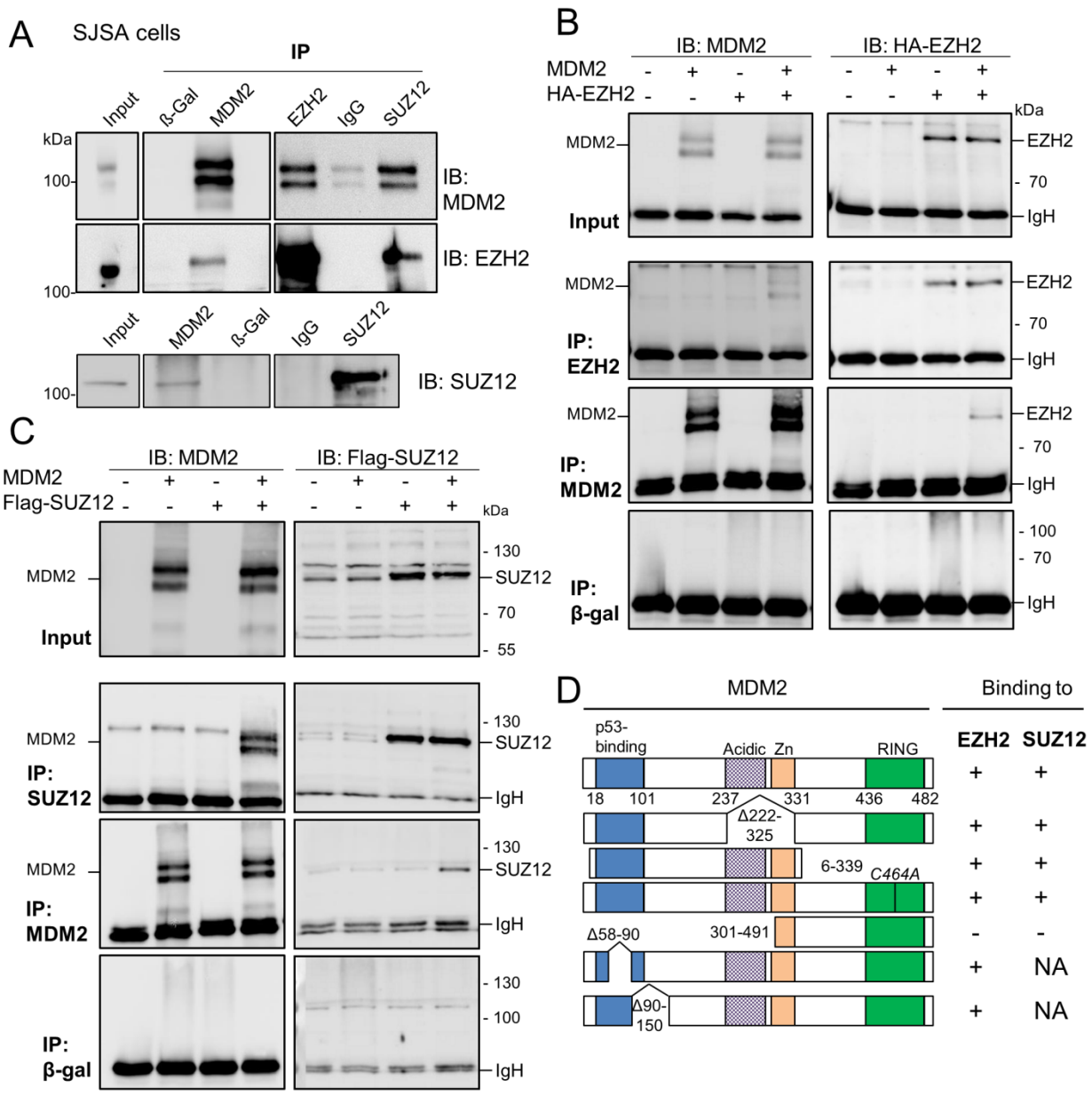

Figure 4-14 MDM2 interacts with the PRC2 components EZH2 and SUZ12.

(A) Endogenous MDM2, EZH2 and SUZ12 were co-immunoprecipitated from MG132-pretreated SJSA cells. Cell lysates (Input) and the immunoprecipitated (IP) material obtained with the indicated antibodies were analyzed by immunoblotting (IB). (**B-C)** Wild type MDM2 was overexpressed by transfection, together with HA-tagged EZH2 (B) or Flag-tagged SUZ12 (C) in H1299 cells, followed by IP and IB as in (A). Note that different appearance of the IgH band was caused by the species specificity of the IP and IB antibody **(D)** Graphical representation of exogenous Co-IP experiments with MDM2 deletion mutants. Indicated MDM2 mutants were transiently overexpressed in H1299 cells together with wt EZH2 or SUZ12 and interaction was monitored as in (B) and (C). For raw data, please refer to Wienken et al, *under review*. Co-IP data was generated in collaboration with A. Dickmanns and M. Weiss. Figure data and legend also published in Wienken et al, *under review*.

4.3.2 MDM2 is recruited to the TSS of MDM2/PRC2 target genes by EZH2

Both MDM2 and the PRC2 have been described to localize in the cell nucleus and bind to chromatin (cf. paragraph 2.1.6 and 2.3.1). Hence, we asked whether MDM2 can directly localize to PRC2 target gene chromatin and performed ChIP analysis (cf. 3.2.3.3 and 3.2.3.4). For this approach SJSA cells were chosen as the most suitable cell system because it provided us with high levels of endogenous MDM2.

Targeted ChIP analysis on promoter regions of previously identified MDM2 target genes (cf. Figure 4-12 C and D) revealed a specific enrichment of MDM2 in comparison to IgG negative control and the negative control gene *MYO* (Figure 4-15 A, siCtrl samples). Most interestingly, the binding of MDM2 to these genes was significantly decreased to background levels upon depletion of EZH2. Thus, Mdm2 was recruited to its target genes by EZH2 (Figure 4-15 A-B). In concordance, MDM2 chromatin binding was not detected on the promoters of genes that are regulated by EZH2 but not MDM2 (Figure 4-15 C; genes identified from microarray data in Figure 4-12).

In order to further validate the recruitment of MDM2 to gene promoters by EZH2, a cell line was used which carried an integrated luciferase gene with a Gal4-binding domain element (Hansen et al, 2008). Upon overexpression of Gal4-fused EZH2 and Myc-tagged MDM2 (Figure 4-15 D), Myc-MDM2 was recruited to the heterologous promoter site (Figure 4-15 E, experiment done by Dr. Xin Zhang). This experiment further confirmed that EZH2 recruits MDM2 to its target gene promoters.

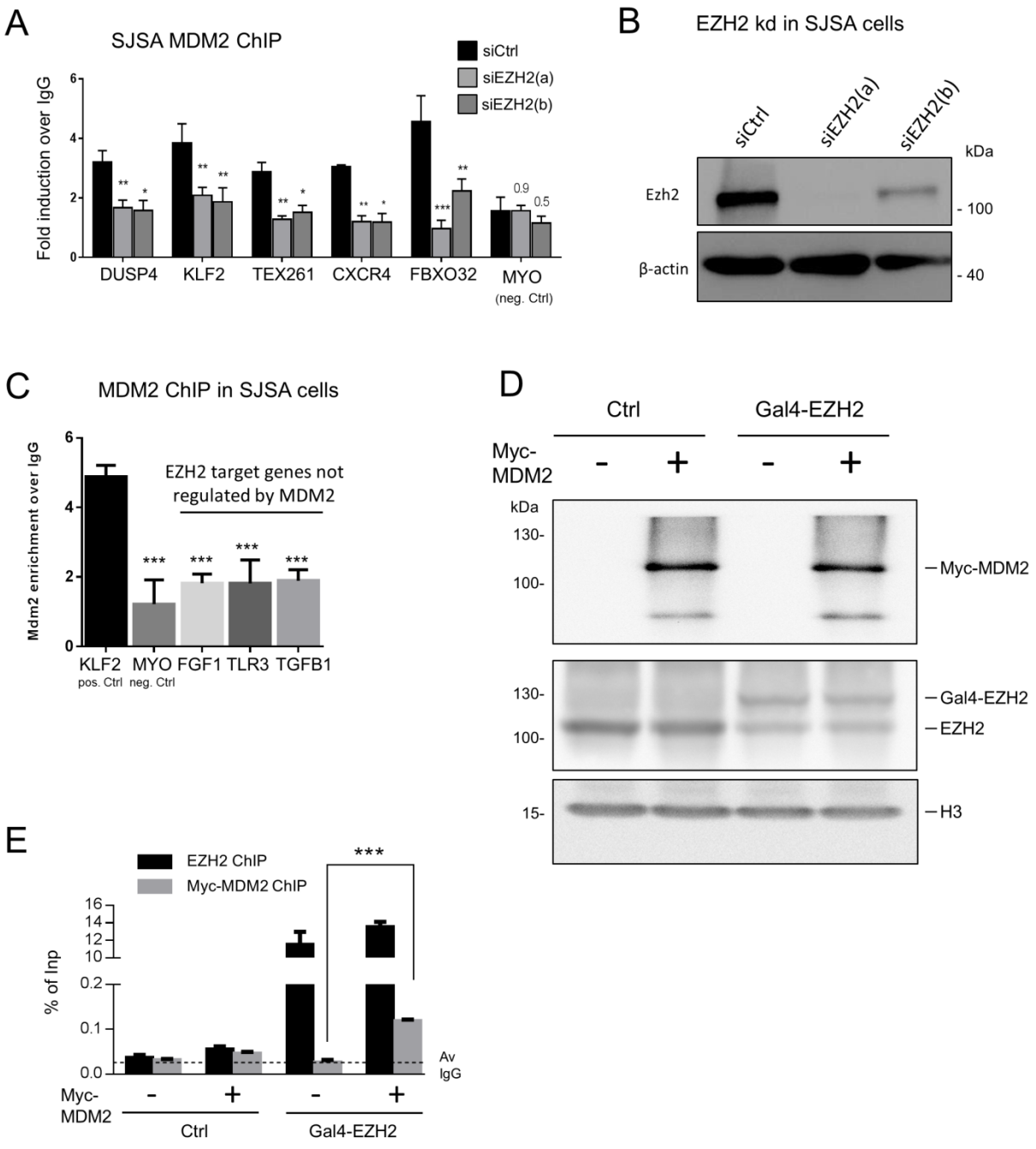

Figure 4-15 MDM2 is recruited to target genes by EZH2.

(A) Chromatin Immunoprecipitation (ChIP) of MDM2 in EZH2 depleted SJSA cells on MDM2/PRC2 target genes (cf. Figure 4-12, enrichment over IgG background; mean ± SEM; n=3). **(B)** Knock down efficiency of EZH2 was monitored via immunoblotting. **(C)** MDM2 enrichment was analyzed via targeted ChIP on the gene promoters of *FGF1, TLR3* and *TGFB1*. These genes responded to EZH2 depletion solely (not in cooperation with MDM2) according to microarray data from HCT116 $p53^{-/-}$ cells (cf. Figure 4-12). Enrichment on *KLF2* and *MYO* was used as positive and negative control, respectively (mean ± SEM, n=3).

Statistical analysis was performed via 1way Anova using Dunnett's multiple comparisons test **(D-E)** HEK293 cells carrying an integrated Upstream Activation Sequence (UAS) that binds Gal4 either contained a tetracycline-inducible expression cassette for EZH2 fused to the Gal4 DNA binding domain, or a control gene (Hansen et al, 2008). Upon tetracycline addition and transient overexpression of MDM2, protein levels were checked via immunoblot analysis **(D)** ChIP was performed with antibodies to EZH2 and Myc, followed by amplification of the UAS **(E)**. Figure data and legend also published in Wienken et al, *under review*.

With the results gathered, we identified a new role for MDM2 in direct gene regulation through the interaction with PRC2 members on the target gene promoters. As of now, these findings did not explain the underlying molecular mechanism of this new function of MDM2. Gene repression through the PcG family follows a widely accepted model in which the distribution of H3K27me3 is followed by H2AK119 monoubiquitination through PRC1 (Cao et al, 2005). Via the usage of targeted ChIP and ChIP-sequencing (ChIP-Seq) experiments in Mdm2 ko MEFs, we investigated whether Mdm2 is involved in this epigenetic interplay.

4.4 Mdm2 supports H3K27me3 on target gene promoters without affecting Ezh2 levels

4.4.1 H3K27me3 on previously identified target gene promoters depends on Mdm2

According to Figure 4-3 specific target genes were de-repressed in total Mdm2 ko MEFs as well as C462A ki (CA/CA) MEFs which are deficient of Mdm2 RING finger domain function. These genes were proven to be direct targets of EZH2 repression (cf. Figure 4-6) and we evaluated whether loss of Mdm2 leads to any H3K27me3 promoter level changes. All three Mdm2 target genes, *Hoxb13, Hoxc13* and *Hhip,* were deprived of H3K27me3 promoter levels in $p53^{-/-}$ $Mdm2^{-/-}$- as well as in $p53^{-/-}$ $Mdm2^{CA/CA}$ MEFs (Figure 4-16 A and A2). This loss of H3K27me3 was not visible at the control genes Evx1 (positive control) and GAPDH (negative control) (Figure 4-16 A2). Loss of H3K27me3 was also not accompanied by a significant change of EZH2 occupancy on these target gene promoters (Figure 4-16 B and B2).

In order to rule out that the effects of Mdm2/PRC2 target gene co-regulation and the loss of H3K27me3 levels on target gene promoters were due to changes in total EZH2 protein levels, immunoblot analysis was performed. According to Figure 4-16 C there are only minor changes between EZH2 and H3K27me3 protein levels comparing $p53^{-/-}$ MEFs with $p53^{-/-}$ $Mdm2^{-/-}$ MEFs as well as $p53^{-/-}$ $Mdm2^{CA/CA}$ MEFs. Co-IP analysis of the PRC2 proteins Suz12

and Ezh2 also ruled out that loss of Mdm2 de-stabilized PRC2 complex formation (Wienken et al, *under review*). To get a broader view of the H3K27me3 epigenetic signature in the p53$^{-/-}$ Mdm2$^{-/-}$ MEFs, DNA from immunoprecipitates was sequenced and analyzed in an experimental procedure called ChIP-Seq (cf. 3.2.2.3).

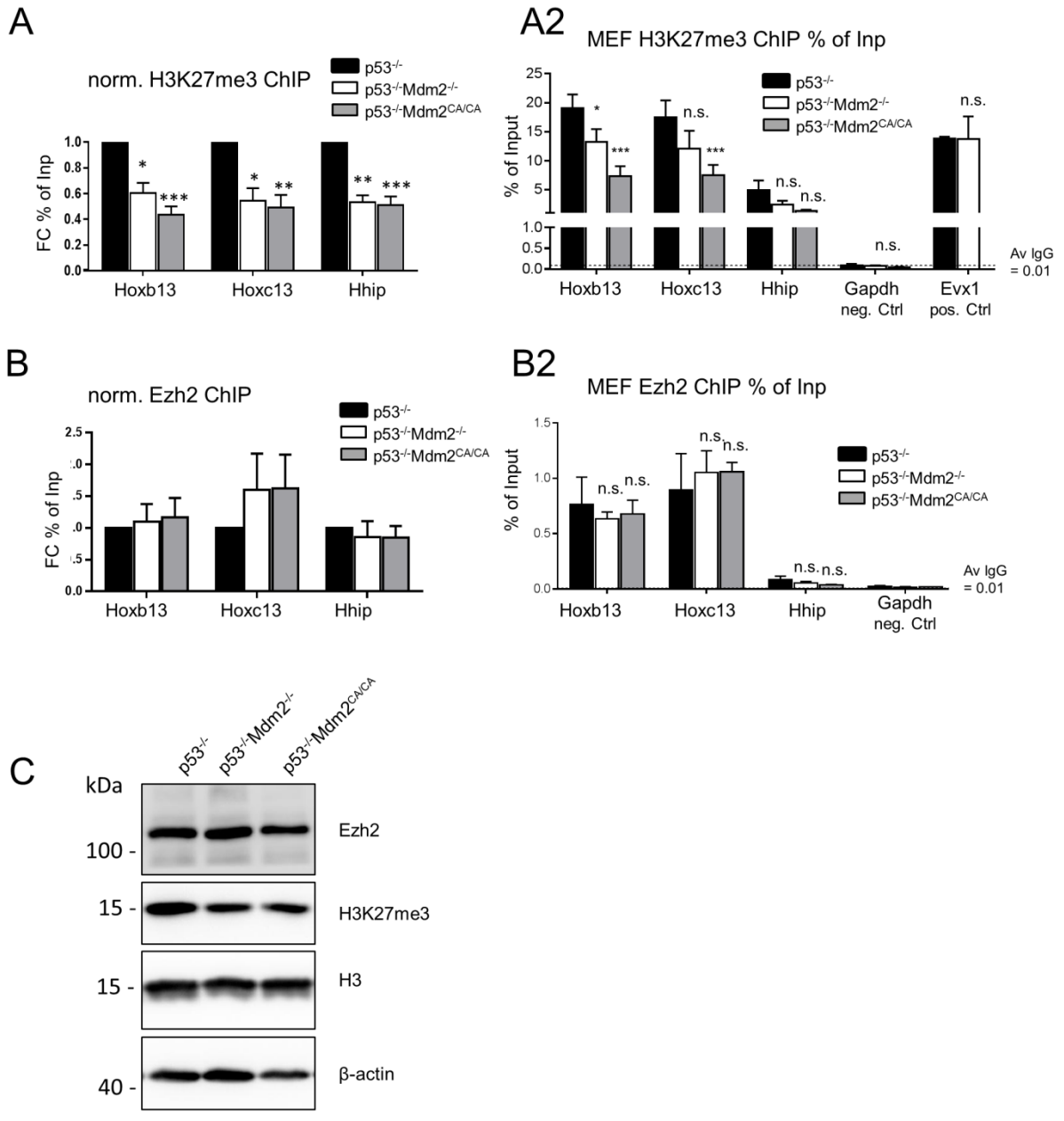

Figure 4-16 Loss of Mdm2 destabilizes histone H3K27 trimethylation (H3K27me3) at Mdm2/PRC2 target gene TSSs without affecting global EZH2 protein levels.

(A-B) p53$^{-/-}$, p53$^{-/-}$ Mdm2$^{-/-}$ and p53$^{-/-}$ Mdm2$^{CA/CA}$ MEFs were used for targeted H3K27me3 (A) and EZH2 ChIP (B). ChIP levels around the TSS of Mdm2/PRC2 target genes (cf. Figure 4-3)

were identified via qRT-PCR analysis and are shown as % of Input relative to $p53^{-/-}$ cells (A and B) together with the corresponding % of Inp values with suitable control genes in A2 and B2. Corresponding % of Input data is also given to prove enrichment of ChIP signal above IgG background. **(C)** Total protein levels of EZH2 and H3K27me3 in $p53^{-/-}$, $p53^{-/-}$ $Mdm2^{-/-}$ and $p53^{-/-}$ $Mdm2^{CA/CA}$ MEFs were evaluated using immunoblot analysis. (H3K27me3 targeted ChIP: mean ± SEM, n=6; EZH2 targeted ChIP: mean ± SEM, n=4.). Figure data and legend also published in Wienken et al, *under review*.

4.4.2 Loss of Mdm2 leads to H3K27me3 removal on target gene TSSs

Sequencing of H3K27me3 ChIP material was conducted by the Transcriptome Analysis Laboratory (TAL) in Göttingen using single end 51 bp sequencing. Mapped fastq files were investigated for peak enrichment using MACS2 in Galaxy and aggregation around the TSS of known genes was done on the Galaxy / deepTools server using UCSC TSS region maps (cf. 3.2.2.4) (Blankenberg et al, 2010; Giardine et al, 2005; Goecks et al, 2010; Karolchik et al, 2004; Ramírez et al, 2014). There was no remarkable change in the general distribution of H3K27me3 around the TSS of known genes comparing $p53^{-/-}$ and $p53^{-/-}$ $Mdm2^{-/-}$ MEFs (Figure 4-17 A). A more sophisticated proof of differential methylation was done using the Biocite DiffBind analysis in R (Stark & Brown, 2011). The differentially methylated regions that were detected via DiffBind localized around transcriptional start sites (Figure 4-17 B). On average, the H3K27me3 signal decreased upon loss of Mdm2 (Figure 4-17 C, all regions). Only a subset of regions were found to add up H3K27me3 (double ko (dko) >single ko (sko)), whereas most regions were significantly deprived of H3K27me3 in the absence of Mdm2 (sko>dko). Aggregating the identified differentially methylated regions around the TSS of their corresponding genes mirrored the same behavior (Figure 4-17 D).

4.4.3 Mdm2 target gene expression is repressed by H3K27me3

Since H3K27me3 is a repressive mark for gene expression, the H3K27me3 status from $p53^{-/-}$ and $p53^{-/-}$ $Mdm2^{-/-}$ MEFs was correlated with the previously detected differential gene expression pattern (cf. Figure 4-3). According to literature and the results obtained, we expected a loss of H3K27me3 on upregulated genes. Indeed, genes that were induced upon loss of Mdm2 were deprived of H3K27me3 whereas genes that were downregulated increased their H3K27me3 levels to some extent (Figure 4-17 E).

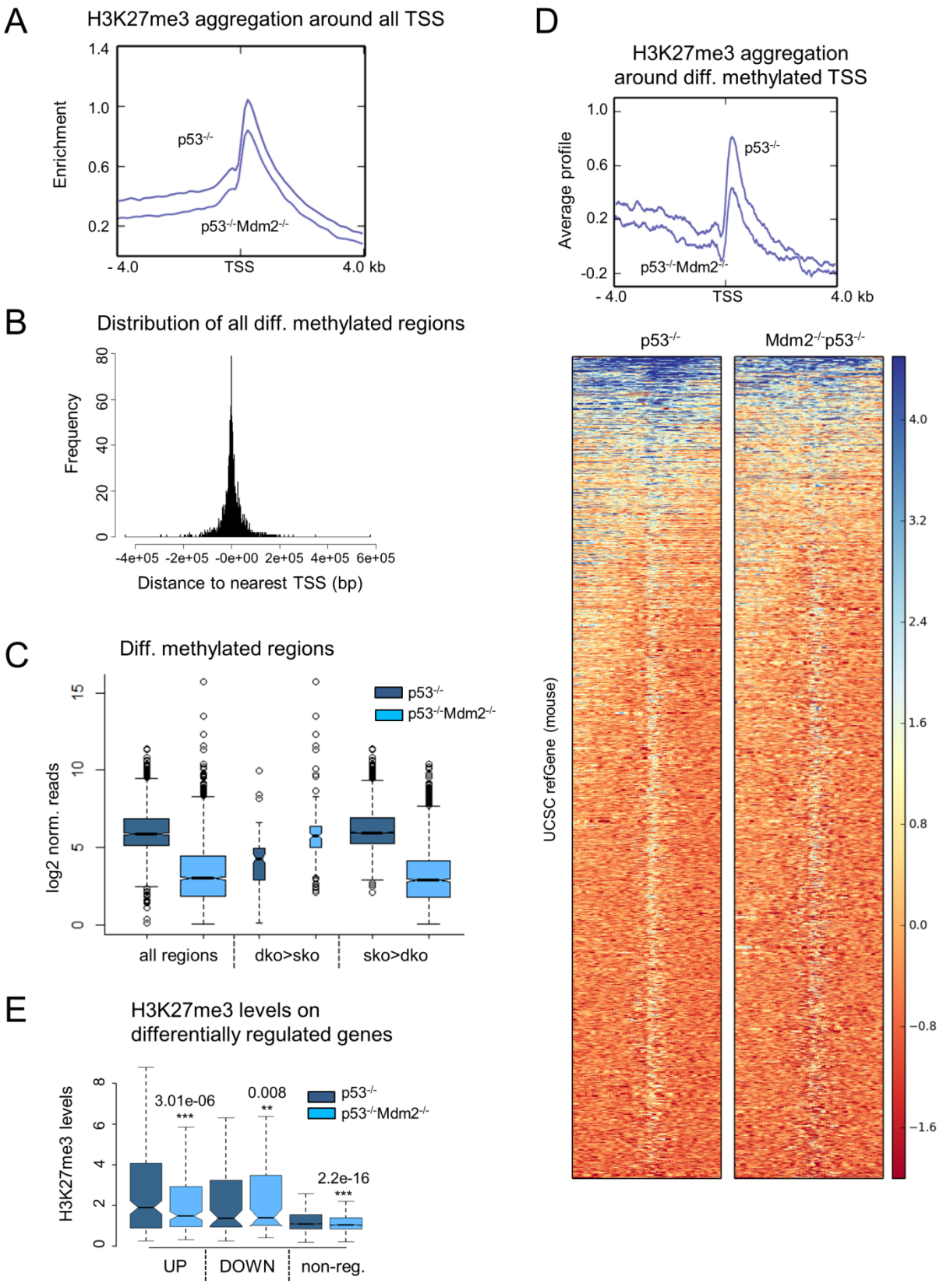
A
H3K27me3 aggregation around all TSS
Enrichment
1.4
1.0
0.6
0.2
p53-/-
p53-/-Mdm2-/-
- 4.0
TSS
4.0 kb
B
Distribution of all diff. methylated regions
Frequency
80
60
40
20
0
-4e+05 -2e+05 -0e+00 2e+05 4e+05 6e+05
Distance to nearest TSS (bp)
C
Diff. methylated regions
log2 norm. reads
15
10
5
0
p53-/-
p53-/-Mdm2-/-
all regions
dko>sko
sko>dko
D
H3K27me3 aggregation around diff. methylated TSS
Average profile
1.0
0.6
0.2
-0.2
p53-/-
p53-/-Mdm2-/-
- 4.0
TSS
4.0 kb
p53-/-
Mdm2-/-p53-/-
UCSC refGene (mouse)
4.0
3.2
2.4
1.6
0.8
0.0
−0.8
−1.6
E
H3K27me3 levels on differentially regulated genes
H3K27me3 levels
8
6
4
2
0
3.01e-06
***
0.008
**
2.2e-16
***
p53-/-
p53-/-Mdm2-/-
UP
DOWN
non-reg.

Figure 4-17 Mdm2 is required for histone H3 trimethylation at K27 (H3K27me3) on various transcription start sites (TSSs).

(A) H3K27me3 ChIP DNA from $p53^{-/-}$ and $p53^{-/-}$ $Mdm2^{-/-}$ MEFs (cf. Figure 4-16 A) was subjected to next generation sequencing and aggregated around the TSS regions of known genes. **(B)** Differentially methylated sites were identified and localized according to their distance to the nearest TSS (Bioconductor packages DiffBind (Stark & Brown, 2011) and ChIPpeakAnno (Zhu et al, 2010)). **(C)** Log2 normalized reads of differentially methylated regions show methylation change of all identified regions as well as discrimination of the regions increased (dko>sko) or decreased (sko>dko) in $p53^{-/-}$ $Mdm2^{-/-}$ MEFs (sko: $p53^{-/-}$; dko: $p53^{-/-}$ $Mdm2^{-/-}$; boxplot widths corresponds to number of identified regions). **(D)** H3K27me3 signal is shown in an aggregation plot around differentially methylated transcriptional start sites that were identified in (C). **(E)** In comparison with the gene expression levels (RNA-Seq; cf. Figure 4-3) relative H3K27me3 enriched genomic sites for either upregulated (UP), downregulated (DOWN) or non-regulated (non-reg.) genes were evaluated (comparing $p53^{-/-}$ $Mdm2^{-/-}$ to $p53^{-/-}$ MEFs) and are presented as boxplots. (H3K27me3 ChIP-Seq n=4). For ChIP-Seq and DiffBind data see also Table S2 and S7, respectively, in Wienken et al, *under review*. Figure data and legend also published in Wienken et al, *under review*.

4.5 Mdm2 enhances H2AK119ub1 without affecting RING1B levels

The influences of Mdm2 on H3K27me3 stabilization were meaningful in respect to the repression of target genes in MEF cells. However, these findings did not reveal anything about the direct functions of Mdm2 in this context. From the CA/CA (C462A ki) MEF data we knew that Mdm2 gene regulatory function was dependent on its ubiquitin ligase activity (cf. Figure 4-3). Therefore, ubiquitination of PRC2 proteins was assessed after overexpression and knock down of Mdm2 but no conclusive results were withdrawn.

Next to PRC2 protein ubiquitination, the histones themselves are a possible target for ubiquitination (cf. 2.2.2). In fact, Minsky and colleagues published that Mdm2 monoubiquitinates histone H2A *in vitro* (Minsky & Oren, 2004). H2AK119 monoubiquitination is usually carried out by the PRC2 complex partner PRC1 and its core enzyme Ring1b (cf. 2.3.2) (Voncken et al, 2003). Thus, we asked whether Mdm2 also stabilizes or enhances H2AK119ub1 in our cell systems and whether it thereby affected the PRC1.

4.5.1 Mdm2 maintains H2AK119ub1 at target genes without affecting Ring1B

According to results from targeted ChIP, a total Mdm2 loss or loss of E3 ubiquitin ligase function significantly reduced the levels of H2AK119ub1 genes on target gene promoters (Figure 4-18 A and A2). These changes were also detected on the positive and negative

control genes Evx1 and Tuba1a (Figure 4-18 A2). However, these control genes did not change their general expression levels in the ko or ki MEFs according to RNA-Seq data from Figure 4-3. The decrease of H2AK119ub1 was not a result of Ring1b loss but was rather accompanied by an increase of Ring1b signal (Figure 4-18 B and B2). Similar results were obtained from HCT116 $p53^{-/-}$ cells depleted of MDM2. Previously identified target genes (cf. Figure 4-12) were decreased in their H2AK119ub1 promoter levels but did not show any change of RING1B levels (Figure 4-18 C-D)

As before, we also investigated for changes in H2AK119ub1 and Ring1b protein levels, both in MEFs and HCT116 $p53^{-/-}$ cells. Immunoblots in Figure 4-18 F and G displayed only minor changes of these proteins in MEFs (F) and no change in HCT116 $p53^{-/-}$ cells (G). Again, these results led us to analysis of the global H2AK119ub1 dependence on Mdm2 and sequenced targeted ChIP DNA as described before (cf. paragraph 3.2.2.4).

4.5.2 H2AK119ub1 levels are enhanced by Mdm2 on the TSS of known genes

After peak calling, global aggregates around the TSS of all known genes were generated from H2AK119ub1 ChIP-Seq signals. According to Figure 4-19 A, Mdm2 stabilizes H2AK119ub1 on gene promoters, since the general signal is decreased in its absence. In concordance, DiffBind analysis revealed on average a reduced H2AK119ub1 signal along all differentially ubiquitinated sites (Figure 4-19 B). As it was detected for H3K27me3, most of these differentially ubiquitinated regions localized around the TSS of known genes (Figure 4-19 C).

4.5.3 Mdm2 target gene activation is accompanied by loss of H2AK119ub1.

According to the ChIP-Seq data presented in Figure 4-19 A and B, we speculated that gene de-repression observed in Figure 4-3 would be accompanied by a loss of H2AK119ub1. Indeed, upregulated (UP) target genes were significant deprived of H2AK119ub1. Moreover, not only these genes were reduced in H2AK119ub1 but also all upregulated and all non-regulated genes (Figure 4-19 D). This was consistent with the aggregation plot in Figure 4-19 A which presented with a rather general drop of H2K119ub at all known TSSs.

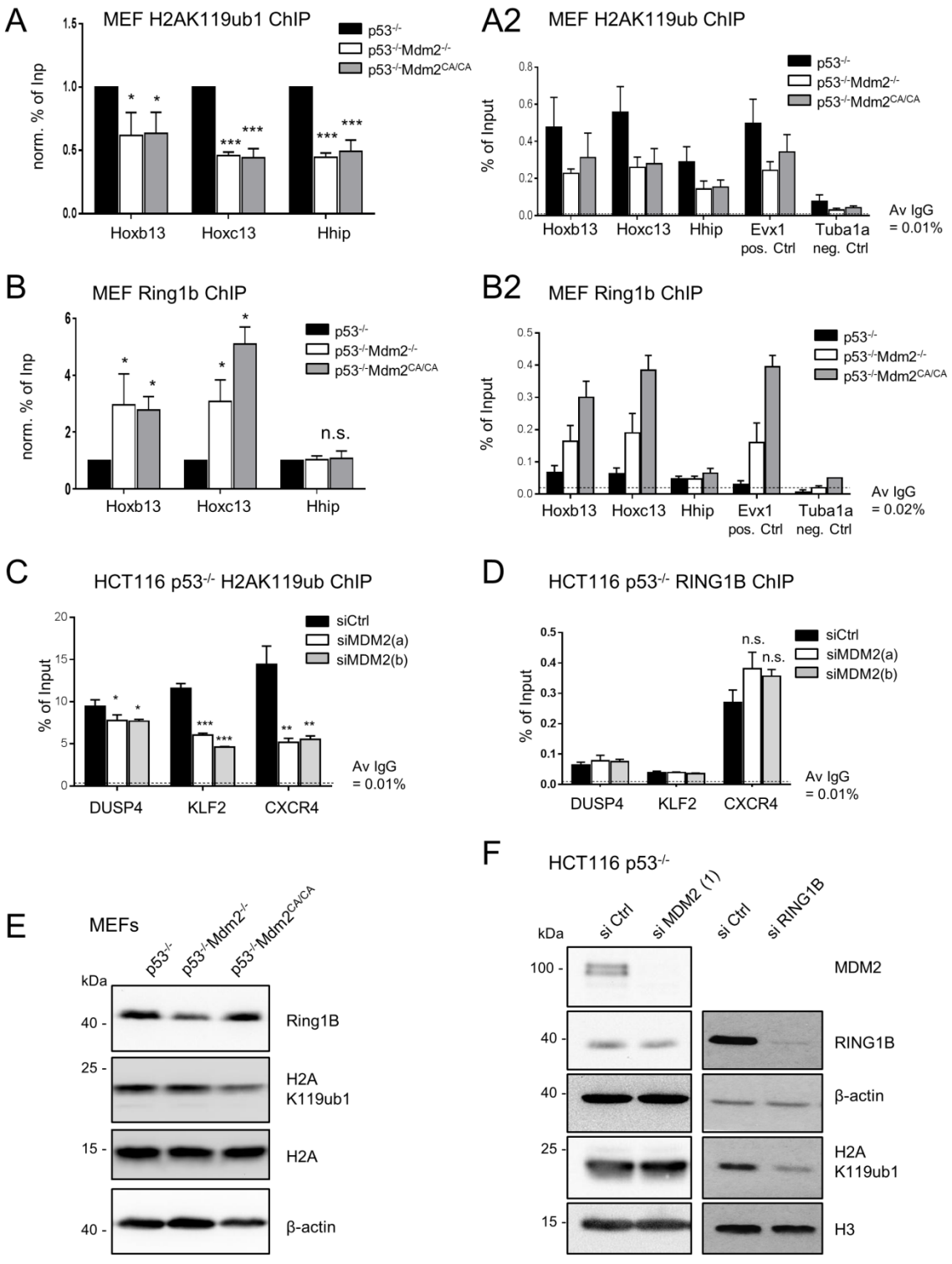

Figure 4-18 Loss of Mdm2 de-stabilizes H2AK119 monoubiquitination (H2AK119ub1) at Mdm2/PRC2 target gene TSSs without affecting global levels of RING1B.

(A-B) $p53^{-/-}$, $p53^{-/-}$ $Mdm2^{-/-}$ and $p53^{-/-}$ $Mdm2^{CA/CA}$ MEFs were used for targeted H2AK119ub1 (A) and RING1B ChIP (B). ChIP levels around the TSS of Mdm2/PRC2 target genes (cf.

Figure 4-3) were identified via qRT-PCR analysis and are shown as fold change of % of Input relative to $p53^{-/-}$ cells (A and B). In addition corresponding % of Inp values over IgG background with suitable control genes in A2 and B2 are given. **(C-D)** HCT116 $p53^{-/-}$ cells were depleted of MDM2 for 96 h using double siRNA transfection. H2AK119ub1 (C) and RING1B (D) levels around the TSS of Mdm2/PRC2 target genes (cf. Figure 4-12) were identified via qRT-PCR analysis and are shown as % of Input. **(E-F)** Total levels of RING1B and H2AK119ub1 protein in $p53^{-/-}$, $p53^{-/-}$ $Mdm2^{-/-}$ and $p53^{-/-}$ $Mdm2^{CA/CA}$ MEFs (E) as well as HCT116 $p53^{-/-}$ cells (F) were evaluated by Immunoblot analysis. (H2AK119ub1 ChIP n=4; RING1B ChIP: mean ± SEM, n=3 for $p53^{-/-}$ and $p53^{-/-}$ $Mdm2^{-/-}$ MEFs, n=2 for $p53^{-/-}$ $Mdm2^{CA/CA}$ MEFs; ChIP data from HCT116 $p53^{-/-}$ cells: n=3).Figure data and legend also published in Wienken et al, *under review*.

4.6 Interdependence and functional classification of Mdm2 enhanced epigenetic modifications

4.6.1 Differentially methylated and ubiquitinated regions overlap

Absence of Mdm2 significantly decreased H3K27me3 on 1441 regions and ubiquitination on 2134 regions according to ChIP-Seq DiffBind analysis (cf. Figure 4-17 C, Figure 4-19 B). Many different publications have illustrated a dependence of these two modifications on each other (see paragraph 2.3.3) which is why we analyzed an overlap of the detected differentially methylated and ubiquitinated regions.

For the calculation, differentially methylated and ubiquitinated TSS regions were isolated and overlapping calculation was done using the Bioconductor ChIPpeakAnno package (Zhu et al, 2010) as well as the intersection function of the Galaxy / deepTools server mentioned before. Iin order to achieve a conclusive result that was true even for different algorhythmic parameters I used the two approaches. Both methods presented withed the same trend and data shown here were derived from the ChIPpeakAnno package calculation. According to Figure 4-20 A, most of the differentially ubiquitinated TSS regions (green) overlapped with the differentially methylated ones (blue). When distinguishing between increased or decreased signals in the $p53^{-/-}$ $Mdm2^{-/-}$ double ko (dko) compared to the $p53^{-/-}$ single ko (sko) MEFs, the methylation and ubiquitination was either simultaneously decreased or enriched.

Genes of the Hox cluster were initially found to be repressed by Mdm2 (cf. Figure 4-3 B). Via the IGV genome browser tool (Robinson et al, 2011), H2AK119ub1 and H3K27me3 ChIP signals were visualized along the Hoxc locus (Figure 4-20 B-C). Overall TSS signals from $p53^{-/-}$ $Mdm2^{-/-}$ MEFs were decreased along the whole locus when compared to $p53^{-/-}$ MEFs. For more detail, the TSS of Hoxc10 is presented as zoomed-in version (Figure 4-20B).

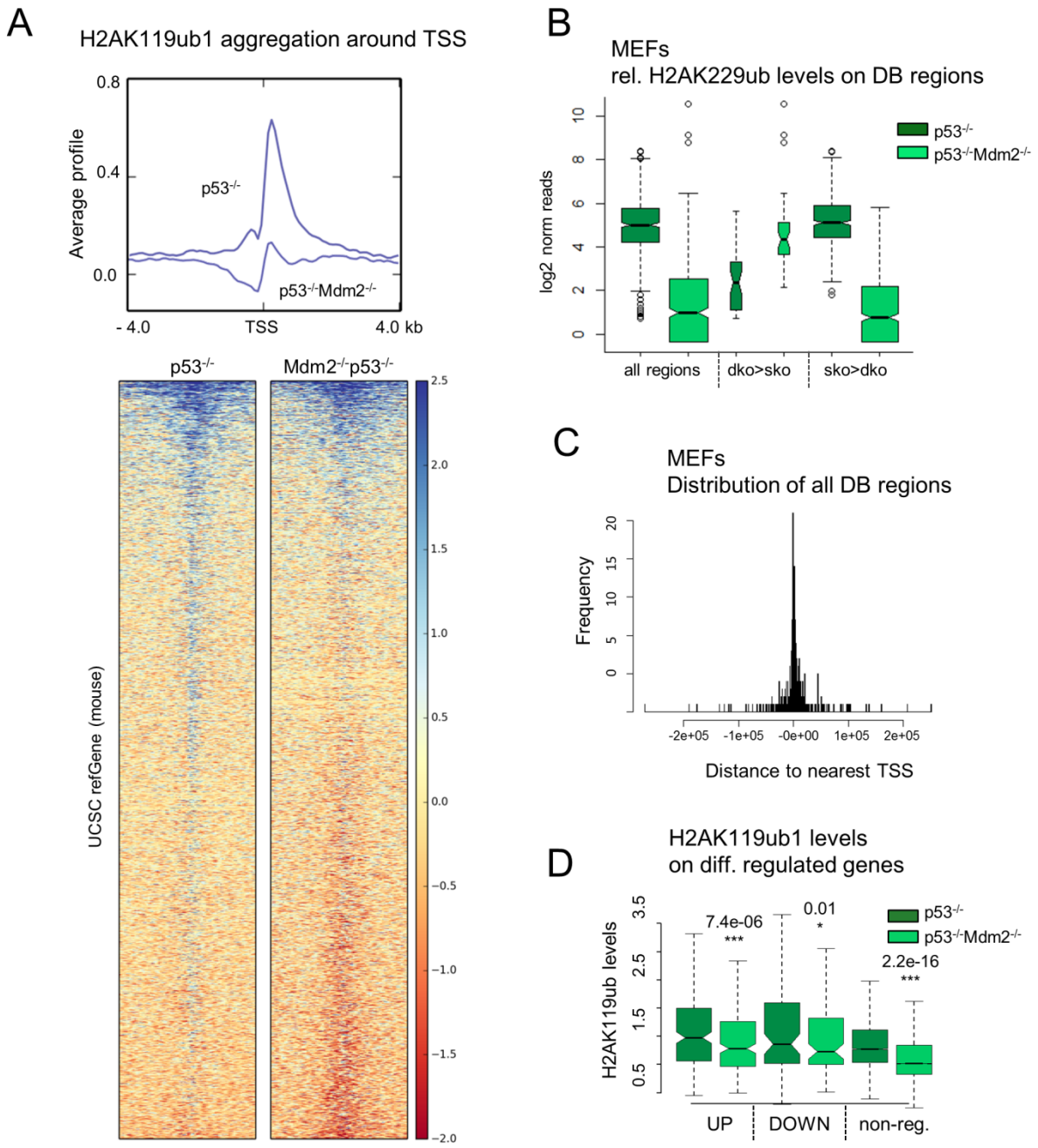

Figure 4-19 Mdm2 is required for the global histone H2A monoubiquitination at K119 (H2AK119ub1) at transcription start sites (TSSs) of known genes.

(A) H2AK119ub1 ChIP DNA from p53$^{-/-}$ and p53$^{-/-}$ Mdm2$^{-/-}$ MEFs was subjected to next generation sequencing, and aggregated around TSS regions of known genes. **(B)** Differentially ubiquitinated sites were identified and log2 normalized reads show the methylation changes of all identified regions as well as discrimination of the regions increased (dko>sko) or decreased (sko>dko) in p53$^{-/-}$ Mdm2$^{-/-}$ MEFs (sko: p53$^{-/-}$; dko: p53$^{-/-}$ Mdm2$^{-/-}$; boxplot widths corresponds to number of identified regions, Bioconductor package DiffBind (Stark & Brown, 2011)). **(C)** Differentially ubiquitinated regions were localized

according to their distance to the nearest gene TSS (Bioconductor package ChIPpeakAnno (Zhu et al, 2010)). **(E)** In comparison with the gene expression levels (RNA-Seq, Figure 4-3), relative H2AK119ub1 levels for either upregulated (UP), downregulated (DOWN) or non-regulated (non-reg.) genes were evaluated (comparing p53$^{-/-}$ Mdm2$^{-/-}$ to p53$^{-/-}$ MEFs) and are presented as boxplots. (H2AK119ub1 ChIP-Seq: n=4). For ChIP-Seq and DiffBind data see also Table S2 and S7, respectively, in Wienken et al, *under review*. Figure data and legend also published in Wienken et al, *under review*.

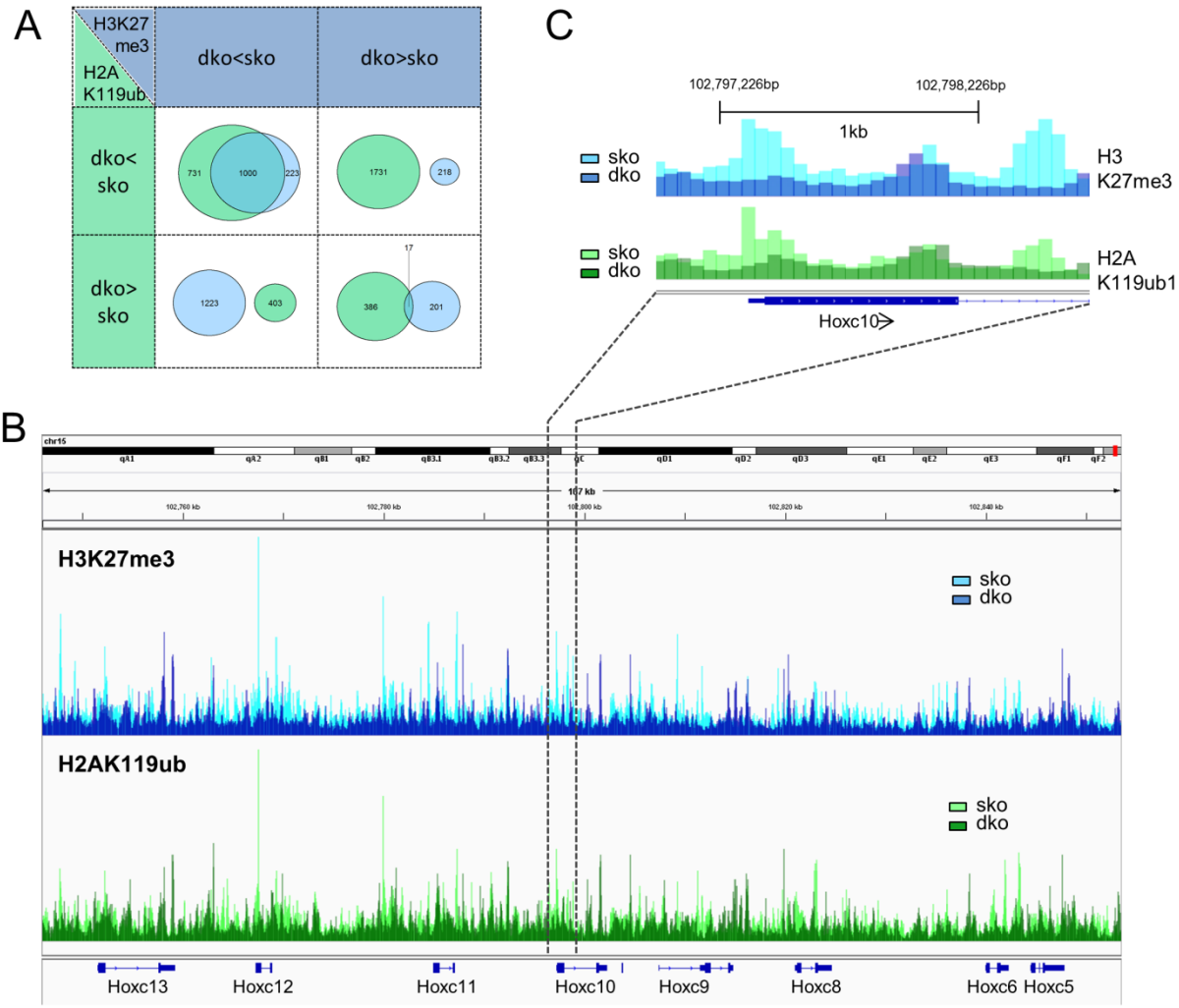

Figure 4-20 Loss of Mdm2 remodels the Polycomb-mediated epigenetic landscape, leading to the simultaneous loss of H2AK119ub1 and H3K27me3 on PRC2 target gene promoters.

(A) Overlap of differentially methylated and ubiquitinated regions from H3K27me3 and H2AK119ub1 ChIP-Seq analysis (cf. Figure 4-17 and Figure 4-19); it was distinguished between sites which are decreased (dko<sko) or increased (dko>sko) for H3K27me3 and H2AK119ub1 in p53$^{-/-}$ Mdm2$^{-/-}$ in comparison to p53$^{-/-}$ MEFs. (B-C) Genomic binding profiles for H3K27me3 and H2AK119ub1 were generated along the Hoxc locus using the IGV genome browser. As an example, the TSS of HoxC10 is zoomed in (C). Figure data and legend also published in Wienken et al, *under review*.

4.6.2 Overlapping regions are involved in development and morphogenesis

Differential gene expression in MEF and MSCs was enriched for developmental and morphogenesis relevant gene ontology (cf. Figure 4-4 and Figure 4-10). GREAT analysis offers a tool for the function prediction of cis-regulatory regions via internal gene annotation and was used to identify common biological processes of the differentially methylated and ubiquitinated regions (http://bejerano.stanford.edu/great/public/html/) (McLean et al, 2010). Remarkably, the biological processes that were enriched for both epigenetic modifications were again mainly involved in development and differentiation which further supported the relation between RNA-Seq and ChIP-Seq data from MEF cells (cf. Figure 4-21).

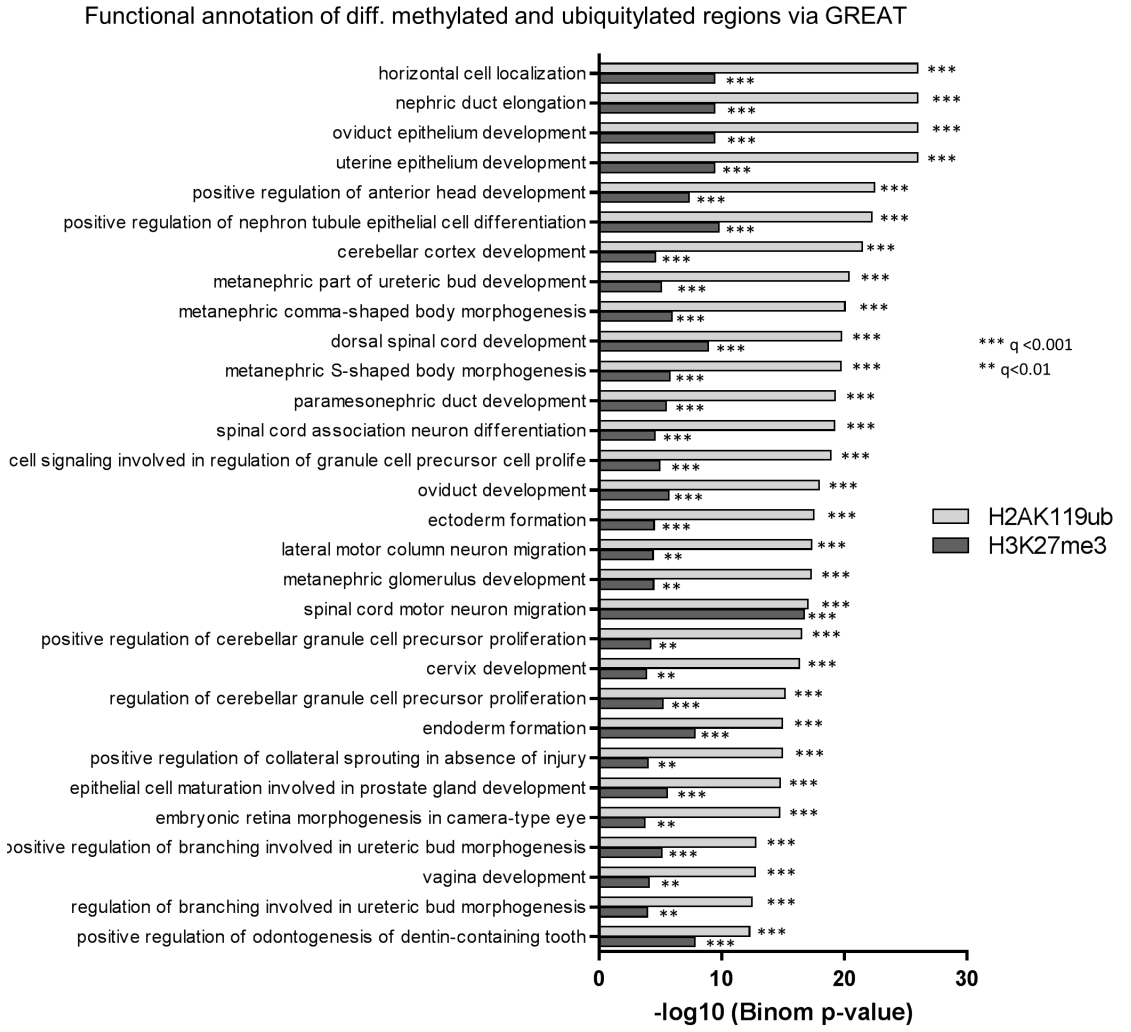

Figure 4-21 Functional annotation of differentially methylated and ubiquitinated regions in p53$^{-/-}$ Mdm2$^{-/-}$ MEFs.

Cis-regulatory regions were predicted from all differentially methylated (cf. Figure 4-17 C) and ubiquitinated (cf. Figure 4-19 B) regions using GREAT and overlapping biological processes for both chromatin modifications are shown. For the total analysis see Table S7 in Wienken et al, *under review*. Figure data and legend also published in Wienken et al, *under review*.

4.7 Mdm2 cooperates with Ring1b in gene repression and cell survival

According to paragraph 4.5, Mdm2 stabilizes H2AK119ub1 levels. The major ubiquitin ligase for H2AK119 is Ring1b, the enzymatic component of the PRC1. In order to identify, whether there is a difference between Mdm2 and Ring1b regulated genes or whether the two factors might even support each other, Ring1b was knocked down via shRNA in $p53^{-/-}$ and $p53^{-/-}$ $Mdm2^{-/-}$ MEFs and target gene expression was assessed. According to the immunoblot in Figure 4-22 A, shRNA kd efficiently deprived the cells of Ring1b and also efficiently depleted total H2AK119ub1 (Figure 4-22 A). The Hox genes *Hoxb13, Hoxc10* and *Hoxc13* were induced upon loss of Ring1b in both cell lines but to a much higher extent in the $p53^{-/-}$ $Mdm2^{-/-}$ cells (Figure 4-22 B). This supported the idea that Ring1b and Mdm2 cooperatively regulate some of their target genes and may therefore also substitute each other. Remarkably, cells that were deprived of both, Mdm2 and Ring1b ceased their proliferation which was quantified by seeding equal amounts of cells and performing Hoechst staining after 48 h of cell growth (Figure 4-22 C-D).

A similar phenotype was detected in HCT116 $p53^{-/-}$ cells after loss of MDM2 and RING1B in combination. Upon 96 h of knock down (Figure 4-23 A), many cells underwent cell cycle arrest or apoptosis (Figure 4-23 B and quantified in C). Fortunately, it was still possible to yield enough cells for ChIP experiments. Upon loss of both, MDM2 and RING1B, previously identified target genes were significantly further deprived of H2AK119ub1 when compared to loss of either MDM2 or RING1B (Figure 4-23 D, cf. Figure 4-12). According to previous experiments, MDM2 is recruited by EZH2 to target gene promoters (cf. Figure 4-15). Loss of RING1B also decreased MDM2 promoter levels on target genes but not as significantly as detected for EZH2 (Figure 4-23 E-F).

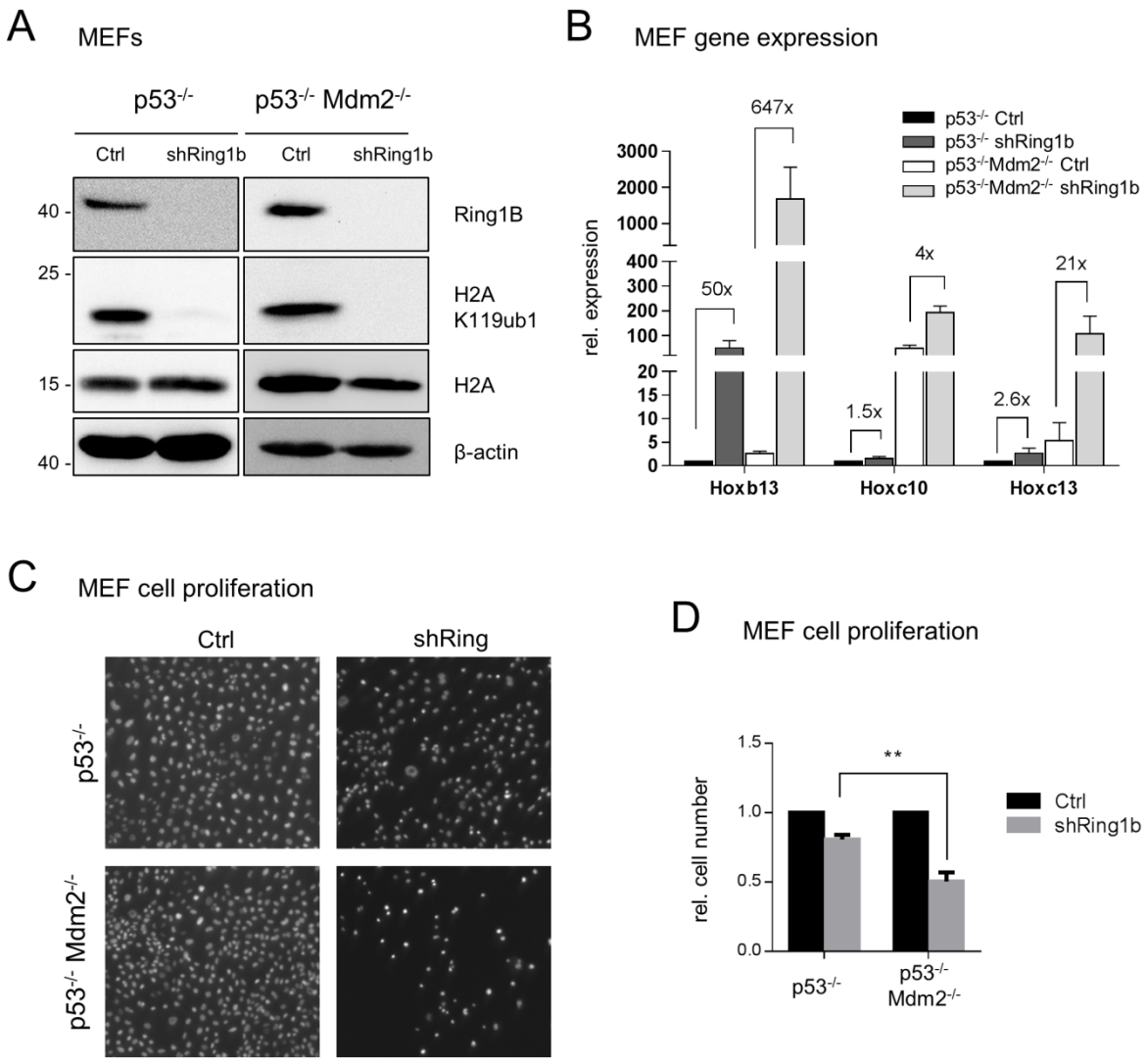

Figure 4-22 Mdm2 and Ring1b cooperatively regulate target gene expression and cell survival in MEFs.

(A) p53$^{-/-}$ and p53$^{-/-}$ Mdm2$^{-/-}$ MEFs were transduced with a shRNA targeting Ring1b. Knock down efficiency was assed via immunoblot. **(B)** Mdm2 target gene expression was assessed using qRT-PCR analysis (cf. Figure 4-3, mean ± SEM, n=3) **(C-D)** The cells from A were plated in equal amounts and grown for 48 h. Subsequent Hoechst staining and fluorescence microscopy with quantitative image analysis was used to quantify cell growth (Celigo cytometer, cf. 3.2.1.10, mean ± SEM, n=5). Figure data and legend also published in Wienken et al, *under review*.

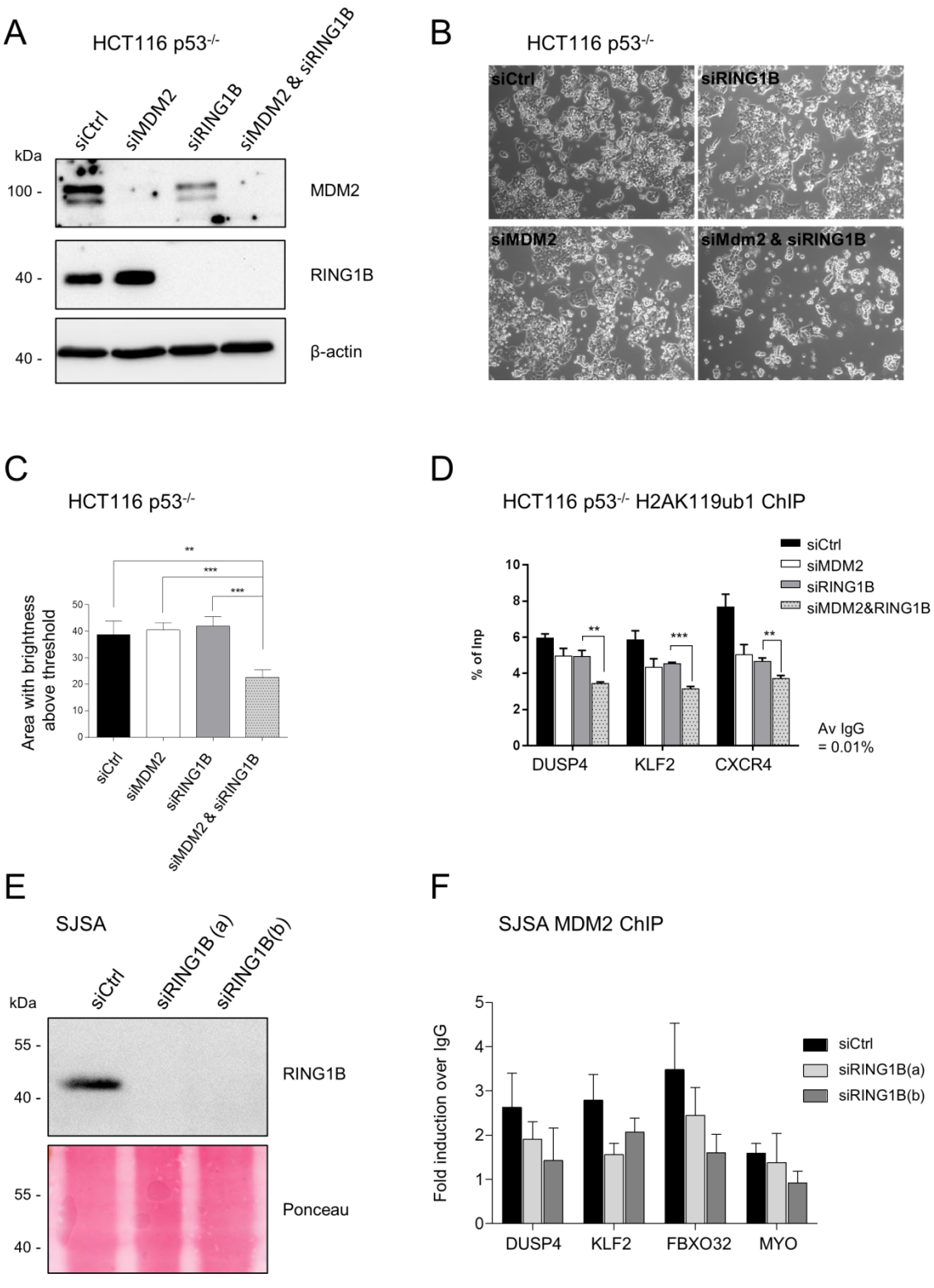

Figure 4-23 MDM2 and RING1B cooperatively ensure cell survival of HCT116 p53$^{-/-}$ cells and ubiquitinate H2AK119.

(A) HCT116 p53$^{-/-}$ cells were depleted of Mdm2 and RING1B for 96h. **(B-C)** For the second knock down equal amounts of cells were plated together with siRNA. After the total kd time of 96 h, cells were imaged using brightfield microscopy (B) and confluence was measured via ImageJ (C; mean ± SEM, n=4). **(D)** Cells treated with the same kd procedure were used for targeted H2AK119ub1 ChIP, amplifying promoter regions of Mdm2/PRC2 target genes described before (cf. Figure 4-12 C, mean ± SEM, n=3). **(E-F)** SJSA cells were depleted of Ring1b and MDM2 recruitment to target gene promoters was analyzed via ChIP (mean ± SEM, n=3; detected differences are not significant). Figure data and legend also published to some extent in Wienken et al, *under review*.

4.8 Mdm4 coregulates Mdm2/PRC2 target genes

4.8.1 The expression of multiple genes is dependent on both, Mdm2 enzymatic function and Mdm4

Mdm2 is not the only Mdm protein encoded in murine and human cells. Its homologue Mdm4 can act in a redundant but also non-redundant manner (Barboza et al, 2008; Grier et al, 2006; Steinman et al, 2005) and we assessed, whether Mmd4 can overtake at least some of the Mdm2 gene regulatory functions described in the last paragraphs. So far we knew that Mdm2 represses PRC2 target genes in different cell systems through stabilization of H3K27me3 and H2AK119ub1. Mdm4 is therefore not able to substitute these functions in an Mdm2 loss of function setting. Mdm4 does not contain intrinsic E3 ubiquitin ligase function but can increase Mdm2-mediated ubiquitination through dimerization (Linares et al, 2003). We therefore hypothesized that loss of Mdm4 in MEF cells de-represses Mdm2/PRC2 target genes through destabilization of the Mdm2-Mdm4 heterodimer and subsequent loss of H2AK119ub1 and H3K27me3.

RNA from p53$^{-/-}$ Mdm4$^{-/-}$ MEF cells was included in the RNA-Seq analysis from Figure 4-3 and indeed genes regulated by Mdm4, Mdm2 and the RING mutant Mdm2^{C462A} overlapped as indicated in Figure 4-24.

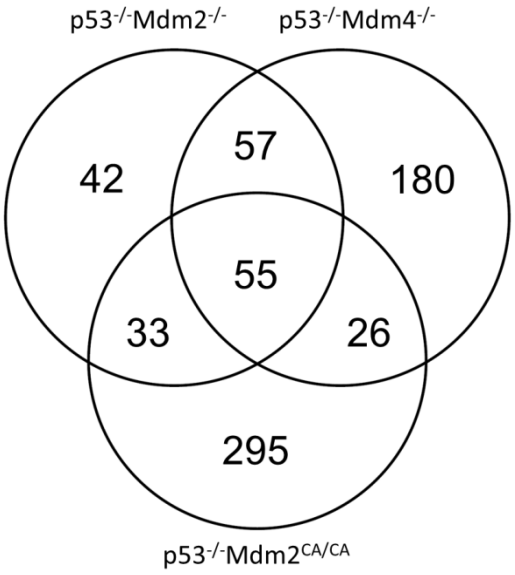

Figure 4-24 Triple Venn diagram of genes regulated in Mdm2$^{-/-}$-, Mdm2$^{CA/CA}$- and Mdm4$^{-/-}$ MEFs.

Differentially regulated genes were identified via DESeq analysis from sequenced RNA of p53$^{-/-}$ Mdm2$^{-/-}$-, p53$^{-/-}$ Mdm2$^{CA/CA}$ and p53$^{-/-}$ Mdm4$^{-/-}$ MEFs in comparison to p53$^{-/-}$ MEFs (cf. Figure 4-3). Overlap of differential gene expression is presented in a triple Venn diagram.

4.8.2 Mdm4 target gene regulation in MEFs is accompanied by loss of H3K27me3

All genes that were significantly deregulated by both, Mdm2 and Mdm4 are visualized in a heatmap in Figure 4-25 A. According to the RNA-Seq data, several previously identified Mdm2 target genes (e.g. *Hoxb13*, *Hhip* and *Eomes*, cf. Figure 4-3 A) were also regulated by Mdm4. It was not possible to verify these results via qRT-PCR since this analysis resulted in only mild induction of some of the Hox genes (Figure 4-25 B). This discrepancy can be caused by biases during RNA library preparation and also due to very low sequencing reads of the corresponding genes, which was at least true for several of the Hox genes.

Nevertheless, we were interested in the H3K7me3 promoter levels because they were diminished before in Mdm2 ko MEFs (cf. Figure 4-16 and Figure 4-17) and indeed detected a comparable decrease (Figure 4-25 C). This decrease was not detectable on the negative Ctrl gene *Gapdh* (Figure 4-25 D). As for p53$^{-/-}$ Mdm2$^{-/-}$ MEFs, EZH2 levels on the promoter of those target genes remained constant. To this end, no significant conclusions were drawn from H2AK119ub1 ChIPs in the p53$^{-/-}$ Mdm4$^{-/-}$ MEFs, since results were not consistent.

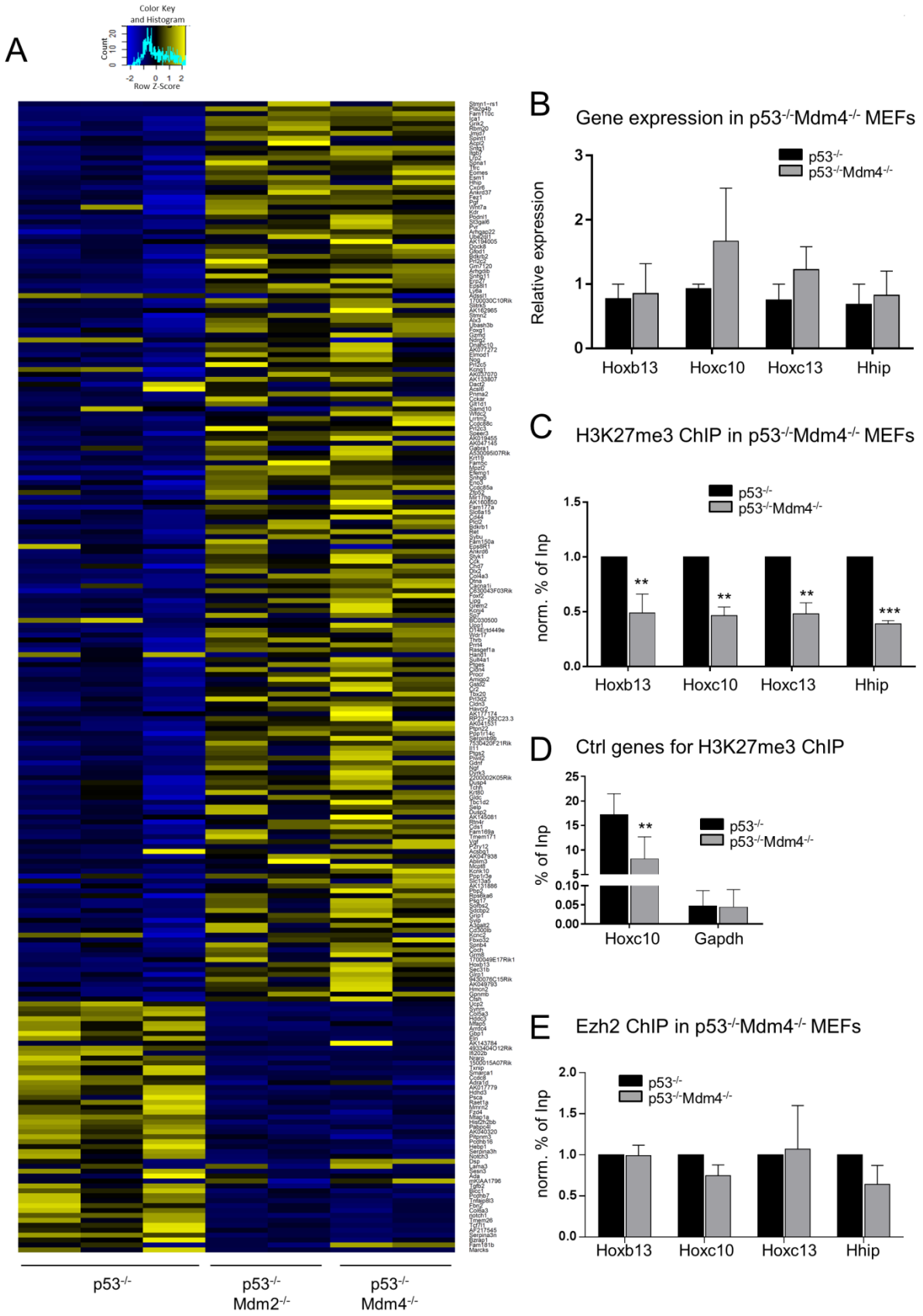
A
Color Key and Histogram
Count
Row Z-Score
p53-/-
p53-/- Mdm2-/-
p53-/- Mdm4-/-
B
Gene expression in p53-/-Mdm4-/- MEFs
Relative expression
p53-/-
p53-/-Mdm4-/-
Hoxb13
Hoxc10
Hoxc13
Hhip
C
H3K27me3 ChIP in p53-/-Mdm4-/- MEFs
norm. % of Inp
D
Ctrl genes for H3K27me3 ChIP
% of Inp
Gapdh
E
Ezh2 ChIP in p53-/-Mdm4-/- MEFs

Figure 4-25 Mdm4 regulates Mdm2 target genes in MEFs to some extent via stabilization of H3K27me3.

(A) $p53^{-/-}$, $p53^{-/-}$ $Mdm2^{-/-}$ and $p53^{-/-}$ $Mdm4^{-/-}$ MEFs were analyzed via next generation RNA-sequencing and differentially expressed genes are shown in a heat map. **(B)** Mdm2 target gene expression (cf. Figure 4-3 B) was evaluated in $p53^{-/-}$ $Mdm4^{-/-}$ MEFs by qRT-PCR (mean ± SEM, n=3). **(C-E)** $p53^{-/-}$ and $p53^{-/-}$ $Mdm4^{-/-}$ MEFs were used for targeted H3K27me3 (C-D) and EZH2 ChIP (E). ChIP levels around the TSS of Mdm2/PRC2 target genes were identified via qRT-PCR analysis and are shown as % of Input relative to $p53^{-/-}$ cells (C, E) together with the corresponding % Inp values for Hoxc10 and with a suitable negative control genes **(D)**.

4.8.3 Mdm4 target genes in MEFs are also involved in stemness and development and are characterized by PRC2 regulation

In concordance to the functional annotation of Mdm2 target genes in MEFs, target genes repressed by Mdm4 were also involved in development and differentiation. No clear accumulation of these gene sets was visible in the activated genes (Figure 4-26 A and B). DAVID analysis of the identified differentially genes confirmed this data, with many maturation-related gene sets in the group of repressed genes and a few in the activated genes (Figure 4-26 C-D).

Since C2 GSEA analysis of the Mdm2 target genes in MEFs, hMSCs and HCT116 cells indicated a connection to PRC2 gene regulation (cf. Figure 4-5, Table 4-1 and Figure 4-13), a possible enrichment was also tested for the $p53^{-/-}$ $Mdm4^{-/-}$ MEFs. According to Table 4-3, genes upregulated upon loss of Mdm4 were targets of PRC2 regulation and were also characterized by the repressive mark, H3K27me3. Fairly reassuring was the appearance of the gene set “MARTORIATI_MDM4_TARGETS_FETAL_LIVER_UP”. Apparently, the genes that were upregulated in our $Mdm4^{-/-}$ MEF system correlated to this gene set which had been identified before to increase its expression upon loss of Mdm4 (Martoriati et al, 2005).

Gene sets downregulated by the loss of Mdm4 were again involved in stemness and also characterized by H3K4me3. This overlap in gene set regulation supported us in the hypothesis that Mdm4 is to some extent involved in the gene regulatory functions of Mdm2.

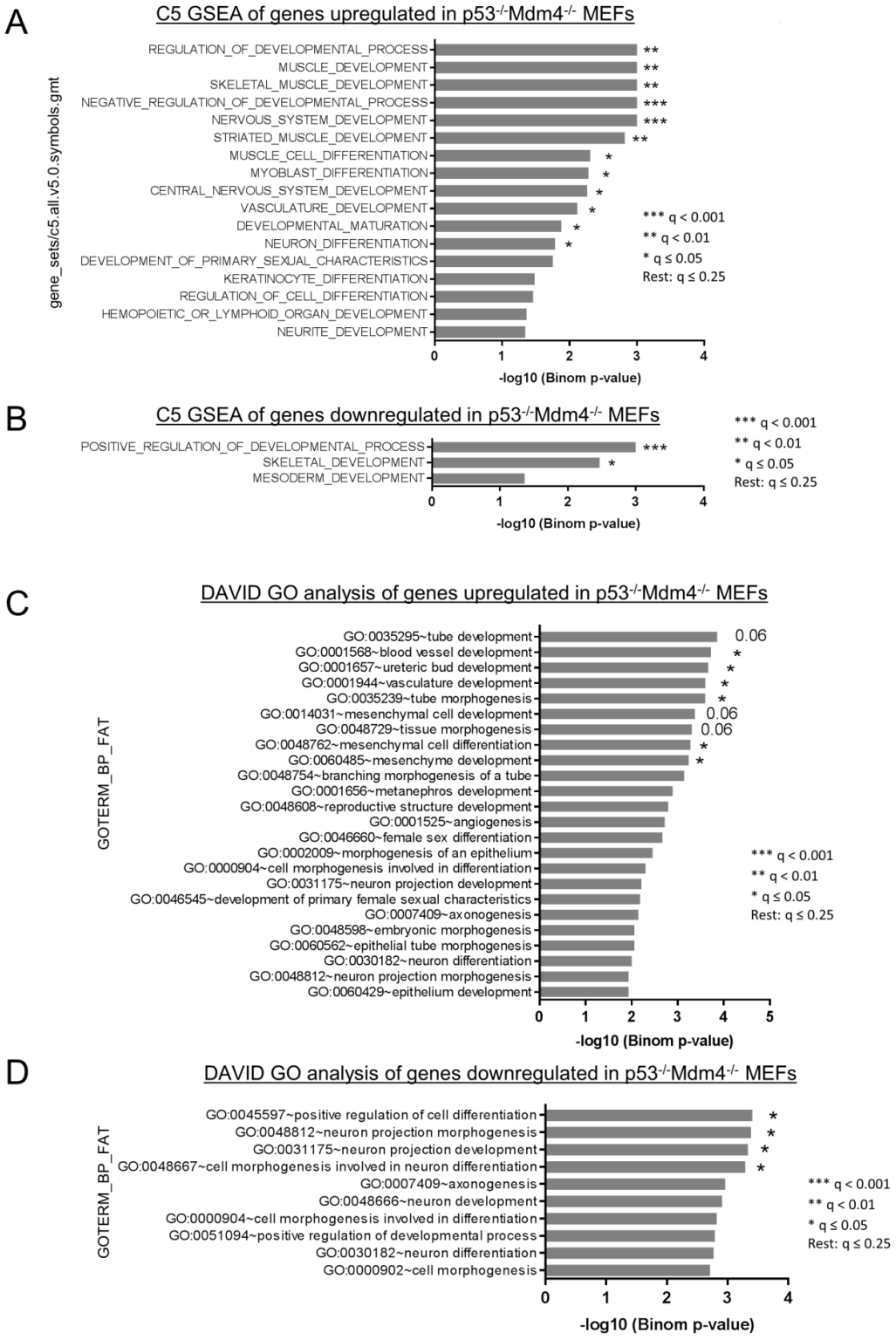

Figure 4-26 GO term analysis of genes regulated by Mdm4 in p53$^{-/-}$ Mdm4$^{-/-}$ MEFs.

(A-B) C5 GSEA was performed based on using normalized RNA-Seq reads comparing p53$^{-/-}$ to p53$^{-/-}$ Mdm4$^{-/-}$ MEFs. Enriched gene sets were filtered as described before (cf. Figure 4-4 A-B) for genes upregulated (A) and downregulated in p53&Mdm2 kd samples

(B). **(C-D)** For comparison, we conducted DAVID annotation analysis from genes that had been identified by DESeq to be differentially regulated in $p53^{-/-}$ $Mdm4^{-/-}$ MEFs in comparison to $p53^{-/-}$ MEFs.

Table 4-3 Mdm4 preferentially regulates stemness related genes controlled by the Polycomb Repressive Complex 2.

(A-B) C2 GSEA based on normalized RNA-Seq reads comparing $p53^{-/-}$ to $p53^{-/-}$ $Mdm4^{-/-}$ MEFs. Enriched gene sets were filtered as described before (cf. Figure 4-5) and are displayed for genes upregulated in $p53^{-/-}$ $Mdm4^{-/-}$ MEFs (A) and genes downregulated in $p53^{-/-}$ $Mdm4^{-/-}$ MEFs (B).

A C2 GSEA of genes upregulated in $p53^{-/-}Mdm4^{-/-}$ MEFs

NAME	NOM p-val	FDR q-val
BOQUEST_STEM_CELL_DN	< 0.001	< 1.16E-05
MIKKELSEN_NPC_HCP_WITH_H3K27ME3	< 0.001	< 1.16E-05
MEISSNER_BRAIN_HCP_WITH_H3K27ME3	< 0.001	< 1.16E-05
MEISSNER_NPC_HCP_WITH_H3K4ME2_AND_H3K27ME3	< 0.001	< 1.16E-05
MEISSNER_NPC_HCP_WITH_H3K4ME3_AND_H3K27ME3	< 0.001	< 1.16E-05
MIKKELSEN_NPC_HCP_WITH_H3K4ME3_AND_H3K27ME3	< 0.001	< 1.16E-05
ACEVEDO_LIVER_CANCER_WITH_H3K27ME3_UP	< 0.001	< 1.16E-05
MIKKELSEN_MCV6_HCP_WITH_H3K27ME3	< 0.001	< 1.16E-05
JAATINEN_HEMATOPOIETIC_STEM_CELL_UP	< 0.001	< 1.16E-05
LIM_MAMMARY_STEM_CELL_UP	< 0.001	< 1.16E-05
HOEBEKE_LYMPHOID_STEM_CELL_UP	< 0.001	< 1.16E-05
MIKKELSEN_ES_ICP_WITH_H3K4ME3_AND_H3K27ME3	< 0.001	< 1.16E-05
SCHAEFFER_PROSTATE_DEVELOPMENT_48HR_UP	< 0.001	< 1.16E-05
PASINI_SUZ12_TARGETS_DN	< 0.001	< 1.16E-05
LU_EZH2_TARGETS_DN	< 0.001	< 1.16E-05
MARTORIATI_MDM4_TARGETS_FETAL_LIVER_UP	< 0.001	< 1.16E-05
OSWALD_HEMATOPOIETIC_STEM_CELL_IN_COLLAGEN_GEL_DN	< 0.001	1.16E-05
IZADPANAH_STEM_CELL_ADIPOSE_VS_BONE_UP	< 0.001	1.85E-05
MIKKELSEN_IPS_WITH_HCP_H3K27ME3	< 0.001	2.18E-05
MIKKELSEN_MEF_ICP_WITH_H3K4ME3_AND_H3K27ME3	< 0.001	2.85E-05

B C2 GSEA of genes downregulated in $p53^{-/-}Mdm4^{-/-}$ MEFs

NAME	NOM p-val	FDR q-val
BOQUEST_STEM_CELL_UP	< 0.001	< 5.3E-06
GAL_LEUKEMIC_STEM_CELL_DN	< 0.001	< 5.3E-06
WONG_EMBRYONIC_STEM_CELL_CORE	< 0.001	< 5.3E-06
MIKKELSEN_MEF_LCP_WITH_H3K4ME3	< 0.001	< 5.3E-06
MIKKELSEN_NPC_ICP_WITH_H3K4ME3	< 0.001	< 5.3E-06
MEISSNER_NPC_HCP_WITH_H3K4ME2	< 0.001	< 5.3E-06
RIZ_ERYTHROID_DIFFERENTIATION	< 0.001	< 5.3E-06
MIKKELSEN_MCV6_LCP_WITH_H3K4ME3	< 0.001	< 5.3E-06
SCHAEFFER_PROSTATE_DEVELOPMENT_6HR_DN	< 0.001	< 5.3E-06
CAIRO_LIVER_DEVELOPMENT_DN	< 0.001	< 5.3E-06
KAMMINGA_EZH2_TARGETS	< 0.001	< 5.3E-06
LU_EZH2_TARGETS_UP	< 0.001	< 5.3E-06
REACTOME_TRANSCRIPTIONAL_REGULATION_OF_WHITE_ADIPOCYTE_DIFFERENTIATION	< 0.001	5.30E-06
MIKKELSEN_NPC_LCP_WITH_H3K4ME3	< 0.001	1.01E-05
BOQUEST_STEM_CELL_CULTURED_VS_FRESH_DN	< 0.001	2.31E-05
URS_ADIPOCYTE_DIFFERENTIATION_DN	< 0.001	2.74E-05
BYSTRYKH_HEMATOPOIESIS_STEM_CELL_AND_BRAIN_QTL_TRANS	< 0.001	2.87E-05
FOURNIER_ACINAR_DEVELOPMENT_LATE_2	< 0.001	3.77E-05
MIKKELSEN_IPS_LCP_WITH_H3K4ME3	< 0.001	3.81E-05
MIKKELSEN_ES_LCP_WITH_H3K4ME3	< 0.001	4.83E-05

5 Discussion

In this project, we analyzed novel functions of the oncoprotein MDM2 in the epigenetic regulation of gene expression (outlined in Figure 5-11). Here, MDM2 stabilized a gene repressive profile correlated to stemness maintenance and cell survival. This led to abrogated iPSC generation and accelerated hMSC differentiation into osteoblasts upon loss of MDM2. The genes that MDM2 regulated in primary-, stem- and cancer cells were direct targets of the PcG family. Remarkably, MDM2 directly interacted with the PcG complex members EZH2 and SUZ12, and was recruited to the promoters of MDM2/PRC2 target genes by EZH2. Presence of MDM2 enhanced the repressive histone modifications H3K27me3 and H2AK119ub1, leading to an induction of gene expression in the absence of it. Concomitant loss of MDM2 and RING1B which is the most well-known H2AK119 ubiquitin ligase abrogated cellular survival of MEF and cancer cells due to further exaggerated gene induction. Preliminary data on a similar gene regulatory function for the MDM2 homolog MDM4 indicated overlapping functions in respect to gene repression of a stemness associated gene profile. Furthermore, loss of MDM4 was also associated with a destabilization of H3K27me3.

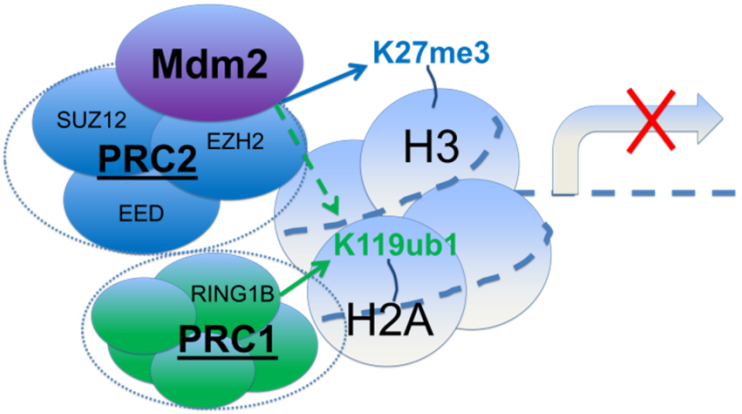

Figure 5-1 Mdm2 regulates gene expression in cooperation with the PcG family

Mdm2 associates with proteins of the PcG family on the chromatin and thereby enhances H3K27 trimethylation and H2AK119 monoubiquitination. Mdm2 facilitates repression of genes involved in stemness and cell proliferation.

5.1 Three cell systems – one conserved mechanism

MDM2 represses PcG target gene expression in primary-, stem- and cancer cells and we investigated its PRC2 interaction and epigenetic function in cancer as well as MEF (primary) cells. Unfortunately, we did not identify shared regulation of many specific genes. However, MDM2 regulated PRC2 target genes in all different systems according to C2 GSEA (cf. Figure 4-5, Table 4-1 and Figure 4-13). The lack of a specific shared gene profile is not completely astonishing. Until now it has been hard to identify a common motif for PRC2 target genes in different cell types, as also outlined in 2.3.3. According to current literature, the PRC2 regulatory profile is strongly dependent on the cellular context which includes presence and absence of DNA methylating agents, accessory proteins and specific chromatin modifications (Simon & Kingston, 2013). Since the recruitment of MDM2 was directly dependent on PRC2 (cf. Figure 4-12 C-D), it was unlikely to detect a common profile of MDM2 chromatin occupancy for the different systems.

Furthermore, the three different cell systems were selected not only to get broad information on the gene regulatory function of MDM2, but also due to technical reasons. MDM2 is a high turnover protein and only present in low amounts in most cell lines. Thus, for endogenous immunoprecipitation assays that are dependent on high protein levels, we used SJSA cells which are characterized by high MDM2 protein levels due to gene amplifications.

Both, Co-IP and ChIP can be done with overexpressed protein, something that we also did in transient short-term experiments for the mapping approaches mentioned earlier (Figure 4-14 B-D; transient overexpression for only 24 h). An obvious experiment would be to overexpress Mdm2 in the $p53^{-/-}$ MEFs and evaluate its chromatin occupancy on the target genes that we described (Figure 4-3). Unfortunately, several groups have tried to set up MDM2-overexpressing cell systems, which failed due to high cell toxicity and overexpression artefacts (cf. paragraph 2.1.5) (Brown et al, 1998; Frum & Deb, 2003). Therefore, we also relied on the SJSA cells for an MDM2 ChIP (Figure 4-15 A). Fortunately, these results were further supported on a heterologous promoter system in HEK cells (Figure 4-15 E).

5.2 MDM2 as a putative H2AK119 ubiquitin ligase

According to our data in Figure 4-18 and Figure 4-19, MDM2 enhances H2AK119ub1 on target gene promoters in MEFs and HCT116 $p53^{-/-}$ cells. Moreover, this function was dependent on its

enzymatic function and together with data from Figure 4-23 D we hypothesize that MDM2 can directly ubiquitinate H2AK119 for gene repression (cf. Figure 4-3 A). However, we did not conclusively prove this. Two publications support our hypothesis that MDM2 is not only able to bind to the promoter DNA of PcG target genes (cf. Figure 4-15) but also to ubiquitinate H2AK119 (Challen et al, 2012; Minsky & Oren, 2004). Especially the data published by Minsky and colleagues showed that MDM2 can bind to the DNA and repress gene expression through a RING dependent H2A ubiquitination, in a p53 independent manner. Using purified histones which were incubated with bacterially expressed GST-MDM2 and HA-tagged ubiquitin they validated that MDM2 ubiquitinates H2A and H2B and that this function is RING domain dependent. The additional value of our data is the connection of this epigenetic regulation with direct cellular functions, namely stem cell maintenance and cancer cell survival.

According to the results in Figure 4-22, Hox gene repression in MEFs relied on both, Ring1b and Mdm2. Since the loss of both, drove cells into arrest and apoptosis (Figure 4-22 C, D and Figure A, B), increased Ring1b promoter levels observed in $p53^{-/-}$ $Mdm2^{-/-}$ MEFs (Figure 4-18 B) could be a rescue effect to prevent a complete loss of H2AK119ub1 or chromatin compaction. A substituting function of Mdm2/Ring1b could also explain the lack of a developmental phenotype in $p53^{-/-}$ $Mdm2^{-/-}$ mice, since Ring1b might compensate for the lack of Mdm2 driven H2AK119 ubiquitination. However, it will be hard to further study this *in vivo* because studies with Ring1b ko systems have already identified a strong lethal phenotype (Román-Trufero et al, 2009; van der Stoop et al, 2008; Voncken et al, 2003). Still, possible attempts are discussed in paragraph 5.10.

5.2.1 PcG protein ubiquitination as a possible function for MDM2?

Despite the strong evidence that Mdm2 is directly involved in H2AK119 ubiquitination (Figure 4-23 D), it is still possible that these functions are mediated indirectly. Such an indirect mechanism could include the ubiquitination of PcG- or accessory proteins by MDM2, driving their proteasomal decay or activation. In MDM2 loss of function and overexpression studies, we did not obtain any data so far which would support this hypothesis. However, several PcG proteins get posttranslationally ubiquitinated, most of them for proteasomal decay (Dimri et al, 2010; Zoabi et al, 2011), but also for increasing their enzymatic activity (Ben-Saadon et al, 2006).

As an example, the H2K119 ubiquitination activity of RING1B is dependent on atypical mixed ubiquitin chains at K6, K27 and K48 (Ben-Saadon et al, 2006). MDM2 can generate K48-based

polyubiquitin chains and it would be interesting to detect whether Ring1b activity is impaired in $p53^{-/-}$ $Mdm2^{-/-}$ and $p53^{-/-}$ $Mdm2^{CA/CA}$ MEFs. Decreased activity could be compensated by increased Ring1b promoter recruitment, as we detected it in Figure 4-18 B. It is still a bit controversial though, why the increased promoter levels were not able to substitute the loss of H2AK119ub1 and the induction of target gene expression (cf. Figure 4-18 A and Figure 4-3 B). Still, this increased recruitment could rescue the gene repression above a specific threshold (since we see further loss of H2AK119ub1 in MDM2/RING1B double kd samples, Figure 4-23 D) that still ensures cell survival (as we detected it in Figure 4-22 B-C and Figure 4-23 A-B).

5.3 MDM2 as a PcG complex member

Corresponding to current literature, it is not completely known how PcG proteins recognize their target genes in the first place, under which circumstances H2AK119ub1 and H3K27me3 depend on each other and how PcG regulation discriminates between different stem cell potencies, lineage commitments and the pathways that determine malignancy. How could the interaction of the PcG proteins with MDM2 contribute to this discussion?

5.3.1 Canonical- and variant PcG activity defined by MDM2

Due to its many complex members, the PRC1 is defined by canonical and variant complex setups (cf. paragraph 2.3.3). Canonical PRC1 complexes contain CBX proteins and their activity strongly depends on upstream H3K27me3, whereas variant (RYBP-containing) complexes ubiquitinate their target genes independent of H3K27me3 (Tavares et al, 2012; Wang et al, 2010).

Along the same line Ku and colleagues identified that the PRC2 can also occupy chromatin independent of the PRC1 (Ku et al, 2008). Through the interaction with MDM2, the PRC2 could build up a variant complex that has intrinsic ubiquitination function which could ensure gene repression maintenance even in the absence of PRC1. In fact, MDM2 would not be the first E3 ubiquitin ligase which is providing this function to the PRC2. TRIM37 and Cullin 4-Ring E3 ligase B (CRL4B) were also detected to interact with the PRC2 and facilitate gene repression through the monoubiquitination of H2AK119 (Bhatnagar et al, 2014; Hu et al, 2012). Because H2AK119ub1 is such an explicit measure to ensure stemness integrity and proper differentiation (Boyer et al, 2006), the occupancy of different ubiquitin ligases can also ensure situation specific signaling as well as redundancy during loss of function.

5.3.2 MDM2 epigenetic contribution in the classic PcG hierarchy

In line with the classic PcG hierarchy, PRC2 methylates H3K27 and thereby recruits PRC1 through the chromodomain protein CBX (Cao et al, 2005). Because the overall decrease of H3K27me3 levels was less prominent upon loss of MDM2 than the decrease of H2AK119ub1 (cf. Figure 4-17 and Figure 4-19) and because EZH2 directly recruited MDM2 to its target genes (cf. Figure 4-15 E) MDM2 mediated ubiquitination of H2AK119 seems to be downstream of H3K27 trimethylation. As a matter of fact, Minsky and colleagues noted a low H2AK119ub1 efficiency of MDM2 in their *in vitro* setting (cf. paragraph 2.1.6.1) and postulated that this might be caused by the absence of further covalent modifications which prime H2A as E3 substrate (Minsky & Oren, 2004). Our data could explain the rather low efficiency of H2AK119 ubiquitination by MDM2 through missing PRC2 proteins to bind to (EZH2 recruits MDM2 to its target gene promoters, cf. Figure 4-15) and absence of H3K27me3. H3K27me3 has previously been identified as an enhancer of intrinsic PRC2 function (Hansen et al, 2008) and PRC2-bound MDM2 could be recruited more efficiently to sites of H3K27me3 and exert accelerated ubiquitin ligase function. Since we detected a cooperative gene regulation of MDM2 and RING1B (cf. Figure 4-22 B), the PRC1 could further maintain gene repression through additional H2AK119 ubiquitination and also through direct chromatin compaction (Eskeland et al, 2010).

5.3.3 MDM2 epigenetic contribution in the non-classic PcG hierarchy

According to our data, the MDM2 epigenetic function directly depended on the presence of PRC2 on the chromatin (cf. Figure 4-15 E). Furthermore, gene repression by MDM2 was partly enhanced by RING1B (Figure 4-22 B). In a possible scenario of the non-classical PcG hierarchy (first H2AK119ub1, then H3K27me3), the PRC1 could provide baseline ubiquitination and chromatin compaction levels which are recognized by the PRC2, as recently described by Kalb and Blackledge (Blackledge et al, 2014; Kalb et al, 2014). PRC2 could subsequently recruit MDM2 to extend, renew and/or maintain the ubiquitination mark. Because the gene regulatory function of the PRC1 is not solely dependent on its ubiquitin ligase function (Eskeland et al, 2010), ubiquitination could be carried out by other ligase like MDM2.

The reverse hierarchy described by Kalb and colleagues was actually based on JARID2 recognition of existing H2AK119ub1, whereas Blackledge hypothesized that the presence of variant PRC1 is responsible for PRC2 recruitment. Interestingly, the variant PRC1 protein RYBP was already described to interact with MDM2 but only in the context of P53 regulation (Chen et

al, 2009). Interaction between RYBP and MDM2 could support the PRC2-MDM2-PRC1 network in the non-classic hierarchy. However, this needs to be clarified through Co-IP experiments.

So far the scientific community does not really agree on how the hierarchical relationship between PRC1 and 2 are set up (or whether there is one) (Comet & Helin, 2014). Further analysis of the PcG-MDM2 functional interaction is needed to evaluate a clear functional hierarchy.

5.4 PRC2/MDM2 interactions through non-coding RNAs

Only 1-2 % of the human genome comprises of protein-coding exons; this finding raised a huge interest in the other 98-99 %, which include repetitive sequences, telomeres, introns and the DNA sequences that give rise to non-coding RNAs (Venter et al, 2001). The long non-coding RNAs XIST and HOTAIR interact with the PRC2 and recruit it to specific target genes (XIST recruits to the X-chromosome and HOTAIR towards the Hox locus (Gupta et al, 2010; Plath et al, 2003)). The PRC2 has further been described to bind to nascent RNAs originating from target genes promoters and thereby halt the transcription machinery in a dynamic fashion (Kaneko et al, 2013).

Along the same line, MDM2 binds to RNA and thereby regulates *TP53* expression (Challen et al, 2012; Elenbaas et al, 1996). Since both, Mdm2 and the PRC2 bind RNA, it would be interesting to know whether their interaction is enhanced or diminished by the presence of RNA. Even though MDM2 has not been detected to bind one of the lncRNAs XIST or HOTAIR, its RNA binding ability could indicate a possible connection. Besides, *HOTAIR* is encoded on the 5' HoxC locus, which we identified to be a target of MDM2/PRC2 regulation. It would be interesting to know whether MDM2 also regulates *HOTAIR* expression and thereby influences its mediated PRC2 recruitment and target gene repression in a feedback loop fashion.

5.5 A role for MDM2 in the development of fat and bone

Lineage differentiation is controlled by specified pathways. Osteoblastic and adipogenic differentiation follow a reciprocal way (cf. Figure 5-2) which is highly influenced by epigenetic PcG regulation (outlined for e.g. EZH2 by Chou et al, 2011). As already mentioned in paragraph 2.1.5, MDM2 overexpression is most commonly found in soft tissue- and osteosarcomas. Since stem cell differentiation and cellular de-differentiation during malignant transformation share molecular pathways (Reya et al, 2001; Sell, 1993), it is important to study MDM2 during e.g. adipogenesis and osteogenesis.

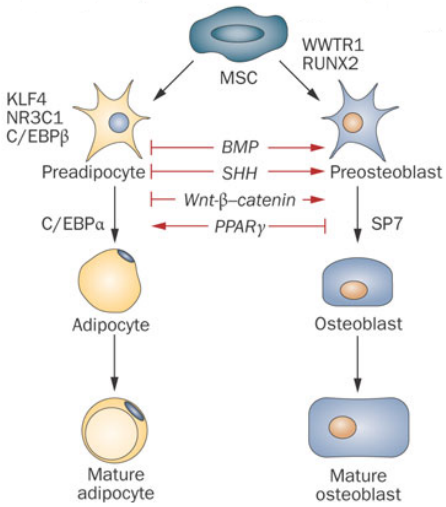

Figure 5-2 Reciprocal development of adipocytes and osteoblasts.

hMSCs differentiated into adipocytes and osteoblasts (among others). These differentiation pathways are controlled by opposing signaling pathways (Takada et al, 2009)

According to our data, loss of MDM2 accelerated osteogenic differentiation from hMSCs (cf. Figure 4-8). On the other hand, Hallenborg and colleagues found that overexpression of MDM2 facilitates adipogenic differentiation through activation of the CREB pathway (cf. Figure 5-2) (Hallenborg et al, 2012). Combining this data concludes that absence of MDM2 not only de-represses early differentiation genes that drive the osteogenic lineage (e.g. *AP* and *BGLAP)* (cf. Figure 4-8 C and F) but also decreases CCAAT/enhancer-binding protein δ (C/EBPδ) expression induction through CREB. This will further shift differentiation along the osteogenic line (cf. Figure 5-2). In the presence of MDM2 this phenotype is reversed, giving rise to cells of the adipogenic lineage and suppressing the osteogenic differentiation. Indeed, when we started these differentiation studies, we also included adipogenic differentiation and did not detect any accelerated adipogenic differentiation after loss of MDM2.

Remarkably, the same behavior was detected for EZH2 by Hemming and colleagues and Dudakovic et al.. According to their data, EZH2 overexpression drove MSC differentiation into the adipogenic lineage whereas loss of EZH2 favored osteoblast differentiation (Dudakovic et al, 2014; Hemming et al, 2014).

Sasaki and colleagues found that the depletion of EZH2 and BMI1 was not enough prevent the survival of osteosarcoma both *in vitro* and *in vivo* (Sasaki et al, 2010). It would be interesting to determine the MDM2 protein levels in the sarcomas that do not respond to EZH2 depletion and whether increased MDM2 levels are responsible for stabilized H3K27me3 and H2AK119ub1. Combining EZH2 inhibition and MDM2 decay (components driving MDM2 self-ubiquitination are under investigation) could be a possible treatment option for those tumor entities.

5.6 Benefits of an MDM2/PcG joint venture

Why would a cell benefit from the connection of a cell cycle regulator and an epigenetic protein complex involved in stem cell maintenance? And how can it circumvent loss of function for one but not the other factor?

5.6.1 MDM2 – link between epigenetics and DNA damage?

The ability to retain a perfect copy of DNA whenever a cell replicates is the major prerequisite a germ cell (and any other dividing cell) must provide. Loss of this proofreading ability will lead to mutation and drive cells into malignant transformation processes (Berg et al, 2002). As a matter of fact, any cell is facing a multitude of stressors every day, including UV radiation, reactive oxygen species, toxins etc. and several systems are making sure that the damage will be recognized and repaired. In case of intensive damage which cannot be repaired, cell death is induced to remove the altered cell from the progeny pool (Jackson & Bartek, 2009). The P53 system is a key player involved in DNA damage recognition and repair as outlined in paragraph 2.1.2.1. Under normal circumstances, DNA damage leads to increased inhibition and degradation of MDM2, releasing P53 from its control. P53 subsequently induces cell cycle arrest and, in case of intensive damage, apoptosis (Oren, 2003; Vogelstein et al, 2000; Vousden, 2000). It furthermore also activates MDM2 expression to ensure autoregulatory feedback.

In line with our data, the shutdown of MDM2 during a cell stress event would not only impede malignant transformation through P53 activation but also through its connection with the PcG gene regulatory network. Upon DNA damage, PcG mediated gene repression would be lifted due to downregulation of MDM2 (as observed in Figure 4-3 A and B, Figure 4-8 C-F and Figure 4-12), enhancing differentiation pathways (cf. Figure 4-8 A-C) and inducing cell cycle arrest (cf. Figure 4-11). Cell cycle arrest promotes DNA repair (Branzei & Foiani, 2008) whereas induction

of differentiation controls proliferation capacity (Sela et al, 2012). We assume that this inter-connection is a further safety measure to keep a perfect germ cell and stem cell pool and proper disposal of cells exhibiting DNA damage. In concordance, many malignancies benefit from high levels of MDM2 or PcG proteins and therapeutic inhibition of these proteins are of great therapeutic value (cf. paragraphs 2.1.5 and 2.3.4.2).

5.6.2 How can MDM2 be dispensable for proper organism development?

One of the most puzzling question of this project is why the epigenetic and stemness related function of MDM2 does not seem to play any role in the development of a murine organism. Embryonic lethality caused by MDM2 ko can be reversed by an additional loss of p53, both in a complete and conditional ko systems (cf. paragraph 2.1.4). Interestingly, a similar question was asked after the p53 ko mouse was generated: How can a factor like p53 be so negligible for development, when it is so indispensable for cell cycle regulation and survival?

At least for p53, this statement has been relativized in the last couple of years especially in murine systems. Two independent groups around Armstrong and Sah reported increased embryonic lethality of the $p53^{-/-}$ mouse. Especially the female mice died due to improper closure of the neural tube and exencephaly, and in general fertility was decreased (Armstrong et al, 1995; Sah et al, 1995). Furthermore, generation of iPS cells from $p53^{-/-}$ MEFs was greatly increased indicating a p53 stem cell barrier function (cf. Figure 4-1 B). This barrier function could also be a reason for the improper nervous system development (Hong et al, 2009; Kawamura et al, 2009).

With our data, we are now able to directly connect gene regulatory and epigenetic functions of Mdm2 with stemness maintenance and cell survival. However, these functions disagree with the fact that the $p53^{-/-}$ $Mdm2^{-/-}$ mouse develops normally. One possible explanation could be based on cellular stress. The whole p53-Mdm2 axis is designed to act during cellular stress which might circumvent its function during development in an unstressed organism, as it is typically the case for laboratory animals.

As mentioned before, Jones and colleagues detected embryonic lethality especially in female $p53^{-/-}$ mice. Female development requires a more intensive amount of epigenetic regulation due to X-chromosome inactivation which could provide a potential cell stress situation. As explained before, Mdm2 expression is induced from the P2 promoter by p53 (cf. paragraph 2.1.3) which is

why you can expect lower MDM2 protein levels in tissues deficient of p53. In fact, we also detected these differences in our MEF cells when compared to wt MEF preparations. Such a decrease in Mdm2 expression could impair PcG target gene repression which is one of the most important factors in X-chromosome silencing (Plath et al, 2003). The additional stress of X-chromosome inactivation can be a reason of induced female lethality. This could be further tested via checking imprinting efficiency of the X-chromosome in p53 ko mice (see also 5.10).

5.6.2.1 *Cell stress in analyzed systems*

Indeed, all systems that we analyzed are characterized by cell stress. Artificial overexpression of transcription factors (Oct3/4, Klf4 and Sox2) are *per se* stress factors and many generated iPSCs are undergoing cell death instead of pursuing reprogramming, due to DNA damage (Marión et al, 2009). Therefore, loss of p53 increases reprogramming but also decrease iPS cell quality as it was stated by Hong and colleagues (Hong et al, 2009). Next to iPS cell generation, MSC differentiation into osteoblasts harbors many stress points. siRNA mediated knock down as well as chemically induced osteoblast differentiation might facilitate MDM2 stemness function.

In fact, we are not the first ones who postulate that p53 independent functions of MDM2 could be hidden under non-stress condition. According to Marine and Lozano, the p53-independent MDM2 functions become relevant under conditions of cellular stress including tumors (Marine & Lozano, 2010).

5.7 MDM2 and PcG – linking cancer and stem cells?

As already outlined in 2.3.4.3, a quite interesting hypothesis has been raised in the last years concerning the concept of cancer stem cells (CSCs). PRC2 proteins and MDM2 are major players in cancer and stemness, and at least the PcG proteins EZH2 and Bmi1 have been extensively discussed in the field of CSC research. As mentioned, elevated EZH2 and H3K27me3 levels were detected in CSCs of breast and prostate cancer (Crea et al, 2011; Suvà et al, 2009; van Vlerken et al, 2013).

According to our data, the MDM2/PRC2 network could combine stemness and malignancy related pathways. MDM2, which is often overexpressed in tumor cells, could facilitate the conversion of differentiated normal cells into cancer stem cells via the induction of a stem cell associated epigenetic- and expression profile. MDM2 could hereby stabilize H3K27me3 and

H2AK119ub1 of target genes involved in differentiation and cell cycle arrest, which explains how high levels of MDM2 can support malignant transformation even in the absence of wt p53 (Cordon-Cardo et al, 1994).

The finding that MDM2 splice variants, which do not contain the P53 binding domain, still confer malignancy is also valid according to our data (Sigalas et al, 1996). The p53 binding domain is not needed for MDM2 interaction with the PRC2 as explained before, and these variants would still be able to repress PcG target genes supporting malignancy.

It would be important know whether CSC maintenance is supported by high levels of MDM2 and how the epigenetic signatures of H3K27me3 and H2AK119ub1 are changed in case of MDM2 loss or inhibition.

5.8 Therapeutic relevance of the MDM2/PRC2 joint venture

The P53-MDM2 system is under intensive therapeutic research. MDM2 binds P53 through the P53-binding domain and the majority of the small chemical compounds that are currently evaluated in animal and patient based trials, target exactly this interaction. Among those are the Nutlins, and the benzodiazepinediones. For these compounds, no therapeutic relevance was found in tumors with mutant or no P53 (Li & Lozano, 2013; Wade et al, 2013). JNJ-26854165 (Kojima et al, 2010), HLI98 (Yang et al, 2005), MPD (Roxburgh et al, 2012) and MEL (Herman et al, 2011) are compounds that were designed to inhibit the E3 ubiquitin ligase function of MDM2. Treatment with these compounds in P53 wt cancers results in a decrease of MDM2 mediated P53 proteasomal degradation, cell cycle arrest and apoptosis related gene expression. Remarkably, treatment with these compounds was also effective to some extent in P53 null systems.

According to our work, the development of drugs which inhibit the MDM2 E3 ubiquitin ligase function or destabilize the whole protein will be of utmost interest. MDM2 interacts with EZH2 and SUZ12 via a region in the first 300 amino acids of the protein but the P53-binding domain is dispensable for this interaction (cf. Figure 4-14 and Wienken et al, *under review*). Compounds that are based on the nutlins and benzodiazepinediones will therefore not target the MDM2-PRC2 interaction and will not have any therapeutic relevance in cells with LOF P53.

Apart from the mapping experiment we also know that MDM2 needs its E3 ubiquitin ligase function for gene repression. Experiments with MEFs expressing MDM2 that lacks E3 ubiquitin function ($MDM2^{CA/CA}$) showed similar outcomes when compared to MDM2 loss of function MEFs

(cf. Figure 4-3 and Figure 4-18). Therefore, inhibitors such as JNJ-26854165 and HLI98 which are designed to target the ubiquitin ligase function may be able to not only target the p53 regulation by MDM2 but also the repression of PRC2 target gene.

As already mentioned in paragraph 5.5, the contributions of MDM2 regarding development of adipocytes and osteoblasts is mainly p53-independent. Since the cancer types that arise from these tissues (lipo- and osteosarcoma) are generally characterized by high levels of MDM2, patients suffering from esp. liposarcoma are included in MDM2 inhibitor clinical trials. During the 8th International MDM2 workshop (New Orleans, 1.11.-4.11.2015) it was intensively discussed whether this could result in misleading conclusions in cases of substances targeting only the P53-MDM2 interaction. Inhibitor treatment could activate P53 to some extent but still ongoing p53-independent functions of MDM2 might be too extensive to drive cells into sufficient apoptosis. This would explain why several clinical trials were recently stopped due to a lack of treatment efficacy (Arnold J. Levine, personal communication) and would further support the idea to run clinical trials with compounds not only targeting the p53-dependent functions of the MDM proteins.

In the context of therapeutic value it will be also important to discuss the role of P53. P53 is a positive regulator of MDM2 and tumors without wt P53 function are most probably characterized by low MDM2 expression (Wu et al, 1993). In the case of H3K27me3- and H2AK119ub1 destabilization due to low MDM2 levels, treatment with EZH2/RING1B inhibitors may be more efficient in cells without wt P53 expression. Indirect evidence for this hypothesis was already given by Sasaki and colleagues as explained before in paragraph 5.5. According to their data, osteosarcomas, which are often characterized by high MDM2 levels, were less responsive towards PcG inhibition therapy (Sasaki et al, 2010). In this case, high MDM2 might have stabilized H3K27me3 and H2AK119ub1 levels, rendering inhibitor treatment ineffective.
Furthermore, precautions have to be taken when using MDM2 inhibitors in a mutant P53 system. In contrast to P53 loss of function, many tumors are characterized by P53 mutations that causes malignant gain of function (GOF) properties of P53 (Brosh & Rotter, 2009). In this case, malignant transformation is supported by P53 and MDM2 can act tumor suppressive because it often still targets mtP53 for degradation (Terzian et al, 2008).

5.9 How can MDM4 contribute to the MDM2/PRC2 gene regulation?

Unfortunately, our knowledge about the relevance of MDM4 in the control of PcG target genes is limited. As described in Figure 4-25, loss of Mdm4 de-repressed an overlapping gene set in MEFs compared to Mdm2 and was also associated to some extent with loss of H3K27me3.

MDM4 does not contain intrinsic E3 ubiquitin ligase function (Shvarts et al, 1997; Shvarts et al, 1996). However, MDM4 can enhance MDM2 E3 function through heterodimerization and also stabilize the MDM2 protein via abrogation of its autoubiquitination (Linares et al, 2003). Due to the impact on MDM2, loss of MDM4 could indirectly regulate PRC2 target genes and thereby change its repressive chromatin state. So far we did not investigate whether MDM4 directly interacts with the PRC2; since it binds to MDM2 and forms dimers, the possibility is quite high though. It will be especially important to study these p53-independent MDM4 functions for potential drug design. Several studies indicated that high MDM4 levels can abrogate the outcome of MDM2 inhibitor therapy and it may be necessary to use compounds that can target both, MDM4 and MDM2 binding and enzymatic function to inhibit the Mdm-PcG gene regulatory network (Li & Lozano, 2013).
Ko studies have revealed that Mdm4 and Mdm2 are functioning in a non-redundant pattern, which means that neither protein can substitute for the loss of the other (although supraphysiological Mdm2 levels were able to substitute loss of Mdm4, cf. paragraph 2.1.2). It could therefore also be plausible that Mdm4 does not share PRC2 co-regulatory functions that are beyond any indirect influences through Mdm2. We have to invest more time into this question in order to gain better insights.

5.10 Concluding remarks and future perspectives

In this study we have evaluated and discussed a novel function of MDM2 in the epigenetic regulation of PcG target genes. This gene regulatory function included enhancement of specific histone modifications and was responsible for stemness maintenance and cancer cell survival.

One of the most interesting findings of the MDM2/PcG relationship was the interdependence of murine primary and human cell on both, RING1B and MDM2. We are now aiming to understand, whether the stabilization of H2AK119ub1 through MDM2 is indeed its major function. This would mean that destabilization of H3K27me3 is a bystander consequence and merely depends on H2AK119ub1 ubiquitination by MDM2 in the first place. Whether the MDM2/RING1B interdependence is a cell-specific phenomenon should be analyzed in various

different systems. Hereby, a mutual gene expression profile could be investigated through global gene expression studies. Accordingly, we have to test, whether the synthetic lethality and gene expression changes can be also observed in $p53^{-/-}$ $Mdm2^{CA/CA}$ MEFs. According to Figure 4-23 D, MDM2 ubiquitinates H2AK119ub1 together with RING1B; from studies in MEFs we know that the enzymatic function of Mdm2 is crucial for gene repression (cf. Figure 4-3) and maintenance of H2AK119ub1 (cf. Figure 4-18). Taken together, loss of Ring1b in $p53^{-/-}$ $Mdm2^{CA/CA}$ MEFs should result in the same synthetic lethality as we observed it for complete loss of Mdm2.

A similar question should be asked for MDM4. Unfortunately, we cannot say for sure how MDM4 is involved in the maintenance of H2AK119ub1. However, loss of it led to the deregulation of similar gene sets compared to MDM2 (cf. Table 4-1 and Table 4-3). Since MDM4 is necessary for the proper enzymatic function of MDM2 it could be plausible, that cells interdepend on RING1B and MDM4 as they do it for MDM2.

Furthermore, we want to understand, whether the relationship between MDM2 and RING1B is unique or can be also determined for other proteins. In paragraph 5.3.1 the existence of other H2AK119 ubiquitin ligases such as BRCA1, TRIM37 and CRL4B was mentioned. It would be interesting to know whether a cell interdepends on TRIM37/CRL4B and MDM2 like it does for RING1B and MDM2. In a possible scenario, we would be able to determine a specific H2AK119 ubiquitin ligase threshold which is needed for cellular survival.

Analyzing whether Ring1b or any other H2AK119 ubiquitin ligase is able to cover up a possible phenotype in the $p53^{-/-}$ $Mdm2^{-/-}$ mouse would be a major breakthrough. Since the ko phenotypes of the $Mdm2^{-/-}$- and the $p53^{-/-}$ $Mdm2^{-/-}$ mouse are apparently ruling out developmental functions for Mdm2 it will always be hard to completely understand the results of this project. Generation of a $p53^{-/-}$ $Mdm2^{-/-}$ mouse that carries an inducible and/or organ specific Ring1b ko could be an option to address this question. However, loss of Ring1b has already been associated with a massive loss of H2AK119ub1 and was also found to be embryonically lethal (Voncken et al, 2003). This means that the majority of H2AK119 ubiquitination is carried out by Ring1b and not Mdm2. It could be hard to discriminate the additional consequences of the loss of Mdm2 in the Ring1b ko system.

Apart from interaction with proteins of the PcG, MDM2 interacts with a multitude of different proteins (cf. Figure 2-5). Since several factors are known transcription factors or modulators of the transcription machinery, we need to know whether they modulate the MDM2 interaction with

the PRC proteins and/or its stabilization of the H2AK119ub1 mark. Possible candidates include P53 (Momand et al, 1992), E2F1 (Zhang et al, 2005) and p300 (Grossman et al, 1998). Further analysis of this interactive network and the consideration of these results into drug design will improve the development of a targeted cancer therapy.

Last but not least, we have to validate the therapeutic relevance of our findings. As outlined in paragraph 5.8, many different compounds have already been developed to target MDM2 or MDM4 but mainly in respect to P53 re-activation. We are especially interested in the compounds that inhibit E3 ubiquitin ligase function or lead to MDM2 degradation, since several of them were correlated with p53-independent functions of MDM2 leading to cell arrest and apoptosis. A possible experiment would include the treatment of p53 wt and p53 ko cells with an inhibitor like JNJ-26854165 or HLI98. Cells responsive towards treatment can be analyzed for PRC2 target gene expression as well as H3K27me3 and H2K119ub1 levels in order to validate whether the p53-independent effects of these compounds are based on the MDM2 epigenetic function described here. As a follow up, xenografts from p53 wt and -ko cells can be tested in an *in vivo* approach.

The results of this project answered a few, and raised many new questions and I want to finish this thesis with a fitting quote from Sir David Lane:

“Why have C. elegans and D. melanogaster evolved new ways to control p53 that nevertheless allow it to respond to the very same damage and developmental clues that the lost system of Mdm2-based control has perfected? How can such highly conserved genes be dispensable for all aspects of development in a mouse? We have much to learn!” (Lane & Verma, 2012)

6 References

Abbas HA, Maccio DR, Coskun S, Jackson JG, Hazen AL, Sills TM, You MJ, Hirschi KK, Lozano G (2010) Mdm2 is required for survival of hematopoietic stem cells/progenitors via dampening of ROS-induced p53 activity. *Cell stem cell* **7:** 606-617

Al-Hajj M, Wicha MS, Benito-Hernandez A, Morrison SJ, Clarke MF (2003) Prospective identification of tumorigenic breast cancer cells. *Proceedings of the National Academy of Sciences* **100:** 3983-3988

Allfrey V, Faulkner R, Mirsky A (1964) Acetylation and methylation of histones and their possible role in the regulation of RNA synthesis. *Proc Natl Acad Sci U S A* **51:** 786

Aloni-Grinstein R, Shetzer Y, Kaufman T, Rotter V (2014) p53: the barrier to cancer stem cell formation. *FEBS letters* **588:** 2580-2589

Aloni-Grinstein R, Zan-Bar I, Alboum I, Goldfinger N, Rotter V (1993) Wild type p53 functions as a control protein in the differentiation pathway of the B-cell lineage. *Oncogene* **8:** 3297-3305

Anders S, Huber W (2010) Differential expression analysis for sequence count data. *Genome biology* **11:** R106

Armstrong JF, Kaufman MH, Harrison DJ, Clarke AR (1995) High-frequency developmental abnormalities in p53-deficient mice. *Current Biology* **5:** 931-936

Artavanis-Tsakonas S, Rand MD, Lake RJ (1999) Notch signaling: cell fate control and signal integration in development. *Science* **284:** 770-776

Arva NC, Gopen TR, Talbott KE, Campbell LE, Chicas A, White DE, Bond GL, Levine AJ, Bargonetti J (2005) A chromatin-associated and transcriptionally inactive p53-Mdm2 complex occurs in mdm2 SNP309 homozygous cells. *Journal of Biological Chemistry* **280:** 26776-26787

Barak Y, Gottlieb E, Juven-Gershon T, Oren M (1994) Regulation of mdm2 expression by p53: alternative promoters produce transcripts with nonidentical translation potential. *Genes Dev* **8:** 1739-1749

Barboza JA, Iwakuma T, Terzian T, El-Naggar AK, Lozano G (2008) Mdm2 and Mdm4 loss regulates distinct p53 activities. *Molecular cancer research* **6:** 947-954

Bartholdy B, Christopeit M, Will B, Mo Y, Barreyro L, Yu Y, Bhagat TD, Okoye-Okafor UC, Todorova TI, Greally JM (2014) HSC commitment–associated epigenetic signature is prognostic in acute myeloid leukemia. *The Journal of clinical investigation* **124:** 1158

Baylin SB, Makos M, Wu J, Yen R, De Bustros A, Vertino P, Nelkin B (1991) Abnormal patterns of DNA methylation in human neoplasia: potential consequences for tumor progression. *Cancer cells (Cold Spring Harbor, NY: 1989)* **3:** 383-390

Beà S, Tort F, Pinyol M, Puig X, Hernández L, Hernández S, Fernández PL, van Lohuizen M, Colomer D, Campo E (2001) BMI-1 gene amplification and overexpression in hematological malignancies occur mainly in mantle cell lymphomas. *Cancer research* **61:** 2409-2412

Ben-Saadon R, Zaaroor D, Ziv T, Ciechanover A (2006) The polycomb protein Ring1B generates self atypical mixed ubiquitin chains required for its in vitro histone H2A ligase activity. *Molecular cell* **24:** 701-711

Berg JM, Tymoczko JL, Stryer L (2002) Biochemistry: International Version (hardcover).

Bernstein E, Allis CD (2005) RNA meets chromatin. *Genes Dev* **19:** 1635-1655

Bhatnagar S, Gazin C, Chamberlain L, Ou J, Zhu X, Tushir JS, Virbasius CM, Lin L, Zhu LJ, Wajapeyee N, Green MR (2014) TRIM37 is a new histone H2A ubiquitin ligase and breast cancer oncoprotein. *Nature* **516:** 116-120

Biderman L, Manley JL, Prives C (2012) Mdm2 and MdmX as regulators of gene expression. *Genes & cancer* **3:** 264-273

Bittner M, Kupferer P, Morris CF (1980) Electrophoretic transfer of proteins and nucleic acids from slab gels to diazobenzyloxymethyl cellulose or nitrocellulose sheets. *Analytical biochemistry* **102:** 459-471

Blackledge NP, Farcas AM, Kondo T, King HW, McGouran JF, Hanssen LL, Ito S, Cooper S, Kondo K, Koseki Y (2014) Variant PRC1 complex-dependent H2A ubiquitylation drives PRC2 recruitment and polycomb domain formation. *Cell* **157:** 1445-1459

Blankenberg D, Von Kuster G, Coraor N, Ananda G, Lazarus R, Mangan M, Nekrutenko A, Taylor J (2010) Galaxy: a web-based genome analysis tool for experimentalists. *Current protocols in molecular biology / edited by Frederick M Ausubel [et al]* **Chapter 19:** Unit 19 10 11-21

Bond GL, Hu W, Bond EE, Robins H, Lutzker SG, Arva NC, Bargonetti J, Bartel F, Taubert H, Wuerl P (2004) A single nucleotide polymorphism in the MDM2 promoter attenuates the p53 tumor suppressor pathway and accelerates tumor formation in humans. *Cell* **119:** 591-602

Bonnet D, Dick JE (1997) Human acute myeloid leukemia is organized as a hierarchy that originates from a primitive hematopoietic cell. *Nature medicine* **3:** 730-737

Boyer LA, Plath K, Zeitlinger J, Brambrink T, Medeiros LA, Lee TI, Levine SS, Wernig M, Tajonar A, Ray MK (2006) Polycomb complexes repress developmental regulators in murine embryonic stem cells. *Nature* **441:** 349-353

Bracken AP, Pasini D, Capra M, Prosperini E, Colli E, Helin K (2003) EZH2 is downstream of the pRB-E2F pathway, essential for proliferation and amplified in cancer. *The EMBO journal* **22:** 5323-5335

Branzei D, Foiani M (2008) Regulation of DNA repair throughout the cell cycle. *Nature reviews Molecular cell biology* **9:** 297-308

Breiling A (2015) Epigenetic Regulation of Pluripotency by Polycomb Group Proteins. In *Epigenetic Mechanisms in Cellular Reprogramming*, pp 121-139. Springer

Brosh R, Rotter V (2009) When mutants gain new powers: news from the mutant p53 field. *Nature Reviews Cancer* **9:** 701-713

Brown DR, Thomas CA, Deb SP (1998) The human oncoprotein MDM2 arrests the cell cycle: elimination of its cell-cycle-inhibitory function induces tumorigenesis. *The EMBO journal* **17:** 2513-2525

Bunz F, Dutriaux A, Lengauer C, Waldman T, Zhou S, Brown JP, Sedivy JM, Kinzler KW, Vogelstein B (1998) Requirement for p53 and p21 to sustain G2 arrest after DNA damage. *Science* **282:** 1497-1501

Cahilly-Snyder L, Yang-Feng T, Francke U, George DL (1987) Molecular analysis and chromosomal mapping of amplified genes isolated from a transformed mouse 3T3 cell line. *Somatic cell and molecular genetics* **13:** 235-244

Cao R, Tsukada Y-i, Zhang Y (2005) Role of Bmi-1 and Ring1A in H2A ubiquitylation and Hox gene silencing. *Molecular cell* **20:** 845-854

Cao R, Wang L, Wang H, Xia L, Erdjument-Bromage H, Tempst P, Jones RS, Zhang Y (2002) Role of histone H3 lysine 27 methylation in Polycomb-group silencing. *Science* **298:** 1039-1043

Cao R, Zhang Y (2004) SUZ12 is required for both the histone methyltransferase activity and the silencing function of the EED-EZH2 complex. *Mol Cell* **15:** 57-67

Challen C, Anderson JJ, Chrzanowska‐Lightowlers Z, Lightowlers RN, Lunec J (2012) Recombinant human MDM2 oncoprotein shows sequence composition selectivity for binding to both RNA and DNA. *Int J Oncol* **40:** 851-859

Chan CS, Rastelli L, Pirrotta V (1994) A Polycomb response element in the Ubx gene that determines an epigenetically inherited state of repression. *The EMBO journal* **13:** 2553

Chavez-Reyes A, Parant JM, Amelse LL, de Oca Luna RM, Korsmeyer SJ, Lozano G (2003) Switching mechanisms of cell death in mdm2-and mdm4-null mice by deletion of p53 downstream targets. *Cancer Res* **63:** 8664-8669

Chen D, Zhang J, Li M, Rayburn ER, Wang H, Zhang R (2009) RYBP stabilizes p53 by modulating MDM2. *EMBO reports* **10:** 166-172

Chen J, Marechal V, Levine AJ (1993) Mapping of the p53 and mdm-2 interaction domains. *Molecular and cellular biology* **13:** 4107-4114

Chen L, Li Z, Zwolinska AK, Smith MA, Cross B, Koomen J, Yuan ZM, Jenuwein T, Marine JC, Wright KL (2010) MDM2 recruitment of lysine methyltransferases regulates p53 transcriptional output. *The EMBO journal* **29:** 2538-2552

Chene P (2003) Inhibiting the p53-MDM2 interaction: an important target for cancer therapy. *Nature reviews Cancer* **3:** 102-109

Chou RH, Yu YL, Hung MC (2011) The roles of EZH2 in cell lineage commitment. *American journal of translational research* **3:** 243-250

Clegg HV, Itahana Y, Itahana K, Ramalingam S, Zhang Y (2012) Mdm2 RING mutation enhances p53 transcriptional activity and p53-p300 interaction. *PLoS One* **7:** e38212

Comet I, Helin K (2014) Revolution in the Polycomb hierarchy. *Nature structural & molecular biology* **21:** 573-575

Cordon-Cardo C, Latres E, Drobnjak M, Oliva MR, Pollack D, Woodruff JM, Marechal V, Chen J, Brennan MF, Levine AJ (1994) Molecular abnormalities of mdm2 and p53 genes in adult soft tissue sarcomas. *Cancer Res* **54:** 794-799

Crea F, Hurt EM, Mathews LA, Cabarcas SM, Sun L, Marquez VE, Danesi R, Farrar WL (2011) Pharmacologic disruption of Polycomb Repressive Complex 2 inhibits tumorigenicity and tumor progression in prostate cancer. *Mol Cancer* **10:** 40

Czermin B, Melfi R, McCabe D, Seitz V, Imhof A, Pirrotta V (2002) Drosophila enhancer of Zeste/ESC complexes have a histone H3 methyltransferase activity that marks chromosomal Polycomb sites. *Cell* **111:** 185-196

Denissov S, van Driel M, Voit R, Hekkelman M, Hulsen T, Hernandez N, Grummt I, Wehrens R, Stunnenberg H (2007) Identification of novel functional TBP-binding sites and general factor repertoires. *The EMBO journal* **26:** 944-954

Dhalluin C, Carlson JE, Zeng L, He C, Aggarwal AK, Zhou M-M (1999) Structure and ligand of a histone acetyltransferase bromodomain. *Nature* **399:** 491-496

Dimri M, Bommi PV, Sahasrabuddhe AA, Khandekar JD, Dimri GP (2010) Dietary omega-3 polyunsaturated fatty acids suppress expression of EZH2 in breast cancer cells. *Carcinogenesis* **31:** 489-495

Dobbelstein M, Wienzek S, Konig C, Roth J (1999) Inactivation of the p53-homologue p73 by the mdm2-oncoprotein. *Oncogene* **18:** 2101-2106

Dolle P, Izpisua-Belmonte J, Brown J, Tickle C, Duboule D, Fallon J, Goetinck P, Kelley R, Stocum D. (1993) Hox genes and the morphogenesis of the vertebrate limb. Wiley-Liss.

Donehower LA, Harvey M, Slagle BL, McArthur MJ, Montgomery Jr CA, Butel JS, Bradley A (1992) Mice deficient for p53 are developmentally normal but susceptible to spontaneous tumours. *Nature* **356:** 215-221

Dudakovic A, Xu F, Camilleri E, McGee-Lawrence M, Lewallen E, Riester S, Hawse JR, Stein G, Montecino M, Westendorf J (2014) Epigenetic control of skeletal development by the histone methyltransferase EZH2. In *Journal of Bone and Mineral Research*, Vol. 29, pp S40-S40.

Duncan AW, Rattis FM, DiMascio LN, Congdon KL, Pazianos G, Zhao C, Yoon K, Cook JM, Willert K, Gaiano N (2005) Integration of Notch and Wnt signaling in hematopoietic stem cell maintenance. *Nature immunology* **6:** 314-322

Eischen CM, Weber JD, Roussel MF, Sherr CJ, Cleveland JL (1999) Disruption of the ARF–Mdm2–p53 tumor suppressor pathway in Myc-induced lymphomagenesis. *Genes Dev* **13:** 2658-2669

El-Deiry WS, Tokino T, Velculescu VE, Levy DB, Parsons R, Trent JM, Lin D, Mercer WE, Kinzler KW, Vogelstein B (1993) WAF1, a potential mediator of p53 tumor suppression. *Cell* **75:** 817-825

Elenbaas B, Dobbelstein M, Roth J, Shenk T, Levine A (1996) The MDM2 oncoprotein binds specifically to RNA through its RING finger domain. *Molecular Medicine* **2:** 439

Eppert K, Takenaka K, Lechman ER, Waldron L, Nilsson B, van Galen P, Metzeler KH, Poeppl A, Ling V, Beyene J (2011) Stem cell gene expression programs influence clinical outcome in human leukemia. *Nature medicine* **17:** 1086-1093

Eskeland R, Leeb M, Grimes GR, Kress C, Boyle S, Sproul D, Gilbert N, Fan Y, Skoultchi AI, Wutz A (2010) Ring1B compacts chromatin structure and represses gene expression independent of histone ubiquitination. *Molecular cell* **38:** 452-464

Ezhkova E, Pasolli HA, Parker JS, Stokes N, Su I-h, Hannon G, Tarakhovsky A, Fuchs E (2009) Ezh2 orchestrates gene expression for the stepwise differentiation of tissue-specific stem cells. *Cell* **136:** 1122-1135

Fåhraeus R, Olivares-Illana V (2013) MDM2's social network. *Oncogene*

Fakharzadeh S, Trusko S, George D (1991) Tumorigenic potential associated with enhanced expression of a gene that is amplified in a mouse tumor cell line. *The EMBO journal* **10:** 1565

Fang S, Jensen JP, Ludwig RL, Vousden KH, Weissman AM (2000) Mdm2 is a RING finger-dependent ubiquitin protein ligase for itself and p53. *The Journal of biological chemistry* **275:** 8945-8951

Faust C, Schumacher A, Holdener B, Magnuson T (1995) The eed mutation disrupts anterior mesoderm production in mice. *Development* **121:** 273-285

Feinberg AP, Vogelstein B (1983) Hypomethylation distinguishes genes of some human cancers from their normal counterparts. *Nature* **301:** 89-92

Finch RA, Donoviel DB, Potter D, Shi M, Fan A, Freed DD, Wang C-y, Zambrowicz BP, Ramirez-Solis R, Sands AT (2002) mdmx is a negative regulator of p53 activity in vivo. *Cancer Res* **62:** 3221-3225

Fischle W, Wang Y, Jacobs SA, Kim Y, Allis CD, Khorasanizadeh S (2003) Molecular basis for the discrimination of repressive methyl-lysine marks in histone H3 by Polycomb and HP1 chromodomains. *Genes Dev* **17:** 1870-1881

Fraga MF, Ballestar E, Villar-Garea A, Boix-Chornet M, Espada J, Schotta G, Bonaldi T, Haydon C, Ropero S, Petrie K (2005) Loss of acetylation at Lys16 and trimethylation at Lys20 of histone H4 is a common hallmark of human cancer. *Nature genetics* **37:** 391-400

Francis NJ, Kingston RE, Woodcock CL (2004) Chromatin compaction by a polycomb group protein complex. *Science* **306:** 1574-1577

Francoz S, Froment P, Bogaerts S, De Clercq S, Maetens M, Doumont G, Bellefroid E, Marine J-C (2006) Mdm4 and Mdm2 cooperate to inhibit p53 activity in proliferating and quiescent cells in vivo. *Proc Natl Acad Sci U S A* **103:** 3232-3237

Frum R, Deb SP (2003) Flow cytometric analysis of MDM2-mediated growth arrest. In *p53 Protocols*, pp 257-267. Springer

Gao Z, Zhang J, Bonasio R, Strino F, Sawai A, Parisi F, Kluger Y, Reinberg D (2012) PCGF homologs, CBX proteins, and RYBP define functionally distinct PRC1 family complexes. *Molecular cell* **45:** 344-356

Giardine B, Riemer C, Hardison RC, Burhans R, Elnitski L, Shah P, Zhang Y, Blankenberg D, Albert I, Taylor J, Miller W, Kent WJ, Nekrutenko A (2005) Galaxy: a platform for interactive large-scale genome analysis. *Genome research* **15:** 1451-1455

Gilkes DM, Pan Y, Coppola D, Yeatman T, Reuther GW, Chen J (2008) Regulation of MDMX expression by mitogenic signaling. *Molecular and cellular biology* **28:** 1999-2010

GM. C (2000) The Cell: A Molecular Approach. 2nd edition. *Sunderland (MA): Sinauer Associates*

Godlewski J, Nowicki MO, Bronisz A, Williams S, Otsuki A, Nuovo G, RayChaudhury A, Newton HB, Chiocca EA, Lawler S (2008) Targeting of the Bmi-1 oncogene/stem cell renewal factor by microRNA-128 inhibits glioma proliferation and self-renewal. *Cancer research* **68:** 9125-9130

Goecks J, Nekrutenko A, Taylor J (2010) Galaxy: a comprehensive approach for supporting accessible, reproducible, and transparent computational research in the life sciences. *Genome biology* **11:** R86

Graham F, Van der Eb A (1973) A new technique for the assay of infectivity of human adenovirus 5 DNA. *Virology* **52:** 456-467

Greer EL, Shi Y (2012) Histone methylation: a dynamic mark in health, disease and inheritance. *Nature Reviews Genetics* **13:** 343-357

Grier JD, Xiong S, Elizondo-Fraire AC, Parant JM, Lozano G (2006) Tissue-specific differences of p53 inhibition by Mdm2 and Mdm4. *Molecular and cellular biology* **26:** 192-198

Grossman SR, Deato ME, Brignone C, Chan HM, Kung AL, Tagami H, Nakatani Y, Livingston DM (2003) Polyubiquitination of p53 by a ubiquitin ligase activity of p300. *Science* **300:** 342-344

Grossman SR, Perez M, Kung AL, Joseph M, Mansur C, Xiao Z-X, Kumar S, Howley PM, Livingston DM (1998) p300/MDM2 complexes participate in MDM2-mediated p53 degradation. *Molecular cell* **2:** 405-415

Gu B, Zhu W-G (2012) Surf the post-translational modification network of p53 regulation. *International journal of biological sciences* **8:** 672

Gupta RA, Shah N, Wang KC, Kim J, Horlings HM, Wong DJ, Tsai M-C, Hung T, Argani P, Rinn JL (2010) Long non-coding RNA HOTAIR reprograms chromatin state to promote cancer metastasis. *Nature* **464:** 1071-1076

Haines DS, Landers JE, Engle LJ, George DL (1994) Physical and functional interaction between wild-type p53 and mdm2 proteins. *Molecular and cellular biology* **14:** 1171-1178

Hallenborg P, Feddersen S, Francoz S, Murano I, Sundekilde U, Petersen R, Akimov V, Olson M, Lozano G, Cinti S (2012) Mdm2 controls CREB-dependent transactivation and initiation of adipocyte differentiation. *Cell Death & Differentiation* **19:** 1381-1389

Hansen KH, Bracken AP, Pasini D, Dietrich N, Gehani SS, Monrad A, Rappsilber J, Lerdrup M, Helin K (2008) A model for transmission of the H3K27me3 epigenetic mark. *Nature cell biology* **10:** 1291-1300

Haupt Y, Maya R, Kazaz A, Oren M (1997) Mdm2 promotes the rapid degradation of p53. *Nature* **387:** 296-299

He J, Kallin EM, Tsukada Y-i, Zhang Y (2008) The H3K36 demethylase Jhdm1b/Kdm2b regulates cell proliferation and senescence through p15Ink4b. *Nature structural & molecular biology* **15:** 1169-1175

Hemming S, Cakouros D, Isenmann S, Cooper L, Menicanin D, Zannettino A, Gronthos S (2014) EZH2 and KDM6A act as an epigenetic switch to regulate mesenchymal stem cell lineage specification. *Stem Cells* **32:** 802-815

Herman AG, Hayano M, Poyurovsky MV, Shimada K, Skouta R, Prives C, Stockwell BR (2011) Discovery of Mdm2-MdmX E3 ligase inhibitors using a cell-based ubiquitination assay. *Cancer discovery* **1:** 312-325

Higuchi R, Fockler C, Dollinger G, Watson R (1993) Kinetic PCR analysis: real-time monitoring of DNA amplification reactions. *Biotechnology* **11:** 1026-1030

Hilliard SA, Yao X, El-Dahr SS (2014) Mdm2 is required for maintenance of the nephrogenic niche. *Developmental biology* **387:** 1-14

Hochedlinger K, Yamada Y, Beard C, Jaenisch R (2005) Ectopic expression of Oct-4 blocks progenitor-cell differentiation and causes dysplasia in epithelial tissues. *Cell* **121:** 465-477

Honda R, Tanaka H, Yasuda H (1997) Oncoprotein MDM2 is a ubiquitin ligase E3 for tumor suppressor p53. *FEBS letters* **420:** 25-27

Hong H, Takahashi K, Ichisaka T, Aoi T, Kanagawa O, Nakagawa M, Okita K, Yamanaka S (2009) Suppression of induced pluripotent stem cell generation by the p53–p21 pathway. *Nature* **460:** 1132-1135

Hu H, Yang Y, Ji Q, Zhao W, Jiang B, Liu R, Yuan J, Liu Q, Li X, Zou Y, Shao C, Shang Y, Wang Y, Gong Y (2012) CRL4B catalyzes H2AK119 monoubiquitination and coordinates with PRC2 to promote tumorigenesis. *Cancer cell* **22:** 781-795

Huang DW, Sherman BT, Lempicki RA (2008) Systematic and integrative analysis of large gene lists using DAVID bioinformatics resources. *Nature protocols* **4:** 44-57

Huang L, Yan Z, Liao X, Li Y, Yang J, Wang Z-G, Zuo Y, Kawai H, Shadfan M, Ganapathy S (2011) The p53 inhibitors MDM2/MDMX complex is required for control of p53 activity in vivo. *Proceedings of the National Academy of Sciences* **108:** 12001-12006

Hunkapiller J, Shen Y, Diaz A, Cagney G, McCleary D, Ramalho-Santos M, Krogan N, Ren B, Song JS, Reiter JF (2012) Polycomb-like 3 promotes polycomb repressive complex 2 binding to CpG islands and embryonic stem cell self-renewal. *PLoS genetics* **8:** e1002576

Iliopoulos D, Lindahl-Allen M, Polytarchou C, Hirsch HA, Tsichlis PN, Struhl K (2010) Loss of miR-200 inhibition of Suz12 leads to polycomb-mediated repression required for the formation and maintenance of cancer stem cells. *Molecular cell* **39:** 761-772

Itahana K, Mao H, Jin A, Itahana Y, Clegg HV, Lindstrom MS, Bhat KP, Godfrey VL, Evan GI, Zhang Y (2007) Targeted inactivation of Mdm2 RING finger E3 ubiquitin ligase activity in the mouse reveals mechanistic insights into p53 regulation. *Cancer Cell* **12:** 355-366

Ito T, Sun B (2009) Epigenetic regulation of developmental timing in floral stem cells. *Epigenetics* **4:** 564-567

Jackson SP, Bartek J (2009) The DNA-damage response in human biology and disease. *Nature* **461:** 1071-1078

Jacobs JJ, Kieboom K, Marino S, DePinho RA, van Lohuizen M (1999) The oncogene and Polycomb-group gene bmi-1 regulates cell proliferation and senescence through the ink4a locus. *Nature* **397:** 164-168

Jin Y, Lee H, Zeng SX, Dai MS, Lu H (2003) MDM2 promotes p21waf1/cip1 proteasomal turnover independently of ubiquitylation. *The EMBO journal* **22:** 6365-6377

Jones SN, Hancock AR, Vogel H, Donehower LA, Bradley A (1998) Overexpression of Mdm2 in mice reveals a p53-independent role for Mdm2 in tumorigenesis. *Proceedings of the National Academy of Sciences* **95:** 15608-15612

Jones SN, Roe AE, Donehower LA, Bradley A (1995) Rescue of embryonic lethality in Mdm2-deficient mice by absence of p53. *Nature* **378:** 206-208

Jürgens G (1985) A group of genes controlling the spatial expression of the bithorax complex in Drosophila.

Kahn TG, Schwartz YB, Dellino GI, Pirrotta V (2006) Polycomb complexes and the propagation of the methylation mark at the Drosophila ubx gene. *Journal of Biological Chemistry* **281:** 29064-29075

Kalb R, Latwiel S, Baymaz HI, Jansen PW, Müller CW, Vermeulen M, Müller J (2014) Histone H2A monoubiquitination promotes histone H3 methylation in Polycomb repression. *Nature structural & molecular biology* **21:** 569-571

Kaneko S, Bonasio R, Saldana-Meyer R, Yoshida T, Son J, Nishino K, Umezawa A, Reinberg D (2014) Interactions between JARID2 and noncoding RNAs regulate PRC2 recruitment to chromatin. *Mol Cell* **53:** 290-300

Kaneko S, Son J, Shen SS, Reinberg D, Bonasio R (2013) PRC2 binds active promoters and contacts nascent RNAs in embryonic stem cells. *Nature structural & molecular biology* **20:** 1258-1264

Karolchik D, Hinrichs AS, Furey TS, Roskin KM, Sugnet CW, Haussler D, Kent WJ (2004) The UCSC Table Browser data retrieval tool. *Nucleic acids research* **32:** D493-D496

Karpiuk O, Najafova Z, Kramer F, Hennion M, Galonska C, Konig A, Snaidero N, Vogel T, Shchebet A, Begus-Nahrmann Y, Kassem M, Simons M, Shcherbata H, Beissbarth T, Johnsen SA (2012) The histone H2B monoubiquitination regulatory pathway is required for differentiation of multipotent stem cells. *Mol Cell* **46:** 705-713

Kawamura T, Suzuki J, Wang YV, Menendez S, Morera LB, Raya A, Wahl GM, Belmonte JCI (2009) Linking the p53 tumour suppressor pathway to somatic cell reprogramming. *Nature* **460:** 1140-1144

Ketel CS, Andersen EF, Vargas ML, Suh J, Strome S, Simon JA (2005) Subunit contributions to histone methyltransferase activities of fly and worm polycomb group complexes. *Molecular and cellular biology* **25:** 6857-6868

Knutson SK, Warholic NM, Wigle TJ, Klaus CR, Allain CJ, Raimondi A, Porter Scott M, Chesworth R, Moyer MP, Copeland RA, Richon VM, Pollock RM, Kuntz KW, Keilhack H (2013) Durable

tumor regression in genetically altered malignant rhabdoid tumors by inhibition of methyltransferase EZH2. *Proc Natl Acad Sci U S A* **110:** 7922-7927

Kojima K, Burks JK, Arts J, Andreeff M (2010) The novel tryptamine derivative JNJ-26854165 induces wild-type p53-and E2F1-mediated apoptosis in acute myeloid and lymphoid leukemias. *Molecular cancer therapeutics* **9:** 2545-2557

Kreso A, Dick JE (2014) Evolution of the cancer stem cell model. *Cell stem cell* **14:** 275-291

Ku M, Koche RP, Rheinbay E, Mendenhall EM, Endoh M, Mikkelsen TS, Presser A, Nusbaum C, Xie X, Chi AS (2008) Genomewide analysis of PRC1 and PRC2 occupancy identifies two classes of bivalent domains. *PLoS genetics* **4:** e1000242

Kussie PH, Gorina S, Marechal V, Elenbaas B, Moreau J, Levine AJ, Pavletich NP (1996) Structure of the MDM2 oncoprotein bound to the p53 tumor suppressor transactivation domain. *Science* **274:** 948-953

Kuzmichev A, Jenuwein T, Tempst P, Reinberg D (2004) Different EZH2-containing complexes target methylation of histone H1 or nucleosomal histone H3. *Molecular cell* **14:** 183-193

Laemmli UK (1970) Cleavage of structural proteins during the assembly of the head of bacteriophage T4. *Nature* **227:** 680-685

Landeira D, Sauer S, Poot R, Dvorkina M, Mazzarella L, Jørgensen HF, Pereira CF, Leleu M, Piccolo FM, Spivakov M (2010) Jarid2 is a PRC2 component in embryonic stem cells required for multi-lineage differentiation and recruitment of PRC1 and RNA Polymerase II to developmental regulators. *Nature cell biology* **12:** 618-624

Lane D, Crawford L (1979) T antigen is bound to a host protein in SY40-transformed cells.

Lane DP, Verma C (2012) Mdm2 in evolution. *Genes & cancer* **3:** 320-324

Langmead B, Salzberg SL (2012) Fast gapped-read alignment with Bowtie 2. *Nature methods* **9:** 357-359

Langmead B, Trapnell C, Pop M, Salzberg SL (2009) Ultrafast and memory-efficient alignment of short DNA sequences to the human genome. *Genome biology* **10:** R25

Lee TI, Jenner RG, Boyer LA, Guenther MG, Levine SS, Kumar RM, Chevalier B, Johnstone SE, Cole MF, Isono K-i (2006) Control of developmental regulators by Polycomb in human embryonic stem cells. *Cell* **125:** 301-313

Leeb M, Pasini D, Novatchkova M, Jaritz M, Helin K, Wutz A (2010) Polycomb complexes act redundantly to repress genomic repeats and genes. *Genes Dev* **24:** 265-276

Lengner CJ, Steinman HA, Gagnon J, Smith TW, Henderson JE, Kream BE, Stein GS, Lian JB, Jones SN (2006) Osteoblast differentiation and skeletal development are regulated by Mdm2–p53 signaling. *The Journal of cell biology* **172:** 909-921

Lessard J, Sauvageau G (2003) Bmi-1 determines the proliferative capacity of normal and leukaemic stem cells. *Nature* **423:** 255-260

Levine SS, Weiss A, Erdjument-Bromage H, Shao Z, Tempst P, Kingston RE (2002) The core of the polycomb repressive complex is compositionally and functionally conserved in flies and humans. *Molecular and cellular biology* **22:** 6070-6078

Levrero M, De Laurenzi V, Costanzo A, Gong J, Wang J, Melino G (2000) The p53/p63/p73 family of transcription factors: overlapping and distinct functions. *Journal of cell science* **113:** 1661-1670

Lewis EB (1978) A gene complex controlling segmentation in Drosophila. *Nature* **276:** 565-570

Li M, Brooks CL, Wu-Baer F, Chen D, Baer R, Gu W (2003) Mono-versus polyubiquitination: differential control of p53 fate by Mdm2. *Science* **302:** 1972-1975

Li Q, Lozano G (2013) Molecular pathways: targeting Mdm2 and Mdm4 in cancer therapy. *Clinical Cancer Research* **19:** 34-41

Lin Y-H, Lee C-C, Chang F-R, Chang W-H, Wu Y-C, Chang J-G (2011) 16-Hydroxycleroda-3, 13-dien-15, 16-olide regulates the expression of histone-modifying enzymes PRC2 complex and induces apoptosis in CML K562 cells. *Life sciences* **89:** 886-895

Linares LK, Hengstermann A, Ciechanover A, Müller S, Scheffner M (2003) HdmX stimulates Hdm2-mediated ubiquitination and degradation of p53. *Proceedings of the National Academy of Sciences* **100:** 12009-12014

Linzer DI, Levine AJ (1979) Characterization of a 54K dalton cellular SV40 tumor antigen present in SV40-transformed cells and uninfected embryonal carcinoma cells. *Cell* **17:** 43-52

Lion M, Bisio A, Tebaldi T, De Sanctis V, Menendez D, Resnick MA, Ciribilli Y, Inga A (2013) Interaction between p53 and estradiol pathways in transcriptional responses to chemotherapeutics. *Cell Cycle* **12:** 1211-1224

Liu T, Ortiz JA, Taing L, Meyer CA, Lee B, Zhang Y, Shin H, Wong SS, Ma J, Lei Y, Pape UJ, Poidinger M, Chen Y, Yeung K, Brown M, Turpaz Y, Liu XS (2011) Cistrome: an integrative platform for transcriptional regulation studies. *Genome biology* **12:** R83

Livak KJ, Schmittgen TD (2001) Analysis of relative gene expression data using real-time quantitative PCR and the 2(-Delta Delta C(T)) Method. *Methods (San Diego, Calif)* **25:** 402-408

Loughran Ö, La Thangue NB (2000) Apoptotic and growth-promoting activity of E2F modulated by MDM2. *Molecular and cellular biology* **20:** 2186-2197

Lu M-L, Wikman F, Orntoft TF, Charytonowicz E, Rabbani F, Zhang Z, Dalbagni G, Pohar KS, Yu G, Cordon-Cardo C (2002) Impact of alterations affecting the p53 pathway in bladder cancer on clinical outcome, assessed by conventional and array-based methods. *Clinical cancer research* **8:** 171-179

Lu X, Ma O, Nguyen T-A, Jones SN, Oren M, Donehower LA (2007) The Wip1 Phosphatase acts as a gatekeeper in the p53-Mdm2 autoregulatory loop. *Cancer cell* **12:** 342-354

Lundgren K, de Oca Luna RM, McNeill YB, Emerick EP, Spencer B, Barfield CR, Lozano G, Rosenberg MP, Finlay CA (1997) Targeted expression of MDM2 uncouples S phase from mitosis and inhibits mammary gland development independent of p53. *Genes Dev* **11:** 714-725

Malekzadeh Shafaroudi A, Mowla SJ, Ziaee SA-M, Bahrami A-R, Atlasi Y, Malakootian M (2008) Overexpression of BMI1, a polycomb group repressor protein, in bladder tumors: a preliminary report. *Urology journal* **5:** 99-105

Margueron R, Li G, Sarma K, Blais A, Zavadil J, Woodcock CL, Dynlacht BD, Reinberg D (2008) Ezh1 and Ezh2 maintain repressive chromatin through different mechanisms. *Molecular cell* **32:** 503-518

Marine J-C, Francoz S, Maetens M, Wahl G, Toledo F, Lozano G (2006) Keeping p53 in check: essential and synergistic functions of Mdm2 and Mdm4. *Cell Death & Differentiation* **13:** 927-934

Marine J-C, Lozano G (2010) Mdm2-mediated ubiquitylation: p53 and beyond. *Cell Death & Differentiation* **17:** 93-102

Marión RM, Strati K, Li H, Murga M, Blanco R, Ortega S, Fernandez-Capetillo O, Serrano M, Blasco MA (2009) A p53-mediated DNA damage response limits reprogramming to ensure iPS cell genomic integrity. *Nature* **460:** 1149-1153

Martin K, Trouche D, Hagemeier C, Sorensen TS, La Thangue NB, Kouzarides T (1995) Stimulation of E2F1/DP1 transcriptional activity by MDM2 oncoprotein. *Nature* **375:** 691-694

Martoriati A, Doumont G, Alcalay M, Bellefroid E, Pelicci PG, Marine J-C (2005) dapk1, encoding an activator of a p19ARF-p53-mediated apoptotic checkpoint, is a transcription target of p53. *Oncogene* **24:** 1461-1466

Matijasevic Z, Steinman HA, Hoover K, Jones SN (2008) MdmX promotes bipolar mitosis to suppress transformation and tumorigenesis in p53-deficient cells and mice. *Molecular and cellular biology* **28:** 1265-1273

Maya R, Balass M, Kim S-T, Shkedy D, Leal J-FM, Shifman O, Moas M, Buschmann T, Ronai Ze, Shiloh Y (2001) ATM-dependent phosphorylation of Mdm2 on serine 395: role in p53 activation by DNA damage. *Genes Dev* **15:** 1067-1077

Mayo LD, Turchi JJ, Berberich SJ (1997) Mdm-2 phosphorylation by DNA-dependent protein kinase prevents interaction with p53. *Cancer Res* **57:** 5013-5016

McDonnell TJ, Montes de Oca Luna R, Cho S, Amelse LL, Chavez-Reyes A, Lozano G (1999) Loss of one but not two mdm2 null alleles alters the tumour spectrum in p53 null mice. *The Journal of pathology* **188:** 322-328

McLean CY, Bristor D, Hiller M, Clarke SL, Schaar BT, Lowe CB, Wenger AM, Bejerano G (2010) GREAT improves functional interpretation of cis-regulatory regions. *Nature biotechnology* **28:** 495-501

Michael D, Oren M (2003) The p53–Mdm2 module and the ubiquitin system. In *Seminars in cancer biology*, Vol. 13, pp 49-58.

Migliorini D, Denchi EL, Danovi D, Jochemsen A, Capillo M, Gobbi A, Helin K, Pelicci PG, Marine J-C (2002) Mdm4 (Mdmx) regulates p53-induced growth arrest and neuronal cell death during early embryonic mouse development. *Molecular and cellular biology* **22:** 5527-5538

Minsky N, Oren M (2004) The RING Domain of Mdm2 Mediates Histone Ubiquitylation and Transcriptional Repression. *Mol Cell* **16:** 631-639

Molchadsky A, Shats I, Goldfinger N, Pevsner-Fischer M, Olson M, Rinon A, Tzahor E, Lozano G, Zipori D, Sarig R (2008) p53 plays a role in mesenchymal differentiation programs, in a cell fate dependent manner. *PLoS One* **3:** e3707

Momand J, Jung D, Wilczynski S, Niland J (1998) The MDM2 gene amplification database. *Nucleic acids research* **26:** 3453-3459

Momand J, Villegas A, Belyi VA (2011) The evolution of MDM2 family genes. *Gene* **486:** 23-30

Momand J, Zambetti GP, Olson DC, George D, Levine AJ (1992) The mdm-2 oncogene product forms a complex with the p53 protein and inhibits p53-mediated transactivation. *Cell* **69:** 1237-1245

Montes de Oca Luna R, Wagner DS, Lozano G (1995) Rescue of early embryonic lethality in mdm2-deficient mice by deletion of p53. *Nature* **378:** 203-206

Mootha VK, Lindgren CM, Eriksson K-F, Subramanian A, Sihag S, Lehar J, Puigserver P, Carlsson E, Ridderstråle M, Laurila E (2003) PGC-1α-responsive genes involved in oxidative phosphorylation are coordinately downregulated in human diabetes. *Nature genetics* **34:** 267-273

Morrison SJ, Shah NM, Anderson DJ (1997) Regulatory mechanisms in stem cell biology. *Cell* **88:** 287-298

Moumen A, Masterson P, O'Connor MJ, Jackson SP (2005) hnRNP K: an HDM2 target and transcriptional coactivator of p53 in response to DNA damage. *Cell* **123:** 1065-1078

Mulay SR, Thomasova D, Ryu M, Anders H-J (2012) MDM2 (murine double minute-2) links inflammation and tubular cell healing during acute kidney injury in mice. *Kidney international* **81:** 1199-1211

Naldini L, Blomer U, Gage FH, Trono D, Verma IM (1996) Efficient transfer, integration, and sustained long-term expression of the transgene in adult rat brains injected with a lentiviral vector. *Proc Natl Acad Sci U S A* **93:** 11382-11388

Nekrasov M, Klymenko T, Fraterman S, Papp B, Oktaba K, Köcher T, Cohen A, Stunnenberg HG, Wilm M, Müller J (2007) Pcl-PRC2 is needed to generate high levels of H3-K27 trimethylation at Polycomb target genes. *The EMBO journal* **26:** 4078-4088

Nemajerova A, Kim S, Petrenko O, Moll U (2012) Two-factor reprogramming of somatic cells to pluripotent stem cells reveals partial functional redundancy of Sox2 and Klf4. *Cell Death & Differentiation* **19:** 1268-1276

Nie F-q, Sun M, Yang J-s, Xie M, Xu T-p, Xia R, Liu Y-w, Liu X-h, Zhang E-b, Lu K-h (2015) Long Noncoding RNA ANRIL Promotes Non–Small Cell Lung Cancer Cell Proliferation and Inhibits Apoptosis by Silencing KLF2 and P21 Expression. *Molecular cancer therapeutics* **14:** 268-277

O'Carroll D, Erhardt S, Pagani M, Barton SC, Surani MA, Jenuwein T (2001) The polycomb-group gene Ezh2 is required for early mouse development. *Molecular and cellular biology* **21:** 4330-4336

Ohta H, Sawada A, Kim JY, Tokimasa S, Nishiguchi S, Humphries RK, Hara J, Takihara Y (2002) Polycomb group gene rae28 is required for sustaining activity of hematopoietic stem cells. *The Journal of experimental medicine* **195:** 759-770

Oliner JD, Kinzler KW, Meltzer PS, George DL, Vogelstein B (1992) Amplification of a gene encoding a p53-associated protein in human sarcomas. *Nature* **358:** 80-83

Oliner JD, Pietenpol JA, Thiagalingam S, Gyuris J, Kinzler KW, Vogelstein B (1993) Oncoprotein MDM2 conceals the activation domain of tumour suppressor p53.

Onder TT, Kara N, Cherry A, Sinha AU, Zhu N, Bernt KM, Cahan P, Mancarci BO, Unternaehrer J, Gupta PB (2012) Chromatin-modifying enzymes as modulators of reprogramming. *Nature* **483:** 598-602

Onel K, Cordon-Cardo C (2004) MDM2 and prognosis. *Molecular cancer research* **2:** 1-8

Oren M (2003) Decision making by p53: life, death and cancer. *Cell death and differentiation* **10:** 431-442

Pant V, Xiong S, Iwakuma T, Quintás-Cardama A, Lozano G (2011) Heterodimerization of Mdm2 and Mdm4 is critical for regulating p53 activity during embryogenesis but dispensable for p53 and Mdm2 stability. *Proceedings of the National Academy of Sciences* **108:** 11995-12000

Parant J, Chavez-Reyes A, Little NA, Yan W, Reinke V, Jochemsen AG, Lozano G (2001) Rescue of embryonic lethality in Mdm4-null mice by loss of Trp53 suggests a nonoverlapping pathway with MDM2 to regulate p53. *Nat Genet* **29:** 92-95

Pardal R, Clarke MF, Morrison SJ (2003) Applying the principles of stem-cell biology to cancer. *Nature Reviews Cancer* **3:** 895-902

Pasini D, Bracken AP, Hansen JB, Capillo M, Helin K (2007) The polycomb group protein Suz12 is required for embryonic stem cell differentiation. *Molecular and cellular biology* **27:** 3769-3779

Pasini D, Bracken AP, Jensen MR, Lazzerini Denchi E, Helin K (2004) Suz12 is essential for mouse development and for EZH2 histone methyltransferase activity. *The EMBO journal* **23:** 4061-4071

Plath K, Fang J, Mlynarczyk-Evans SK, Cao R, Worringer KA, Wang H, Cecile C, Otte AP, Panning B, Zhang Y (2003) Role of histone H3 lysine 27 methylation in X inactivation. *Science* **300:** 131-135

Ramírez F, Dündar F, Diehl S, Grüning BA, Manke T (2014) deepTools: a flexible platform for exploring deep-sequencing data. *Nucleic acids research* **42:** W187-W191

Reik W, Dean W, Walter J (2001) Epigenetic reprogramming in mammalian development. *Science* **293:** 1089-1093

Renart J, Reiser J, Stark GR (1979) Transfer of proteins from gels to diazobenzyloxymethyl-paper and detection with antisera: a method for studying antibody specificity and antigen structure. *Proc Natl Acad Sci U S A* **76:** 3116-3120

Reya T, Morrison SJ, Clarke MF, Weissman IL (2001) Stem cells, cancer, and cancer stem cells. *Nature* **414:** 105-111

Richly H, Aloia L, Di Croce L (2011) Roles of the Polycomb group proteins in stem cells and cancer. *Cell death & disease* **2:** e204

Robinson JT, Thorvaldsdottir H, Winckler W, Guttman M, Lander ES, Getz G, Mesirov JP (2011) *Integrative genomics viewer*: Nat Biotechnol. 2011 Jan;29(1):24-6. doi: 10.1038/nbt.1754.

Román-Trufero M, Méndez-Gómez HR, Perez C, Hijikata A, Fujimura Yi, Endo T, Koseki H, Vicario-Abejón C, Vidal M (2009) Maintenance of Undifferentiated State and Self-Renewal of Embryonic Neural Stem Cells by Polycomb Protein Ring1B. *Stem Cells* **27:** 1559-1570

Rothbart SB, Strahl BD (2014) Interpreting the language of histone and DNA modifications. *Biochimica et Biophysica Acta (BBA)-Gene Regulatory Mechanisms* **1839:** 627-643

Roxburgh P, Hock AK, Dickens MP, Mezna M, Fischer PM, Vousden KH (2012) Small molecules that bind the Mdm2 RING stabilize and activate p53. *Carcinogenesis* **33:** 791-798

Sah VP, Attardi LD, Mulligan GJ, Williams BO, Bronson RT, Jacks T (1995) A subset of p53-deficient embryos exhibit exencephaly. *Nat Genet* **10:** 175-180

Saiki RK, Scharf S, Faloona F, Mullis KB, Horn GT, Erlich HA, Arnheim N (1985) Enzymatic amplification of beta-globin genomic sequences and restriction site analysis for diagnosis of sickle cell anemia. *Science* **230:** 1350-1354

Santos-Rosa H, Schneider R, Bannister AJ, Sherriff J, Bernstein BE, Emre NT, Schreiber SL, Mellor J, Kouzarides T (2002) Active genes are tri-methylated at K4 of histone H3. *Nature* **419:** 407-411

Sasaki H, Setoguchi T, Matsunoshita Y, Gao H, Hirotsu M, Komiya S (2010) The knock-down of overexpressed EZH2 and BMI-1 does not prevent osteosarcoma growth. *Oncology reports* **23:** 677-684

Schmitges FW, Prusty AB, Faty M, Stützer A, Lingaraju GM, Aiwazian J, Sack R, Hess D, Li L, Zhou S (2011) Histone methylation by PRC2 is inhibited by active chromatin marks. *Molecular cell* **42:** 330-341

Schuettengruber B, Cavalli G (2009) Recruitment of polycomb group complexes and their role in the dynamic regulation of cell fate choice. *Development* **136:** 3531-3542

Schwartz YB, Kahn TG, Nix DA, Li X-Y, Bourgon R, Biggin M, Pirrotta V (2006) Genome-wide analysis of Polycomb targets in Drosophila melanogaster. *Nat Genet* **38:** 700-705

Schwartz YB, Pirrotta V (2007) Polycomb silencing mechanisms and the management of genomic programmes. *Nature Reviews Genetics* **8:** 9-22

Sela Y, Molotski N, Golan S, Itskovitz-Eldor J, Soen Y (2012) Human embryonic stem cells exhibit increased propensity to differentiate during the G1 phase prior to phosphorylation of retinoblastoma protein. *Stem Cells* **30:** 1097-1108

Seligson DB, Horvath S, Shi T, Yu H, Tze S, Grunstein M, Kurdistani SK (2005) Global histone modification patterns predict risk of prostate cancer recurrence. *Nature* **435:** 1262-1266

Sell S (1993) Cellular origin of cancer: dedifferentiation or stem cell maturation arrest? *Environmental health perspectives* **101:** 15

Shah N, Sukumar S (2010) The Hox genes and their roles in oncogenesis. *Nature reviews Cancer* **10:** 361-371

Shao Z, Raible F, Mollaaghababa R, Guyon JR, Wu C-t, Bender W, Kingston RE (1999) Stabilization of chromatin structure by PRC1, a Polycomb complex. *Cell* **98:** 37-46

Shapiro AL, Vinuela E, Maizel JV, Jr. (1967) Molecular weight estimation of polypeptide chains by electrophoresis in SDS-polyacrylamide gels. *Biochemical and biophysical research communications* **28:** 815-820

Sher F, Boddeke E, Olah M, Copray S (2012) Dynamic changes in Ezh2 gene occupancy underlie its involvement in neural stem cell self-renewal and differentiation towards oligodendrocytes. *PLoS One* **7:** e40399

Sherr CJ (2001) The INK4a/ARF network in tumour suppression. *Nature reviews Molecular cell biology* **2:** 731-737

Shin YJ, Kim J-H (2012) The role of EZH2 in the regulation of the activity of matrix metalloproteinases in prostate cancer cells. *PLoS One* **7:** e30393

Shogren-Knaak M, Ishii H, Sun J-M, Pazin MJ, Davie JR, Peterson CL (2006) Histone H4-K16 acetylation controls chromatin structure and protein interactions. *Science* **311:** 844-847

Shvarts A, Bazuine M, Dekker P, Ramos YF, Steegenga WT, Merckx G, van Ham RC, van Oordt WvdH, van der Eb AJ, Jochemsen A (1997) Isolation and identification of the human homolog of a new p53-binding protein, Mdmx. *Genomics* **43:** 34-42

Shvarts A, Steegenga WT, Riteco N, van Laar T, Dekker P, Bazuine M, van Ham RC, van der Houven van Oordt W, Hateboer G, van der Eb AJ, Jochemsen AG (1996) MDMX: a novel p53-binding protein with some functional properties of MDM2. *The EMBO journal* **15:** 5349-5357

Sigalas I, Calvert AH, Anderson JJ, Neal DE, Lunec J (1996) Alternatively spliced mdm2 transcripts with loss of p53 binding domain sequences: transforming ability and frequent detection in human cancer. *Nature medicine* **2:** 912-917

Simon J, Chiang A, Bender W, Shimell MJ, O'Connor M (1993) Elements of the Drosophila bithorax complex that mediate repression by Polycomb group products. *Developmental biology* **158:** 131-144

Simon JA, Kingston RE (2013) Occupying chromatin: Polycomb mechanisms for getting to genomic targets, stopping transcriptional traffic, and staying put. *Molecular cell* **49:** 808-824

Sing A, Pannell D, Karaiskakis A, Sturgeon K, Djabali M, Ellis J, Lipshitz HD, Cordes SP (2009) A vertebrate Polycomb response element governs segmentation of the posterior hindbrain. *Cell* **138:** 885-897

Singh SK, Clarke ID, Terasaki M, Bonn VE, Hawkins C, Squire J, Dirks PB (2003) Identification of a cancer stem cell in human brain tumors. *Cancer Res* **63:** 5821-5828

Slifer EH (1942) A mutant stock of Drosophila with extra sex-combs. *Journal of Experimental Zoology* **90:** 31-40

Smith KS, Chanda SK, Lingbeek M, Ross DT, Botstein D, van Lohuizen M, Cleary ML (2003) Bmi-1 regulation of INK4A-ARF is a downstream requirement for transformation of hematopoietic progenitors by E2a-Pbx1. *Molecular cell* **12:** 393-400

Sparmann A, van Lohuizen M (2006) Polycomb silencers control cell fate, development and cancer. *Nature Reviews Cancer* **6:** 846-856

Spiegelman S, Watson K, Kacian D (1971) Synthesis of DNA complements of natural RNAs: a general approach. *Proceedings of the National Academy of Sciences* **68:** 2843-2845

Spivakov M, Fisher AG (2007) Epigenetic signatures of stem-cell identity. *Nature reviews Genetics* **8:** 263-271

Stark R, Brown G (2011) DiffBind: differential binding analysis of ChIP-Seq peak data. *In R package version* **100**

Steinman HA, Hoover KM, Keeler ML, Sands AT, Jones SN (2005) Rescue of Mdm4-deficient mice by Mdm2 reveals functional overlap of Mdm2 and Mdm4 in development. *Oncogene* **24:** 7935-7940

Stewart SA, Dykxhoorn DM, Palliser D, Mizuno H, Yu EY, An DS, Sabatini DM, Chen IS, Hahn WC, Sharp PA, Weinberg RA, Novina CD (2003) Lentivirus-delivered stable gene silencing by RNAi in primary cells. *RNA* **9:** 493-501

Stier S, Cheng T, Dombkowski D, Carlesso N, Scadden DT (2002) Notch1 activation increases hematopoietic stem cell self-renewal in vivo and favors lymphoid over myeloid lineage outcome. *Blood* **99:** 2369-2378

Strahl BD, Allis CD (2000) The language of covalent histone modifications. *Nature* **403:** 41-45

Subramanian A, Tamayo P, Mootha VK, Mukherjee S, Ebert BL, Gillette MA, Paulovich A, Pomeroy SL, Golub TR, Lander ES (2005) Gene set enrichment analysis: a knowledge-based approach for interpreting genome-wide expression profiles. *Proceedings of the National Academy of Sciences of the United States of America* **102:** 15545-15550

Suvà M-L, Riggi N, Janiszewska M, Radovanovic I, Provero P, Stehle J-C, Baumer K, Le Bitoux M-A, Marino D, Cironi L (2009) EZH2 is essential for glioblastoma cancer stem cell maintenance. *Cancer Res* **69:** 9211-9218

Takada I, Kouzmenko AP, Kato S (2009) Wnt and PPARγ signaling in osteoblastogenesis and adipogenesis. *Nature Reviews Rheumatology* **5:** 442-447

Takahashi K, Yamanaka S (2006) Induction of pluripotent stem cells from mouse embryonic and adult fibroblast cultures by defined factors. *Cell* **126:** 663-676

Talbert PB, Henikoff S (2010) Histone variants—ancient wrap artists of the epigenome. *Nature reviews Molecular cell biology* **11:** 264-275

Tanaka Y, Hysolli E, Su J, Xiang Y, Kim K-Y, Zhong M, Li Y, Heydari K, Euskirchen G, Snyder MP (2015) Transcriptome Signature and Regulation in Human Somatic Cell Reprogramming. *Stem cell reports*

Tange S, Oktyabri D, Terashima M, Ishimura A, Suzuki T (2014) JARID2 is involved in transforming growth factor-beta-induced epithelial-mesenchymal transition of lung and colon cancer cell lines. *PLoS One* **9:** e115684

Tanikawa C, Nakagawa H, Furukawa Y, Nakamura Y, Matsuda K (2012) CLCA2 as a p53-inducible senescence mediator. *Neoplasia* **14:** 141-IN149

Tanimura S, Ohtsuka S, Mitsui K, Shirouzu K, Yoshimura A, Ohtsubo M (1999) MDM2 interacts with MDMX through their RING finger domains. *FEBS letters* **447:** 5-9

Tavares L, Dimitrova E, Oxley D, Webster J, Poot R, Demmers J, Bezstarosti K, Taylor S, Ura H, Koide H (2012) RYBP-PRC1 complexes mediate H2A ubiquitylation at polycomb target sites independently of PRC2 and H3K27me3. *Cell* **148:** 664-678

Terzian T, Suh Y-A, Iwakuma T, Post SM, Neumann M, Lang GA, Van Pelt CS, Lozano G (2008) The inherent instability of mutant p53 is alleviated by Mdm2 or p16INK4a loss. *Genes & development* **22:** 1337-1344

Thorvaldsdottir H, Robinson JT, Mesirov JP (2013) Integrative Genomics Viewer (IGV): high-performance genomics data visualization and exploration. *Brief Bioinform* **14:** 178-192

Toledo F, Krummel KA, Lee CJ, Liu C-W, Rodewald L-W, Tang M, Wahl GM (2006) A mouse p53 mutant lacking the proline-rich domain rescues Mdm4 deficiency and provides insight into the Mdm2-Mdm4-p53 regulatory network. *Cancer cell* **9:** 273-285

Towbin H, Staehelin T, Gordon J (1979) Electrophoretic transfer of proteins from polyacrylamide gels to nitrocellulose sheets: procedure and some applications. *Proc Natl Acad Sci U S A* **76:** 4350-4354

Trotta R, Vignudelli T, Candini O, Intine RV, Pecorari L, Guerzoni C, Santilli G, Byrom MW, Goldoni S, Ford LP (2003) BCR/ABL activates mdm2 mRNA translation via the La antigen. *Cancer cell* **3:** 145-160

Truong AH, Cervi D, Lee J, Ben-David Y (2005) Direct transcriptional regulation of MDM2 by Fli-1. *Oncogene* **24:** 962-969

Turner BM (2000) Histone acetylation and an epigenetic code. *Bioessays* **22:** 836-845

Twine NA, Chen L, Pang CN, Wilkins MR, Kassem M (2014) Identification of differentiation-stage specific markers that define the ex vivo osteoblastic phenotype. *Bone* **67:** 23-32

Uchida C, Miwa S, Kitagawa K, Hattori T, Isobe T, Otani S, Oda T, Sugimura H, Kamijo T, Ookawa K (2005) Enhanced Mdm2 activity inhibits pRB function via ubiquitin-dependent degradation. *The EMBO journal* **24:** 160-169

van der Stoop P, Boutsma EA, Hulsman D, Noback S, Heimerikx M, Kerkhoven RM, Voncken JW, Wessels L, van Lohuizen M (2008) Ubiquitin E3 ligase Ring1b/Rnf2 of polycomb repressive complex 1 contributes to stable maintenance of mouse embryonic stem cells. *PLoS One* **3:** e2235-e2235

van Vlerken LE, Kiefer CM, Morehouse C, Li Y, Groves C, Wilson SD, Yao Y, Hollingsworth RE, Hurt EM (2013) EZH2 is required for breast and pancreatic cancer stem cell maintenance and can be used as a functional cancer stem cell reporter. *Stem cells translational medicine* **2:** 43-52

Vanharanta S, Shu W, Brenet F, Hakimi AA, Heguy A, Viale A, Reuter VE, Hsieh JJ, Scandura JM, Massagué J (2013) Epigenetic expansion of VHL-HIF signal output drives multiorgan metastasis in renal cancer. *Nature medicine* **19:** 50-56

Varambally S, Cao Q, Mani RS, Shankar S, Wang X, Ateeq B, Laxman B, Cao X, Jing X, Ramnarayanan K, Brenner JC, Yu J, Kim JH, Han B, Tan P, Kumar-Sinha C, Lonigro RJ, Palanisamy N, Maher CA, Chinnaiyan AM (2008) Genomic loss of microRNA-101 leads to overexpression of histone methyltransferase EZH2 in cancer. *Science* **322:** 1695-1699

Venter JC, Adams MD, Myers EW, Li PW, Mural RJ, Sutton GG, Smith HO, Yandell M, Evans CA, Holt RA (2001) The sequence of the human genome. *Science* **291:** 1304-1351

Villasante A, Piazzolla D, Li H, Gomez-Lopez G, Djabali M, Serrano M (2011) Epigenetic regulation of Nanog expression by Ezh2 in pluripotent stem cells. *Cell Cycle* **10:** 1488-1498

Vogelstein B, Lane D, Levine AJ (2000) Surfing the p53 network. *Nature* **408:** 307-310

Voigt P, LeRoy G, Drury WJ, Zee BM, Son J, Beck DB, Young NL, Garcia BA, Reinberg D (2012) Asymmetrically modified nucleosomes. *Cell* **151:** 181-193

Voncken JW, Roelen BA, Roefs M, de Vries S, Verhoeven E, Marino S, Deschamps J, van Lohuizen M (2003) Rnf2 (Ring1b) deficiency causes gastrulation arrest and cell cycle inhibition. *Proceedings of the National Academy of Sciences* **100:** 2468-2473

Vousden KH (2000) p53: death star. *Cell* **103:** 691-694

Wade M, Li Y-C, Wahl GM (2013) MDM2, MDMX and p53 in oncogenesis and cancer therapy. *Nature Reviews Cancer* **13:** 83-96

Walker E, Chang WY, Hunkapiller J, Cagney G, Garcha K, Torchia J, Krogan NJ, Reiter JF, Stanford WL (2010) Polycomb-like 2 associates with PRC2 and regulates transcriptional networks during mouse embryonic stem cell self-renewal and differentiation. *Cell stem cell* **6:** 153-166

Wang H, Wang L, Erdjument-Bromage H, Vidal M, Tempst P, Jones RS, Zhang Y (2004) Role of histone H2A ubiquitination in Polycomb silencing. *Nature* **431:** 873-878

Wang R, Taylor AB, Leal BZ, Chadwell LV, Ilangovan U, Robinson AK, Schirf V, Hart PJ, Lafer EM, Demeler B (2010) Polycomb group targeting through different binding partners of RING1B C-terminal domain. *Structure* **18:** 966-975

Wang X, Jiang X (2012) Mdm2 and MdmX partner to regulate p53. *FEBS letters* **586:** 1390-1396

Weikert S, Christoph F, Köllermann J, Müller M, Schrader M, Miller K, Krause H (2005) Expression levels of the EZH2 polycomb transcriptional repressor correlate with aggressiveness and invasive potential of bladder carcinomas. *International journal of molecular medicine* **16:** 349-353

Weinreb M, Shinar D, Rodan GA (1990) Different pattern of alkaline phosphatase, osteopontin, and osteocalcin expression in developing rat bone visualized by in situ hybridization. *Journal of Bone and Mineral Research* **5:** 831-842

Whitcomb SJ, Basu A, Allis CD, Bernstein E (2007) Polycomb Group proteins: an evolutionary perspective. *TRENDS in Genetics* **23:** 494-502

Wienken M, Dickmanns A, Nemajerova A, Weiss M, Kramer D, Najafova Z, Karpiuk O, Kassem M, Zhang Y, Lozano G, Johnsen SA, Moll UM, Zhang X, Dobbelstein M (under review) MDM2 Associates with Polycomb Repressor Complex 2 and Enhances Stemness-Promoting Chromatin Modifications Independent of p53. *Mol Cell*

Woo CJ, Kharchenko PV, Daheron L, Park PJ, Kingston RE (2010) A region of the human HOXD cluster that confers polycomb-group responsiveness. *Cell* **140:** 99-110

Wu H, D'Alessio AC, Ito S, Xia K, Wang Z, Cui K, Zhao K, Sun YE, Zhang Y (2011) Dual functions of Tet1 in transcriptional regulation in mouse embryonic stem cells. *Nature* **473:** 389-393

Wu X, Bayle JH, Olson D, Levine AJ (1993) The p53-mdm-2 autoregulatory feedback loop. *Genes & development* **7:** 1126-1132

Wu X, Johansen JV, Helin K (2013) Fbxl10/Kdm2b recruits polycomb repressive complex 1 to CpG islands and regulates H2A ubiquitylation. *Molecular cell* **49:** 1134-1146

Xiao ZX, Chen J, Levine AJ, Modjtahedi N, Xing J, Sellers WR, Livingston DM (1995) Interaction between the retinoblastoma protein and the oncoprotein MDM2. *Nature* **375:** 694-698

Xu E, Zhang J, Chen X (2013) MDM2 expression is repressed by the RNA-binding protein RNPC1 via mRNA stability. *Oncogene* **32:** 2169-2178

Yan MS-C, Matouk CC, Marsden PA (2010) Epigenetics of the vascular endothelium. *Journal of applied physiology* **109:** 916-926

Yang J-Y, Zong CS, Xia W, Wei Y, Ali-Seyed M, Li Z, Broglio K, Berry DA, Hung M-C (2006) MDM2 promotes cell motility and invasiveness by regulating E-cadherin degradation. *Molecular and cellular biology* **26:** 7269-7282

Yang J-Y, Zong CS, Xia W, Yamaguchi H, Ding Q, Xie X, Lang J-Y, Lai C-C, Chang C-J, Huang W-C (2008) ERK promotes tumorigenesis by inhibiting FOXO3a via MDM2-mediated degradation. *Nature cell biology* **10:** 138-148

Yang Y, Ludwig RL, Jensen JP, Pierre SA, Medaglia MV, Davydov IV, Safiran YJ, Oberoi P, Kenten JH, Phillips AC (2005) Small molecule inhibitors of HDM2 ubiquitin ligase activity stabilize and activate p53 in cells. *Cancer cell* **7:** 547-559

Yuan W, Wu T, Fu H, Dai C, Wu H, Liu N, Li X, Xu M, Zhang Z, Niu T (2012) Dense chromatin activates Polycomb repressive complex 2 to regulate H3 lysine 27 methylation. *Science* **337:** 971-975

Zacchetti G, Duboule D, Zakany J (2007) Hox gene function in vertebrate gut morphogenesis: the case of the caecum. *Development* **134:** 3967-3973

Zhang Y, Liu T, Meyer CA, Eeckhoute J, Johnson DS, Bernstein BE, Nusbaum C, Myers RM, Brown M, Li W (2008) Model-based analysis of ChIP-Seq (MACS). *Genome biology* **9:** R137

Zhang Z, Wang H, Li M, Rayburn ER, Agrawal S, Zhang R (2005) Stabilization of E2F1 protein by MDM2 through the E2F1 ubiquitination pathway. *Oncogene* **24:** 7238-7247

Zhao Y, Yu H, Hu W (2014) The regulation of MDM2 oncogene and its impact on human cancers. *Acta biochimica et biophysica Sinica* **46:** 180-189

Zhu LJ, Gazin C, Lawson ND, Pagès H, Lin SM, Lapointe DS, Green MR (2010) ChIPpeakAnno: a Bioconductor package to annotate ChIP-seq and ChIP-chip data. *BMC bioinformatics* **11:** 237

Zindy F, Eischen CM, Randle DH, Kamijo T, Cleveland JL, Sherr CJ, Roussel MF (1998) Myc signaling via the ARF tumor suppressor regulates p53-dependent apoptosis and immortalization. *Genes & development* **12:** 2424-2433

Zoabi M, Sadeh R, de Bie P, Ciechanover A (2011) PRAJA1 is a ubiquitin ligase for the polycomb repressive complex 2 proteins. *Biochemical and biophysical research communications* **408:** 393-398

CURRICULUM VITAE

MAGDALENA WIENKEN

Address: Untere-Masch-Str. 10, 37073 Göttingen, Germany
Phone: +49-1713136071
E-mail: magdalenawienken@web.de
Born: December 18th 1986 in Quakenbrueck, Germany
Nationality: German

I. STUDIES

PhD studies in Molecular Oncology **June 2012 – now**

University Medical Center Göttingen, Institute of Molecular Oncologoy (Prof. Dr. M. Dobbelstein)

- Title of thesis: A regulatory network of Mdm2 and members of the Polycomb Group (PcG) family
- Member of the Göttingen Graduate School for Neurosciences, Biophysics, and Molecular Biosciences (GGNB)

M.Sc. Molecular Medicine **2010 – 2012**

University Medical Center Göttingen

- **overall rating: 1.1**
- Title of Master thesis: Mdm2 as a Novel Player in Chromatin Modification and Stemness
    - Supervisor: Prof. Dr. M. Dobbelstein (Institute of Molecular Oncology)
    - **Grade: 1.0**

B.Sc. Applied Biology / B.Hons. Genetics (Immunology) **2007-2010**

Bonn, University of Applied Sciences Bonn-Rhein-Sieg
University of Aberdeen, Scotland (UK)

- **Overall rating: 1.3**
- integrated study programme with a one year stay in Aberdeen, UK
- Title of Bachelor thesis: The Role of Factor XIII in Stabilizing Fibrin against Fibrinolysis
    - Supervisor: Prof. Dr. Nuala Booth (University of Aberdeen)
      Prof. Dr. E. Tobiasch (Bonn-Rhein-Sieg University)
    - **Grade: 1.3**

II. FORMAL EDUCATION

High School **1999-2006**

Gymnasium ULF, Cloppenburg **(Final examination 1,9)**

III. PRICES AND SCHOLARSHIPS

PhD Fellowship Studienstiftung des deutschen Volkes (04/2013 – 03/2016)

M.Sc. Molecular Medicine Scholarship (University Medical Center Göttingen, 2010)

- awarded to 2 students out of 20
- assigned due to excellent performances in the application exam and interview as well as outstanding ratings in the Bachelor studies

Brenda Page Prize for Genetics (University of Aberdeen, 2010)

- awarded to 1 student out of 25
- assigned due to excellent oral and written examination

Free Mover scholarship (Deutscher Akademischer Austauschdienst (DAAD, 2009-2010)

IV. ADDITIONAL QUALIFICATIONS

10/2015	2 day expertise workshop organized by the Studienstiftung des deutschen Volkes, headed by Eva Schuster ***(Communication, negotiation, conflict management)***
08/2014	1 week summer school by the Studienstiftung des deutschen Volkes ***(Introduction into entrepreneurship and consulting, supervised by undconsorten business consultants)***
04/2014 – 07/2014	Graded course *Introduction into Business Consulting and Entrepreneurship* at the University of Göttingen (***2 SWS, Grade: 1.0)***
Since 10/2013	Organization of the 3rd and 4th Women's Careers and Networks symposium (2014 and 2016) in Göttingen ***(writing press releases, managing website and facebook appearance)***
Since 07/2013	IT Manager of the Molecular Oncology workgroup (2013-now)
2009	Advanced training: Quality Assurance (Good Medical Practice, GMP) Prof. Dr. Jürgen Pomp, *University of Applied Sciences Bonn-Rhein-Sieg* **(Grade: 1.7)**

V. CONFERENCES

08/2013	8th International Mdm2 Conference (New Orleans, USA)	***Poster presentation***
2013 & 2014	Molecular Biology Summer Symposium (GZMB, Göttingen)	***Oral presentations***
08/2013	7th International Mdm2 Conference (Cambridge, UK)	***Poster presentation***
10/2012	7th Heinrich F.C. Behr Symposium on Stem Cells and Cancer (Heidelberg)	
09/2012	2nd symposium of the Göttingen Chromatin Club	***Oral presentation***

VI. SUPERVISION AND TEACHING

2013 - 2014	Supervision of 2 molecular biology master students during 8-week-lab rotations
10/2013 & 10/2014	Instruction of a 4 day method course for molecular biology master students "*DNA Techniques*"
04/2013	Instruction of a 2 day method course for PhD students "*Polymerase chain reaction and advanced applications*"

VII. VOLUNTEERING & INTERNSHIPS

Since 10/2013	Organization of the 3rd and 4th Women's Careers and Networks symposium (***Head organizer of the public relations team in 2014)***
11/2010 – 01/2011	Internship at the Department of Cellular and Molecular Immunology, Prof. Dr. Holger Reichardt (University Medical Center Göttingen)
03/2011 – 04/2011	Internship at the Stem Cell Biology Unit, Prof. Dr. Rüdiger Behr (German Primate Center, Göttingen)
2008-2009	Member of the student committee of the University of Applied Sciences Bonn-Rhein-Sieg
2004-2007	Regular organization of youth camps and children leisure activities

VIII. STAY ABROAD

09/2009-06/2010	Aberdeen, Scotland, UK *integrated study program at the University of Aberdeen*
07/2006-05/2007	Work and Travel Australia

IX. LANGUAGE PROFIENCY

German	Native speaker
English	Fluent spoken and written
Norwegian	Beginner

Göttingen, 20.11.2015

Magdalena Wienken